PHYSICOCHEMICAL CHARACTERISATION OF CYCLODEXTRIN-DRUG COMPLEXES

by

VIVIENNE JEAN GRIFFITH

Thesis Presented for the Degree of

DOCTOR OF PHILOSOPHY

in the Department of Chemistry

Faculty of Science

UNIVERSITY OF CAPE TOWN

March 1996

ACKNOWLEDGEMENTS

My sincere thanks to:

Professor Mino Caira, for his time, patience and outstanding supervision.

my co-supervisor, Professor Luigi Nassimbeni, for his advice and encouragement.

Dr. Leonard Barbour, for his useful computer programs, especially "torsion".

my parents, for providing me with the opportunity of acquiring a tertiary education.

my husband, Manolis, for his love and support.

the Foundation for Research Development, the University of Cape Town and South African Druggists for financial support.

PUBLICATIONS, CONFERENCES AND PATENTS.

PARTS OF THIS THESIS HAVE BEEN PUBLISHED:

1. M.R. Caira, V.J. Griffith, L.R. Nassimbeni and M.C.B. van Oudtshoorn. Synthesis and X-ray crystal structure of β-cyclodextrin diclofenac sodium undecahydrate, a β-CD complex with a unique crystal packing arrangement. *J. Chem. Soc., Chem. Commun.*, 1994, 1061.

2. M.R. Caira, V.J. Griffith, L.R. Nassimbeni and M.C.B. van Oudtshoorn. X-ray structure and thermal analysis of a 1:1 complex between sulfathiazole and β-cyclodextrin. *J. Incl. Phenom.*, 1994, **17**, 187.

3. M.R. Caira, V.J. Griffith, L.R. Nassimbeni and B. van Oudtshoorn. Unusual $^1C_4$ conformation of a methylglucose residue in crystalline permethyl-β-cyclodextrin monohydrate. *J. Chem. Soc., Perkin Trans. 2*, 1994, 2071.

4. M.R. Caira, V.J. Griffith, L.R. Nassimbeni and B. van Oudtshoorn. X-ray structure and thermal analysis of a 1:1 complex between (*S*)-naproxen and heptakis(2,3,6-tri-O-methyl)-β-cyclodextrin. *J. Incl. Phenom.*, 1995, **20**, 277.

5. M. R. Caira, V. J. Griffith, L. R. Nassimbeni and B. van Oudtshoorn. X-ray structures of 1:1 complexes of (*L*)-menthol with β-cyclodextrin and permethylated β-cyclodextrin. *Supramol. Chem.*, 1995, in press.

PARTS OF THIS THESIS HAVE BEEN PRESENTED AT THE FOLLOWING CONFERENCES:

14th Annual Congress of the Academy of Pharmaceutical Sciences, Durban, 21-23 June 1993.
M. R. Caira, **V. J. Griffith**, L. R. Nassimbeni and B. van Oudtshoorn. Structure and thermal analysis of a 1:1 complex between β-cyclodextrin and sulfathiazole.

15th Annual Congress of the Academy of Pharmaceutical Sciences, Grahamstown, 27-29 June 1994.
M. R. Caira, **V. J. Griffith**, L. R. Nassimbeni and B. van Oudtshoorn. A study of the interaction between diclofenac sodium and β-cyclodextrin in the solid state and in solution.

XXth International Symposium on Macrocyclic Chemistry, Jerusalem, 2-7 July 1995.
M. R. Caira, **V. J. Griffith**, L. R. Nassimbeni and B. van Oudtshoorn. X-ray structures and thermal analyses of 1:1 complexes of (*L*)-menthol with β-cyclodextrin and permethylated β-cyclodextrin.

PATENTS

1. European patent. Application no. 94307380.9-. 21/12/94 Diclofenac sodium-β-cyclodextrin inclusion complex.

2. South African preliminary patent application, no. 94/4466, filed February 1995. Inclusion complexes of naproxen and ibuprofen with (2,3,6-tri-O-methyl)-β-cyclodextrin.

ABSTRACT

The cyclodextrins and their derivatives are finding increasing application in the pharmaceutical industry as carrier molecules for many drugs, as complexation can result in improved physical characteristics such as increased aqueous solubility and dissolution rates. The aim of this work was to prepare solid cyclodextrin complexes with selected drugs which have already been shown to interact with cyclodextrins in solution and ultimately to grow crystals of these inclusion complexes of sufficient quality for single crystal X-ray structure determination. The designated drugs included an antibacterial, sulfathiazole; three non-steroidal anti-inflammatory drugs (NSAIDs), (*S*)-naproxen and the sodium salts of diclofenac and meclofenamic acid; and (*L*)-menthol, a compound used in many pharmaceutical preparations. The chosen host molecules were β-cyclodextrin, γ-cyclodextrin, heptakis(2,6-di-O-methyl)-β-cyclodextrin (DIMEB) and heptakis(2,3,6-tri-O-methyl)-β-cyclodextrin (TRIMEB).

The unit cell parameters of thirteen cyclodextrin-drug complexes and of TRIMEB monohydrate were determined by X-ray photography and the crystal structures of six of these complexes and of TRIMEB monohydrate were solved. The water content of the complexes was established by thermogravimetric analysis and the host:guest stoichiometries of those complexes whose crystal structures were not solved were determined by UV spectrophotometry or, in one case, by a combination of NMR and thermogravimetric analysis. The complexes were also characterised by differential scanning calorimetry.

Hot stage microscopy was a useful method for initial testing for the formation of inclusion complexes of the native cyclodextrins, since their behaviour on heating differs markedly from that of the relevant host alone. The events observed could be correlated with the thermal analyses of the complexes. Complexes which contained alkali metal cations appeared to retain water molecules of crystallisation to higher temperatures, on average, than those which did not. XRD patterns were calculated from the crystal structures which were solved and matched the experimental patterns of the prepared samples well. The calculated patterns serve as the best references for establishing the identity and purity of prepared complexes.

Host-guest interactions included hydrogen bonding, van der Waals contacts and

hydrophobic interactions. Guest molecules maintained similar conformations on the whole as those observed in other crystal structures containing these particular guests. Conformations of the hosts were akin to those found in known crystal structures, except in TRIMEB monohydrate, where the TRIMEB conformation was distorted to a remarkable extent even in comparison with the distorted conformations observed in its complexes. In addition, one of the methylglucose residues is present in the $^1C_4$ inverted chair conformation which has not been observed before in the cyclodextrins or their complexes in the solid state. The invariable occurrence in the TRIMEB host of $C(6G_n)$-H$\cdots$O$(5G_{n-1})$ hydrogen bonds noted in this study is partly responsible for the uniformity in the conformation of TRIMEB in its complexes.

The packing arrangement found in the diclofenac sodium-β-CD complex is unique and is the first example of a β-CD complex crystallising in the hexagonal crystal system. The inclusion by β-CD of meclofenamate sodium (a structural isomer of diclofenac sodium) is similar to that of diclofenac sodium, but the packing arrangement is different and while unique for a complex of unsubstituted β-CD, resembles the packing arrangement found in most of the known TRIMEB complexes.

ABBREVIATIONS AND SYMBOLS.

CSD	Cambridge Structural Database
DSC	differential scanning calorimetry
E	normalised structure factor
e.s.d.	estimated standard deviation
M_r	molecular mass
NMR	nuclear magnetic resonance spectroscopy
NSAID	non-steroidal anti-inflammatory drug
τ	torsion angle
s.o.f.	site occupancy factor
TG	thermogravimetry
UV	ultraviolet
V	cell volume
XRD	X-ray powder diffraction
SULF*	sulfathiazole (*N*-(2-thiazolyl)sulfanilamide)
DICLOF*	diclofenac sodium (sodium salt of 2-[(2,6-dichlorophenyl)amino]benzeneacetic acid)
FENAC*	diclofenac sodium
MECLOF*	meclofenamate sodium (sodium salt of (2-[2,6-dichloro-3-methyl-phenyl)amino]benzoic acid)
NAP*	(*S*)-naproxen ((*S*)-6-methoxy-α-methyl-2-naphthaleneacetic acid)
MENTH*	(*L*)-menthol ((1α,2β,5α)-5-methyl-2-(1-methylethyl) cyclohexanol
MEN*	(*L*)-menthol
CD	cyclodextrin or circular dichroism
β-CD	β-cyclodextrin
B*	β-cyclodextrin
γ-CD	γ-cyclodextrin
G*	γ-cyclodextrin
DIMEB	heptakis(2,6-di-O-methyl)-β-cyclodextrin
DMB*	heptakis(2,6-di-O-methyl)-β-cyclodextrin
TRIMEB	heptakis(2,3,6-tri-O-methyl)-β-cyclodextrin
TMB*	heptakis(2,3,6-tri-O-methyl)-β-cyclodextrin

* combinations of these refer to complexes e.g SULFB is the sulfathiazole-β-cyclodextrin complex and NAPTMB is the (*S*)-naproxen-heptakis(2,3,6-tri-O-methyl)-β-cyclodextrin complex.

TABLE OF CONTENTS

	Acknowledgements	i
	Publications, conferences and patents	ii
	Abstract	iii
	Abbreviations and symbols	v
	Table of contents	vi
Chapter 1	**Introduction**	
	Introduction	1
	The uses of cyclodextrins in the pharmaceutical industry	2
	Metabolism and toxicity of cyclodextrins	4
	Cyclodextrin derivatives	5
	Host-guest interactions and the driving force of complexation	8
	Investigation of complexation in solution	9
	Preparation of solid complexes	11
	Investigation of solid complexes	12
	Single crystal X-ray structure analysis	13
	Molecular modelling	21
	Objectives of this study	23
	References	24
Chapter 2	**Materials and Methods**	
	Host compounds	28
	Guest compounds	28
	Crystal growth	28
	Hot stage microscopy	28
	Density measurement	29
	Thermal analysis	29
	UV spectrophotometry	30
	NMR spectroscopy	30
	Microanalysis	30
	X-ray powder diffraction	31
	Crystal structure analysis, solution and refinement	31
	References	35

Chapter 3 Sulfathiazole

Introduction 36
Preparation of the CD complex 37
Hot stage microscopy 38
Thermal analysis 38
Microanalysis 39
Crystal structure solution 39
Crystal structure 41
XRD 49
UV spectrophotometry 50
References 51

Chapter 4 Diclofenac sodium

Introduction 52
Preparation of the CD complexes 53
Diclofenac sodium-β-cyclodextrin complex (DICLOFB)
Diclofenac-β-cyclodextrin complexes with potassium and caesium (FENACBK and FENACBCs)
Diclofenac sodium-γ-cyclodextrin complex (DICLOFG)
Hot stage microscopy 54
Thermal analysis 56
UV spectrophotometry 59
Microanalysis 59
Crystal data 60
Crystal structure solution 61
DICLOFB
FENACBK
Crystal structure (DICLOFB) 63
XRD 78
References 79

Chapter 5 Meclofenamate sodium

Introduction 80
Preparation of the complex 80
Thermal analysis 81
Microanalysis 82
Crystal structure solution 82
Crystal structure 83
XRD 99
References 100

Chapter 6 Permethylated β-cyclodextrin

Introduction 101
Preparation of TRIMEB monohydrate 101
Thermal analysis 101
Microanalysis 102
Crystal structure solution 103
Crystal structure 103
XRD 111
References 112

Chapter 7 Naproxen

Introduction 113
Preparation of the CD complexes 113
(*S*)-Naproxen-β-cyclodextrin complex (NAPBmono)
(*S*)-Naproxen sodium-β-cyclodextrin complex (NAPBorth)
(*S*)-Naproxen-γ-cyclodextrin complex (NAPG)
(*S*)-Naproxen-TRIMEB complex (NAPTMB)
Thermal analysis 115
UV spectrophotometry 118
Microanalysis 119
Crystal data for NAPBmono, NAPBorth and NAPG 120
Crystal structure solution (NAPTMB) 121
Crystal structure (NAPTMB) 121
XRD 131
References 132

Chapter 8 Menthol

Introduction 134

Preparation of the CD complexes 134

(L)-menthol-β-cyclodextrin complex (MENTHB)

(L)-menthol-DIMEB complex (MENDMB)

(L)-menthol-TRIMEB complex (MENTMB)

Thermal analysis 136

Microanalysis 139

Crystal data for MENDMB 140

Crystal structure solutions 141

MENTHB complex

MENTMB complex

Crystal structure 145

MENTHB complex

MENTMB complex

Thermal analyses of the menthol-CD complexes in relation to their crystal structures.

XRD 162

References 164

Chapter 9 Conclusion

Hot stage microscopy - a useful tool 166

Thermal Analysis 167

Crystal structure 167

XRD 169

References 170

Chapter 1 INTRODUCTION

The cyclodextrins are cyclic oligosaccharides made up of α-1,4 linked D-glucopyranose units[1]. (Figure 1) They were first noted by Villiers in 1891 and later characterised by Schardinger in 1904[2]. They have been called Schardinger dextrins, cycloglucans and cycloamyloses, but are now almost exclusively referred to as the cyclodextrins. α-, β- and γ-cyclodextrin, six, seven and eight glucopyranose units respectively, are the most common naturally occurring cyclodextrins. They are the products of the action on starch of a bacterial amylase, cyclodextrin glucosyltransferase (CGTase), which was first isolated from *Bacillus macerans*. The digestion of starch by this enzyme also yields much smaller amounts of cyclodextrins containing more than eight glucose moieties, but they are more difficult to isolate and purify because of their low yield and higher solubility. Despite this, the crystal structure of δ-cyclodextrin[3] (9 glucose units) and its physicochemical properties[4] have been reported and, more recently, η-cyclodextrin (12 glucose units) has been purified and characterised[5].

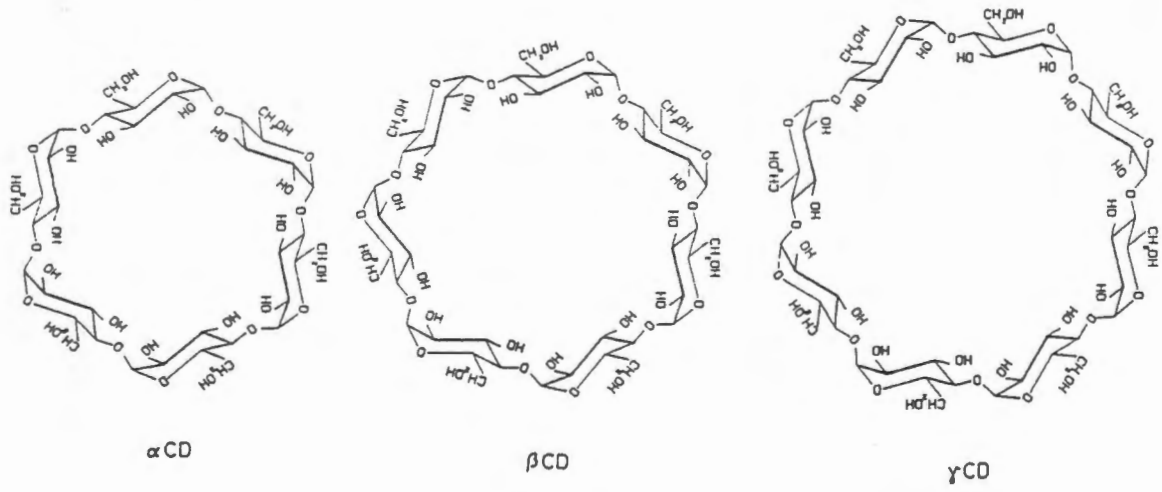

Figure 1 Chemical structure of the cyclodextrins (taken from reference 1)

The cyclodextrins have the shape of a truncated cone with a cavity in the centre. Figure 2 shows a schematic diagram of α- β- and γ-cyclodextrin with their approximate dimensions. The cavity is relatively hydrophobic since the lone pairs of the glycosidic oxygen atoms are directed inwards towards the cavity as are the hydrogen atoms attached to C(3) and C(5) of each glucose moiety[1]. The hydroxyl

groups at the rims of the cyclodextrin render the molecule soluble in aqueous solution. The wider rim of the molecule is lined with secondary hydroxyl groups and the narrower rim with primary hydroxyl groups. A guest molecule of lower polarity than water can be accommodated in the cyclodextrin cavity in aqueous solution providing that it is of appropriate size and shape. This complexing ability of the cyclodextrins was discovered by Pringsheim and has been exploited because of the altered physical and chemical properties that are conferred on the guest[1,2]. Complexation of some guests can lead to a catalytic action in the hydrolysis, oxidation, decarboxylation or isomerisation of the guest[6] and therefore cyclodextrins have also been used as enzyme models[7,8,9]. The cavity of the cyclodextrin is a permanent structural feature and this distinguishes cyclodextrins from most other host molecules which can only provide cavities or channels suitable for the inclusion of guest molecules by crystallisation[10]. In contrast, inclusion of guest molecules by cyclodextrins can be observed in solution as well as in the solid state.

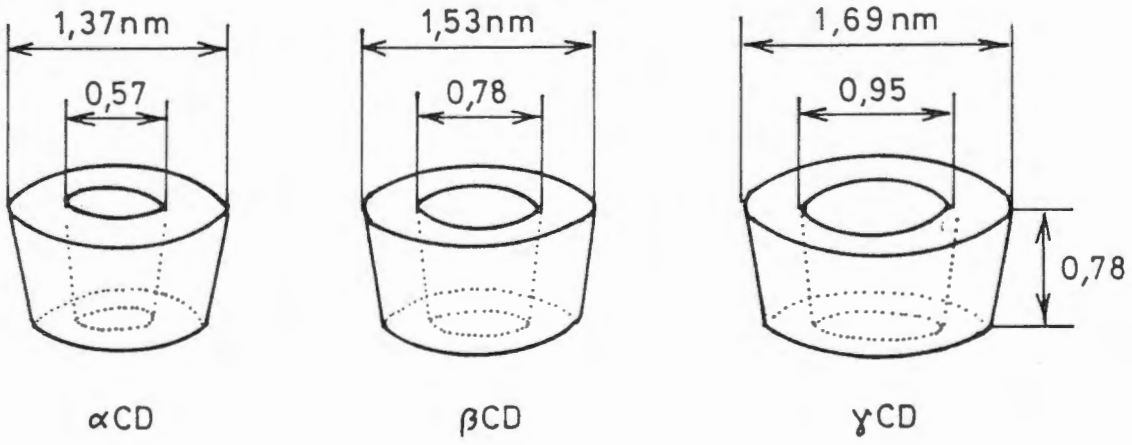

Figure 2 Schematic diagram of α-, β- and γ-cyclodextrin (taken from reference 1)

The uses of cyclodextrins in the pharmaceutical industry.

Although cyclodextrins are utilised in foods, cosmetics, toiletries and in agriculture, only their uses in the pharmaceutical industry will be discussed as only guest molecules classified as drugs were investigated for this thesis.

There are many advantages in complexing drug molecules with cyclodextrins[1,6,11,12]:

- increased dissolution rate and aqueous solubility which can lead to enhanced bioavailability.
- stabilisation of guest from heat, light, hydrolysis and oxidation.
- transformation of liquid compounds to solids suitable for tabletting.
- masking of bad smell and sometimes taste.
- mixing of incompatible compounds if one is complexed with a cyclodextrin.
- preparation of stable solutions suitable for injectables or eye-drops.
- utilisation of highly swelling cyclodextrin polymers in small amounts can result in rapid tablet disintegration on contact with water.
- separation of drug stereoisomers.
- reduction in ulcerogenic potencies of several acidic anti-inflammatory drugs.

The bioavailability is defined as the rate and extent of absorption of a drug from its dosage form into the systemic circulation. For intravenously administered drugs the absorption is rapid and complete. However, for reasons of convenience and stability, most drugs are administered orally and hence their rate and extent of absorption are not known precisely. Since a drug must dissolve in the gastrointestinal tract prior to absorption, the dissolution rate and aqueous solubility play a major role in the bioavailability of the drug. These, in turn, are dependent to some extent on other parameters like particle size, pK_a and polymorphism (crystal structure).

The pharmacokinetic behaviour of a drug in the body can be described by pharmacokinetic models. Figure 3 shows such a model for peroral administration of a cyclodextrin-drug complex. If the rate of dissolution is slower than the rate of absorption as is the case for poorly water-soluble drugs, then dissolution is the rate-limiting step. The absorption of the drug is also dependent on the stability constant of the complex, since only the free drug is absorbed. A low stability constant will result in rapid absorption of the drug. Higher blood levels can be achieved through complexation with cyclodextrins and therefore therapeutic effects with lower doses are possible. Lower doses of drug also decrease the possibility of side effects.

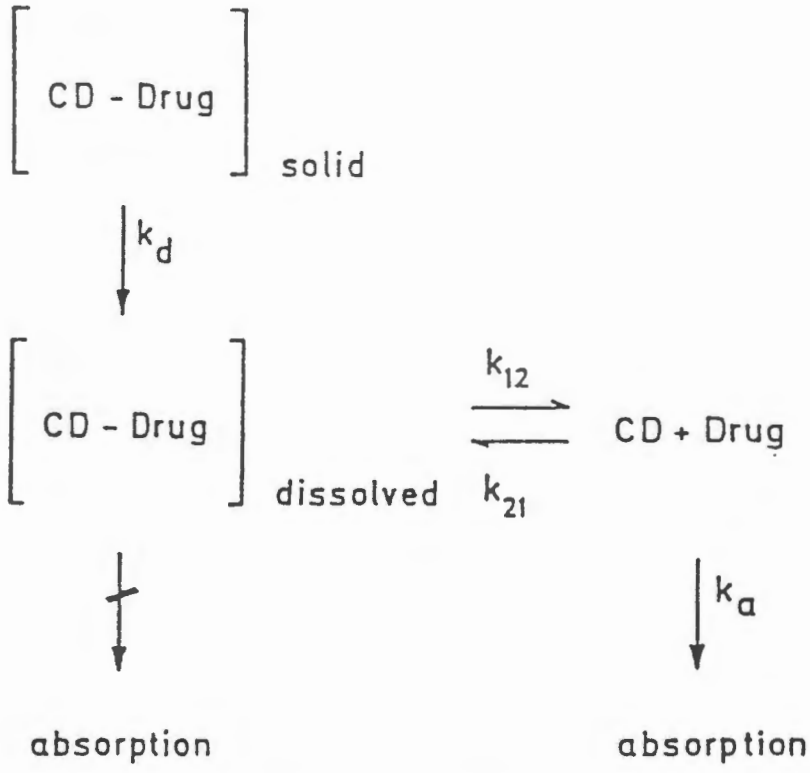

Figure 3 Pharmacokinetic model (taken from reference 6).

Although cyclodextrins are rather non-specific regarding their guest molecules, it has been found in cases of certain optically active drugs that β-cyclodextrin can distinguish between and/or show a slight preference for one enantiomer of a drug over the other[13,14,15,16,17]. This can be used to achieve separation of drug stereoisomers by immobilised β-cyclodextrin. Many drugs are administered as racemates because of difficulties in separation or with stereoselective syntheses and numerous examples exist where the undesired effects of one isomer limit the overall effectiveness of the active species because of host toxicities, biodistribution problems, altered metabolism and unwanted drug interactions[13,18].

Metabolism and toxicity of cyclodextrins

The cyclodextrins are cleaved much more slowly by α-amylases than starch and are not hydrolysed at all by β-amylases which attack terminal groups[12]. Negligible amounts are absorbed intact from the gastrointestinal tract. They are, however, broken down by enzymes of the flora found in the colon and therefore the major difference between the metabolism of starch and that of the cyclodextrins is that starch is metabolised in the small intestine and the cyclodextrins in the colon[1,6].

The primary metabolites (acyclic maltodextrins, maltose and glucose) are then further metabolised, and absorbed, and finally excreted as CO_2 and H_2O. Toxicity studies have shown that orally administered natural cyclodextrins are harmless, particularly γ-cyclodextrin.

Parenteral administration of the natural cyclodextrins, especially β-cyclodextrin, results in nephrotoxicity (due to accumulation in the kidneys) and haemolysis of erythrocytes, but only with relatively large doses. Although low concentrations of cyclodextrins actually protect erythrocytes from haemolysis, at higher concentrations sequestration of cholesterol (mostly by β-cyclodextrin) and phospholipids (mostly by α-cyclodextrin) from the erythrocyte cell membrane result in its disruption. In both these respects, γ-cyclodextrin has been found to cause the least damage, probably because of its higher solubility and more rapid enzymatic degradation[6].

Cyclodextrin derivatives

Due to the above-mentioned problems, caused essentially by relatively low solubility, the use of the natural cyclodextrins is limited, especially for parenterally administered drugs. This has been shown in particular for β-cyclodextrin[1,6], which has an anomalously low aqueous solubility[19]. In addition, the solubility of cyclodextrin complexes is sometimes lower than that of the host itself[6,20]. At 25°C the solubilities of α-, β- and γ-cyclodextrin are 127, 18.8 and 256 $mg.ml^{-1}$, respectively. Consequently, much attention has been focussed on the derivatisation of the natural cyclodextrins in an effort to increase the aqueous solubility while retaining, and in some cases enhancing, the complexing ability[21,22,23,24,25,26,27]. In contrast, more lipophilic cyclodextrin derivatives (e.g. ethylated derivatives) are being investigated for their sustained release properties[6,27].

The hydroxyl groups of the cyclodextrins are characterised by different reactivities and can be selectively substituted[25]. The C(6)-OH groups are the most reactive and the C(3)-OH the least reactive. However, the preparation of homogeneous, selectively modified cyclodextrins is difficult and these are not yet produced on an industrial scale. Since β-cyclodextrin is inexpensive and has a cavity of suitable size for the complexation of most pharmaceuticals, its derivatives have attained practical importance in pharmacy[6]. Table 1 shows some of the characteristics of

pharmaceutically useful β-cyclodextrin derivatives. Since the methylated β-cyclodextrin hosts, heptakis(2,6-di-O-methyl)-β-cyclodextrin (DIMEB) and heptakis(2,3,6-tri-O-methyl)-β-cyclodextrin (TRIMEB), have been employed in this thesis, a brief summary of their properties will be given.

derivative	characteristic	possible use (dosage form)
ß-CD	crystalline, relatively low water-soluble (1·85%)	oral, mucosal[a], dermal
hydrophilic derivatives:		
methylated ßCD: • DMßCD • TMßCD	soluble in cold water and in organic solvents, surface active, haemolytic	oral, dermal
hydroxyalkylated ßCD: • 2-HEßCD • 2-HPßCD • 3-HPßCD • 2,3-DHPßCD	amorphous mixture with different degrees of substitution, highly water-soluble, low haemolytic activity	oral, mucosal, parenteral (IV)
branched ßCD: • G_1ßCD • G_2ßCD • $(G_2)_2$ßCD	homogeneous compound, highly water-soluble, low haemolytic activity	oral, mucosal, parenteral (IV)
hydrophobic derivatives:		
ethylated ßCD: • DEßCD • TEßCD	water-insoluble, surface active	oral, sub-cutaneous, (sustained-release)
ionizable derivatives:		
anionic ßCD: • CMEßCD	pKa = 3 to 4, enteric	oral, dermal, mucosal (delayed-release)
• ßCD sulphate • ßCD phosphate	pKa < 1, water-soluble in wide pH range	oral, dermal, mucosal

DM	2,6-di-O-methyl	TM	2,3,6-tri-O-methyl
2-HE	2-hydroxyethyl	2-HP	2-hydroxypropyl
3-HP	3-hydroxypropyl	2,3-DHP	2,3-dihydroxypropyl
G_1	glycosyl	G_2	maltosyl
$(G_2)_2$	di-maltosyl	DE	2,6-di-O-ethyl
TE	2,3,6-tri-O-ethyl	CME	O-carboxymethyl-O-ethyl

(a) mucosal: nasal, sublingual, ophthalmic, pulmonary, rectal, vaginal etc.

Table 1 Characteristics of pharmaceutically useful β-CD derivatives (taken from reference 27).

The methylated β-cyclodextrin derivatives are much more water-soluble than the parent cyclodextrin and, in fact, the solubility (in cold water) increases with increasing degree of methylation until about two thirds of the hydroxyl groups are methylated and then decreases again. Therefore DIMEB (14 hydroxyl groups methylated) shows a higher solubility than TRIMEB (all 21 hydroxyl groups methylated), although the solubility of TRIMEB is still considerably higher than that of the parent cyclodextrin[25]. The reason for the higher solubility on methylation is not clear, but it has been found that DIMEB and TRIMEB do not form large aggregates in solution like the native cyclodextrins because of their decreased hydrogen bonding capacity (although the presence of the O(3) hydroxyl groups may allow dimerisation of DIMEB in solution)[19]. DIMEB and TRIMEB have an unusual property in that their solubility decreases with increasing temperature[6]. This behaviour suggests hydrophobic interactions probably correlated with hydration around the methylated CDs[10]. Figure 4 shows the dissolution and recrystallisation of DIMEB and the solubility of β-cyclodextrin as a function of temperature. This inverse solubility behaviour is a potential problem for the preparation of aqueous injectable solutions because of the need for heat-sterilisation of such formulations[24].

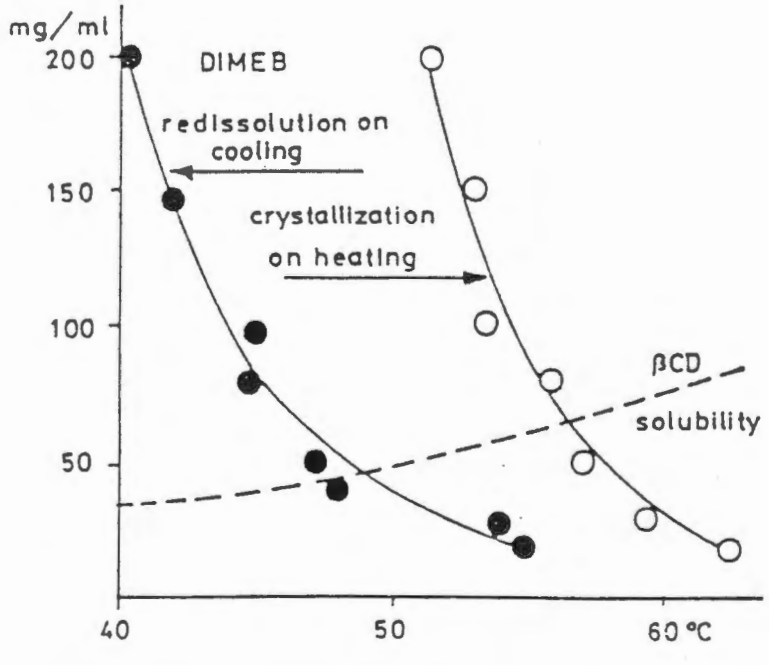

Figure 4 Dissolution and recrystallisation of DIMEB and the solubility of β-cyclodextrin as a function of temperature (taken from reference 6).

The inclusion ability of DIMEB is generally greater than that of the parent host molecule and other derivatives due to an increase in hydrophobic space of the cyclodextrin cavity[12] and the presence of this host can enhance the solubility of drugs by up to 10^3 times[11]. Although this is obviously an advantage, it has been found that DIMEB has a high affinity for cholesterol and therefore causes haemolysis even at fairly low concentrations[11]. TRIMEB shows a lower haemolytic activity, but also a decreased complexing ability. However, it has been suggested that the chiral recognition ability of TRIMEB is superior because of its distorted conformation relative to the more symmetrical conformations of β-cyclodextrin and DIMEB[28,29]. Another advantage of the methylated cyclodextrins is that they are less hygroscopic and so may provide better protection in the solid state for drugs that are susceptible to hydrolysis. The dissolution rates of their complexes also increase with increasing temperature probably due to the dissociation of the complexes during the dissolution process[12].

Host-guest interactions and the driving force of complexation

The interactions between host and guest are mainly due to van der Waals forces, hydrophobic interactions and hydrogen bonding, and the extent to which these forces contribute is dependent on the nature of the guest[2,30]. The "driving force" of complexation is not yet fully understood, but many workers have suggested that one of the most important factors is the release of "high-energy" water molecules from the cavity of the cyclodextrin molecule. Since the tetrahedral hydrogen bonding capacity of the water molecules cannot be satisfied in the cavity, they are regarded as molecules of enhanced energy and therefore the release of these molecules into the bulk solvent, where their hydrogen bonding capacity can be fulfilled, is favourable[2]. Likewise, the removal of a hydrophobic guest from the polar solvent into the cavity is desirable. The thermodynamic parameters enthalpy (ΔH) and entropy (ΔS) can either be calculated from the temperature dependence of the dissociation constant or, more accurately, by microcalorimetry. A linear relationship is found when plotting ΔH against ΔS for complexation of different guests. This compensation effect implies a role for water molecules in the complexation process[2].

Investigation of complexation in solution

Amongst the most popular methods of investigating complexation by cyclodextrins in solution are the phase-solubility method, ^{1}H NMR, UV spectroscopy and circular dichroism.

The phase-solubility method[31] involves stirring excess guest (the drug) at a constant temperature with varying concentrations of host (the cyclodextrin) in a suitable solvent (water). Once equilibrium has been attained, the solution phases are analysed for the total drug concentration. If the guest is indeed complexed by the host, then increasing concentrations of host should result in an apparent increase in the solubility of guest provided that the solubility limit of the resultant complex is not exceeded. Plotting the apparent solubility of the guest against the host concentration can yield various solubility isotherm types. Figure 5 shows the various types of solubility isotherms which can be expected.

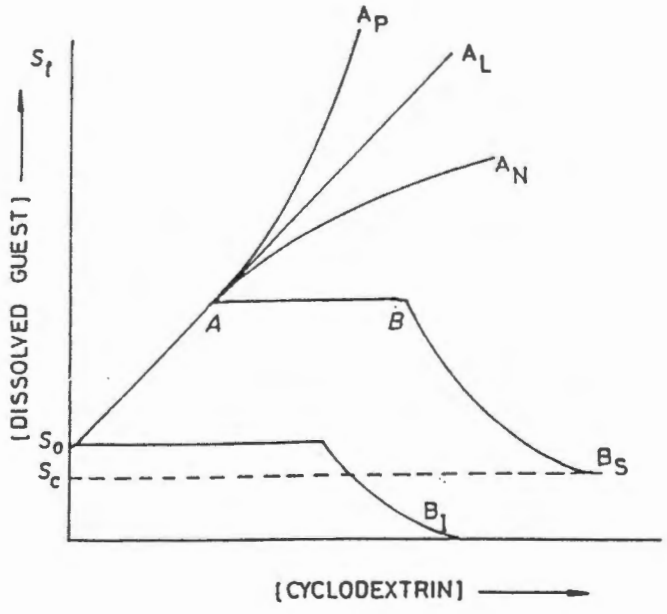

Figure 5 Solubility isotherm types. S_0 = solubility of the guest in the absence of CD; S_t = concentration of dissolved guest (free + complexed); S_c = solubility limit of the poorly soluble complex; Isotherm types A_P, A_L and A_N = soluble complexes formed (solubility determined by solubility of the CD); Isotherm B_S = complex of limited solubility is formed; Isotherm B_I = insoluble complex is formed (taken from reference 6).

The slope of the initial straight line portion of the graph and the y-intercept (i.e. the aqueous solubility of the drug in the absence of cyclodextrin) can be used to estimate the association constant for a 1:1 complex and in the case of the formation of a poorly soluble complex (type B_S curve), the stoichiometry of the solid complex can be established by analysing the plateau region of the graph. Deviation from linearity for the A type curves is explained by the presence in solution of complexes of differing stoichiometry. Although the phase-solubility approach has been a very popular method of investigating complexation in solution, a number of draw-backs have been pointed out. Firstly, an increase in solubility of a guest in the presence of a cyclodextrin could be accounted for by interactions other than inclusion of the guest in the host cavity and secondly the estimation of the association constant is based on the assumption of a host-guest complex with 1:1 stoichiometry. However, since for applications in the pharmaceutical industry, it is often merely an increase in solubility that is required, whether this is due to true inclusion or not, the technique is valuable for assessing the potential usefulness of cyclodextrins and derivatives for improving the solubility of particular drugs[27].

^1H NMR spectroscopy has been used extensively to investigate complexation by cyclodextrins in solution[27,32,33,34,35]. Shifts (usually upfield) in the presence of a guest molecule of the signals of the host protons attached to C(3) and C(5) (and to a lesser extent C(6)), which line the inside of the cavity, are generally accepted to be evidence of inclusion of a guest molecule in solution. Shifts of the guest protons can also be observed on complexation. Splitting of signals is not generally observed on complexation and this is indicative of a rapid exchange between the complexed and uncomplexed states on the NMR time-scale. The change in chemical shift of a particular guest proton (or host proton) on increasing guest:host ratio (host:guest ratio) can be used to estimate the association constant[27]. However, this can be technically difficult due to the low solubility of the complexes or either component in D_2O[11]. ^{13}C NMR has also been used, but to a lesser extent, because even higher concentrations are needed in order to obtain good spectra with high signal to noise ratios. It has been shown that the compounds tetramethylsilane (TMS) and sodium 2,2-dimethylsilapentane-5-sulphonate (DSS), commonly used as internal references in NMR spectroscopy, are also included by cyclodextrins in solution and therefore, the use of an **external** reference, preferably DSS, is recommended for studying changes in shifts on cyclodextrin complexation[36]. An advantage of NMR spectroscopy in comparison with other spectroscopic methods like UV and circular

dichroism is that both host and guest can be observed simultaneously. Difficulties can be encountered, however, when there is overlap of host and guest signals.

Changes in the UV spectrum of a given guest can be observed in the presence of excess cyclodextrin. The changes involve shifts in λ_{max} and/or an increased (or decreased) absorption in the presence of the host. The change in absorbance on increasing cyclodextrin concentration can be utilised to estimate association constants[34,37,38]. Circular dichroism has also been used to demonstrate inclusion of a guest in solution[34,39,40,41,42] especially that of an optically inactive guest which, on complexation, displays an **induced** circular dichroism spectrum on account of being transferred to the asymmetric environment of the host cavity. Changes in the induced CD spectrum on increasing guest:host ratio are used for the calculation of the association constant and the sign of the induced CD spectrum can give an indication of the orientation of the included guest molecule in the cavity of the host[42]. To a lesser extent, fluorescence spectroscopy is also used to study the interaction of some guests with cyclodextrins in solution[43].

The Job's plot[44] method has been used extensively to establish the host:guest stoichiometry in solution. Briefly, the method involves keeping the sum of the concentrations of host and guest constant, while varying the host:guest ratio. The change in a parameter (e.g. chemical shift or UV absorbance at a particular wavelength) is then plotted against the host:guest ratio. The maximum (or minimum) of the Job's plot then corresponds to the stoichiometry in solution.

Preparation of solid complexes.

The method of preparation of solid cyclodextrin inclusion complexes is generally guest dependent and must be tailor-made[1]. Solid complexes can be prepared by mixing host and guest in an appropriate molar ratio in aqueous solution at elevated temperature. The complex can then be precipitated by cooling or pH adjustment followed by filtration, or the solution can be spray- or freeze-dried to yield an amorphous solid product. Elevated temperatures are used to increase the solubility of both host and guest (except in the case of the methylated cyclodextrins). In the case of guests which are very insoluble in water, cosolvents like methanol, ethanol and acetone can be used, but this is to be avoided if possible, as the stability

constant is decreased in the presence of cosolvents due to competition of the drug and the cosolvent for the host cavity[45]. Complexes can also be prepared in suspension, by kneading where a small amount of water or other solvent is used, or by grinding. Complexes prepared in these ways are often not homogeneous true inclusion complexes, but contain significant amounts of uncomplexed host and guest. Complexes with the methylated derivatives can be prepared by stirring host and guest together in water at room temperature or in an ice bath and then crystallising at elevated temperature.

Investigation of solid complexes.

It is somewhat difficult to detect the difference between a true inclusion complex and an intimate physical mixture between host and guest in the solid state. However, a combination of a number of the following methods can give strong evidence in favour of the formation of a true inclusion complex.

The X-ray powder diffraction pattern (XRD) of a true inclusion complex should differ from the XRD pattern of a physical mixture of host and guest in the relevant molar ratio. The appearance of new peaks and the disappearance of peaks relative to the pattern for the physical mixture can be evidence in favour of the formation of an inclusion complex. However, this is merely evidence of a new phase i.e. the presence of a new species with different unit cell parameters and could just as easily represent a polymorph of the guest. Therefore XRD patterns can only be used as proof of complex formation in conjunction with other methods.

Thermogravimetric analysis (TG), differential scanning calorimetry (DSC) and evolved gas analysis (EGA) can give good indications of whether an inclusion complex has been made. The traces obtained can be compared with traces for physical mixtures in the appropriate molar ratio. In general, true inclusion complex formation results in the retention of the guest until well above its melting point and, in most cases, until the onset of decomposition of the host[1,6,46]. Other methods which can be used include IR spectroscopy, solid state ^{13}C NMR, reflectance spectroscopy and thin-layer chromatography.

Single crystal X-ray structure analysis

Single crystal X-ray analysis is the best method for detecting complex formation in the solid state. This technique not only provides information regarding stoichiometry and host-guest geometry, but also about host-guest interactions[1,6,10,12,27]. However, there is some difficulty in obtaining crystals of a suitable size for analysis and crystal lattice effects are expected to affect the structure relative to that found in solution.

Application of cyclodextrins in the pharmaceutical industry is limited mainly to β-cyclodextrin and γ-cyclodextrin and their derivatives because most commonly used pharmaceuticals are too large to fit into the α-cyclodextrin cavity[24]. Since the hosts employed in this thesis have been restricted to β-cyclodextrin, DIMEB, TRIMEB and γ-cyclodextrin, a summary of the crystal packing arrangements found thus far for these hosts and their complexes will be given.

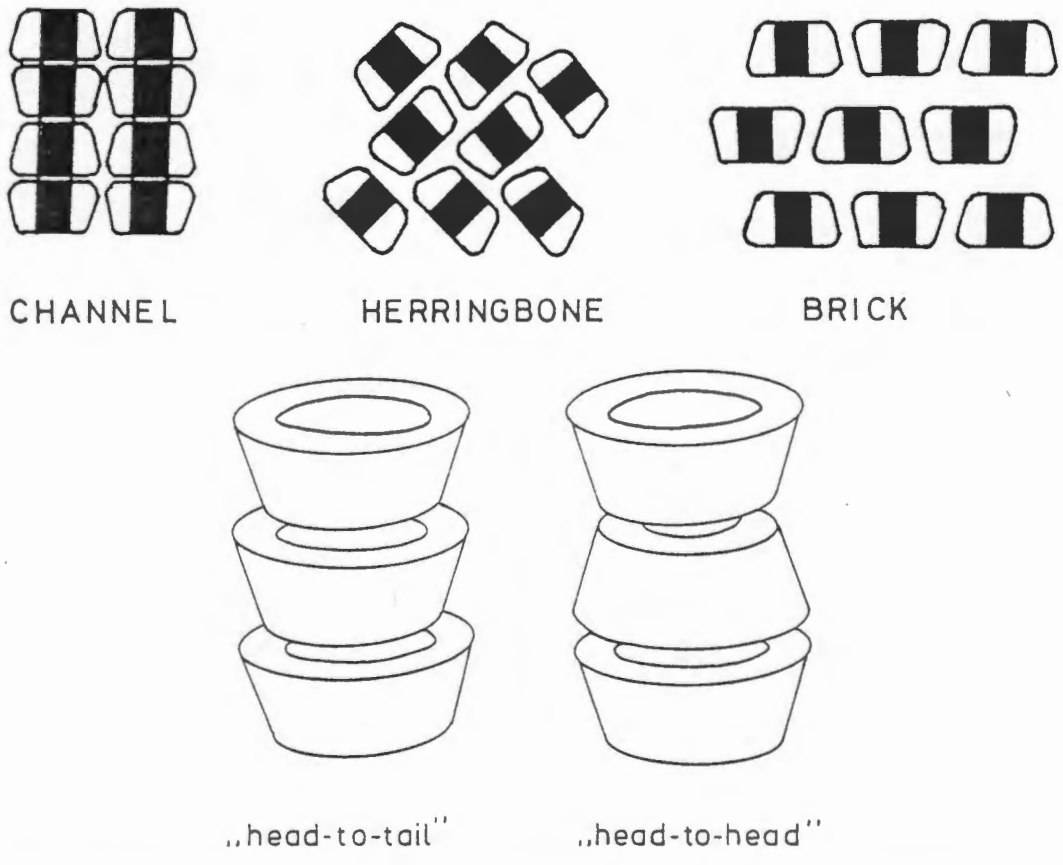

Figure 6 Crystal packing arrangements and stacking modes of CDs and their complexes (taken from reference 1.)

The packing arrangements found in the crystal structures of cyclodextrins and their complexes can be broadly classified into channel and cage type packing arrangements[1,10,47]. Figure 6 is a schematic diagram showing these different arrangements. Channel type packing results from stacking of cyclodextrin molecules either in a head-to-head or head-to-tail fashion. The cage type packing, where the cavity of each host molecule is blocked on either side by an adjacent cyclodextrin, can be either "herring-bone" or "bricks in a wall" type packing. The latter therefore has a layered appearance.

A search of the Cambridge Structural Database[48] yields 59 β-cyclodextrin, 9 DIMEB, 6 TRIMEB and 6 γ-cyclodextrin crystal structures. In all of these crystal structures, the D-glucopyranose moieties are found exclusively in the $^4C_1$ chair conformation, with one exception. One of the glucopyranose moieties in the m-iodophenol-TRIMEB crystal structure is found in the $^{O}S_2$ twist conformation[49]. Another feature which is found systematically in the crystal structures of these host molecules (except for TRIMEB) is intramolecular O(2)···O(3') hydrogen bonding between adjacent glucose residues[10,50]. Neutron diffraction studies have shown that this intramolecular hydrogen bonding is of a "flip-flop" nature in β- and γ-cyclodextrin crystal structures, constantly oscillating between O(2)-H···O(3') and O(2)···H-O(3') in the solid state[51,52,53]. Methylation of all the hydroxyl groups results in the loss of this intramolecular hydrogen bonding and, consequently, the increased conformational flexibility observed in the TRIMEB molecule[54].

In addition to the O(2)···O(3') intramolecular hydrogen bonding found in the crystal structures of cyclodextrins, there is extensive intermolecular hydrogen bonding involving the hosts and the water molecules which fill the intermolecular spaces. Although hydrogen atoms very often cannot be placed with certainty in X-ray crystal structures, a statistical analysis of high resolution neutron crystal structures of cyclodextrin complexes has shown that all O···O contact distances of 3 Å and less are actually associated with hydrogen bonds[55]. Another common, but frequently ignored, weak electrostatic interaction in carbohydrate crystal structures is the C-H···O hydrogen bond[56,57]. These interactions play a role in completing the tetrahedral coordination geometry around water molecules[58] as well as in host-guest interactions[59,60]. The primary hydroxyl groups in β-CD complexes are usually found in the (-)-gauche conformation[10] i.e. pointing away from the host cavity, unless they are involved in hydrogen bonding with a guest molecule, in which case

the (+)-gauche conformation is observed i.e. pointing inwards.

Figure 7 is a diagram of β-CD, showing the accepted numbering scheme used for the glucose moieties in cyclodextrins. The macrocyclic conformation of the host molecule and an indication of its deviation from 7-fold (8-fold in the case of γ-cyclodextrin) symmetry can be described by certain well established parameters[10,29]. Amongst these are the distances between the linking glycosidic oxygen atoms (O(4) atoms), the radius of the O(4) heptagon (or octagon for γ-CD) which is defined as the distance from the centre of gravity of the O(4) atoms to each O(4) atom, and the O(4)···O(4')···O(4") angle. The average of these angles is usually close to the ideal value of 128.6° (135°) for a regular heptagon (octagon). The larger the ranges spanned by the values of these parameters, the greater the departure from seven-fold (eight-fold) symmetry in the macrocyclic conformation. Another useful parameter is the tilt angle, which is defined as the angle between the O(4) plane and the plane through C(1), C(4), O(4) and O(4') of each glucose residue[61]. If the glucose moiety is inclined with its O(6) side towards the centre of the cavity, then the tilt angle is positive, but if the glucose moiety is inclined away from the cavity, then the tilt angle is assigned a negative value. Finally, the torsion-angle index[62] gives some idea of small variations in the ring geometry of the glucose residues. It is defined as $|\phi(C(1)\text{-}C(2))| + |\phi(C(2)\text{-}C(3))| - |\phi(C(3)\text{-}C(4))| - |\phi(C(4)\text{-}C(5))| + |\phi(C(5)\text{-}O(5))| + |\phi(O(5)\text{-}C(1))|$, where $\phi(C(1)\text{-}C(2))$ is the torsion angle O(5)-C(1)-C(2)-C(3).

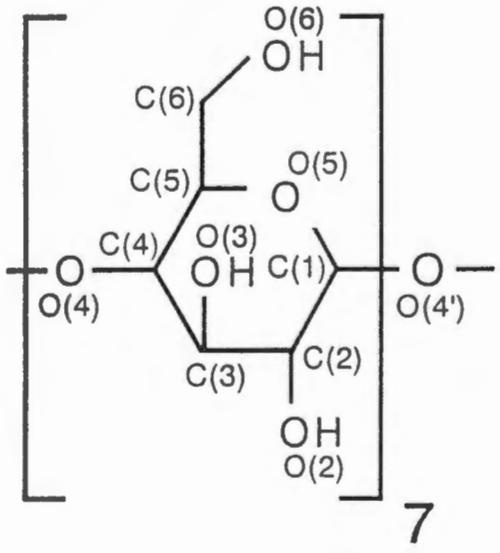

7

Figure 7 A diagram of β-CD showing the accepted numbering scheme.

The β-cyclodextrin dodecahydrate[63,64] has been studied extensively. It has a "herring-bone" packing arrangement and some of the water molecules are located inside the cavity and are characterised by high thermal motion and disorder. The remaining water molecules are located in the intermolecular spaces between the host molecules and suffer less from high thermal motion and disorder than the water molecules occupying the cavity. The hydrate dehydrates reversibly at ambient temperature in air[65,66]. A recent paper follows the partial dehydration of β-cyclodextrin dodecahydrate by X-ray diffraction[67], determining the crystal structure at various humidities. The crystal packing arrangement, hydrogen-bonding pattern and conformation of the host are retained down to 15% humidity with a loss of approximately 2.5 water molecules per host molecule.

The majority of β-cyclodextrin complexes are dimeric whereby two cyclodextrin molecules form a head-to-head dimer stabilised by hydrogen bonding between the secondary hydroxyl groups. A larger cavity is formed in this manner and usually accommodates two guest molecules. The dimers always pack in layers and four different types of dimeric packing have been described, namely: channel, intermediate, screw channel and chessboard[50,68]. These four types of dimeric packing arrangements are illustrated in Figure 8. The two-dimensional hydrogen bond network involving the water molecules and the cyclodextrin hydroxyl groups, characteristic of all four classes, is divided into two sub-networks[69]. One is associated with the secondary hydroxyl groups of the host and therefore extends the intramolecular and intradimer hydrogen bond network while the other is associated with the primary hydroxyl groups of the host and links the layers of dimers via water molecules.

Monomeric β-cyclodextrin complexes have cage-type packing of the "herring-bone" variety, except for the 1,4-diazabicyclo[2.2.2]octane complex[70], which packs in layers, but, unlike the brick packing arrangement, the cyclodextrin cavity is not completely blocked off by the hosts above and below (Figure 9). Another exception is the 8:1 pyridine-β-CD complex, which also packs in layers and is less compact than both known monomeric and dimeric structures[71]. In this case, the guest molecules occupy not only the cyclodextrin cavity, but also the intermolecular space and there are few water molecules present since the compound was not crystallised from water. The cyclodextrin conformation in the monomeric packing arrangements seems to be slightly more distorted in comparison with that found in

the dimeric complexes, where the macrocyclic conformation is round and rather symmetrical. Closer packing is achieved in the monomeric herring-bone packing arrangement than in dimeric packing arrangements and it has been suggested for this reason that this arrangement is preferred with small guest molecules which do not protrude from the host cavity[47,50].

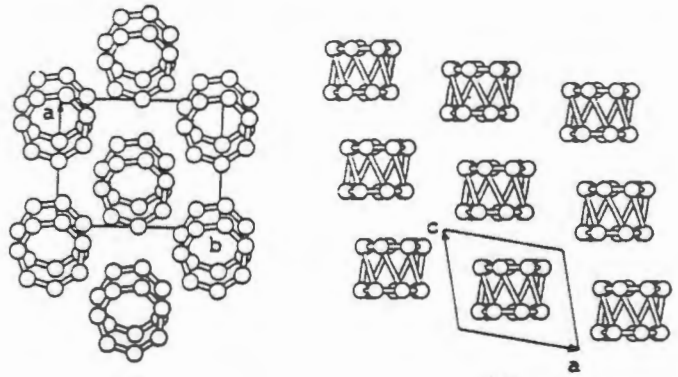

Projections of β-CD dimers for the channel packing mode. Each β-CD molecule is represented by its O(4) heptagon. (a) - Projection onto the average plane of the O(4) heptagon. The dimer is represented by one heptagon only. (b) - Projection along the *b*-axis.

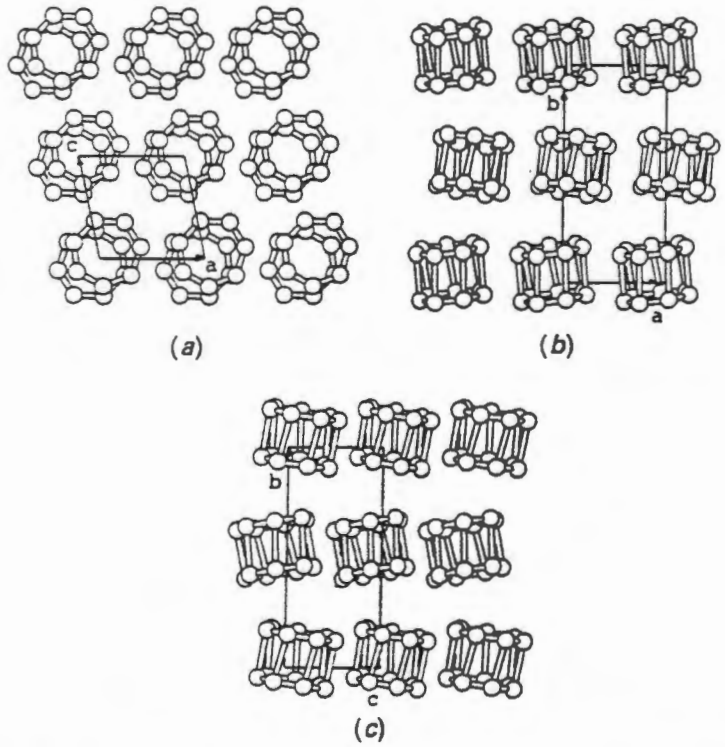

Projections of the β-CD dimers for the **screw channel** packing mode. Projections onto: (a) - the *ac*-plane (the dimer is represented by one heptagon only), (b) - the *ab*-plane, (c) - the *bc*-plane.

Figure 8 Dimeric packing arrangements observed in β-CD complexes (taken from reference 50).

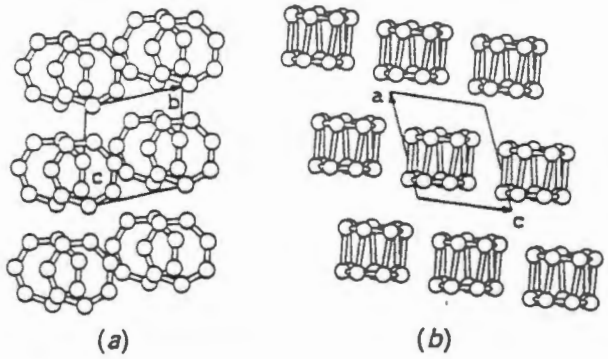

Projections of β-CD dimers for the **intermediate** packing mode. (a) - Projection onto the average plane of the O(4) heptagons. The dimer is represented by one heptagon only. (b) - Projection along the normal to the *ac*-plane.

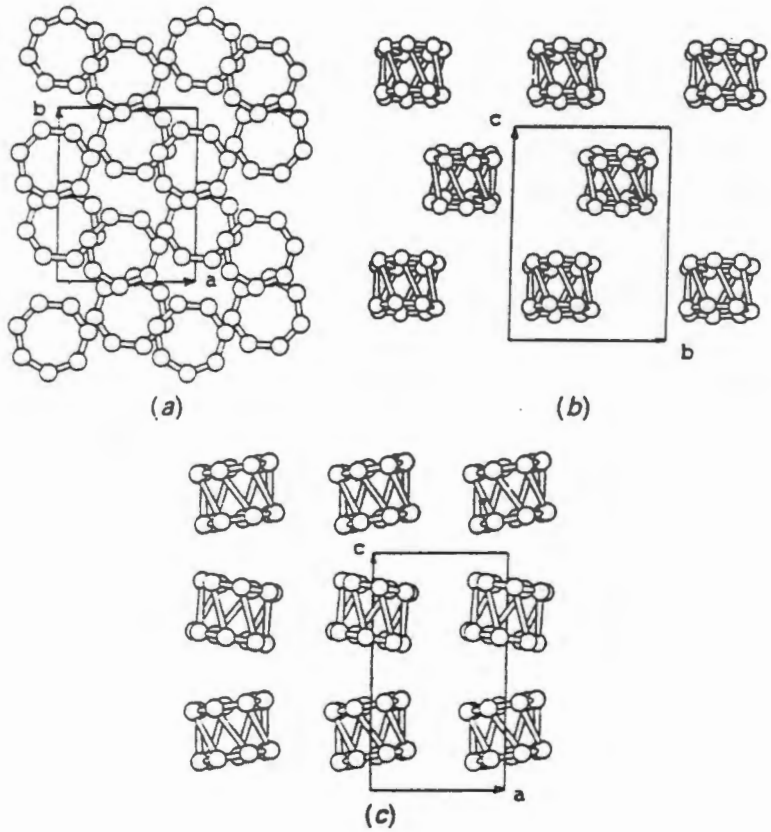

Projections of the β-CD dimers for the **chessboard** packing mode. Projections onto: (a) - the *ab*-plane (the dimer is represented by one heptagon only), (b) - the *bc*-plane, (c) - the *ac*-plane.

Figure 8 cont'd. Dimeric packing arrangements observed in β-CD complexes (taken from reference 50).

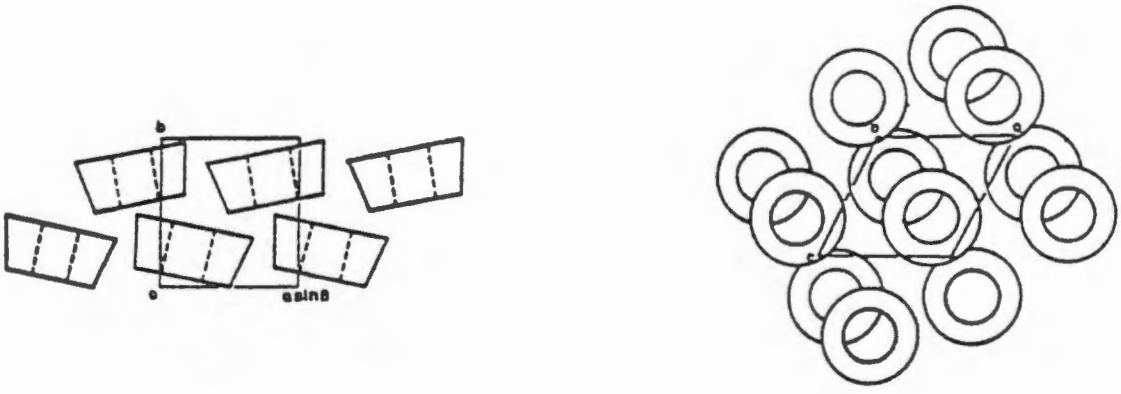

Figure 9 Schematic diagrams of the packing arrangement in the 1,4-diazabicyclo[2.2.2]octane-β-CD complex (taken from reference 70).

A "tetrameric" β-CD complex has been reported[72], in which there are two dimers in the asymmetric unit. However, atomic co-ordinates are not available.

Although the Cambridge Structural Database has unit cell parameters for nine DIMEB complexes, crystal co-ordinates are not available for the hydrate and two of the complexes. Therefore only six of the structures will be discussed[73,74,75,76,77]. One of these is the (15,22,dioxo-2,5,8,11,26,29,32,35-octaoxa-14,23-diaza(15.15.0)paracyclophane)-DIMEB catenane monohydrate[77], which because of the size of the "guest" does not permit packing in the "normal" way. Amongst the five remaining structures, there are 3 different types of packing, namely, channel type packing with head-to-tail stacking of the host molecules, but with adjacent columns antiparallel[73]; modified bricks in a wall type packing[75] like that of the 1,4-diazabicyclo[2.2.2]octane-β-CD complex[70]; and a modified herring-bone packing, where the cavity of the cyclodextrin is blocked on the O(2), O(3) side by an adjacent cyclodextrin, but is open to the intermolecular space at the O(6) side[74,76]. In two of the latter three complexes, the *p*-nitrophenol and *p*-iodophenol complexes[74], the guest is actually situated outside the cavity of the host molecule at the position where the host cavity is open to the intermolecular space and the cavity is occupied by water molecules (Figure 10). This packing arrangement is characterised by "self-inclusion" i.e. one of the cyclodextrin O(6) methoxy groups is included in the cavity of a screw-related host molecule at the O(2), O(3) side. Although the packing

arrangement for the host is very similar in the naphthoic acid complex[76], the guest is shifted so that it is half inserted in the host cavity at the O(6) side and the water molecules are found occupying the intermolecular space. In the carmofur complex[75], the guest is disordered over two sites. In the major site, a part of the guest is included in the host cavity, but in the minor site the guest occupies the intermolecular space. There is no explanation for the guest occupying the intermolecular space instead of the cyclodextrin cavity in some of the DIMEB complexes, except that perhaps the intermolecular space has a more hydrophobic character than the intermolecular spaces of the parent cyclodextrin because of the presence of the methyl groups[74]. The macrocyclic conformation of the host molecule is much the same as that of β-cyclodextrin because O(2)···H-O(3') intramolecular hydrogen bonding is present.

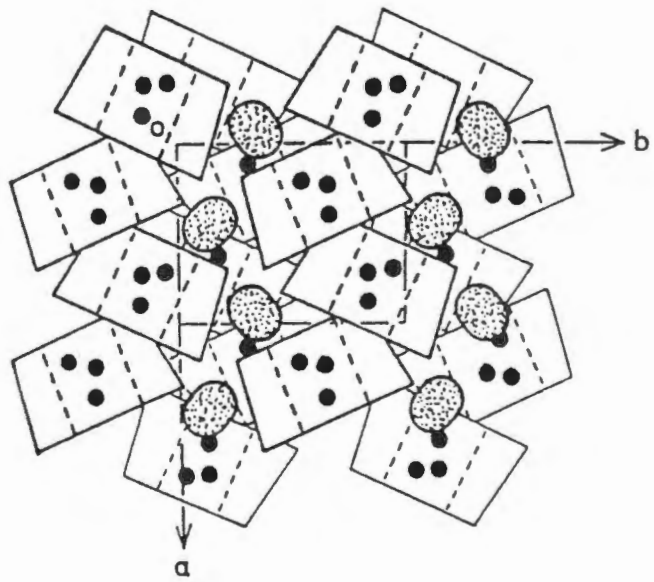

Figure 10 Packing arrangement in the iodophenol- and nitrophenol-DIMEB complexes (taken from reference 74).

Five of the six TRIMEB crystal structures found in the Cambridge Structural Database pack in screw channel mode in a head-to-tail fashion with the axes of the host molecules almost parallel to the *b*-axis and adjacent columns of complex units antiparallel[78,79,80,81]. In the sixth, that of the *m*-iodophenol-TRIMEB complex[80,82], the axis of the TRIMEB molecule makes an angle of 26.2° with the *b*-axis, resulting in more of a cage-type packing arrangement. As already

mentioned, one of the methylglucose residues in this complex adopts the $^{O}S_2$ twist conformation. Despite this, the authors note that the macrocyclic conformation of the host is similar to the conformation observed in the 4-biphenylacetic acid complex. In all of these structures, the host molecule is cup-shaped and five of the glucose residues have positive tilt angles, the two remaining having negative tilt angles i.e. with their O(6) sides tilted away from the centre of the CD cavity. In addition, the positive tilt angles are larger than those observed in complexes of native β-CD and this has been attributed to the host's inability to form intramolecular hydrogen bonds and to steric hindrance involving the methyl groups attached to O(3) which are directed towards the cavity in all TRIMEB structures[54]. The crystal structure of the uncomplexed host is not amongst the structures in the Cambridge Structural Database.

The γ-cyclodextrin hydrate[83] has a herring-bone packing arrangement like that of the β-cyclodextrin hydrate. However, there is closer contact between host molecules and two of the glucose residues have their primary hydroxyl sides partially inserted into the cavity of an adjacent cyclodextrin molecule at the secondary hydroxyl side. As in the β-cyclodextrin hydrate, some water molecules occupy the cavity of the host and the remaining water molecules are found in intermolecular spaces. The other five γ-cyclodextrin structures[84,85,86,87] all have the same packing arrangement, crystallising in the space group $P42_12$. It is a channel type packing arrangement, but differs from all the channel type packing arrangements in β-cyclodextrin, DIMEB and TRIMEB structures in that both head-to-head and head-to-tail packing is observed within each column of host molecules (Figure 11). The axes of the host molecules coincide with the crystallographic fourfold axis and therefore the asymmetric unit contains three one-quarter host molecules.

Molecular modelling

The number of theoretical studies on cyclodextrins and their complexes appearing in the literature has begun to increase relatively recently[88,89,90,91,92,93]. These involve a variety of computational approaches - molecular mechanics, molecular dynamics and molecular orbital calculations[94]. However, the results of these studies are of limited use in a solid state study since they are applicable *in vacuo* and the role of the solvent is often neglected.

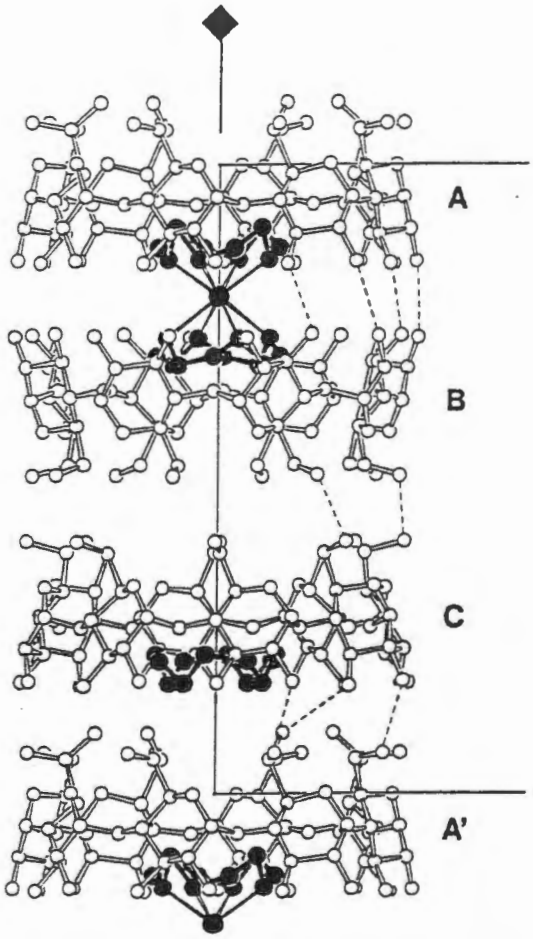

Figure 11 Channel packing arrangement in the 12-crown-4.LiSCN-γ-CD complex (taken from reference 85).

A molecular mechanics study of the conformation of native cyclodextrins[95] has revealed that conformations of lower energy than the rather symmetrical conformations observed in X-ray structures could be located by the removal of symmetry constraints. In another study, the dipole moments of α-CD and its guest, *p*-nitrophenol, were calculated separately using the conformations observed in the crystal structure of the complex[96]. A relatively large dipole moment of 13.5 D directed from the side of the secondary hydroxyl groups towards the side of the primary hydroxyl groups (at an angle of 27° to the host axis) was found for the host. A dipole moment of 5 D was calculated for the guest and the vectors of the dipole moments for host and guest were found to be almost antiparallel. The authors therefore propose that electrostatic effects could play an essential role in binding and determining the orientation of the guest in the host cavity.

Objectives of this study

Although there have been many reports of complexation of pharmaceuticals with cyclodextrins, both in solution and in the solid state, comparatively few crystal structures of pharmaceuticals complexed with cyclodextrins have been reported. Therefore, the main aim of this work was to take some of these drugs and attempt to grow single crystals of their inclusion complexes with the hosts β-cyclodextrin, DIMEB, TRIMEB and γ-cyclodextrin for crystal structure solution in order to shed light on the nature of the host-guest interactions and the mode of inclusion.

Amongst the drugs chosen were three non-steroidal anti-inflammatories (NSAIDs), diclofenac sodium, meclofenamate sodium and (S)-naproxen. They are all weak acids and are well known for their irritation of the mucosa of the gastrointestinal tract. It has already been demonstrated with another NSAID, piroxicam, that gastric irritation can be reduced by complexation of the drug with β-cyclodextrin. In addition, since diclofenac sodium and meclofenamate sodium are structural isomers, it is interesting to see whether there are differences in their interactions with a particular host molecule. The other guests which were chosen were sulfathiazole and (L)-menthol. Sulfathiazole is an anti-bacterial which has a rather low aqueous solubility. (L)-menthol is used in many pharmaceutical preparations since it has mild antipruritic and antibacterial properties.

Another aim was to characterise complexes by X-ray powder diffraction (XRD), thermogravimetric analysis (TG), differential scanning calorimetry (DSC) and UV spectrophotometry. In cases where crystal structures could be solved, powder patterns are calculated from the refined single crystal data. XRD patterns calculated from crystal structures are useful as standards for comparison when bulk preparation of inclusion complexes is desired in the pharmaceutical industry. TG and DSC can give information about water content and how tightly held different populations of water molecules are in the crystal structures. Since the water molecules in crystal structures are characterised by disorder and high thermal motion, it is difficult to locate them and therefore the crystal structure very often is not a true reflection of the water content. Attempts will also be made to reconcile the crystal structures which have been solved with the thermal analysis. For those complexes for which only unit cell parameters have been obtained, these methods are used to establish the stoichiometry of the complexes.

References

1. J. Szejtli, *Topics in Inclusion Science - Cyclodextrin Technology*, Chapter 1, Kluwer Academic Publishers, Dordrecht, The Netherlands, 1988.
2. W. Saenger, *Angew. Chem. Int. Ed. Engl.*, 1980, **19**, 344.
3. T. Fujiwara, N. Tanaka and S. Kobayashi, *Chem. Lett.*, 1990, 739.
4. I. Miyazawa, H. Ueda, H. Nagase, T. Endo, S Kobayashi and T. Nagai, *Eur. J. Pharm. Sci.*, 1995, **3**, 153.
5. T. Endo, H. Ueda, S. Kobayashi and T. Nagai, *Carb. Res.*, 1995, **269**, 369.
6. K-H. Frömming and J. Szejtli, *Topics in Inclusion Science - Cyclodextrins in Pharmacy*, Volume 5, Dordrecht, The Netherlands, Kluwer Academic Publishers, 1994.
7. R. Breslow, *Science*, 1982, **218**, 532.
8. I. Tabushi, *Acc. Chem. Res.*, 1982, **15**, 66.
9. M. Komiyama and H. Hirai, *J. Am. Chem. Soc.*, 1984, **106**, 174.
10. W. Saenger, *Inclusion Compounds*, ed. J. L. Atwood, J. E. D. Davies and D. D. MacNicol, 1984, Volume 2, Chapter 8, 231.
11. S. P. Jones, D. J. W. Grant, J. Hadgraft and G. D. Parr, *Acta Pharmaceutica Technologica*, 1984, **30**, 213.
12. K. Uekama and M. Otagiri, *Critical Reviews in Therapeutic Drug Carrier Systems*, 1987, **3**, 1.
13. D. W. Armstrong, T. J. Ward, R. D. Armstrong and T. E. Beesley, *Science*, 1986, **232**, 1132.
14. J. A. Hamilton and L. Chen, *J. Am. Chem. Soc.*, 1988, **110**, 5833.
15. J. A. Hamilton and L. Chen, *J. Am. Chem. Soc.*, 1988, **110**, 4379
16. K. Harata, K. Uekama, T. Imai, F. Hirayama and M. Otagiri, *J. Incl. Phenom.*, 1988, **6**, 443.
17. I. J. Colquhoun and B. J. Goodfellow, *J. Chem. Soc. Perkin Trans. 2*, 1994, 1803.
18. A. Brossi, *Medicinal Research Reviews*, 1994, **14**, 665.
19. A. W. Coleman, I. Nicolis, N. Keller and J. P. Dalbiez, *J. Incl. Phenom.*, 1992, **13**, 139.
20. J. Cohen and J. L. Lach, *J. Pharm. Sci.*, 1963, **52**, 132.
21. B. Casu, M. Reggiani and G. R. Sanderson, *Carb. Res.*, 1979, **76**, 59.
22. J. Szejtli, *J. Incl. Phenom.*, 1983, **1**, 135.
23. B. W. Müller and U. Brauns, *Int. J. Pharm.*, 1985, **26**, 77.

24. J. Pitha and J. Pitha, *J. Pharm. Sci.*, 1985, **74**, 987.
25. J. Szejtli, *J. Incl. Phenom.*, 1992, **14**, 25.
26. G. Wenz, *Angew. Chem. Int. Ed. Engl.*, 1994, **33**, 803.
27. *New Trends in Cyclodextrins and Derivatives*, edited by D. Duchene, Editions de Sante, Paris, France, 1991.
28. K. Harata, K. Uekama, M. Otagiri and F. Hirayama, *J. Incl. Phenom.*, 1984, **1**, 279.
29. K. Harata, *Inclusion Compounds*, Volume 5, Chapter 9, edited by J. L. Atwood, J. E. D. Davies and D. D. MacNicol, Oxford University Press, 1991.
30. R. J. Bergeron, *Inclusion Compounds*, Volume 3, Chapter 12, edited by J. L. Atwood, J. E. D. Davies and D. D. MacNicol, Oxford University Press, 1984.
31. T. Higuchi and K. A. Connors, *Adv. Anal. Chem. Instr.*, 1965, **4**, 117.
32. P. V. Demarco and A. L. Thakkar, *J. Chem. Soc., Chem. Commun.*, 1970, 2.
33. R. Fornasier, V. Lucchini, P. Scrimin and U. Tonnelato, *J. Incl. Phenom.*, 1986, **4**, 292.
34. S. Li and W. C. Purdy, *Anal. Chem.*, 1992, **64**, 1405.
35. P. Berthault and B. Perly, *Supramol. Chem.*, 1993, **2**, 225.
36. Z. Li, Q. Guo, T. Ren, X. Zhu and Y Liu, *J. Incl. Phenom.*, 1993, **15**, 37.
37. S. Divakar, *J. Incl. Phenom.*, 1993, **15**, 305.
38. M. C. Ramusino, L. Rufini and C. Mustazza, *J. Incl. Phenom.*, 1993, **15**, 359.
39. H. Shimizu, A. Kaito and M. Hatano, *Bull. Chem. Soc. Jpn.*, 1979, **52**, 2678.
40. H. Yamaguchi and M. Higashi, *J. Incl. Phenom.*, 1987, **5**, 725.
41. H. Yamaguchi, M. Higashi, J. Nakayama and M. Hoshino, *J. Incl. Phenom.*, 1990, **9**, 253.
42. M. Kodaka, *J. Am. Chem. Soc.*, 1993, **115**, 3702.
43. S. Hamai, T. Ikeda, A. Nakamura, H. Ikeda, A. Ueno and F. Toda, *J. Am. Chem. Soc.*, 1992, **114**, 6012.
44. P Job, *Ann. Chim.*, 1928, **9**, 113.
45. J. Huang, G. C. Catena and F. V. Bright, *Applied Spectroscopy*, 1992, **46**, 606.
46. L. Szente, J. Szejtli and M. Gal-Füzy, *J. Incl. Phenom.*, 1984, **2**, 631.
47. W. Saenger, *J. Incl. Phenom.*, 1984, **2**, 445.
48. *Cambridge Structural Database and Cambridge Structural Database System*, October 1995, Version 2.3.7, Cambridge Crystallographic Data Centre, University Chemical Laboratory, Cambridge, England.
49. K. Harata, F. Hirayama, H. Arima, K. Uekama and T. Miyaji, *J. Chem. Soc.,*

Perkin Trans. 2, 1992, 1159.

50. D. Mentzafos, I. M. Mavridis, G. Le Bas and G. Tsoucaris, *Acta Crystallog.*, 1991, B**47**, 746.
51. B. Hingerty, B. Klar, G. L. Hardgrove, C. Betzel and W. Saenger, *Journal of Biomolecular Structure and Dynamics*, 1984, *2*, 249.
52. C. Betzel, W. Saenger, B. E. Hingerty and G. M. Brown, *J. Am. Chem. Soc.*, 1984, **106**, 7545.
53. V. Zabel, W. Saenger and S. A. Mason, *J. Am. Chem. Soc.*, 1986, **108**, 3664.
54. K. Harata, K. Uekama, M. Otagiri anf F. Hirayama, *J. Incl. Phenom.*, 1984, **1**, 279.
55. T. Steiner and W. Saenger, *Carb. Res.*, 1994, **259**, 1.
56. T. Steiner and W. Saenger, *J. Am .Chem. Soc.*, 1992, **114**, 10146.
57. T. Steiner, *J. Chem. Soc., Chem. Commun.*, 1994, 2341.
58. T. Steiner and W. Saenger, *J. Am. Chem. Soc.*, 1993, **115**, 4540.
59. T. Steiner, G. Koellner, K. Gessler and W. Saenger, *J. Chem. Soc., Chem. Commun.*, 1995, 511.
60. T. Steiner and W. Saenger, *J. Chem. Soc., Chem. Commun.*, 1995, 2087.
61. K. Harata, *Bull. Chem. Soc. Jpn.*, 1979, **52**, 2451.
62. A. D. French and V. G. Murphy, *Carb. Res.*, 1973, **27**, 391.
63. K. Lindner and W. Saenger, *Angew. Chem. Int. Ed. Engl.*, 1978, **17**, 694.
64. K. Lindner and W. Saenger, *Carb. Res.*, 1982, **99**, 103.
65. T. Steiner, G. Koellner, S. Ali, D. Zakim and W. Saenger, *Biochem. Biophys. Res. Commun.*, 1992, **188**, 1060.
66. J. A. Ripmeester, *Supramol. Chem.*, 1993, **2**, 89.
67. T. Steiner and G. Koellner, *J. Am. Chem. Soc.*, 1994, **116**, 5122.
68. G. Le Bas and G. Tsoucaris, *Mol. Cryst. Liq. Cryst.*, 1986, **137**, 287.
69. G. Le Bas and G. Tsoucaris, *Supramol. Chem.*, 1994, **4**, 13.
70. K. Harata, *Bull. Chem. Soc. Jpn.*, 1982, **55**, 2315.
71. C. de Rango, P. Charpin, J. Navaza, N. Keller, I. Nicolis, F. Villain and A. W. Coleman, *J. Am .Chem. Soc.*, 1992, **114**, 5475.
72. J. Vicens, T. Fujiwara and K. Tomita, *J. Incl. Phenom.*, 1988, **6**, 577.
73. M. Czugler, E. Eckle and J. J. Stezowski, *J. Chem. Soc.*, Chem. Commun., 1981, 1291.
74. K. Harata, *Bull. Chem. Soc. Jpn.*, 1988, **61**, 1939.
75. K. Harata, F. Hirayama, K. Uekama and G. Tsoucaris, *Chem. Lett.*, 1988,

1585.

76. K. Harata, *J. Chem. Soc., Chem. Commun.*, 1993, 546.
77. D. Armspach, P. R. Ashton, C. P. Moore, N. Spencer, J. F. Stoddart, T. J. Wear and D. J. Williams, *Angew. Chem. Int. Ed. Engl.*, 1993, **32**, 854.
78. K. Harata, K. Uekama, M. Otagiri anf F. Hirayama, *Bull. Chem. Soc. Jpn.*, 1983, **56**, 1732.
79. K. Harata, K. Uekama, T. Imai, F. Hirayama and M. Otagiri, *J. Incl. Phenom.*, 1988, **6**, 443.
80. K. Harata, F. Hirayama, H. Arima, K. Uekama and T. Miyaji, *J. Chem. Soc., Perkin Trans. 2*, 1992, 1159.
81. D. Mentzafos, I. M. Mavridis and H. Schenk, *Carb. Res.*, 1994, **253**, 39.
82. K. Harata, *J. Chem. Soc., Chem. Commun.*, 1988, 928.
83. K. Harata, *Bull. Chem. Soc. Jpn.*, 1987, **60**, 2763.
84. S. Kamitori, K. Hirotsu and T. Higuchi, *J. Chem. Soc., Chem. Commun.*, 1986, 690.
85. S. Kamitori, K. Hirotsu and T. Higuchi, *J. Am. Chem. Soc.*, 1987, **109**, 2409.
86. S. Kamitori, K. Hirotsu and T. Higuchi, *Bull. Chem. Soc. Jpn.*, 1988, **61**, 3825.
87. J. Ding, T. Steiner and W. Saenger, *Acta Cryst.*, 1991, B**47**, 731.
88. M. J. Sherrod, *Carb. Res.*, 1989, **192**, 17.
89. D. Wouessidjewe, A. Crassous, D. Duchene, A. Coleman, N. Rysanek, G. Tsoucaris, B. Perly and F. Djedaini, *Carb. Res.*, 1989, **192**, 313.
90. M. E. Amato, F. Djedaini-Pilard, B. Perly and G. Scarlata, *J. Chem. Soc., Perkin Trans. 2*, 1992, 2065.
91. M. E. Amato, G. C. Pappalardo and B. Perly, *Magnetic Resonance in Chemistry*, 1993, **31**, 455.
92. N. S. Bodor, M. Huang and J. D. Watts, *J. Pharm. Sci.*, 1995, **84**, 330.
93. Ch. Th. Klein, G. Köhler, B. Mayer, K. Mraz, S. Reiter, V. Viernstein and P. Wolschann, *J. Incl. Phenom.*, 1995, **22**, 15.
94. M. J. Sherrod, *Topics in Inclusion Science - Spectroscopic and Computational Studies of Supramolecular Systems*, Volume 4, Edited by J. E. D. Davies, Dordrecht, The Netherlands, Kluwer Academic Publishers, 1992.
95. K. B. Lipkowitz, *J. Org. Chem.*, 1991, **56**, 6357.
96. M. Kitagawa, H. Hoshi, M. Sakurai, T. Inoue and R. Chujo, *Carb. Res.*, 1987, **163**, C1

Chapter 2 Materials and Methods

Host Compounds

β-cyclodextrin was obtained from Chinoin-Reanal, Hungary and Sigma Chemical Company, U.S.A. γ-cyclodextrin, heptakis(2,6-di-O-methyl)-β-cyclodextrin (DIMEB) and heptakis(2,3,6-tri-O-methyl)-β-cyclodextrin (TRIMEB) were obtained from Cyclolab, Hungary. All were used as received.

Guest Compounds

Sulfathiazole (Aldrich Chemical Company, U.S.A.), diclofenac sodium (Syntex, U.S.A.), meclofenamate sodium (Sigma Chemical Company, U.S.A.), (*S*)-naproxen (Syntex, U.S.A.) and (*L*)-menthol (Sigma Chemical Company, U.S.A.) were used as received.

Crystal Growth

Crystals were always obtained by dissolving host and guest in a known molar ratio in distilled water and using common crystallisation techniques such as slow evaporation and slow cooling. More detailed methods shall be described in individual cases. Cosolvents such as methanol, ethanol, propanol and acetone were also used, but this was generally not successful because of competition of the cosolvent with the guest for the host cavity.

Hot stage microscopy

One of the most reliable methods for preliminary testing of putative cyclodextrin-drug inclusion complexes was the observation of thermal events on a Linkam TH600 hot stage mounted on a Nikon microscope with camera attached. The temperature was controlled using a Linkam CO600 temperature controller. Crystals of the relevant host and guest alone were often observed simultaneously with the inclusion complex.

Density Measurement

Density was measured using two miscible organic solvents of differing density such that the density of the inclusion complex was expected to fall between the two. A few crystals of good quality were chosen and immersed in the solvent of lower density. The solvent of higher density was then added in small amounts until the density of the solvent mixture was equal to that of the crystals i.e the crystals neither sank to the bottom nor floated to the top, but remained suspended in the solvent mixture. The density of the solvent mixture was then measured with a Paar DMA35 digital density meter. The procedure was performed in triplicate and reported values given as the mean of the three values. Solvent pairs used were either chloroform and toluene or benzene and carbon tetrachloride. Densities of DIMEB and TRIMEB complexes were not measured because of the high solubility of these host compounds in both aqueous solutions and organic solvents.

Thermal Analysis

Thermogravimetric (TG) and differential scanning calorimetric (DSC) traces were recorded on a Perkin-Elmer PC7-Series Thermal Analysis System at a scanning rate of $10°min^{-1}$ (unless otherwise stated) under N_2 gas-purge with a flow rate of 30 $ml.min^{-1}$. Temperature ranges over which traces were recorded were generally 30 - 300°C for β-CD and γ-CD complexes, 30 - 360°C for the DIMEB complex and 30 - 200°C for TRIMEB and its complexes. Sample masses were of the order of 5-10 mg, except in cases where vigorous foaming of the melt resulted in unsatisfactory traces, in which case smaller masses were used. Samples for TG were placed in an open platinum pan while those for DSC were placed in a crimped, vented aluminium pan with an empty pan used as reference . The TG analyser was calibrated using built-in procedures for furnace and weight calibration. The Curie points for alumel (163°C) and perkalloy (596°C) were also used to calibrate the furnace. The DSC analyser was calibrated using the melting points of indium (156.4°C) and zinc (419.5°C) and the enthalpy of melting of indium (28.5 $J.g^{-1}$). The temperature ranges over which weight loss occurs in the TG traces are given in each case. The temperature given as marking the termination of a weight loss is the temperature at which the derivative of the TG trace returns to baseline (i.e. zero). The onset and peak temperatures as well as temperature ranges for the exotherms and endotherms observed in the DSC traces have been tabulated in most cases. In

the absence of a table, the onset temperature at least is quoted.

UV Spectrophotometry

UV spectra were recorded on a Philips PU8700 series UV/visible spectrophotometer. Samples were dissolved in distilled water. Calibration curves at the appropriate λ_{max} were set up for the relevant drugs in concentration ranges such that the absorbance range fell between zero and one. Correlation coefficients and λ_{max} values used are quoted in the relevant chapters. Solutions of the complexes were then made in distilled water, the absorbance was measured at the appropriate λ_{max} and the concentration of the drug was estimated from its calibration curve. The percentage by weight of the drug in the complex could then be calculated and the water content of the complex was known from thermogravimetric analysis. The remaining weight was then assumed to be the host and the stoichiometry of guest:host could be calculated. The effect of the host on the UV absorbance spectrum of the guests in the concentration ranges used and at ratios of guest:host close to unity was tested and found to be negligible (i.e. no significant shift in λ_{max} or change in absorbance values). Therefore the calibration curve set up for the guest alone in distilled water was also a sufficiently accurate reflection of the concentration of the guest in the presence of the host. The sulfathiazole-β-CD, diclofenac sodium-β-CD and naproxen-TRIMEB complexes, for which the stoichiometries were known to be 1:1 because the crystal structures had been solved in this study, were then used as standards for further verification of the reliability of the method. This method could not be used for the menthol complexes because menthol does not absorb in the UV range and therefore NMR had to be used.

Nuclear Magnetic Resonance Spectroscopy

^1H nuclear magnetic resonance spectra were recorded at 25°C in D_2O on a Varian Unity 400 MHz spectrometer using sodium 2,2-dimethylsilapentane-5-sulphonate (DSS) as internal reference.

Microanalysis

C, H, N (where appropriate) and S (where appropriate) elemental analyses were

performed in duplicate on a Carlo Erba elemental analyser Model 1106. Samples were not weighed under vacuum as this could have resulted in loss of water of crystallisation. Loss of even one water molecule per complex unit in most cases could lead to a difference of more than 0.3% in the calculated percentage of carbon in the complex.

X-ray Powder Diffraction (XRD)

X-ray powder diffraction patterns were obtained using a Philips PW1050/80 goniometer with Ni-filtered CuKα radiation (λ = 1.5418 Å). The sample was lightly ground, but not sieved (as this could lead to loss of water molecules of crystallisation) and packed in an Al sample holder. Step scans (0.1° 2θ, 2s counting times) were performed from 6 to 32° 2θ. Automatic receiving and divergence slits were used. For each crystal structure determined in this study, space group data, refined unit cell parameters, atomic coordinates and thermal parameters were used as input to the program LAZY PULVERIX[1] in order to generate an idealised X-ray powder pattern. Such a pattern is regarded as the best representation of the pure phase[2]. The purity of a laboratory sample of the phase can be conveniently assessed by comparison of its experimental XRD pattern with the idealised pattern.

Crystal Structure Analysis, Solution and Refinement

Preliminary unit cell parameters and space groups were established by X-ray photography for all inclusion complexes of which sufficiently good quality crystals had been grown. Oscillation, Weissenberg, Cone-axis, de Jong-Bouman and Buerger precession photographs were taken on Stoë goniometers using Ni-filtered CuKα radiation.

Attempts were then made to optimise the crystallisation conditions for each complex to obtain crystals of the highest possible quality for intensity data collection. Crystals were chosen for data collection on the basis of size (approximately equal length in all dimensions) and their ability to extinguish plane polarised light uniformly. In a few cases it was necessary to cleave crystals to an appropriate size because they were plate-like or needle-shaped and therefore always much shorter in at least one dimension. Crystals were generally mounted in Lindemann capillaries (0.3 or 0.5 mm diameter - see Figure 1) either because they

were unstable or, in the case of the TRIMEB complexes, because they dissolved in the cyanoacrylate glue and therefore could not be glued to glass fibres. The exception was the sulfathiazole-β-cyclodextrin complex, which was exceptionally stable out of mother liquor at room temperature. The latter was mounted on the end of a thin glass rod for data collection. Some crystals were mounted in Lindemann capillaries without mother liquor while others required complete immersion in mother liquor. The (*L*)-menthol-β-cyclodextrin complex, which was particularly unstable out of mother liquor (developing cracks within seconds of being dried), was mounted in a capillary which had been filled with quick-setting cyanoacrylate glue. Many attempts were made at mounting this complex before a satisfactory result was achieved. The ends of the capillaries were either heat-sealed or sealed with sealing wax.

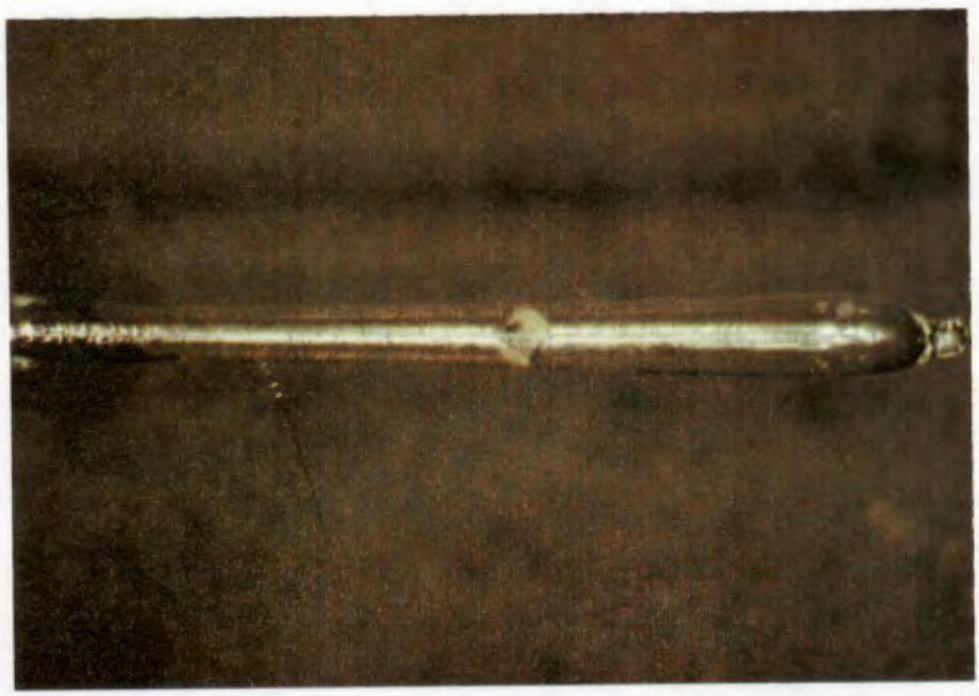

Figure 1 A single crystal of the diclofenac sodium-β-cyclodextrin complex mounted in a Lindemann capillary (15 X).

Reflection intensities were collected on an Enraf-Nonius CAD-4 diffractometer using graphite-monochromated MoKα radiation (λ = 0.71069 Å). Accurate cell dimensions were obtained by least-squares analysis of the setting angles of 24 reflections in the range $16° \leq \theta \leq 17°$. Intensity data were collected by the ω-2θ or ω-scan techniques to $(\sin\theta/\lambda)_{max}$ = 0.595 $Å^{-1}$. For low-temperature data collections, air was compressed and passed through a drying unit before being cooled by an FTS Systems Air Jet refrigeration unit (model XR-85-1). The crystal was therefore cooled by a constant stream of cold air with a flow rate of 20 $l.min^{-1}$. Temperatures lower than the dew point, which was -50°C, could not be attained. Three standard reflections were checked periodically (usually every 60 min) during data collection to detect any crystal decay and orientation control was performed after every 200 measured reflections. Data were corrected for Lorentz-polarisation effects and linear decay corrections were applied if crystal decay was significant. In the case of the sulfathiazole-β-cyclodextrin complex, data were corrected for absorption although it was not strictly necessary. Azimuthal scans for nine reflections with χ near 90° were recorded in order to measure the effect of crystal orientation on the reflection intensity. Absorption corrections were then made with program EAC[3]. The μR_{min} values (linear absorption coefficient multiplied by the minimum radius of the particular crystal specimen) for all the compounds ranged from 0.021 to 0.036 and those of μR_{max} from 0.032 to 0.074. Absorption correction factors (A^*) for any μR value in the range μR_{min} to μR_{max} was constant with increasing θ and for constant θ the A^* values for μR_{min} and μR_{max} never differed by more than approximately 7% (in most cases it was lower). Therefore absorption corrections were deemed unnecessary.

Crystal structures were solved either by direct methods using programs SHELX86[4] and SIR92[5] or by isomorphous replacement, using published co-ordinates for the skeleton cyclodextrin atoms of an isomorphous complex. Refinement was by block-diagonal (SHELX76[6], minimisation of $\Sigma w||F_o| - |kF_c||^2$) or full-matrix (SHELX93[7], minimisation of $\Sigma(w(F_o^2 - kF_c^2))$) least-squares techniques. The R-factor, which is a measure of the agreement between the calculated (based on the model) and observed structure factors, was calculated as follows:

SHELX76:

$$R = \Sigma(|F_o| - |F_c|)/\Sigma(|F_o|)$$

$$Rw = \Sigma(w^{\frac{1}{2}}(|F_o| - |F_c|)/\Sigma(w^{\frac{1}{2}}|F_o|))$$

where $w = [\sigma^2(F_o) + gF_o^2]^{-1}$

SHELX93:

$R1$ = Same as R in SHELX76 for comparison

$$wR2 = [\Sigma(w(F_o^2 - F_c^2)^2/\Sigma(w(F_o^2)^2)]^{\frac{1}{2}}$$

$$\text{where } w = [\sigma^2(F_o)^2 + (aP)^2 + (bP)]^{-1}$$

$$P = (\max(F_o^2,0 + F_c^2)/3)$$

The terms g, a and b in the above weighting schemes were chosen to yield constant distributions of $\Sigma w(\Delta F)^2$ with $\sin\theta$ and $(F_o/F_{max})^{\frac{1}{2}}$. Further details of structure solution and refinement are tabulated under individual structures.

Molecular parameters with esds were calculated with programs PARST[8] and SHELX93. Molecular and packing diagrams were drawn with PLUTO[9]. Atomic coordinates, bond lengths, bond angles, torsion angles and structure factor tables have been recorded on the two stiffy discs supplied on the inside back cover of the thesis. The information has been recorded in two different ways. The files with the extension, **.doc**, are files generated by the word processing package MSWORD (version 5.0) and can be read by any word processing package capable of importing MSWORD files. Alternatively, files have been saved as text files with the extension, **.tex**, and can be read by a modern DOS editor.

References

1. K. Yvon, W. Jeitschko and E. Parthe, *J. Appl. Crystallog.*, 1977, **10**, 73.
2. I. Bar and J. Bernstein, *J. Pharm. Sci.*, 1985, **74**, 255.
3. *Enraf-Nonius: Structure Determination Package*, Enraf-Nonius, Delft, The Netherlands, 1979.
4. G. M. Sheldrick, *Crystallographic Computing*, edited by G. M. Sheldrick, C. Kruger and R. Goddard, Oxford University Press, 1985, Volume 3, 175.
5. M. C. Burla, M. Camalli, G. Cascarano, C. Giacovazzo, G. Polidori, R. Spagna and D. Viterbo, *J. Appl. Crystallog.*, 1989, **22**, 389.
6. G. M. Sheldrick, *SHELX76*, Program for crystal structure determination, University of Cambridge, England, 1976.
7. G. M. Sheldrick, *J. Applied Crystallog.*, in preparation
8. M. Nardelli, *Comput. Chem.*, 1983, **7**, 95.
9. W. D. S. Motherwell, *PLUTO89*, program for plotting molecular and crystal structures, University of Cambridge, England, 1989.

Chapter 3 Sulfathiazole

Introduction

Sulfathiazole is one of a group of drugs with bacteriostatic properties referred to as the sulfonamides. It is a sparingly water-soluble drug, which exerts its bacteriostatic effect by blocking folic acid synthesis. The structure, together with the numbering scheme used in the crystal structure analysis, is shown in Figure 1. The sulfonamides are often administered as mixtures in particular ratios as it has been found that they display additive mutual solubilisation and in so doing not only enhance the bioavailability of the drug, but also reduce the incidence of crystalluria[1]. Sulfathiazole has also been investigated on account of its ability to crystallise in a number of polymorphic forms[2,3,4]. This has obvious applications in that different polymorphs of a particular compound often have significantly different dissolution rates[5].

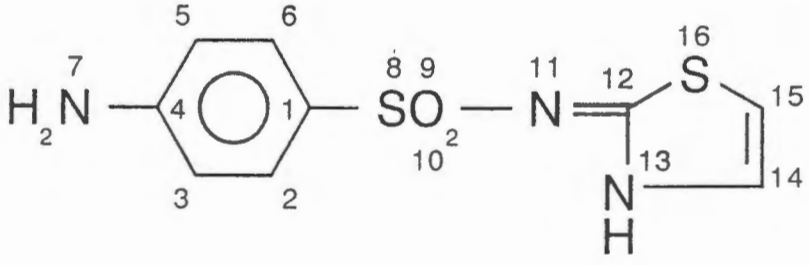

Figure 1 Sulfathiazole

The sulfonamides are therefore good candidates for complexation with the cyclodextrins and various studies have been carried out on their inclusion by cyclodextrins in aqueous media and in the solid state[6,7,8,9]. These studies have reported proposals on the mode of inclusion, values for stability constants as well as the stoichiometry in solution[7,8,9]. The stability constant for the sulfathiazole-β-cyclodextrin complex in solution (reported as 1860 M^{-1} in 0.1 M phosphate buffer at pH 3 by the HPLC method, 1800 M^{-1} in distilled water by the solubility method and 1650 M^{-1} in 0.1 M phosphate buffer at pH 7 by the UV method[8,9]) has been found to be higher than those of other sulfonamide-β-cyclodextrin complexes and in view of the lack of structural data for such complexes[10], a solid state complex of sulfathiazole with β-cyclodextrin has been crystallised and characterised and the structure solved by X-ray diffraction methods.

Preparation of the CD complex

Crystals of the sulfathiazole-β-cyclodextrin complex, which are prismatic and colourless (Figure 2), were prepared by stirring 0.18 mmol of sulfathiazole and 0.16 mmol of β-cyclodextrin in 18ml of distilled water at 70°C until both had dissolved and the volume had reduced to approximately 10 ml. The solution was allowed to cool spontaneously and left at room temperature for 24 to 48 hours in which time good single crystals grew (Figure 2).

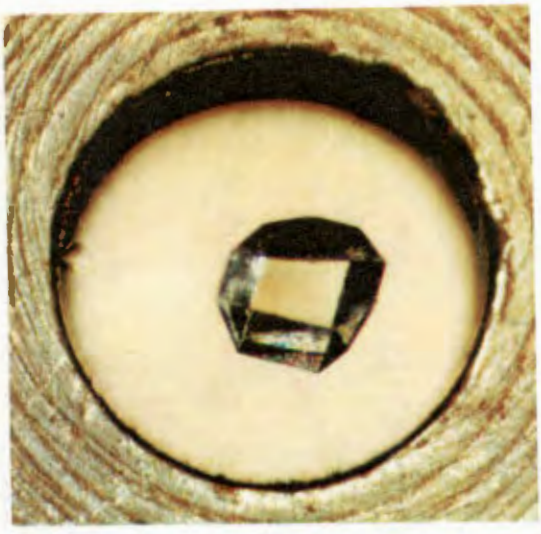

Room temperature (24 X)

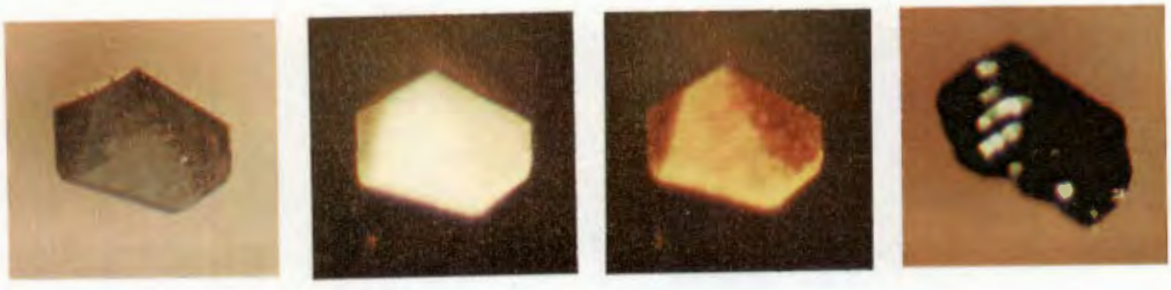

70°C 100°C 230°C 285°C

Magnification: 73 X

Figure 2 Sulfathiazole-β-cyclodextrin complex (SULFB)

Hot stage microscopy

Figure 2 also shows SULFB at various temperatures on the hot stage microscope. The initially clear crystal becomes opaque as water molecules of crystallisation are lost and the dehydrated complex begins to turn brown as decomposition commences at approximately 230°C. By 285°C, the complex is completely black and has expanded slightly, but there is no clear melting point.

Thermal analysis

TGA (Figure 3) of the complex shows a loss of 9.7 weight % between 30 and 130°C, corresponding to the loss of 8.3 water molecules of crystallisation for a 1:1 sulfathiazole-β-cyclodextrin complex, followed by onset of decomposition at about 250°C. The DSC trace shows three endothermic peaks, A, B and C, with onset temperatures of 80, 224, and 253°C respectively. The first is associated with loss of water while the second and third correspond to a phase change of the dehydrated complex followed by melting with concomitant decomposition.

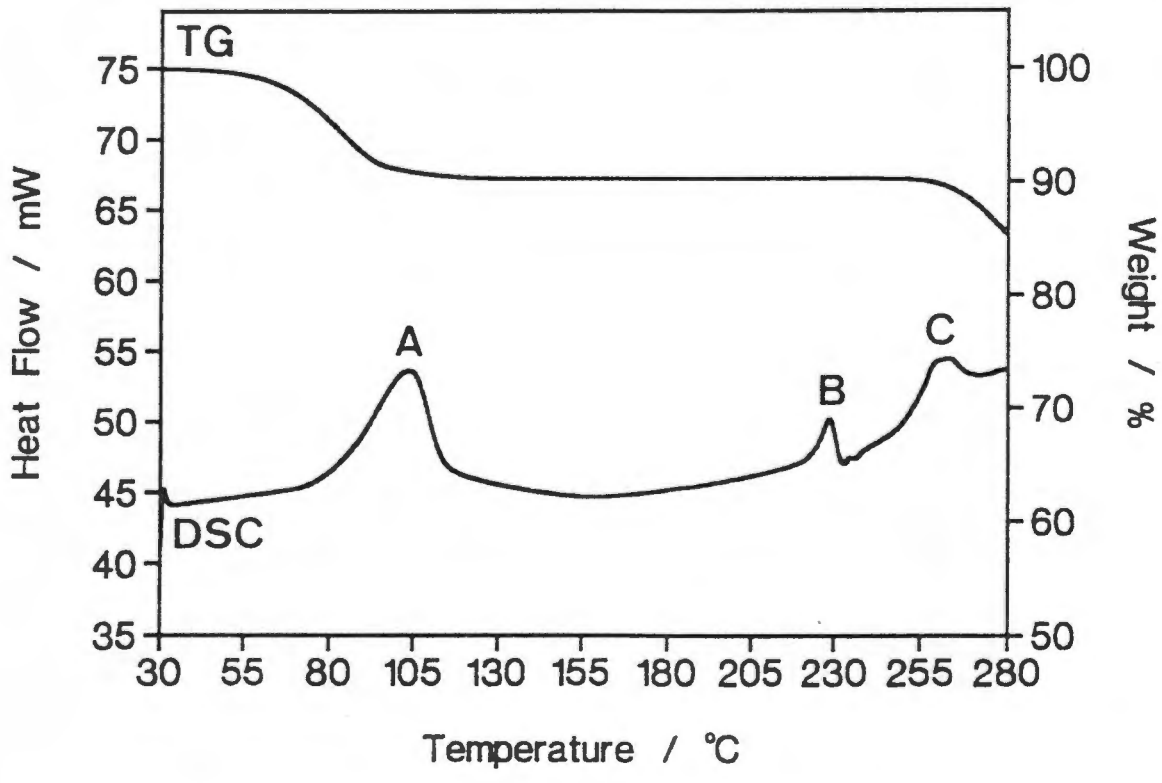

Figure 3 TG and DSC traces for SULFB.

Microanalysis

The results of the elemental analysis are given as the average of duplicate determinations. The calculated values are for a 1:1:8.3 sulfathiazole:β-cyclodextrin:H_2O complex and the water content is based on the thermogravimetric analysis result. The molecular formula is:

$$C_{42}H_{70}O_{35}.C_9H_9N_3S_2O_2.8.3H_2O$$

	Calculated (%)	Experimental (%)
Carbon	39.78	39.97
Hydrogen	6.26	6.23
Nitrogen	2.73	2.60
Sulphur	4.16	4.02

Crystal structure solution

The numbering scheme for the host is given in Figure 4. The structure was solved using published co-ordinates for the non-hydrogen cyclodextrin atoms (excluding the primary hydroxyl oxygen atoms) of the isomorphous 1,4-diazabicyclo[2.2.2]octane-β-cyclodextrin complex[11]. The *y* co-ordinate of atom C(1G1) was fixed (space group $P2_1$) and the resulting difference Fourier map revealed all but one of the non-hydrogen atoms of the guest and some of the primary hydroxyl oxygen atoms. The remaining non-hydrogen atoms, including those of eight water molecules, were located on subsequent difference Fourier maps during isotropic refinement by full-matrix least-squares techniques[12]. Many cyclodextrin hydrogen atoms were found and therefore all cyclodextrin hydrogen atoms linked to carbon atoms were inserted at idealised positions with C-H = 1.00 Å. All the hydrogen atoms of each glucose residue were assigned common variable isotropic temperature factors. At this stage all non-hydrogen atoms were assigned anisotropic temperature factors and further refinement was carried out by the block-diagonal least-squares method, ensuring adequate simultaneous refinement of different parts of the model. All of the cyclodextrin hydroxyl hydrogens except one were found and allowed to refine subject to a distance constraint (O-H = 1.00 Å, σ = 0.05 Å). All the hydrogens attached to carbons on the guest were inserted at idealised positions and the hydrogens attached to the nitrogens were located and allowed to refine with a distance constraint (N-H = 1.00 Å, σ = 0.05 Å). The hydrogen atoms of the guest

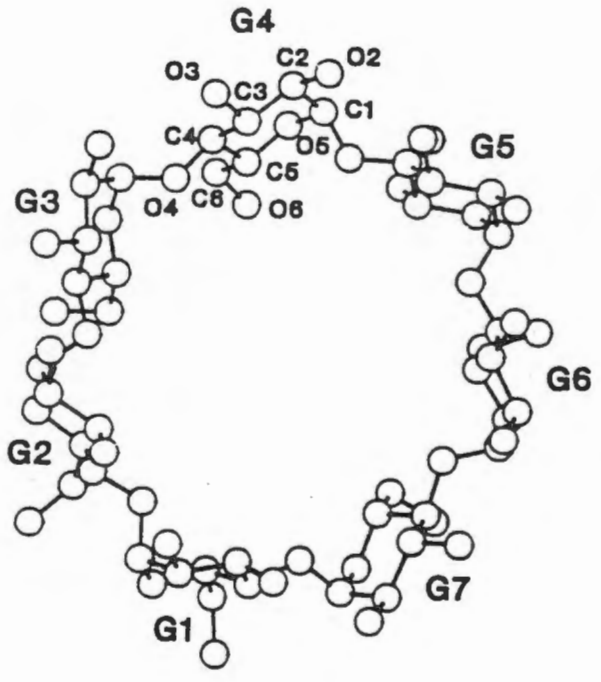

Figure 4 Numbering scheme for the host in SULFB

were assigned a common variable isotropic temperature factor. The hydrogen atoms of all the water molecules, except O(8W), were also found and refined in a similar manner with a common fixed temperature factor (U_{iso} = 0.1 $Å^2$). Thermogravimetric analysis of the complex consistently gave a weight loss which corresponded to 8.3 water molecules. The isotropic temperature factor of O(8W) had been relatively high prior to anisotropic refinement, indicating possible disorder, and there were two additional peaks on the difference Fourier map of significantly higher electron density than the rest. These were therefore inserted as water molecules O(9WA) and O(9WB) and their site occupancy factors were refined along with that of O(8W). The site occupancy factors were 0.7, 0.3 and 0.3 for atoms O(8W), O(9WA) and O(9WB) respectively, giving a total of 8.3 water molecules in the asymmetric unit, in good agreement with the TG results. The hydrogen atoms of these three water molecules of fractional site occupancy were not located.

Crystal structure

Crystal data, refinement and experimental parameters are shown in Table 1.

Table 1 Crystal data, experimental and refinement parameters for SULFB (structure refined on F using SHELX76)

Molecular formula	$C_{42}H_{70}O_{35}.C_9H_9N_3S_2O_2.8.3H_2O$
M_r (g.mol^{-1})	1539.83
Crystal system	Monoclinic
Space group	$P2_1$
Z	2
a (Å)	15.264(4)
b (Å)	16.500(6)
c (Å)	15.559(5)
β (°)	117.29(3)
V (Å^3)	3483(2)
D_m (g.cm^{-3})	1.46(1)
D_c (g.cm^{-3})	1.469
μ (Mo Kα) (cm^{-1})	1.76
F(000)	1634
Crystal dimensions (mm)	0.28 x 0.31 x 0.41
Temperature of dat coll.	294K
Range scanned θ (°)	$1 \leq \theta \leq 25$
Scan type	ω-2θ
Index range	h 0,18: k 0,19: l -18,18
Scan width (°)	0.8 + 0.35 tanθ
Aperture width (mm)	1.12 + 1.05 tanθ
Std reflections monitored for decay	-11,6,7 -5,1,12 -6,10,7
Decay (%)	0.3
No. of reflections collected	6603
No. of unique reflections	5690
R_{int}	0.081
No. of reflections with I > 2σ(I)	4706

cont'd

Table 1 cont'd

No. of L.S. parameters	980
R	0.061
wR	0.061
w	$[\sigma^2(F_o) + 2.20 \times 10^{-4} F_o^2]^{-1}$
S	6.34
Shift/e.s.d. max, average	0.451, 0.003
$\Delta\rho_{max}$ final (e.Å^{-3})	0.38
$\Delta\rho_{min}$ final (e.Å^{-3})	-0.41
Absorption correction factor range	0.8903 - 0.9992

Figure 5 is a stereoview of the SULFB complex. All seven α-D-glucose moieties of the β-cyclodextrin molecule are in the $^4C_1$ chair conformation. The primary hydroxyl groups are in the (-)-*gauche* conformation[13] except for that of the G4 residue, which is in the (+)-*gauche* conformation, owing to hydrogen bonding from O(2G2) to O(6G4). Furthermore, O(6G4) is within hydrogen bonding distance of O(9WB). The conformation of the macrocycle is maintained by intramolecular O(2)···O(3') hydrogen bonding as in β-cyclodextrin hydrate[14] and other β-cyclodextrin complexes[13]. However, O(2G3) and O(3G4) are 3.1 Å apart compared with a range of 2.75 - 2.85 Å for all the other O(2)···O(3') distances. This is due to the relatively large tilt angles of G3 and G4 with their secondary hydroxyl groups inclined away from the cavity. The G7 residue also has a relatively large tilt angle with its secondary hydroxyl groups inclined away from the cavity. The large tilt angles of these glucose residues are explained by the elliptical distortion of the cyclodextrin molecule induced by complexation with sulfathiazole.

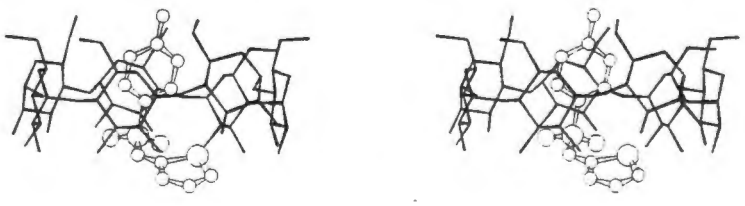

Figure 5 Stereoview of the SULFB complex viewed perpendicular to the axis of the host.

Table 2 lists values for the O(4)···O(4')···O(4") angles of the O(4) heptagon, radii of the O(4) heptagon, O(4)···O(4') distances, tilt angles and the deviation of each O(4) atom from the least-squares plane through the seven O(4) atoms. Comparison of radii, O(4)···O(4') distances and tilt angles of the sulfathiazole-β-cyclodextrin complex with those of the isomorphous 1,4-diazabicyclo[2.2.2]octane-β-cyclodextrin complex[11] shows that the cyclodextrin molecule is relatively more distorted by sulfathiazole as guest because the radii and O(4)···O(4') distances are spread over larger ranges and the tilt angles are larger.

Table 2 Geometrical data for β-cyclodextrin.

i. Glycosidic oxygen angle(°) and radius (Å) of the O(4) heptagon (measured from the centre of gravity of seven O(4) atoms to each O(4) atom).

O(4G7)···O(4G1)···O(4G2)	124.3	G1	5.14
O(4G1)···O(4G2)···O(4G3)	125.8	G2	5.08
O(4G2)···O(4G3)···O(4G4)	133.1	G3	4.81
O(4G3)···O(4G4)···O(4G5)	125.9	G4	5.09
O(4G4)···O(4G5)···O(4G6)	126.5	G5	5.17
O(4G5)···O(4G6)···O(4G7)	127.9	G6	4.97
O(4G6)···O(4G7)···O(4G1)	133.8	G7	4.79
Average	128.2	Average	5.01

ii. O(4)···O(4') distance (Å) and tilt angle (°).

O(4G1)···O(4G2)	4.25	G1	8.3
O(4G2)···O(4G3)	4.40	G2	3.9
O(4G3)···O(4G4)	4.48	G3	25.7
O(4G4)···O(4G5)	4.34	G4	19.6
O(4G5)···O(4G6)	4.29	G5	7.0
O(4G6)···O(4G7)	4.48	G6	3.0
O(4G7)···O(4G1)	4.25	G7	26.1
Average	4.36	Average	13.4

cont'd

Table 2 cont'd

iii. Deviations of O(4) atoms (Å) from the least-squares plane through the seven O(4) atoms.

O(4G1)	O(4G2)	O(4G3)	O(4G4)	O(4G5)	O(4G6)	O(4G7)
0.320(5)	0.300(5)	0.030(5)	0.174(6)	0.040(5)	0.218(5)	0.014(5)

The sulfathiazole molecule, present as the imido tautomer (with atom N(13) protonated, rather than N(11)), is almost completely included in the cyclodextrin cavity with the thiazole ring protruding slightly from the secondary hydroxyl side and the phenyl ring near the primary hydroxyl side of the host molecule as shown in the stereoview (Figure 5). The sulfathiazole molecule is held in the cavity primarily by hydrophobic forces, but also by two weak C-H···O hydrogen bonds which are often found in carbohydrate crystal structures[15]. The first is between C(3G4)-H of the host and O(10) of the guest and the second is between C(15)-H in the thiazole ring of the drug and O(3G1), a secondary hydroxyl oxygen atom of the cyclodextrin molecule. The latter type of C-H···O hydrogen bond has also been reported in a sulfathiazole-crown ether-acetonitrile complex[16].

There is another C-H···O interaction between C(14)-H of the thiazole ring and O(6G1) of a neighbouring cyclodextrin molecule as well as an O-H···N hydrogen bond between O(6G3) of another neighbouring cyclodextrin molecule and N(11). The latter two interactions thus contribute to the stabilisation of the crystal packing rather than to the stability of the complex. A fourth C-H···O hydrogen bond is present between C(5)-H and O(7W). This particular type of hydrogen bond occurs frequently and its significance has been discussed by Steiner and Saenger[17]. The remaining two nitrogen atoms of the guest are also hydrogen bonded to water molecules. These interactions between guest and host/water molecules are listed in Table 3. Apart from the hydrogen bonding between host and guest, there are only two further close contacts which are also listed in Table 3. Stereo space-filling diagrams illustrate the otherwise relatively loose fit of the guest in the cyclodextrin cavity (Figures 6 and 7).

Table 3 Guest-host/water interactions*.

D	H	A		D-H	Distance (Å) H···A	D···A	Angle (°) D-H···A
C(15)-H(15)		O(3G1)	(a)	1.00	2.58	3.34(1)	132
C(3G4)-H(3G4)		O(10)	(a)	1.00	2.51	3.47(1)	161
C(5)-H(5)		O(7W)	(a)	1.00	2.48	3.30(2)	139
N(7)-H(72)		O(6W)	(a)	1.02	2.04	3.01(2)	157
N(7)-H(71)		O(7W)	(a)	1.01	2.09	3.02(2)	152
N(13)-H(13)		O(2W)	(b)	1.00	1.81	2.76(1)	158
O(6G3)-H(63O)		N(11)	(c)	1.00	2.14	3.04(1)	150
C(14)-H(14)		O(6G1)	(d)	1.00	2.39	3.35(1)	162
O(8W)		N(7)	(a)			3.03(2)	
O(9WB)		N(7)	(a)			2.95(4)	
O(8W)		O(10)	(c)			2.91(2)	

Equivalent positions

(a)	x,	y,	z
(b)	-x+1,	y+1/2,	-z+1
(c)	-x+1,	y-1/2,	-z+1
(d)	-x,	y+1/2,	-z

Close contacts (Å)**

H(3G1)···S(16)	2.787(9)***
H(5G5)···H(2)	2.35 (2)

* Distances involving hydrogen atoms in C-H···O hydrogen bonds are based on calculated positions.

** Van der Waals radii used here and throughout this thesis taken from reference 18.

*** The e.s.d.s quoted (here and throughout this thesis) for close contact distances between host and guest involving hydrogen atoms inserted at idealised positions are based on the carbon atoms to which they are attached.

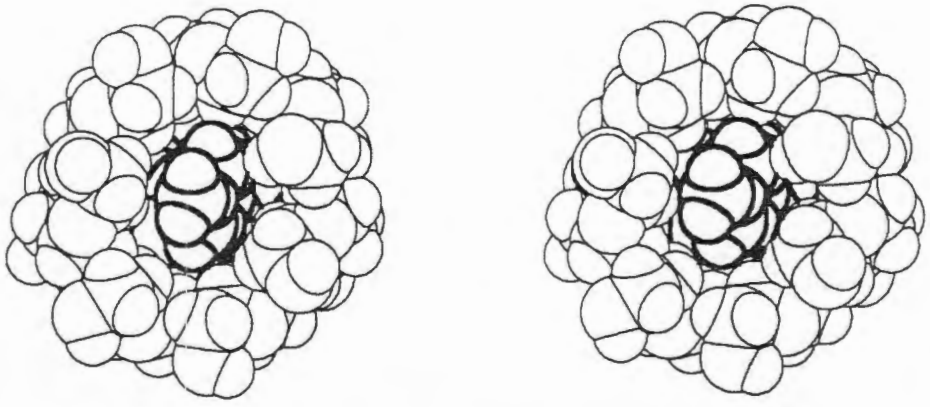

Figure 6 Stereo space-filling diagram of the SULFB complex viewed from the primary hydroxyl side.

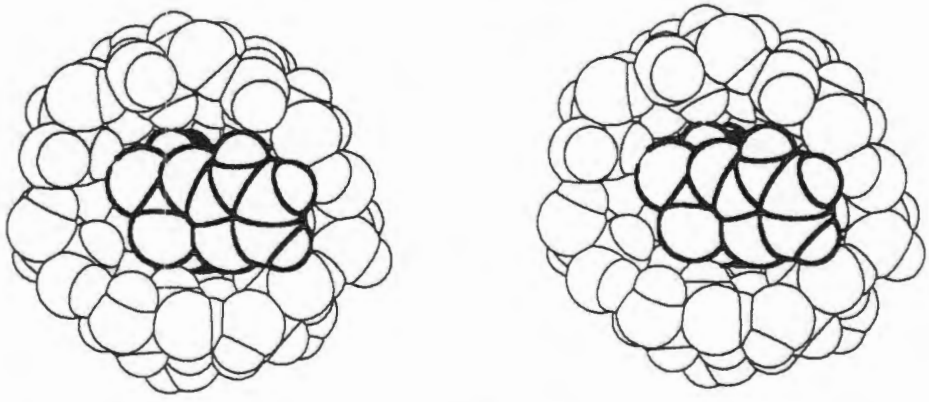

Figure 7 Stereo space-filling diagram of the SULFB complex viewed from the secondary hydroxyl side.

The conformation of the sulfathiazole molecule is defined completely by three torsion angles, namely C(6)-C(1)-S(8)-N(11), C(1)-S(8)-N(11)-C(12) and S(8)-N(11)-C(12)-S(16) (see Figure 1 for numbering scheme of the sulfathiazole molecule). The values for these torsion angles are 108(1)°, -76(1)° and -3(2)°, respectively, and they have been compared with the corresponding torsion angles in sulfathiazole polymorphs I, II and III as well as those in the sulfathiazole-crown ether-acetonitrile complex[2,3,16]. The conformation of the sulfathiazole molecule in the title compound is closest to that observed in the sulfathiazole-crown ether-acetonitrile complex, for which the corresponding torsion angles are 122°, -85° and -5° (e.s.d.s $\leq$ 1°). From the comparison of these torsion angles in all the above structures, there appears to be a preferred narrow range for each torsion angle. Therefore, the conformation adopted by sulfathiazole is presumably one of relatively low energy which must contribute to the high stability constant of the complex.

Table 4 Hydrogen bond table for SULFB.

O H	O		Distance (Å) O-H	H···O	Angle (°) O···O	O-H···O
O(3G1)-H(31O)	O(2G7)	(a)	1.00	1.85	2.806(8)	158
O(3G2)-H(32O)	O(2G1)	(a)	1.00	1.77	2.758(7)	171
O(6G2)-H(62O)	O(4W)	(a)	1.00	1.77	2.770(9)	173
O(3G3)-H(33O)	O(2G2)	(a)	0.99	1.99	2.862(8)	146
O(2G4)-H(24O)	O(3G5)	(a)	0.99	1.91	2.856(7)	158
O(2G5)-H(25O)	O(3G6)	(a)	1.00	1.87	2.828(8)	159
O(6G5)-H(65O)	O(1W)	(a)	1.00	1.66	2.651(7)	170
O(3G7)-H(37O)	O(2G6)	(a)	1.00	2.12	2.818(9)	126
O(3W)-H(1W3)	O(4W)	(a)	1.00	1.84	2.80 (1)	161
O(3W)-H(2W3)	O(6G3)	(a)	1.00	1.8	2.70 (1)	142
O(7W)-H(2W7)	O(9WA)	(a)	1.00	2.0	2.76 (4)	133
O(6G1)-H(61O)	O(6G5)	(b)	1.00	2.07	2.91 (1)	140
O(2G3)-H(23O)	O(8W)	(c)	1.00	2.26	2.90 (2)	121
O(3G6)-H(36O)	O(2W)	(c)	0.99	1.82	2.77 (1)	160
O(3G4)-H(34O)	O(8W)	(c)	1.00	2.08	2.76 (2)	123
O(3G4)-H(34O)	O(9WA)	(c)	1.00	1.73	2.68 (3)	157
O(2G2)-H(22O)	O(6G4)	(c)	1.00	1.85	2.76 (1)	148*
O(3G5)-H(35O)	O(3W)	(c)	0.99	1.77	2.742(8)	165
O(6W)-H(2W6)	O(3G3)	(d)	1.00	2.01	2.91 (1)	149
O(6G6)-H(66O)	O(3W)	(e)	1.00	1.66	2.662(9)	178
O(2G7)-H(27O)	O(2G3)	(f)	1.00	2.15	2.998(8)	141
O(7W)-H(1W7)	O(3G7)	(g)	1.00	2.00	2.84 (1)	140
O(6G7)-H(67O)	O(3G1)	(g)	1.00	1.80	2.75 (1)	158*
O(5W)-H(1W5)	O(3G7)	(g)	1.00	2.14	3.00 (1)	143
O(1W)-H(2W1)	O(5W)	(h)	1.00	2.1	2.78 (1)	124
O(4W)-H(1W4)	O(6G7)	(i)	1.00	1.9	2.78 (1)	153
O(9WB)	O(6G4)	(a)			2.89 (5)	
O(2G6)	O(6G5)	(j)			2.73 (1)*	

* Direct hydrogen bond between hosts in adjacent layers.

cont'd

Table 4 cont'd

Equivalent positions			
(a)	x,	y,	z
(b)	x,	y,	z-1
(c)	-x+1,	y-1/2,	-z+1
(d)	x+1,	y,	z
(e)	x-1,	y,	z
(f)	x-1,	y,	z-1
(g)	-x,	y-1/2,	-z
(h)	x,	y,	z+1
(i)	x+1,	y,	z
(j)	-x,	y+1/2,	-z+1

All 8.3 water molecules are located outside the cyclodextrin cavity. Crystal stabilisation is achieved by extensive hydrogen bonding mediated chiefly by these water molecules. There are also intramolecular and intermolecular hydrogen bonds involving the hydroxyl groups of the cyclodextrin moieties (Table 4). Seven water molecules are ordered and the remaining 1.3 water molecules are disordered over three sites with fractional site occupancies of 0.7, 0.3 and 0.3.

The complex packs in layers parallel to the *ac* plane and the layers are linked mostly by water molecules. However there are three direct hydrogen bonds between hosts in adjacent layers. These have been indicated in Table 4. Packing diagrams are shown in Figures 8 and 9. The molecular axis of the β-cyclodextrin molecule makes an angle of 7° with the *b*-axis and therefore molecules in successive layers, related by the twofold screw axis, are not in parallel orientation. This is an unusual packing arrangement for a β-cyclodextrin complex. Only one other similar structure has been reported, namely that of the 1,4-diazabicyclo[2.2.2]octane-β-cyclodextrin complex[11].

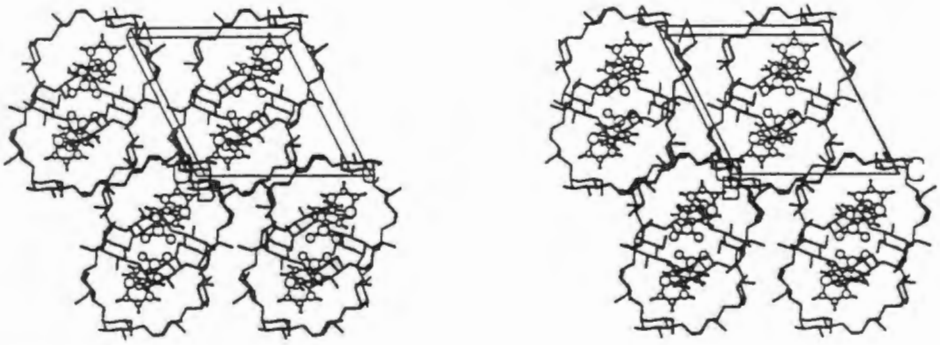

Figure 8 Stereo packing diagram of SULFB viewed down the *b*-axis (water molecules omitted for clarity).

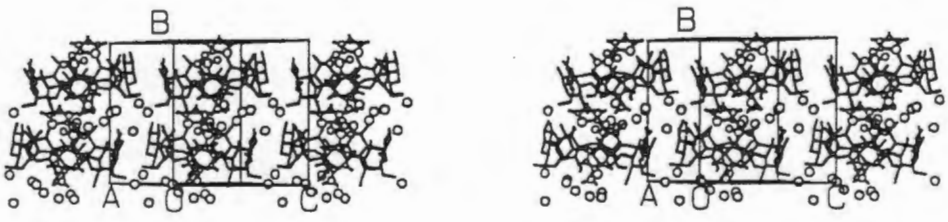

Figure 9 Stereo packing diagram of SULFB viewed perpendicular to the *b*-axis (water molecules are indicated as open circles).

Uekama *et al.* concluded from their circular dichroism, UV and N.M.R. studies[6,7] that the interaction between sulfathiazole and β-cyclodextrin is predominantly hydrophobic, that the phenyl ring is inserted in the cyclodextrin cavity and that the stoichiometry is 1:1. Furthermore, they proposed that there may be hydrogen bonding between the amino group of sulfathiazole and some part of the cyclodextrin molecule. Their results are consistent with what is reported here. However, in the solid state the amino group of the sulfathiazole molecule is hydrogen bonded to water molecules and there are also some guest-host/water hydrogen bonds which may either be too transient or not present in solution.

XRD

Calculated and experimental XRD patterns for SULFB are shown in Figure 10. The very close match in the peak positions (2θ values) confirms the high purity of

the SULFB sample as demonstrated by elemental analysis. The differences in relative intensities between the two patterns means that the sample which gives rise to the experimental pattern is suffering from preferred orientation of the crystallites.

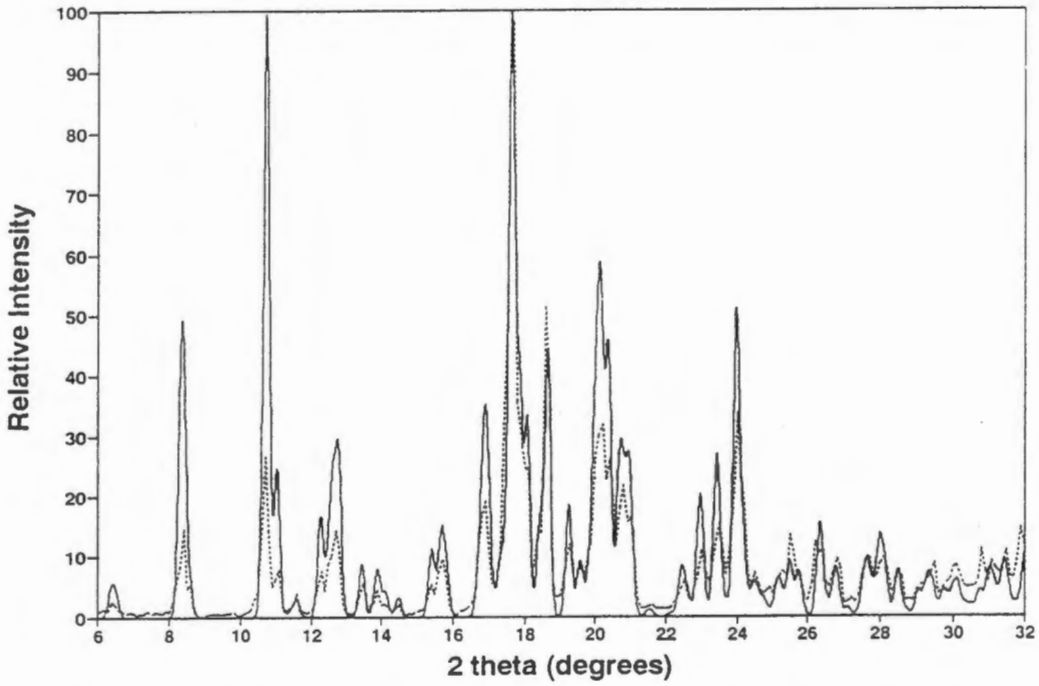

Figure 10 Calculated (——) and experimental (· · · · ·) XRD patterns for SULFB.

UV spectrophotometry

Although the stoichiometry of the complex was known because the crystal structure of the complex had been solved, the complex was used as a standard to verify the reliability of the UV method used in determining the stoichiometries of other complexes whose crystal structures were not solved. The wavelength used for sulfathiazole was 285 nm and the correlation coefficient for the standard curve was 0.992. The host:guest ratio obtained was 1.00 : 1.07.

References

1. E. Holz, A. G. Onandia and S. Holz, *Acta Cient. Venezolana*, 1955, **6**, 68.
2. G. J. Kruger and G. Gafner, *Acta Crystallog.*, 1971, B**27**, 326.
3. G. J. Kruger and G. Gafner, *Acta Crystallog.*, 1972, B**28**, 272.
4. J. Anwar, S. E. Tarling and P. Barnes, *J. Pharm. Sci.*, 1989, **78**, 337.
5. W. I. Higuchi, P. D. Bernado and S.C. Mehta, *J. Pharm. Sci.*, 1967, **56**, 200.
6. K. Uekama, F. Hirayama and H. Koinuma, *Chem. Lett.*, 1977, 1393.
7. K. Uekama, F. Hirayama, M. Otagiri, Y. Otagiri and K. Ikeda, *Chem. Pharm. Bull.*, 1978, **26**, 1162.
8. K. Uekama, F. Hirayama, S. Nasu, N. Matsuo and T. Irie, *Chem. Pharm. Bull.*, 1978, **26**, 3477.
9. M. Wang, H. Ueda and T. Nagai, *Drug Dev. Ind. Pharm.*, 1990, **16**, 571.
10. *Cambridge Structural Database and Cambridge Structural Database System*, April 1993, Version 5.05, Cambridge Crystallographic Data Centre, University Chemical Laboratory, Cambridge, England.
11. K. Harata, *Bull. Chem. Soc. Jpn.*, 1982, **55**, 2315.
12. G. M. Sheldrick, *SHELX76*, Program for crystal structure determination. University of Cambridge, England, 1976.
13. W. Saenger, *Inclusion Compounds* Volume 2, Chapter 8, London, Academic Press, edited by J. L. Atwood, J. E. D. Davies and D. D. MacNicol, 1984.
14. C. Betzel, W. Saenger, B. E. Hingerty and G. M. Brown, *J. Am. Chem. Soc.*, 1984, **106**, 7545.
15. T. Steiner and W. Saenger, *J. Am. Chem. Soc.*, 1992, **114**, 10146.
16. M. R. Caira and R. Mohamed, *Acta Crystallog.*, 1993, B**49**, 760.
17. T. Steiner and W. Saenger, *J. Am. Chem. Soc.*, 1993, **115**, 4540.
18. (a) A. Bondi, *J. Phys. Chem.*, 1964, **68**, 441.
    (b) S. C. Nyburg and C. H. Faerman, *Acta Crystallog.*, 1985, B**41**, 274.

Chapter 4 Diclofenac sodium

Introduction

The therapeutic properties of the non-steroidal anti-inflammatory drugs (NSAIDs) are characteristic of the prototype aspirin (acetylsalicylic acid) and include analgesic and antipyretic effects in addition to the anti-inflammatory effect. The action of these drugs is attributable to the inhibition of prostaglandin synthesis[1]. The NSAIDs fall into a number of classes[2]:

- Salicylic acid derivatives
- Aminoarylcarboxylic acid derivatives
- Arylacetic acid derivatives
- Arylpropionic acid derivatives
- Arylbutyric acid derivatives
- Arylcarboxylic acids
- Pyrazoles
- Pyrazolones
- Thiazinecarboxamides

Non-steroidal agents other than salicylates are often preferred to aspirin to relieve painful conditions such as osteoarthritis, rheumatoid arthritis and gout, since high doses of aspirin are needed for a significant anti-inflammatory effect[1]. Although NSAIDs are very widely used, they are well known for causing gastrointestinal ulceration and bleeding. Complexation with cyclodextrins is a possible way of reducing local irritation in the gastrointestinal tract by promoting more rapid absorption and therefore shorter exposure to the drug[3]. This has, in fact, already been demonstrated for a β-cyclodextrin complex with piroxicam[4].

Diclofenac is an arylacetic acid derivative and the structure of the sodium salt of the drug together with the numbering scheme used in the crystal structure analysis is shown in Figure 1. An advantage of this drug is that therapeutic effects are elicited at lower doses than for most other NSAIDs[5]. The crystal structure of diclofenac sodium tetrahydrate has been reported[6] and the interaction between diclofenac acid and β-cyclodextrin has been studied in solution by phase solubility, UV and circular dichroism techniques[7]. The stoichiometry of the complex in solution was established

as 1:1 by a continuous variation plot and stability constants calculated by phase solubility, UV and CD methods were 150 M^{-1} (distilled water), 510 M^{-1} and 340 M^{-1} (both in 0.1 M sodium phosphate buffer, pH 7.0), respectively.

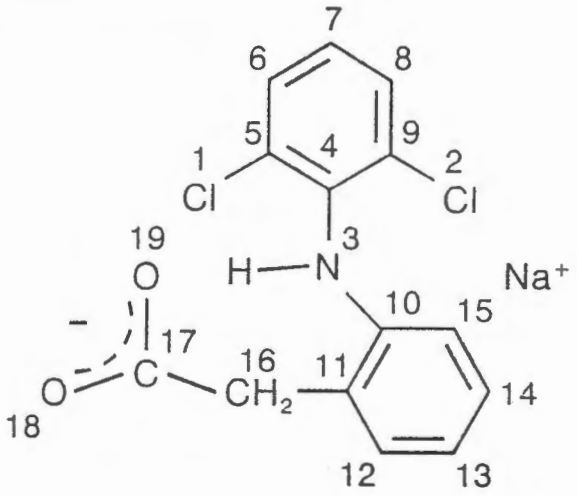

Figure 1 Diclofenac sodium

Preparation of the CD Complexes

Diclofenac sodium-β-cyclodextrin complex (DICLOFB)

0.18 mmol of diclofenac sodium and 0.16 mmol of β-cyclodextrin were dissolved in 2 ml of distilled water at 70°C. After about 4 months at room temperature, the complex crystallised as colourless needles with an hexagonal cross-section (Figure 2).

Diclofenac-β-cyclodextrin complexes with potassium and caesium (FENACBK and FENACBCs)

0.19 mmol of diclofenac sodium and 0.16 mmol of β-cyclodextrin were dissolved at 70°C in 5 ml distilled water with either 150 mg KCl or 337 mg CsCl. The solutions were left at room temperature in summer to evaporate quickly and crystals of the respective complexes crystallised after 2 to 3 days (Figure 2).

Diclofenac sodium-γ-cyclodextrin complex (DICLOFG)

0.06 mmol of diclofenac sodium and 0.06 mmol of γ-cyclodextrin were dissolved in 1.8 ml of distilled water at 70°C. The solution was left at room temperature to evaporate very slowly. The complex crystallised as colourless flat needles after about 3 months (Figure 2).

Hot stage Microscopy

Figure 2 also shows photographs of DICLOFB, β-CD hydrate and diclofenac sodium tetrahydrate at various temperatures. The behaviour of the complex is similar to that of the SULFB complex (Chapter 3) and most of the other native β-CD and γ-CD complexes presented in this thesis also behave in the same way. The complexes retain the shape of their crystals during water loss, but the β-CD hydrate expands, becoming almost feathery and then melts, bubbling gently. The diclofenac sodium tetrahydrate also goes opaque as it loses water and then turns black just a few degrees before melting.

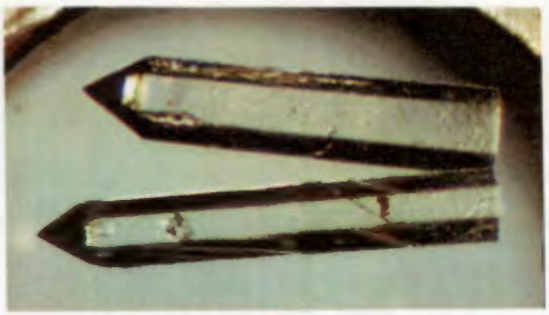

DICLOFB (42 X)

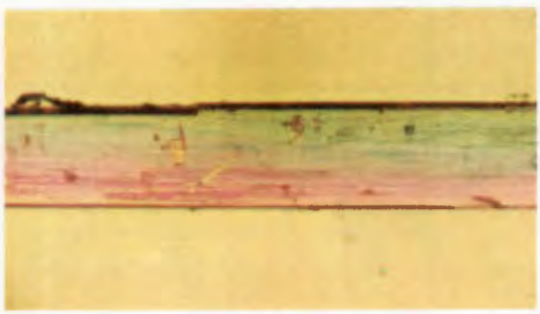

DICLOFG (47 X , polarised light)

FENACBK (32 X)

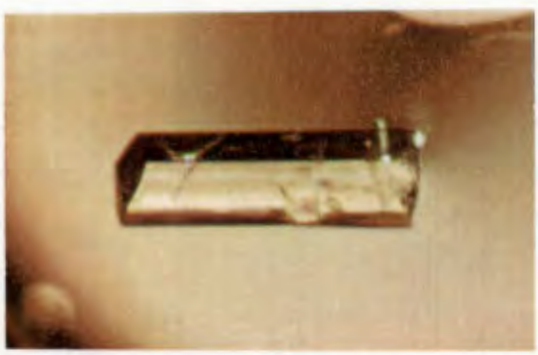

FENACBCs (47 X)

Figure 2 Photographs of DICLOFB, FENACBK, FENACBCs and DICLOFG.

cont'd

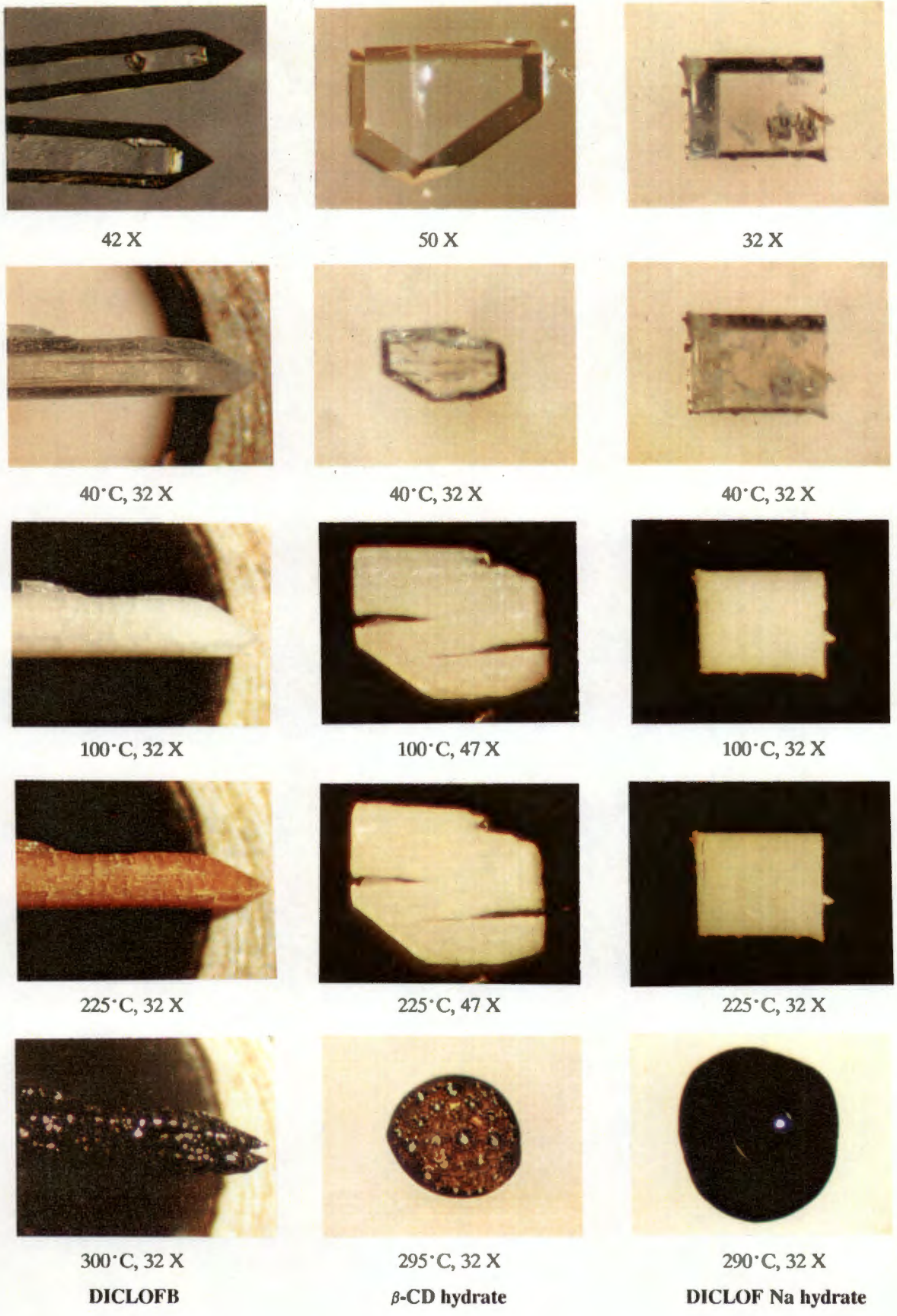

Figure 2 cont'd Photographs of DICLOFB, β-CD hydrate and diclofenac sodium hydrate.

Thermal Analysis

TG and DSC traces for the four complexes are shown in Figure 3. Table 1 summarises the TGA results for the four complexes.

Table 1 TG data for the four diclofenac complexes.

Complex	% weight loss	Temperature range (°C)	No. of water molecules
DICLOFB	12.0	30 - 170	11.0
FENACBK	11.4	30 - 160	10.5
FENACBCs	10.6	30 - 152	10.3
DICLOFG	13.8	30 - 185	14.4

The DSC results are summarised in Table 2.

Table 2 DSC data for the four diclofenac complexes.

Complex	Peak	Temperature range (°C)	Onset (°C)	Peak/s (°C)
DICLOFB	Endotherm A	30 - 115	48	58, 72, 81
	Endotherm B	118 - 160	120	130
	Exotherm C	219 - 244	221	228
FENACBK	Endotherm A	30 - 165	60	87
	Exotherm B	220 - 240	224	231
	Exotherm C	244 - 270	245	254
FENACBCs	Endotherm A	30 - 166	62	93
	Exotherm B	216 - 240	218	228
	Exotherm C	244 - 278	255	260
DICLOFG	Endotherm A	40 - 173	72	104
	Exotherm B	217 - 248	221	228
	Exotherm C	251 - 270	254	258

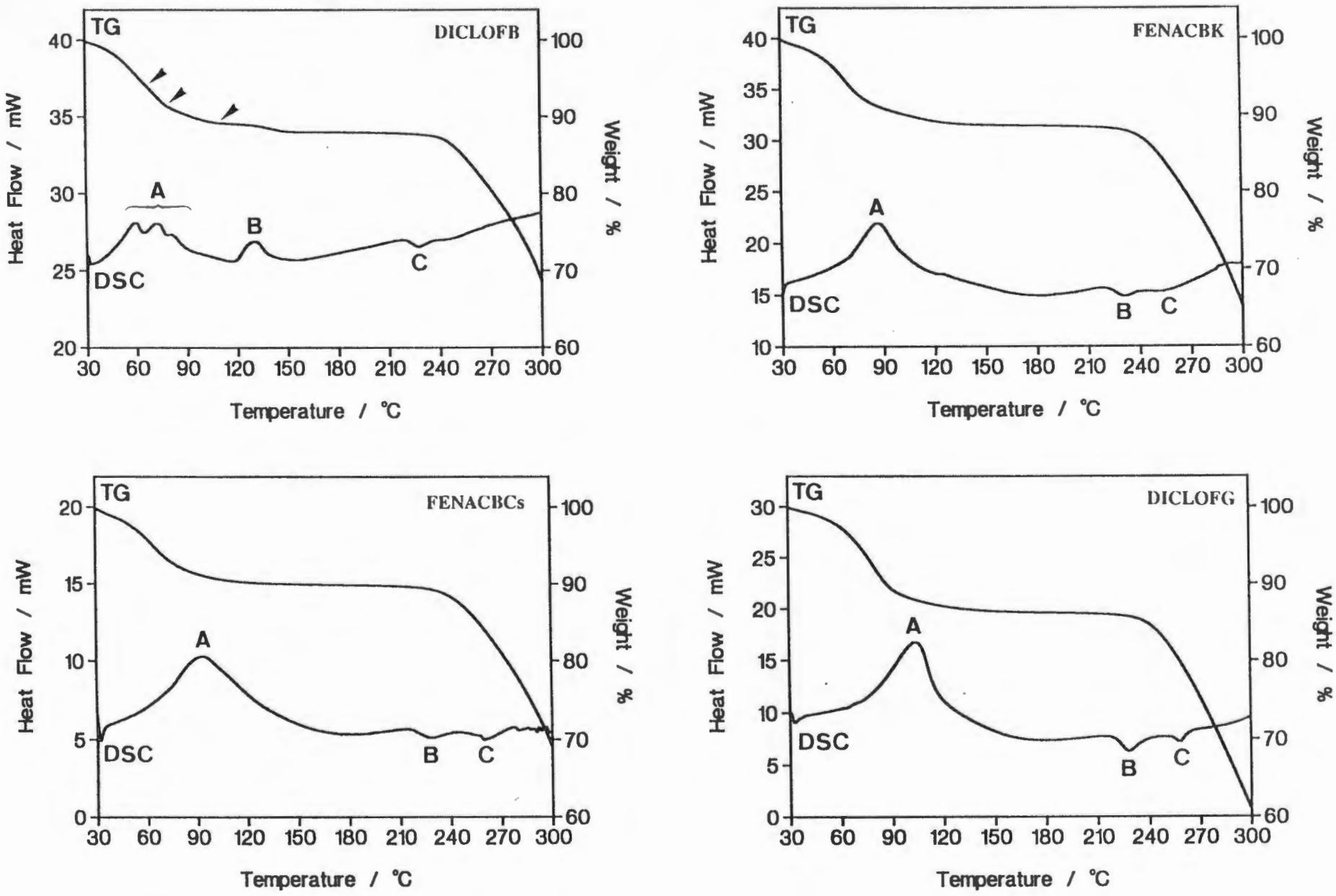

Figure 3 TG and DSC traces for DICLOFB, FENACBK, FENACBCs and DICLOFG.

The relatively high temperatures to which water molecules of crystallisation are retained by the four complexes are noteworthy. It is possible that this is due to the strong coordination of water molecules by the cations which are present in all four complexes. A trend which seems to support this explanation is the decrease in the temperature at which water loss is terminated in going from DICLOFB to FENACBK to FENACBCs. A sodium ion would be expected to coordinate water molecules most strongly because it has the highest charge density. Since packing arrangement is also a factor which determines how tightly water molecules are bound in crystal structures, it is perhaps unwise to make comparisons in this respect between complexes with different packing arrangements. However, the FENACBK and FENACBCs complexes are isomorphous (unit cell parameters given later) and therefore a direct comparison is justified.

The profiles of the endotherms representing water loss (A in each case) in the FENACBK, FENACBCs and DICLOFG complexes are similar. The shoulders on the peaks indicate in each case that the water losses are multi-step processes, but no attempt was made to estimate the number of water molecules in different steps from the TG traces because the derivatives of the traces showed that there are no obvious points of inflection. The broad endotherm for water loss in the FENACBK complex does seem, however, to be slightly more suggestive of multiple endotherms than that of the FENACBCs complex. In the case of the DICLOFB complex, water loss is represented by four endotherms, three of which are overlapping, but nevertheless have definite peaks. The derivative of the TG trace for the complex shows that there are three points of inflection in the TG trace. The four separate weight losses correspond to 6.0, 2.2, 1.8 and 1.0 water molecules, respectively. The last water molecule lost must therefore be particularly tightly bound in the crystal structure and will be discussed in more detail in the crystal structure analysis.

A common feature in the DSC traces of all four complexes is the small, but reproducible exotherm at approximately 220°C, which seems to be correlated in each case with the onset of decomposition of the dehydrated complex. There is a second small, but equally reproducible exotherm at about 250°C following the first exotherm in the DSC traces of the FENACBK, FENACBCs and DICLOFG complexes which also is hinted at in the trace of the DICLOFB complex. This common exotherm may represent a specific event in decomposition, indicating a similar path of decomposition for the four complexes.

UV spectrophotometry

Host:guest ratios determined by UV spectrophotometry are as follows. The DICLOFB complex, whose structure had been solved in this study (host:guest ratio of 1:1), was used as a reference compound to verify the reliability of the method as it is well-known that the UV spectrum of a guest can be significantly altered in the presence of cyclodextrins. The wavelength used for diclofenac was 274 nm and the correlation coefficient of the standard curve was 0.999.

Complex	Host:guest ratio
DICLOFB	1.00 : 0.90
FENACBK	1.00 : 1.08
FENACBCs	1.00 : 1.04
DICLOFG	1.00 : 1.14

Microanalysis

The ratio given in parentheses is the host:guest:water stoichiometry. Water content is based on the thermogravimetric analysis results. Molecular formulae are as follows:

DICLOFB (1:1:11)	$C_{42}H_{70}O_{35}.C_{14}H_{10}Cl_2NO_2^-Na^+.11H_2O$
FENACBK (1:1:10.5)	$C_{42}H_{70}O_{35}.C_{14}H_{10}Cl_2NO_2^-K^+.10.5H_2O$
FENACBCs (1:1:10.3)	$C_{42}H_{70}O_{35}.C_{14}H_{10}Cl_2NO_2^-Cs^+.10.3H_2O$
DICLOFG (1:1:14.4)	$C_{48}H_{80}O_{40}.C_{14}H_{10}Cl_2NO_2^-Na^+.14.4H_2O$

The results of the microanalyses are given as the average of duplicate determinations.

	Calculated (%)			Experimental (%)		
	C	H	N	C	H	N
DICLOFB	40.73	6.23	0.85	40.87	5.68	0.68
FENACBK	40.77	6.12	0.85	40.95	6.00	0.90
FENACBCs	38.47	5.80	0.80	38.23	5.55	0.52
DICLOFG	39.72	6.39	0.75	39.83	6.12	0.72

Crystal data

Table 3 shows the crystal data for complexes for which crystal structures were not determined.

Table 3 Crystal data for complexes for which crystal structures were not determined.

Complex	FENACBK
Molecular formula	$C_{42}H_{70}O_{35}.C_{14}H_{10}Cl_2NO_2^-K^+.10.5H_2O$
M_r (g.mol^{-1})	1658.39
Crystal system	Orthorhombic
Space group	$P2_12_12_1$
Z	8
a (Å)	15.529(4)
b (Å)	26.070(9)
c (Å)	37.15(1)
V (Å^3)	15040(8)
D_m (g.cm^{-3})	1.47(1)
D_c (g.cm^{-3})	1.465
Complex	FENACBCs
Molecular formula	$C_{42}H_{70}O_{35}.C_{14}H_{10}Cl_2NO_2^-Cs^+.10.3H_2O$
M_r (g.mol^{-1})	1748.59
Crystal system	Orthorhombic
Space group	$P2_12_12_1$
Z	8
a (Å)	15.54(5)
b (Å)	26.12(8)
c (Å)	37.3 (2)
V (Å^3)	15140(106)
D_m (g.cm^{-3})	1.55(1)
D_c (g.cm^{-3})	1.53

cont'd

Table 3 cont'd

Complex	DICLOFG
Molecular formula	$C_{48}H_{80}O_{40}.C_{14}H_{10}Cl_2NO_2^-Na^+.14.4H_2O$
M_r (g.mol^{-1})	1874.68
Crystal system	Monoclinic
Space group	$P2_1$
Z	8
a (Å)	15.24(5)
b (Å)	33.4 (1)
c (Å)	34.4 (1)
β (°)	103.8(3)
V (Å^3)	17005(93)
D_m (g.cm^{-3})	1.47(1)
D_c (g.cm^{-3})	1.46

The FENACBK and FENACBCs complexes are isomorphous as their unit cell parameters are very similar. No other β-CD complex (unsubstituted β-CD) with these cell dimensions and crystallising in the space group $P2_12_12_1$ has been reported. All the γ-CD complexes reported to date have similar packing arrangements and crystallise in the space group $P42_12$. The DICLOFG complex, which crystallises in the space group $P2_1$, may therefore represent a different packing arrangement for a γ-CD complex and could be dimeric since the cell parameters indicate that there are four complex units in the asymmetric unit (possibly two dimers).

Crystal structure solution

DICLOFB

Data were first collected from a crystal of DICLOFB at room temperature and extensive attempts to solve the structure by direct methods (SHELX86), heavy-atom methods and the "search for a fragment of known geometry" (program PATSEE[8]) failed. Data were then recollected from a bigger crystal at 233K with a forced scan for all reflections. The structure was then solved relatively easily (TREF 200, SUBS 6) by direct methods (SHELX86) and all the non-hydrogen atoms of the host

and guest were located in the direct methods solution. The model was refined isotropically by full-matrix least-squares techniques (SHELX76) and eleven water molecules were found on subsequent difference Fourier maps and included in the model. Hydrogen atoms attached to the carbon atoms of host and guest were inserted at idealised positions with C-H = 1.00 Å and the hydrogen atoms of each glucose residue and those of the guest were assigned common variable isotropic temperature factors. All non-hydrogen atoms other than carbon atoms were assigned anisotropic temperature factors and further refinement was carried out by the block-diagonal least-squares method. All of the cyclodextrin hydroxyl hydrogen atoms were found and allowed to refine subject to a distance constraint (O-H = 1.00 Å, C···H = 1.99 Å, σ = 0.005 Å). The hydrogen atom attached to the nitrogen atom of the guest and the hydrogen atoms of the water molecules were also located and refined with distance constraints (N-H = 1.00 Å, σ = 0.005 Å and O-H = 1.00 Å, H···H of each water molecule = 1.58 Å, σ = 0.005 Å). The hydrogen atom attached to the nitrogen atom was assigned the same temperature factor as the rest of the guest hydrogen atoms and the hydrogen atoms of the water molecules were also assigned their own common variable isotropic temperature factor.

FENACBK

Data were also collected at 250K from a crystal of FENACBK. The low temperature equipment broke down after half the data had been collected and the crystal did not survive the resultant thermal shock. Therefore the second half of the data were collected from a different crystal. This required the collection of some common reflections (4 - 5° θ) in order to calculate a factor by which to scale the one half of the data to the other. This was further complicated by a decay of 11.5% during the first 60 hours of the first half of the data collection. A linear decay correction was applied up to this point (60 hours) and the rest of this half of the data was corrected by a constant. Finally, the intensities of the first half of the data were multiplied by the scale factor which was calculated from the common reflections in the two halves of the data. Lengthy attempts to solve the structure by direct methods (SHELX86 and SIR92) and with PATSEE using many different parameters were unsuccessful, probably due to poor data and the large number of non-hydrogen atoms in the asymmetric unit (2:2:21 cyclodextrin:drug:water molecules). The skeleton non-hydrogen atoms of a single cyclodextrin molecule as well as those of a dimer were used as input for the fragment of known geometry in the program PATSEE.

Crystal structure (DICLOFB)

Crystal data, experimental and refinement parameters for DICLOFB are listed in Table 4.

Table 4 Crystal data, experimental and refinement parameters for DICLOFB (structure refined on F using SHELX76)

Molecular formula	$C_{42}H_{70}O_{35}.C_{14}H_{10}Cl_2NO_2^-Na^+.11H_2O$
M_r (g.mol^{-1})	1651.29
Crystal system	Hexagonal
Space group	$P6_1$
Z	6
a (Å)	15.956(8)
c (Å)	50.95(1)
V (Å^3)	11233(8)
D_m (g.cm^{-3})	1.47(1)
D_c (g.cm^{-3})	1.451
μ (Mo Kα) (cm^{-1})	1.92
F(000)	5244
Crystal dimensions (mm)	0.38 x 0.38 x 0.45
Temperature of data collection	233K
Range scanned θ (°)	$1 \leq \theta \leq 25$
Scan type	ω
Index range	h 0,19: k 0,19: l 0,60
Scan width (°)	0.7 + 0.35 tanθ
Aperture width (mm)	1.12 + 1.05 tanθ
Std reflections monitored for decay	-12,3,9 -3,-9,9 12,-3,9
Decay (%)	7.3
No. of reflections collected	7490
No. of unique reflections	6167
R_{int}	0.0344
No. of reflections with I > 2σ(I)	5489
No. of L.S. parameters	915

cont'd

Table 4 cont'd

R	0.056
wR	0.051
w	$[\sigma^2(F_o)]^{-1}$
S	4.65
Shift/e.s.d. max, average	0.455, 0.001
$\Delta\rho_{max}$ final (e.Å^{-3})	0.57
$\Delta\rho_{min}$ final (e.Å^{-3})	-0.36

Figure 4 is a stereodiagram of the diclofenac sodium-β-cyclodextrin complex in which the glucose residues have been numbered. As usual, all α-D-glucose moieties are in the $^4C_1$ chair conformation and all the primary hydroxyl groups are found in the *(-)-gauche*[9] conformation, except that of residue G6, which adopts the *(+)-gauche* conformation on account of a hydrogen bond to a carboxylate oxygen atom of the guest molecule. Table 5 lists values for the O(4)···O(4')···O(4") angles of the O(4) heptagon, radii of the O(4) heptagon, O(4)···O(4') distances, tilt angles and the deviation of each O(4) atom from the least-squares plane through the seven O(4) atoms. Residues G4 and G7 have rather large tilt angles because of the intermolecular hydrogen bond O(2G4)-H···O(3G7)^I (I = x, y-1, z). Despite this, the O(2)···O(3') distances are still within the range for the usual intramolecular hydrogen bonding, 2.716(6) - 3.022(7) Å.

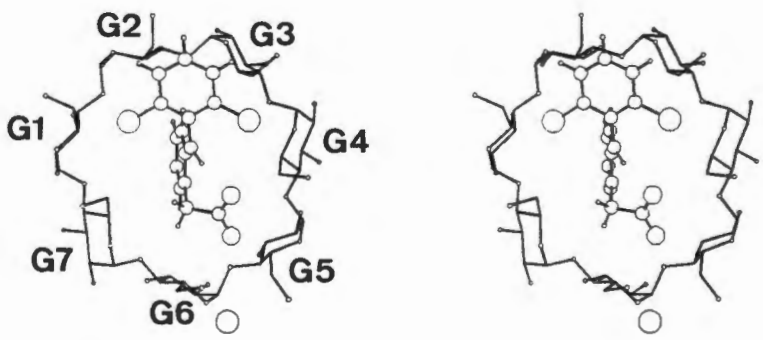

Figure 4 A stereodiagram of the DICLOFB complex viewed down the axis of the host molecule (the Na+ ion is shown as a single open circle).

Table 5 Geometrical data for host.

i. Glycosidic oxygen angle (°) and radius (Å) of the O(4) heptagon (measured from the centre of gravity of the seven O(4) atoms to each O(4) atom.)

O(4G7)···O(4G1)···O(4G2)	124.5	G1	5.14
O(4G1)···O(4G2)···O(4G3)	127.4	G2	5.09
O(4G2)···O(4G3)···O(4G4)	129.3	G3	4.89
O(4G3)···O(4G4)···O(4G5)	131.8	G4	4.90
O(4G4)···O(4G5)···O(4G6)	120.1	G5	5.23
O(4G5)···O(4G6)···O(4G7)	130.3	G6	4.86
O(4G6)···O(4G7)···O(4G1)	131.6	G7	4.83
Average	127.9	Average	4.99

ii. O(4)···O(4') distance(Å) and tilt angle (°)

O(4G1)···O(4G2)	4.36	G1	5.4
O(4G2)···O(4G3)	4.33	G2	4.2
O(4G3)···O(4G4)	4.50	G3	13.5
O(4G4)···O(4G5)	4.24	G4	28.7
O(4G5)···O(4G6)	4.32	G5	7.1
O(4G6)···O(4G7)	4.40	G6	11.7
O(4G7)···O(4G1)	4.31	G7	31.6
Average	4.35	Average	14.6

iii. Deviation (Å) of each O(4) atom from the least-squares plane through the seven O(4) atoms.

O(4G1)	O(4G2)	O(4G3)	O(4G4)	O(4G5)	O(4G6)	O(4G7)
0.303(5)	0.007(5)	0.258(5)	0.004(4)	0.439(5)	0.396(5)	0.091(5)

The phenylacetate ring of the drug anion is included in the host cavity from the primary hydroxyl side (Figure 5) and the interaction is stabilised by the hydrogen bond between a carboxylate oxygen atom, O(18), and a primary hydroxyl group of the host molecule. The dichlorophenyl moiety protrudes from the host molecule, but is included at the secondary hydroxyl side of a sixfold screw-related cyclodextrin

molecule (Figure 6). The plane through Cl(1)···C(4)···Cl(2) makes an angle of approximately 10° with the least-squares plane through the O(4) atoms of the screw-related host and consequently Cl(1) is situated slightly deeper inside the host cavity than Cl(2). The angle of inclusion of the dichlorophenyl ring as a whole (angle between the plane through Cl(1)···C(7)···Cl(2) and the least-squares plane through the O(4) atoms of the screw-related cyclodextrin molecule) is 26.6°. The interaction of the dichlorophenyl ring with the host molecule is stabilised by three weak $C(3G_n)$-$H(3_n)$···Cl hydrogen bonds and a weak C-H···O hydrogen bond between a phenyl carbon atom and a glycosidic oxygen atom of the host. Table 6 lists the parameters of these host/guest interactions along with other guest-involved hydrogen bonds and the numerous additional close contacts between host and guest.

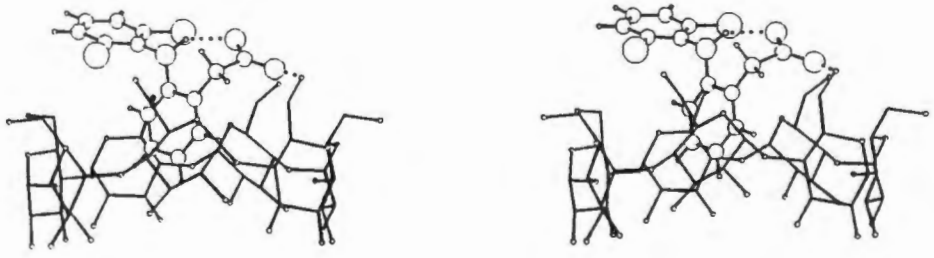

Figure 5 Stereoview of DICLOFB viewed perpendicular to the host axis showing the drug intramolecular hydrogen bond and the hydrogen bond between O(18) of the guest and O(6G6) of the host.

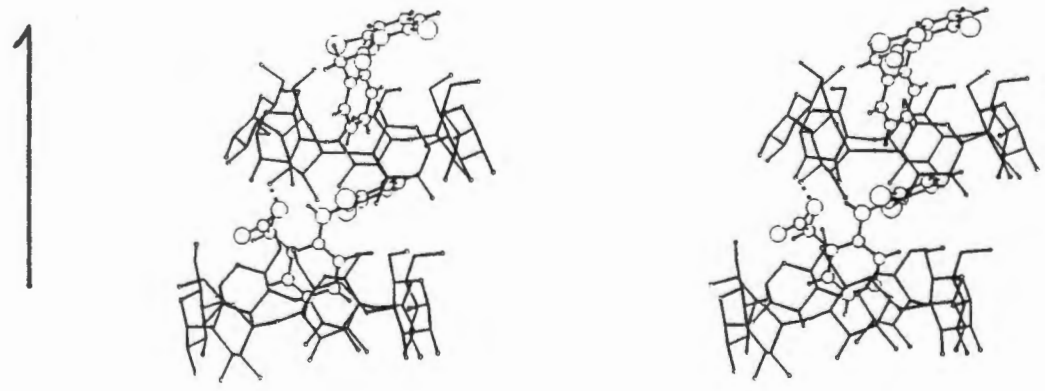

Figure 6 Two complex units related by the sixfold screw axis. The dotted line shows the hydrogen bond between O(3G6) of the host and O(19) of the guest.

Table 6 Guest-involved hydrogen bonds and host/guest close contacts.

			Distance(Å)			Angle(°)
D H	A		D-H	H···A	D···A	D-H···A
O(6G6)-H(66)	O(18)		1.00	1.84	2.729(6)	147
O(1W)-H(2W1)	O(18)		1.00	1.72	2.693(7)	163
N(3)-H(3)	O(19)		1.01	1.95	2.820(7)	143
O(3G6)-H(36)	O(19)	(a)	1.00	1.57	2.565(6)	171
C(3G5)-H(35)	Cl(1)	(a)	1.00	2.844	3.540(7)	127
C(3G6)-H(36)	Cl(1)	(a)	1.00	2.659	3.544(6)	148
C(3G2)-H(32)	Cl(2)	(a)	1.00	2.928	3.697(7)	134
C(7)-H(7)	O(4G3)	(a)	1.00	2.636	3.589(9)	160
C(13)-H(13)	π	(b)	1.00	2.77	3.542	135

Close Contacts

C(5) ···H(623)		2.810(9)			
C(6G3)···Cl(1)		3.472(5)			
H(621)···Cl(2)		2.904(8)			
C(11) ···H(627)		2.82 (1)			
C(12) ···H(5G7)		2.71 (1)	Equivalent positions		
H(14) ···H(5G2)		2.364(6)			
C(16) ···H(66)		2.79 (2)	(a)	x-y, x,	z+1/6
C(16) ···H(627)		2.77 (1)	(b)	y, -x+y,	z - 1/6
C(7) ···H(3G3)	(b)	2.83 (1)			
H(7) ···H(3G3)	(b)	2.164(7)			
C(8) ···H(3G3)	(b)	2.896(8)			
H(8) ···H(3G3)	(b)	2.343(5)			
C(17) ···H(36)	(b)	2.56 (4)			

Stereo space-filling diagrams in Figures 7 and 8 illustrate the interaction of the guest at the primary and secondary hydroxyl sides of the host molecule, respectively. The Na^+ ion is situated at the periphery of the *β*-cyclodextrin molecule and is approximately octahedrally coordinated by oxygen atoms of three water molecules, a primary hydroxyl group of *β*-cyclodextrin and two secondary hydroxyl groups of a symmetry-related host molecule (Figure 9). The Na^+···O distances and

O···Na^+···O angles are listed in Table 7.

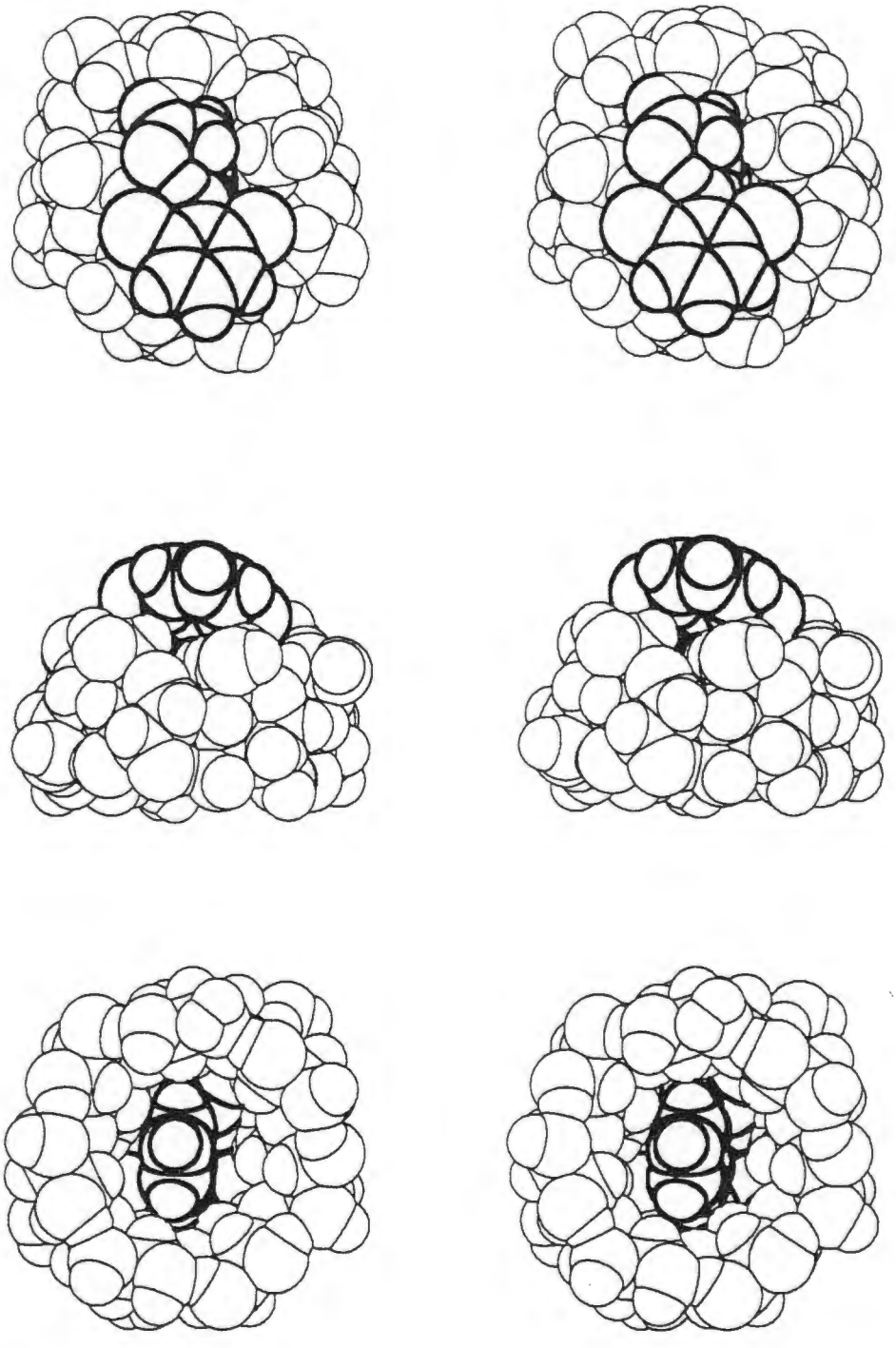

Figure 7 Stereo space-filling diagrams of the inclusion of the phenylacetate moiety of the diclofenac anion at the primary hydroxyl side of the host viewed: top - from the primary hydroxyl side, middle - perpendicular to the host axis, bottom - from the secondary hydroxyl side.

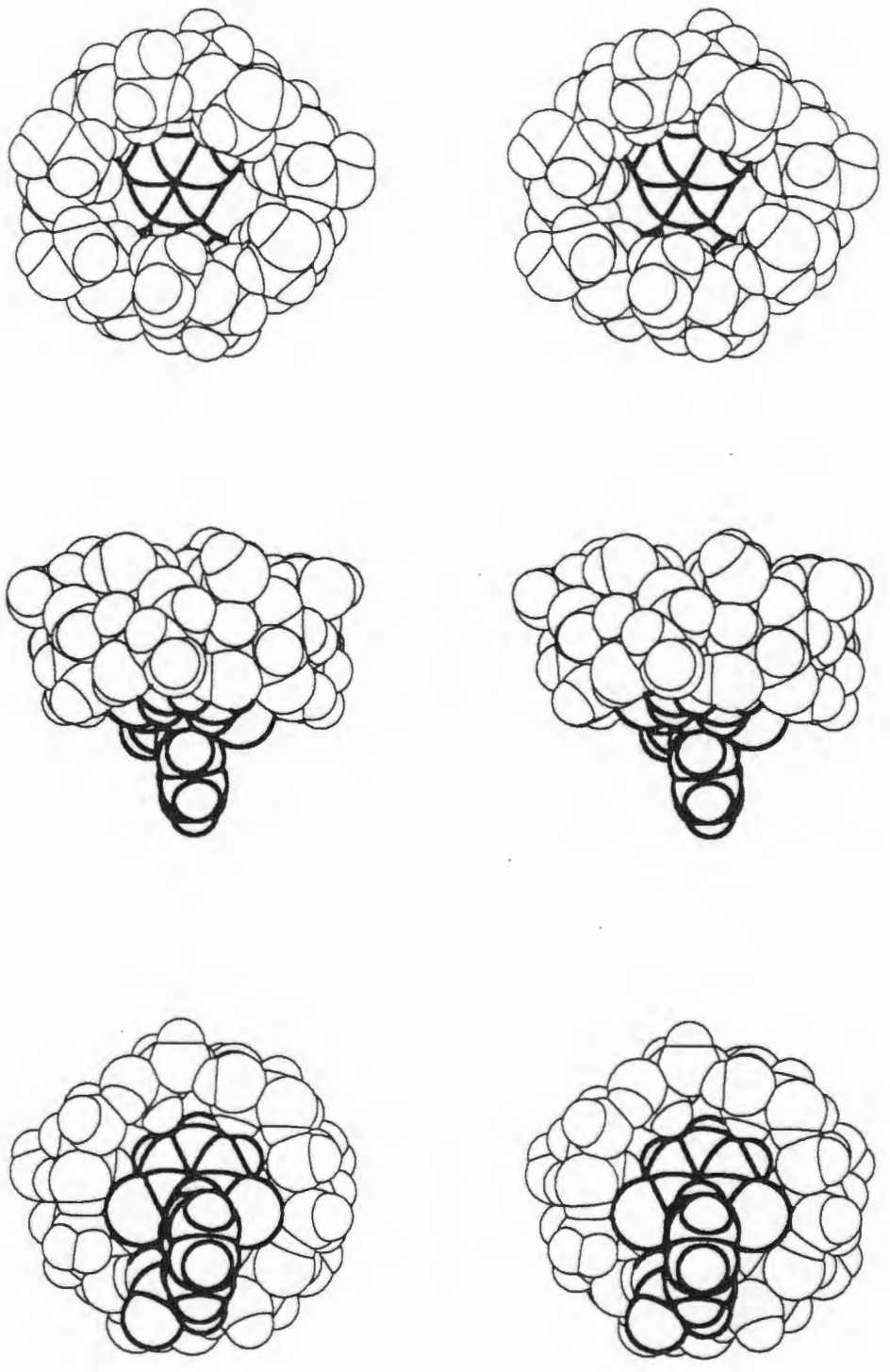

Figure 8 Stereo space-filling diagrams of the inclusion of the dichlorophenyl moiety of the diclofenac anion at the secondary hydroxyl side of a screw-related host molecule viewed: top - from the primary hydroxyl side, middle - perpendicular to the host axis, bottom - from the secondary hydroxyl side.

Table 7 Na+···O distances (Å) and O···Na+···O angles (°) in DICLOFB

Na(1)···O(6G6)	2.269(6)
Na(1)···O(1W)	2.401(5)
Na(1)···O(6W)	2.299(7)
Na(1)···O(9W)	2.461(7)
Na(1)···O(2G4)$^{(a)}$	2.613(6)
Na(1)···O(3G4)$^{(a)}$	2.350(6)
O(2G4)$^{(a)}$···Na(1)···O(3G4)$^{(a)}$	68.1(2)
O(9W) ···Na(1)···O(3G4)$^{(a)}$	86.7(2)
O(6W) ···Na(1)···O(3G4)$^{(a)}$	101.3(2)
O(6W) ···Na(1)···O(2G4)$^{(a)}$	91.5(2)
O(6W) ···Na(1)···O(9W)	85.7(2)
O(1W) ···Na(1)···O(3G4)$^{(a)}$	78.1(2)
O(1W) ···Na(1)···O(2G4)$^{(a)}$	90.0(2)
O(1W) ···Na(1)···O(9W)	92.4(2)
O(6G6) ···Na(1)···O(2G4)$^{(a)}$	97.6(2)
O(6G6) ···Na(1)···O(9W)	108.8(2)
O(6G6) ···Na(1)···O(6W)	94.8(2)
O(6G6) ···Na(1)···O(1W)	86.3(2)
O(9W) ···Na(1)···O(2G4)$^{(a)}$	153.6(2)
O(1W) ···Na(1)···O(6W)	178.0(2)
O(6G6) ···Na(1)···O(3G4)$^{(a)}$	158.6(2)

Equivalent position

(a) 1+y, 1-x+y, -1/6+z

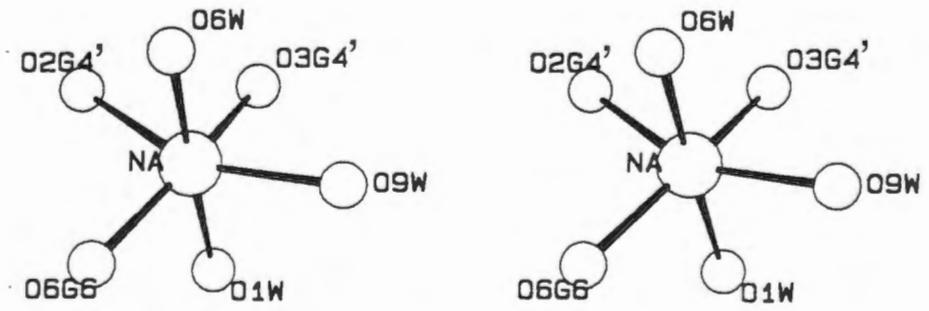

Figure 9 Coordination of the Na^+ ion by three water molecules, a primary hydoxyl oxygen atom of the host and two secondary hydroxyl oxygen atoms of a symmetry-related host molecule.

The diclofenac anion has an intramolecular N-H···O hydrogen bond (parameters listed in Table 6 and shown in Figure 6) which has also been observed in the crystal structure of diclofenac sodium tetrahydrate[10]. The orientation of the two phenyl rings of the drug with respect to one another in the complex is described by torsion angles $\tau 1$ and $\tau 2$, C(5)-C(4)-N(3)-C(10) and C(4)-N(3)-C(10)-C(11), with values of -113.6(7) and -173.6(6)°, respectively. The orientation of the carboxylate group with respect to its attached phenyl ring is described by two further torsion angles, $\tau 3$ and $\tau 4$, C(10)-C(11)-C(16)-C(17) and C(11)-C(16)-C(17)-O(19), with values of -80.9(8) and 74.9(8)°, respectively. Values for all the corresponding torsion angles in the two crystallographically independent molecules of the crystal structure of diclofenac sodium tetrahydrate have been calculated from the published coordinates[6]. The values obtained for the two independent molecules are:

Molecule A	$\tau 1$ -131°,	$\tau 2$ -170°	$\tau 3$ -73°,	$\tau 4$ 24°
Molecule B	$\tau 1$ 126°,	$\tau 2$ 166°	$\tau 3$ 80°,	$\tau 4$ -68°

They are approximate mirror images of one another except for the rotation of the carboxylate group around C(16)-C(17) and are therefore presumably of similar energy. Since the space group ($P2_1/m$) is centrosymmetric, the exact mirror images of the two independent molecules are also generated in the crystal structure by symmetry. The conformation of the diclofenac anion in DICLOFB is most similar to that of the mirror image of molecule B.

Eleven water molecules per asymmetric unit were located and refined in the X-ray analysis. The water molecules were exceptionally well-behaved at the low temperature of the X-ray analysis, yielding final U_{eq} values in the range 0.03 - 0.08 $Å^2$ and showed no signs of disorder. O(1W) is hydrogen bonded to O(18), a carboxylate oxygen atom of the drug molecule (parameters listed in Table 6). This water molecule is also coordinated to the Na^+ ion (Figure 9) and is involved in two further hydrogen bonds, one to another water molecule and the second to a secondary hydroxyl oxygen atom of the host. O(1W) is thus a likely candidate for the last water molecule lost on heating in thermogravimetric analysis assuming that there are no major structural changes during dehydration. (This is a reasonable assumption because it has been shown that the partial isothermal dehydration of β-CD hydrate at room temperature at successively lower humidities is not accompanied by any major structural changes[11]. In addition, Debye-Scherrer

photographs of some of the β-CD complexes presented in this thesis following dehydration match those of the hydrated material, although admittedly the dehydrated complexes do rehydrate to a certain extent.) It is also probable that the two water molecules lost in the second last step of water loss are the other two water molecules which are coordinated to the Na^+ ion. The water molecules are involved in many hydrogen bonds which stabilise the crystal packing. Hydrogen bonding data and other O···O contacts less than 3.0 Å are given in Table 8.

Table 8 Hydrogen bonding data for β-cyclodextrin-diclofenac sodium complex.

			Distance (Å)		Angle (°)
O H	O	O-H	H···O	O···O	O-H···O
O(3G1)-H(31)	O(2G2) (a)	1.00	1.81	2.791(6)	166
O(2G3)-H(23)	O(3G2) (a)	1.00	1.83	2.775(8)	157
O(3G3)-H(33)	O(2G4) (a)	1.00	2.11	3.022(7)	151
O(3G4)-H(34)	O(2G5) (a)	1.00	1.84	2.716(6)	145
O(6G4)-H(64)	O(7W) (a)	1.00	1.78	2.664(8)	145
O(3G5)-H(35)	O(2G6) (a)	1.00	1.86	2.857(8)	174
O(2G7)-H(27)	O(3G6) (a)	1.00	1.83	2.813(8)	166
O(3G7)-H(37)	O(2G1) (a)	1.00	1.95	2.877(5)	153
O(2W)-H(1W2)	O(1W) (a)	1.00	1.8	2.723(9)	163
O(2W)-H(2W2)	O(9W) (a)	1.00	2.28	3.024(9)	130
O(4W)-H(1W4)	O(8W) (a)	1.00	2.0	2.758(7)	131
O(5W)-H(1W5)	O(4W) (a)	1.00	1.79	2.783(9)	172
O(9W)-H(1W9)	O(6G5) (a)	1.00	2.13	2.871(7)	129
O(2G1)-H(21)	O(11W)(b)	1.00	1.72	2.68 (1)	162
O(6G2)-H(62)	O(5W) (c)	1.00	1.75	2.740(9)	169
O(6G1)-H(61)	O(7W) (c)	1.00	1.77	2.731(6)	160
O(2G2)-H(22)	O(2W) (d)	1.00	1.72	2.722(7)	175
O(3G2)-H(32)	O(3W) (d)	1.00	1.71	2.676(6)	162
O(1W)-H(1W1)	O(2G7) (e)	1.00	1.91	2.797(7)	146
O(6G7)-H(67)*	O(3G1) (e)	1.00	1.65	2.639(7)	175
O(3W)-H(2W3)	O(3G6) (e)	1.00	1.79	2.754(8)	160
O(2G4)-H(24)**	O(3G7) (f)	1.00	1.78	2.752(7)	161
O(10W)-H(110)	O(6G7) (f)	1.00	2.0	2.69 (1)	124

cont'd

Table 8 cont'd

		Distance (Å)			Angle (°)
O H	O	O-H	H···O	O···O	O-H···O
O(2G6)-H(261)*	O(6G4) (g)	1.00	1.81	2.690(8)	146
O(2G5)-H(25)	O(10W)(g)	1.00	1.67	2.663(8)	171
O(6G5)-H(65)**	O(6G1) (h)	1.00	2.07	2.979(8)	151
O(6G5)-H(65)**	O(5G1) (h)	0.99	2.51	3.196(8)	126
O(2W)-H(2W2)	O(10W)(i)	1.00	2.24	3.091(8)	143
O(6W)-H(1W6)	O(6G2) (i)	1.00	1.9	2.833(9)	150
O(5W)-H(2W5)	O(2G3) (j)	1.00	1.91	2.863(7)	160
O(11W)-H(111)	O(3G3) (j)	1.00	2.17	2.814(7)	121
O(5W)	O(7W) (a)			2.906(9)	
O(8W)	O(11W)(a)			2.76 (1)	
O(8W)	O(3G5) (e)			2.74 (1)	
O(8W)	O(6G7) (f)			2.806(6)	
O(10W)	O(5G1) (f)			2.898(8)	
O(2W)	O(6G1) (h)			2.731(8)	
O(6W)	O(6G2) (i)			2.833(9)	
O(9W)	O(6G3) (i)			2.929(7)	

Equivalent positions

(a)	x,	y,	z
(b)	x-y-1,	x,	z+1/6
(c)	x-1,	y,	z
(d)	x-y-1,	x-1,	z+1/6
(e)	y,	-x+y,	z-1/6
(f)	x,	y-1,	z
(g)	x-y,	x,	z+1/6
(h)	x+1,	y,	z
(i)	x+1,	y+1,	z
(j)	y+1,	-x+y,	z-1/6

* Direct hydrogen bond between screw-related host molecules which links successive layers.
** Direct hydrogen bond between adjacent host molecules in the *ab*-plane.

Apart from the hydrogen bond between the guest and O(1W) mentioned above, the diclofenac anion is almost completely enveloped in an infinite helical host channel created by the 6_1-axis which passes through the cavity of the host. Figure 10 shows that the only part of the drug which is accessible from the outside of the host channel is the carboxylate oxygen atom which is hydrogen bonded to O(1W). In addition, it is evident from this drawing that the carboxylate group is also partly responsible for the large tilt angle of G7 which was explained earlier only by an intermolecular hydrogen bond. Successive drug molecules inside the helical channel are in contact with one another by means of a weak C-H$\cdots\pi$ interaction shown in Figure 11 (parameters listed in Table 6). There is also a strong hydrogen bond between a secondary hydroxyl group of the host molecule and a carboxylate oxygen atom of a screw-related guest (see Figure 6 - parameters listed in Table 6). The latter is an important interaction contributing to the head-to-tail stacking of complex units along the sixfold screw axis which is parallel to the *c*-axis (Figure 12).

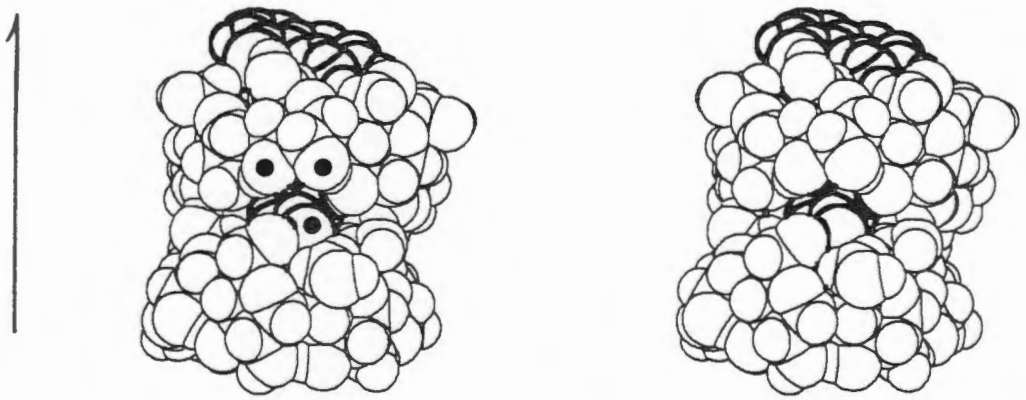

Figure 10 Space-filling stereodiagram of two screw-related complex units. The exposed carboxylate oxygen atom and the secondary hydroxyl groups of G7 are indicated.

The helical columns of complex units pack in hexagonal array forming molecular layers parallel to the *ab*-plane (Figure 13). This figure is a representation of one layer of complex units in the *ab*-plane and is **not** a projection of the structure down the *c*-axis. There are three direct hydrogen bonds between any given host and its neighbours in the *ab*-plane, but otherwise adjacent complex units in this plane are linked via water molecules. Since each complex unit is equivalent by symmetry, the given host must necessarily also act as acceptor for these same hydrogen bonds, which brings the total number of direct hydrogen bonds to six. There are only two

direct hydrogen bonds between the primary face of the host and the secondary face of a screw-related cyclodextrin molecule with all other inter-layer links mediated by water molecules. The direct hydrogen bonds have been indicated in the hydrogen bond table (Table 8).

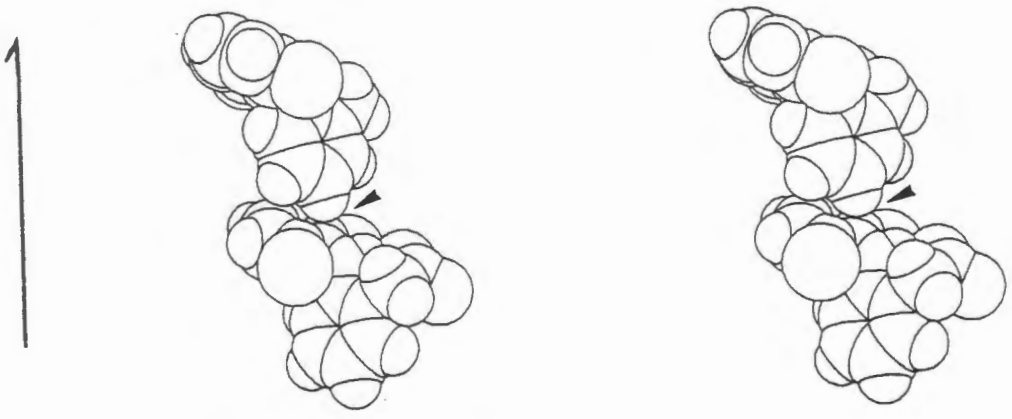

Figure 11 Two screw-related guest molecules illustrating the C-H···π interaction.

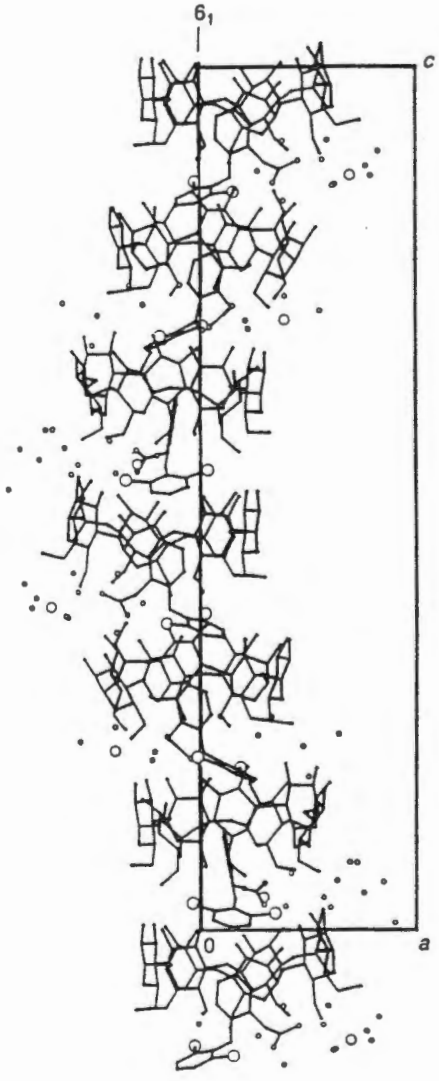

Figure 12 (010) Projection showing the helical arrangement in one stack of complex units.

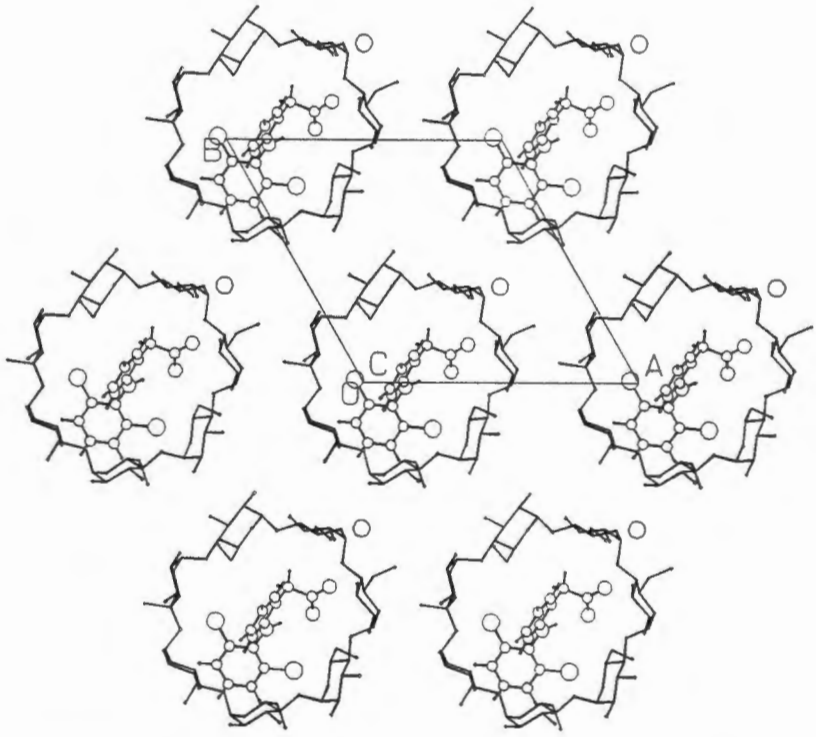

Figure 13 A view down the *c*-axis of the hexagonal packing arrangement in one layer of complex units parallel to the *ab*-plane (water molecules have been omitted).

This is the only known example of a β-CD complex occurring in the hexagonal crystal system and the packing arrangement is unique. A model of this helical packing arrangement is shown on the following page.

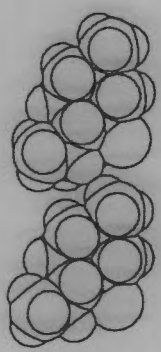

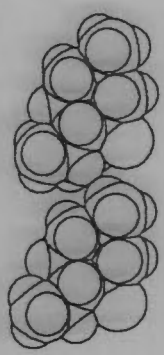

XRD

Calculated and experimental XRD patterns for DICLOFB are shown in Figure 14. The very close match between the calculated and experimental patterns shows the high purity of the sample.

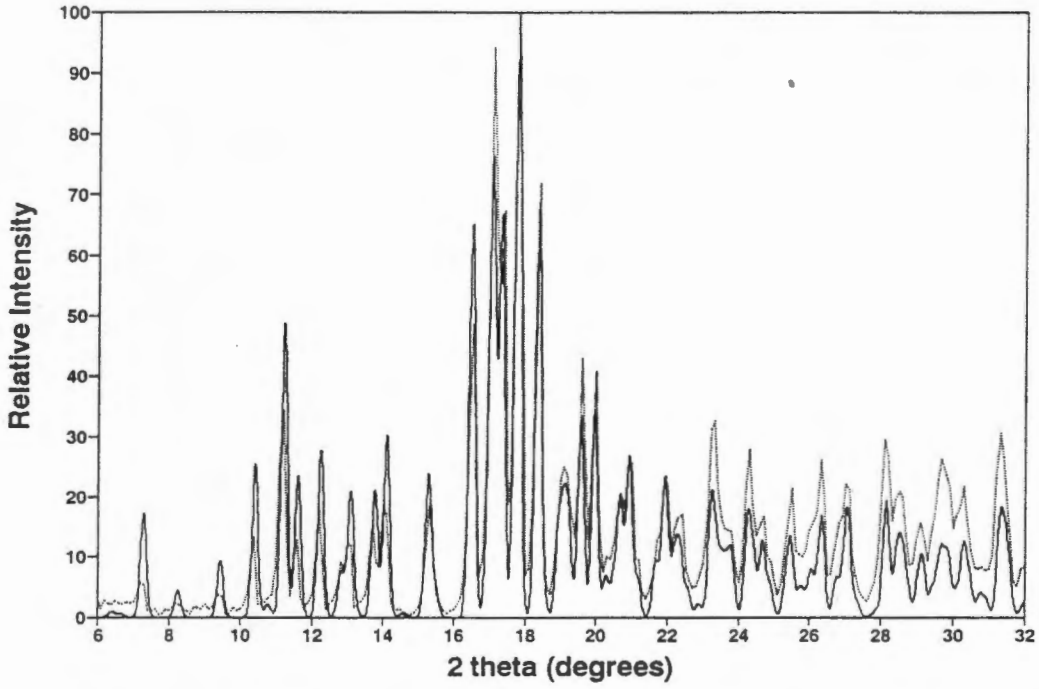

Figure 14 Calculated (——) and experimental (· · · · ·) XRD patterns for DICLOFB.

References

1. *South African Medicines Formulary*, edited by C. J. Gibbon and C. R. Swanepoel, CTP Book Printers, Western Cape, South Africa, 1995.
2. *The Merck Index*, 11th edition, edited by S. Budavari, M. J. O'Neil, A. Smith and P. E. Heckelman, Merck and Co., Inc., New Jersey, U.S.A., 1989.
3. T. Loftsson, B. J. Olafsdottir, H. Frioriksdottir and S. Jonsdottir, *Eur. J. Pharm. Sci.*, 1993, **1**, 95.
4. L. Santucci, S. Fiorucci, L. Patoia, F. Farroni, A. Sicilia, S. Chiucchiu, L. Bufalino and A. Morelli, *Drug Invest.*, 1990, **2** (Suppl. 4), 56.
5. C. M. Adeyeye and P. Li, *Analytical Profiles of Drug Substances*, Volume 19, Academic Press, Inc., California, U.S.A., 1990.
6. G. Reck, G. Faust and G. Dietz, *Pharmazie*, 1988, **43**, 771.
7. K. Ikeda, K. Uekama and M. Otagiri, *Chem. Pharm. Bull.*, 1975, **23**, 201.
8. E. Egert and G. M. Sheldrick, *Acta Crystallog.*, 1985, A**41**, 262.
9. W. Saenger, *Inclusion Compounds*, (Eds. J.L Atwood, J.E.D. Davies and D.D. MacNicol, Volume 2, 1984, 231.
10. E.C. van Tonder, M.R. Caira, S.A. Botha and A.P Lötter, *Pharm. Res.*, 1993, **10**, S-163.
11. T. Steiner and G. Koellner, *J. Am. Chem. Soc.*, 1994, **116**, 5122.

Chapter 5 Meclofenamate sodium

Introduction

Meclofenamic acid is a structural isomer of diclofenac and belongs to the aminoarylcarboxylic acid derivative class of NSAIDs[1]. The interaction between meclofenamic acid and β-cyclodextrin has been studied in solution by phase solubility, UV and CD techniques[2,3,4]. The stoichiometry in solution was established to be 1:1 and stability constants calculated by phase solubility, UV and CD methods are 470 M^{-1} (distilled water), 640 M^{-1} and 490 M^{-1} (both in 0.1 M sodium phosphate buffer, pH 7.0), respectively. Analogous studies on the related drug, diclofenac, were described in Chapter 4.

Figure 1 shows the structure of meclofenamate sodium together with the numbering scheme used in the crystal structure analysis. Although the crystal structure of meclofenamate sodium has not been reported[5], two crystal structures containing the meclofenamate anion have been published[6], namely those of ethanolamine meclofenamate and choline meclofenamate monohydrate.

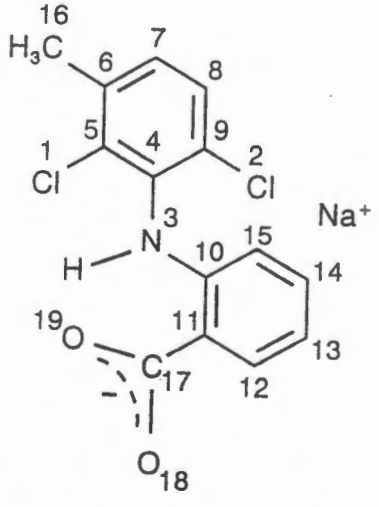

Figure 1 Meclofenamate sodium

Preparation of the CD Complex (MECLOFB)

0.13 mmol of meclofenamate sodium and 0.16 mmol of β-cyclodextrin were dissolved in 4 ml of distilled water at 70°C. The solution was filtered and then cooled slowly to room temperature over about 3 days in a thermos flask (Figure 2).

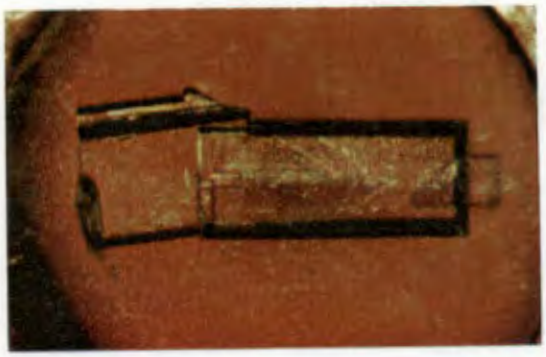

Figure 2 MECLOFB complex (32.5 X)

Thermal Analysis

Figure 3 shows the TG and DSC traces for MECLOFB.

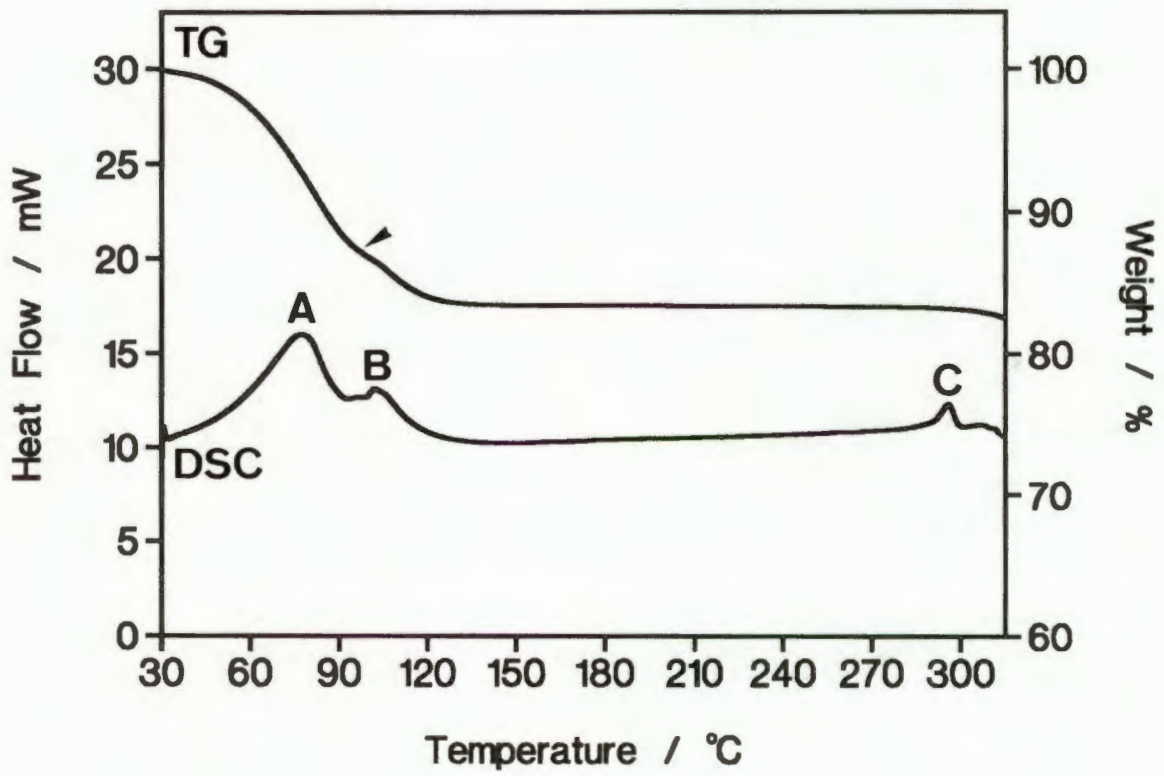

Figure 3 TG and DSC traces for MECLOFB.

TGA of the complex shows a weight loss of 16.6% over the temperature range 30 - 150°C. This corresponds to 16.0 water molecules per 1:1 cyclodextrin:meclofenamate sodium complex unit. The point of inflection in the TG trace shows that 11.2 and 3.8 water molecules are lost in the first and second steps of weight loss, respectively. This will be discussed again later in the crystal structure analysis. The DSC results are summarised in Table 1. Water loss is represented by at least two overlapping endotherms (A and B), suggesting again that water loss is a multi-step process, comparable with the water loss observed in the diclofenac sodium complexes. A small endotherm (C) occurring at the onset of decomposition at 296°C is contrary to what is observed for DICLOFB and the other diclofenac complexes, where small exotherms are present.

Table 1 DSC data for MECLOFB.

Peak	Temperature range (°C)	Onset (°C)	Peak (°C)
Endotherm A	30 - 95	52	77
Endotherm B	95 - 136	99	103
Endotherm C	282 - 302	291	296

Microanalysis

The results of the microanalysis are given as the average of duplicate determinations. The host:guest:water ratio is 1:1:16, with molecular formula as follows: $C_{42}H_{70}O_{35}.C_{14}H_{10}Cl_2NO_2^-Na^+.16H_2O$

Calculated (%)			Experimental (%)		
C	H	N	C	H	N
38.63	6.48	0.80	38.86	6.13	0.81

Crystal structure solution

During the data collection, there was a period of fairly rapid decay following which the standard reflections remained constant. Therefore a linear decay correction was applied only over the period of decay and all the remaining reflections were corrected by a constant. The structure was solved by direct methods (program

SIR92, default run including the SEMINVARIANTS routine) and the model was refined isotropically using SHELX93. All the non-hydrogen atoms of the host and guest except the Na^+ ion were located in the direct methods solution. Hydrogen atoms attached to carbon atoms on both the host and guest were inserted at idealised positions in a riding model (C-H = 1.00 Å). All hydrogen atoms of each glucose residue and all the hydrogen atoms of the guest were assigned common variable isotropic temperature factors. The non-hydrogen atoms of the host and guest anion were then assigned anisotropic temperature factors. There were still many peaks of relatively high electron density on the difference Fourier map representing water molecules and the sodium cation. However, the position of the sodium ion was not obvious from the peak heights. A search of the Cambridge Structural Database for $Na^+ \cdots O$ contacts revealed a minimum distance of 2.1 Å and an average of approximately 2.4 Å. The sodium ion was then assigned on the basis of $Na^+ \cdots O$ distances and geometry. The isotropic temperature factor of the sodium ion was quite high, indicating disorder, and there was a peak 1.7 Å away from it. Since this distance is too short for an $Na^+ \cdots O$ contact and chemical analysis for sodium indicated one sodium atom per 1:1 complex, the peak was inserted as an alternative position for the sodium ion with site occupancies of 0.6 for the former peak and 0.4 for the latter peak. Twelve water molecules were placed with full site occupancy and although the temperature factors of the last three were rather high (0.27, 0.24 and 0.31 $Å^2$, respectively), their site occupancies were not refined because their temperature factors refined to a constant value and there were no abnormally short contacts with neighbouring non-hydrogen atoms. A further eight sites for water molecules were found, their temperature factors were fixed at 0.2 $Å^2$ (average of those for the water molecules with full site occupancy) and their site occupancies were refined. This gave a total of 15.5 water molecules. Water molecules O(1W), O(2W), O(3W) and O(4W) were then assigned anisotropic temperature factors. The hydrogen atoms of the hydroxyl groups of the host, except that of the disordered group, were found and inserted with geometrical constraints (O-H 0.98 Å, σ = 0.05 Å or 0.005 Å in some cases, $C \cdots H$ = 1.99 Å, σ = 0.05 Å or 0.005 Å). No attempt was made to locate the hydrogen atoms of the water molecules.

Crystal structure

Table 2 lists crystal data, experimental and refinement parameters for MECLOFB.

Table 2 Crystal data, experimental and refinement parameters for MECLOFB (structure refined on F^2 using SHELX93)

Molecular formula	$C_{42}H_{70}O_{35}.C_{14}H_{10}Cl_2NO_2^-Na^+.16H_2O$
M_r (g.mol^{-1})	1741.36
Crystal system	Orthorhombic
Space group	$P2_12_12_1$
Z	4
a (Å)	15.087(2)
b (Å)	17.967(2)
c (Å)	29.634(4)
V (Å^3)	8032(2)
D_m (g.cm^{-3})	1.44(1)
D_c (g.cm^{-3})	1.440
μ (Mo Kα) (cm^{-1})	1.88
F(000)	3696
Crystal dimensions (mm)	0.50 x 0.50 x 0.33
Temperature of data collection	294K
Range scanned θ (°)	$1 \leq \theta \leq 25$
Scan type	ω
Index range	h 0,17: k 0,21: l 0,35
Scan width (°)	0.8 +0.35 tanθ
Aperture width (mm)	1.12 + 1.05 tanθ
Std reflections monitored for decay	11,3,7 9,5,13 2,14,2
Decay (%)	11.5
No. of reflections collected	7766
No. of unique reflections	7729
R_{int}	0.00
No. of reflections with I > 2σ(I)	5349
No. of L.S. parameters	1042
R1 (I > 2σ(I))	0.0759
wR2 (F^2)	0.2450 (0.2080 obs refs)
w	$[\sigma^2(F_o)^2 + (0.1581\ P)^2 + 4.1681\ P]^{-1}$
	$P = (\max(F_o^2, 0) + (2 \times F_c^2))/3$

cont'd

Table 2 cont'd

Goof	1.039
Shift/e.s.d. max, average	1.136, 0.026
$\Delta\rho_{max}$ final (e.Å^{-3})	0.63
$\Delta\rho_{min}$ final (e.Å^{-3})	-0.38

Figure 4 is a stereodiagram of the meclofenamate sodium-β-cyclodextrin complex in which the glucose residues have been numbered. All glucose residues are in the $^4C_1$ chair conformation. Atom O(6G4) is disordered over two sites with site occupancies of 0.575 and 0.425. The C(6)-O(6) bonds of all the glucose residues are directed away from the cavity in the (-)-*gauche* conformation[7], except those of G1 and the major site of O(6) in G4, which point inwards towards the cavity in the (+)-*gauche* conformation. O(6G1) is hydrogen bonded to O(2G4) of a screw-related cyclodextrin molecule and O(64A) is within hydrogen bonding distance of O(19) of the guest and is coordinated to the minor position of the Na^+ ion, Na1B. Table 3 lists values for the O(4)···O(4')···O(4") angles of the O(4) heptagon, radii of the O(4) heptagon, O(4)···O(4') distances, tilt angles of the glucose residues and the deviations of the O(4) atoms from their least-squares plane. Comparison of the O(4)···O(4')···O(4") angles, tilt angles and the deviations of the O(4) atoms from their least-squares plane with those in DICLOFB, shows that the conformation of the cyclodextrin molecule in MECLOFB is not as distorted as that in DICLOFB. O(2)···O(3') distances of adjacent glucose residues are in the expected range of 2.77(1) - 2.886(9) Å, consistent with intramolecular hydrogen bonding.

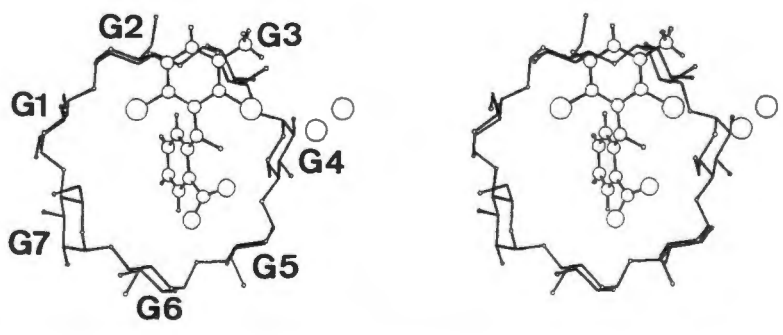

Figure 4 A stereodiagram of the MECLOFB complex viewed down the host axis. The disordered Na+ ion is shown as two open circles - Na1A (right) and Na1B (left).

Table 3 Geometrical data for host.

i. Glycosidic oxygen angle (°) and radius (Å) of the O(4) heptagon (measured from the centre of gravity of the seven O(4) atoms to each O(4) atom.

O(4G7)···O(4G1)···O(4G2)	125.1	G1	5.13
O(4G1)···O(4G2)···O(4G3)	132.3	G2	4.89
O(4G2)···O(4G3)···O(4G4)	126.5	G3	5.03
O(4G3)···O(4G4)···O(4G5)	128.8	G4	5.05
O(4G4)···O(4G5)···O(4G6)	126.4	G5	5.04
O(4G5)···O(4G6)···O(4G7)	131.4	G6	4.88
O(4G6)···O(4G7)···O(4G1)	127.9	G7	5.05
Average	128.3	Average	5.01

ii. O(4)···O(4') distance (Å) and tilt angle (°).

O(4G1)···O(4G2)	4.408	G1	5.2
O(4G2)···O(4G3)	4.375	G2	2.2
O(4G3)···O(4G4)	4.342	G3	12.2
O(4G4)···O(4G5)	4.344	G4	21.0
O(4G5)···O(4G6)	4.319	G5	5.2
O(4G6)···O(4G7)	4.412	G6	7.9
O(4G7)···O(4G1)	4.278	G7	26.4
Average	4.354	Average	11.4

iii. Deviation (Å) of each O(4) atom from the least-squares plane through the seven O(4) atoms.

O(4G1)	O(4G2)	O(4G3)	O(4G4)	O(4G5)	O(4G6)	O(4G7)
0.167(4)	0.055(4)	0.226(4)	0.058(4)	0.228(4)	0.211(4)	0.070(4)

Figure 5 is a stereodiagram of the meclofenamate sodium-β-cyclodextrin complex viewed perpendicular to the axis of the host. The phenylcarboxylate ring of the drug anion is included in the host cavity from the primary hydroxyl side and the interaction is stabilised by the hydrogen bond between a carboxylate oxygen atom,

O(19), and the major site of a primary hydroxyl group, O(64A), of the host molecule. This same carboxylate oxygen atom is involved in the intramolecular N-H···O hydrogen bond of the drug molecule. This is in contrast to DICLOFB, where each carboxylate oxygen atom is involved in one of these interactions. The angle of inclusion of this moiety is 70.4° as opposed to 82.9° in DICLOFB.

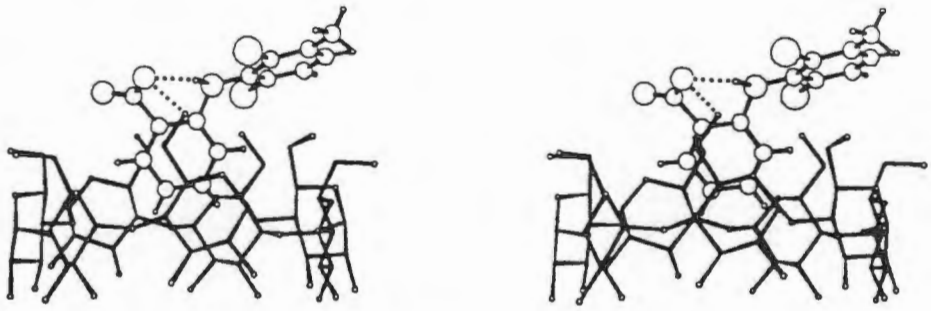

Figure 5 A stereodiagram of the MECLOFB complex viewed perpendicular to the host axis. Dotted lines represent hydrogen bonds.

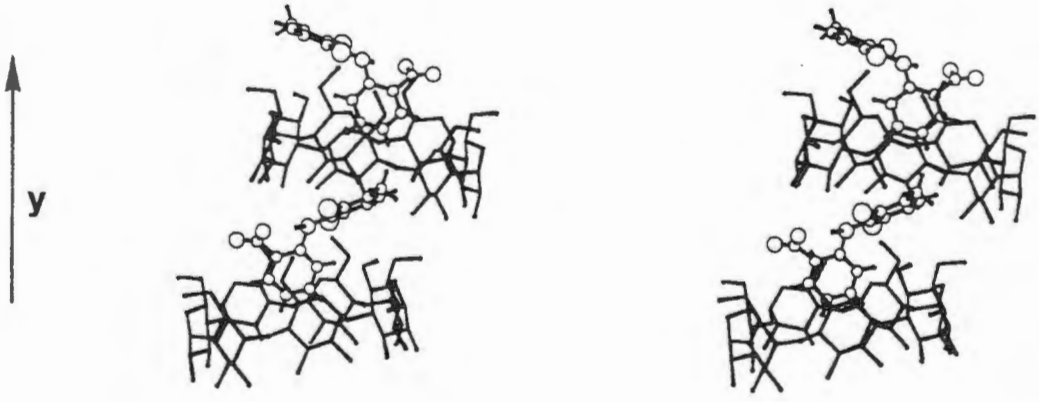

Figure 6 Two complex units related by the twofold screw axis parallel to the *b*-axis.

The dichloromethylphenyl moiety, which protrudes from the host cavity as does the dichlorophenyl moiety in the DICLOFB complex, is included at the secondary hydroxyl side of a 2_1-related host molecule (Figure 6). The angle of inclusion is 28.6° compared with 26.6° in DICLOFB. The interactions observed between the dichlorophenyl moiety and the secondary hydroxyl side of the host in DICLOFB are not present in the MECLOFB complex and other close contacts between host and guest are few in comparison. These are listed in Table 4 with other guest-involved hydrogen bonds.

Table 4 Drug-involved hydrogen bonds and close contacts between guest and host/guest.

			Distance (Å)		Angle (°)
D H	A	D-H	H···A	D···A	D-H···A
N(3)-H(3)	O(19)	0.97	2.27	2.83 (1)	116
O(3G2)-H(32)	O(19) (a)	0.99	2.02	2.676(8)	122
O(19)	O(64A)			2.89 (1)	
O(19)	O(5W)			2.77 (1)	
O(18)	O(6W)			2.91(1)	
O(18)	O(2G6) (b)			2.650(9)	
Close Contacts					
Cl(2) ···O(64A)				3.32(1)	
Cl(2) ···O(20W)				3.52(4)	
C(5) ···H(63A)				2.70(1)	
H(12) ···H(5G6)				2.27(1)	
Cl(1) ···H(3G4)		(a)		2.954(8)	
C(16) ···H(3G7)		(a)		2.853(1)	
C(17) ···H(32)		(a)		2.86 (6)	
H(16B)···H(13)*		(a)		2.23 (2)	

Equivalent positions

(a)	-x,	y-1/2,	-z+1/2
(b)	-x+1,	y+1/2,	-z+1/2

* Close contact between screw-related guest molecules.

Stereo space-filling diagrams in Figures 7 and 8 illustrate the interaction of the guest at the primary and secondary hydroxyl sides of the host, respectively. Comparison of these diagrams with those of DICLOFB shows the much snugger fit of the diclofenac anion in the β-CD cavity at the secondary hydroxyl side of the host. In MECLOFB, the dichloromethylphenyl moiety is shifted relative to what is observed in DICLOFB in order to accommodate the methyl group in the host cavity. Consequently, the chlorine substituents are shifted from the middle of the cavity

(i.e. the widest part) towards the side where they can no longer fit into the cavity and therefore protrude slightly, which explains the lack of C-H···Cl hydrogen bonds between host and guest.

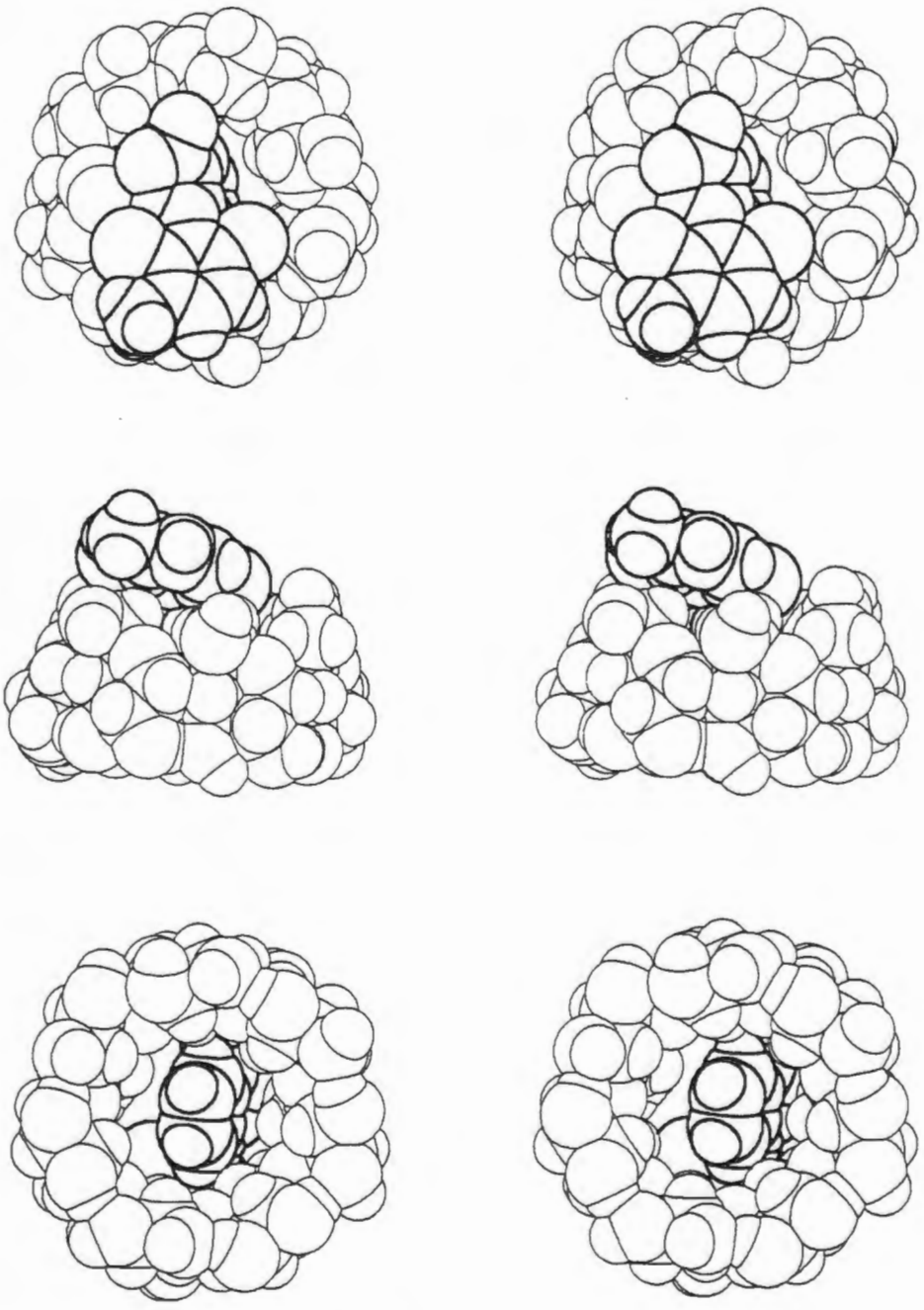

Figure 7 Space-filling diagrams of MECLOFB illustrating the inclusion of the phenyl carboxylate moiety at the primary hydroxyl side of the host viewed: top - from the primary hydroxyl side, middle - perpendicular to the host axis, bottom - from the secondary hydroxyl side.

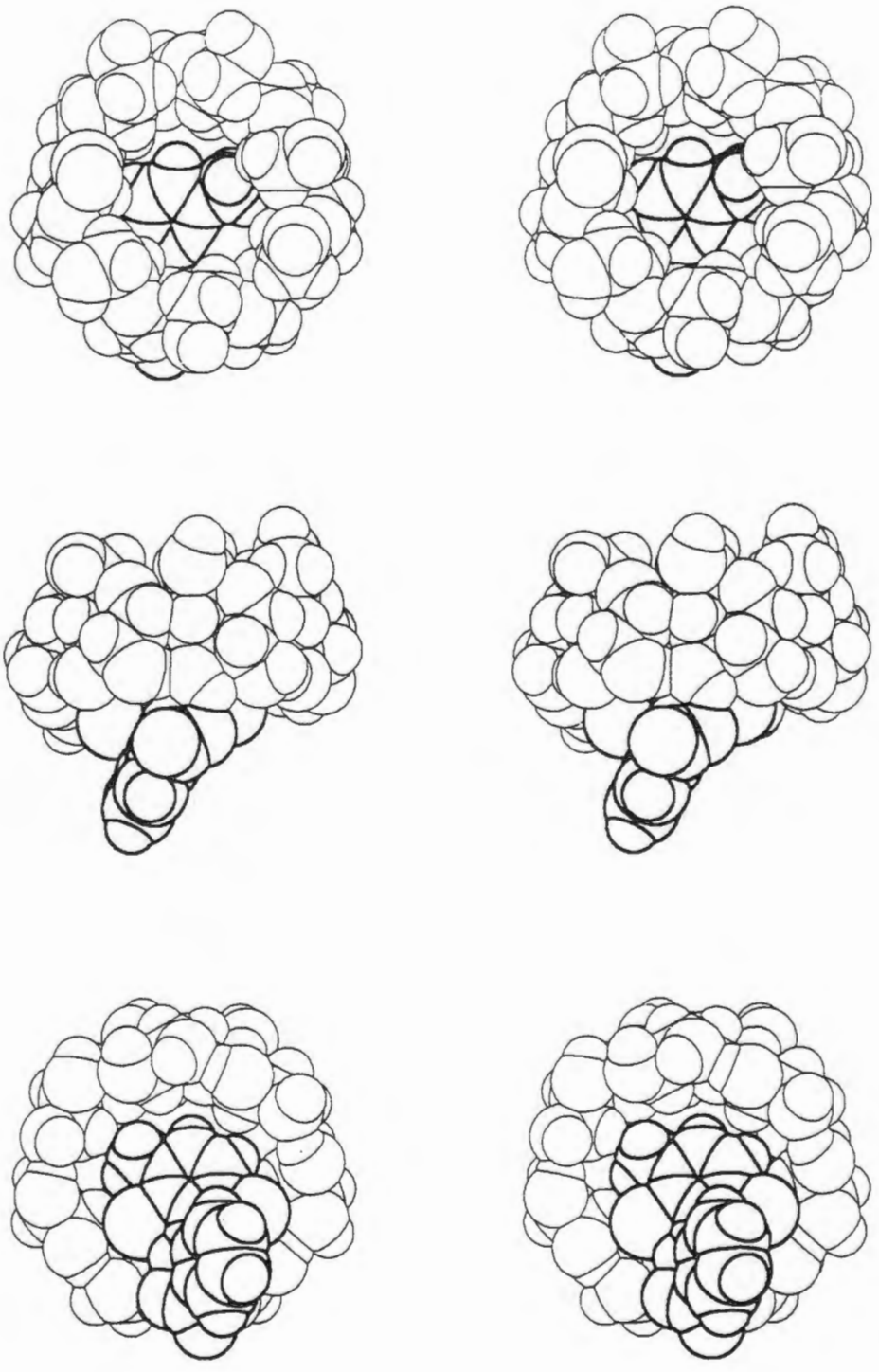

Figure 8 Space-filling diagrams illustrating the inclusion of the dichloromethylphenyl moeity at the secondary hydroxyl side of a screw-related host molecule viewed: top - from the primary hydroxyl side of the screw-related host molecule, middle - perpendicular to the host axis, bottom - from the secondary hydroxyl side.

The Na^+ ion is disordered over two sites with site occupancies of 0.6 and 0.4. Figure 9 shows how the Na^+ ion with the greater site occupancy is approximately octahedrally coordinated to two secondary hydroxyl oxygen atoms of the host molecule and four water molecules. The Na^+ ion with the smaller site occupancy is approximately tetrahedrally coordinated to the major site of a primary hydroxyl oxygen atom of the host molecule, a secondary hydroxyl oxygen atom of a symmetry related cyclodextrin molecule and two water molecules.

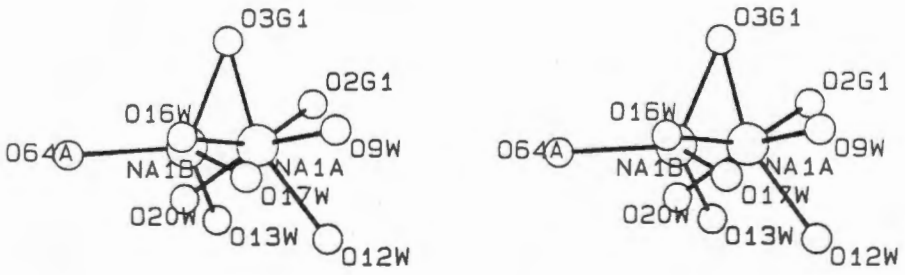

Figure 9 Coordination of the disordered Na+ ion in MECLOFB.

The $Na^+ \cdots O$ distances and the $O \cdots Na^+ \cdots O$ angles for the two sodium positions are listed in Table 5. It is difficult to say whether the Na^+ ion is truly disordered in the MECLOFB complex or whether (since during the data collection there was a relatively short period of fairly rapid decay) the major sodium site reflects the true scenario in the complex and the minor site represents the situation following the period of decay during data collection. The second step in the water loss seen in thermogravimetric analysis corresponds to about four water molecules (actually 3.8). This could support an argument in favour of the latter hypothesis, since the Na^+ ion in the major position is coordinated to four water molecules. However, if one examines the disordered scenario, addition of the fractional site occupancies of the water molecules coordinated to both sites of the disordered Na^+ ion gives a total of [(4 X 0.6) + (2 X 0.4)] = 3.2 water molecules. Since the two steps of the weight loss in the TG trace overlap, the estimation of the number of water molecules involved in the second step may not be sufficiently accurate to distinguish between the two possibilities. In addition, the fractional site occupancies used in the above calculation were based on the assumption that the water molecules would have the same fractional site occupancy as the Na^+ ion to which they are coordinated (those of O(13W), O(16W), O(17W) and O(20W) could well be lower).

Table 5 $Na^+ \cdots O$ distances (Å) and the $O \cdots Na^+ \cdots O$ angles (°) for the two Na^+ ion positions in MECLOFB.

Na(1A)···O(2G1)$^{(a)}$	2.34(2)	Na(1B)···O(3G1)$^{(a)}$	2.76(3)
Na(1A)···O(3G1)$^{(a)}$	2.60(2)	Na(1B)···O(64A)	2.83(3)
Na(1A)···O(9W)$^{(b)}$	2.21(2)	Na(1B)···O(13W)	2.71(5)
Na(1A)···O(12W)$^{(b)}$	2.68(3)	Na(1B)···O(17W)	2.46(5)
Na(1A)···O(16W)	2.32(4)		
Na(1A)···O(20W)	2.15(4)		

O(2G1)$^{(a)}$···Na(1A)···O(3G1)$^{(a)}$	69.4(5)
O(2G1)$^{(a)}$···Na(1A)···O(16W)	147 (1)
O(2G1)$^{(a)}$···Na(1A)···O(20W)	118 (1)
O(2G1)$^{(a)}$···Na(1A)···O(9W)$^{(b)}$	83.8(7)
O(2G1)$^{(a)}$···Na(1A)···O(12W)$^{(b)}$	89.5(8)
O(3G1)$^{(a)}$···Na(1A)···O(9W)$^{(b)}$	97.9(8)
O(3G1)$^{(a)}$···Na(1A)···O(12W)$^{(b)}$	157.1(9)
O(3G1)$^{(a)}$···Na(1A)···O(16W)	77 (1)
O(3G1)$^{(a)}$···Na(1A)···O(20W)	108 (1)
O(9W)$^{(b)}$···Na(1A)···O(12W)$^{(b)}$	70.3(8)
O(9W)$^{(b)}$···Na(1A)···O(16W)	102 (1)
O(9W)$^{(b)}$···Na(1A)···O(20W)	151 (1)
O(12W)$^{(b)}$···Na(1A)···O(16W)	123 (1)
O(12W)$^{(b)}$···Na(1A)···O(20W)	90 (1)
O(16W) ···Na(1A)···O(20W)	72 (2)

O(13W) ···Na(1B)···O(17W)	95 (2)
O(64A) ···Na(1B)···O(13W)	106 (1)
O(64A) ···Na(1B)···O(17W)	123 (1)
O(3G1)$^{(a)}$···Na(1B)···O(64A)	114 (1)
O(3G1)$^{(a)}$···Na(1B)···O(13W)	111 (1)
O(3G1)$^{(a)}$···Na(1B)···O(17W)	106 (1)

Equivalent positions

(a) -x, y+1/2, -z+1/2 (b) x-1/2, -y+1/2, -z

As already mentioned, the drug anion has an intramolecular hydrogen bond (parameters listed in table 4) which, as in the case of diclofenac sodium, is also observed in two crystal structures where the meclofenamate anion is present[6]. The orientation of the two phenyl rings of the drug with respect to one another in the complex is described by the torsion angles $\tau 1$ and $\tau 2$, C(5)-C(4)-N(3)-C(10) and C(4)-N(3)-C(10)-C(11), with values of -126(1) and -176.1(8)°, respectively. The orientation of the carboxylate group with respect to its attached phenyl ring is described by the torsion angle $\tau 3$, C(10)-C(11)-C(17)-O(19), with a value of -42(1)°. Values for the corresponding angles in the two crystallographically independent molecules in two crystal structures which contain the meclofenamate anion have been calculated from the atomic coordinates which were retrieved from the CSD[5]. The two crystal structures are ethanolamine meclofenamate (ETHMECLO) and choline meclofenamate (CHOMECLO)[6]. The values obtained for the three torsion angles are:

ETHMECLO	Molecule A	$\tau 1$	113	$\tau 2$	-175	$\tau 3$	10
	Molecule B	$\tau 1$	99	$\tau 2$	-175	$\tau 3$	0
CHOMECLO	Molecule A	$\tau 1$	111	$\tau 2$	-174	$\tau 3$	0
	Molecule B	$\tau 1$	-109	$\tau 2$	175	$\tau 3$	-9

The conformations of the two independent molecules in ETHMECLO are very similar and, since the space group $P\bar{1}$ is centrosymmetric, the mirror images of the two molecules are also generated. CHOMECLO does not crystallise in a centrosymmetric space group, but the two independent molecules in this case are very nearly mirror images of one another. The conformation of the meclofenamate anion in the MECLOFB complex is most similar to that of the mirror image of molecule A in ETHMECLO, the largest difference lying in $\tau 3$. In the crystal structures of ETHMECLO and CHOMECLO, the carboxylate group is always coplanar or nearly coplanar with its attached phenyl ring. However in MECLOFB it is twisted out of the plane of the phenyl ring to maintain the drug intramolecular N-H···O hydrogen bond.

TG of the complex indicated the presence of 16 water molecules in the crystal structure of MECLOFB. However, location of all the water molecules was difficult, due to crystal decay, which probably involves mostly loss of water molecules. As is usually the case in cyclodextrin complexes, the water molecules are responsible for

the stabilisation of the crystal packing by means of extensive hydrogen bonding. Hydrogen bonding data and other O···O contacts less than 3.0 Å are given in Table 6.

Table 6 Hydrogen bonding data for β-cyclodextrin-meclofenamate sodium complex.

		Distance (Å)			Angle (°)
O H	O	O-H	H···O	O···O	O-H···O
O(2G7)-H(21)	O(3G7)	1.01	1.87	2.87 (1)	172
O(3G1)-H(31)	O(2G2)	0.93	1.88	2.80 (1)	167
O(2G3)-H(23)	O(3G2)	0.96	1.90	2.773(9)	150
O(3G3)-H(33)	O(2G4)	0.96	1.89	2.846(9)	175
O(6G3)-H(63)	O(11W)	0.96	2.00	2.78 (3)	136
O(3G4)-H(34)	O(2G5)	0.94	1.95	2.830(9)	156
O(3G5)-H(35)	O(2G6)	0.92	1.98	2.886(8)	167
O(2G7)-H(27)	O(8W)	0.98	2.09	2.98 (2)	150
O(6G7)-H(67)	O(2W)	0.98	2.07	2.73 (1)	123
O(6G2)-H(62)*	O(3G5) (a)	0.99	1.77	2.711(8)	158
O(6G1)-H(61)*	O(3G4) (a)	1.00	1.93	2.90 (1)	162
O(2G2)-H(22)	O(8W) (b)	1.00	2.17	3.09 (2)	152
O(2G6)-H(26)	O(4W) (c)	0.93	1.95	2.79 (1)	150
O(2G4)-H(24)	O(8W) (d)	0.98	2.33	3.07 (2)	132
O(2G5)-H(25)	O(1W) (d)	0.98	1.82	2.776(9)	163
O(6G6)-H(66)**	O(6G2) (e)	0.98	1.87	2.843(9)	173
O(6G5)-H(65)	O(4W) (e)	0.98	1.88	2.83 (1)	160
O(3G6)-H(36)	O(5W) (f)	0.96	1.93	2.88 (1)	176
O(3G7)-H(37)	O(10W)(g)	0.98	2.2	2.82 (4)	120

* Direct hydrogen bond between successive host molecules in the columns of complex units along the *b*-axis.

** Direct hydrogen bond between adjacent columns of complex units along the *a*-axis.

cont'd

Table 6 cont'd

O(6G1)···O(2W)	2.78 (1)		O(1W) ···O(2W)		2.81(1)
O(6G2)···O(4W)	2.97 (1)		O(3W) ···O(6W)		2.76(1)
O(6G3)···O(13W)	2.65 (4)		O(4W) ···O(11W)		2.77(2)
O(6G3)···O(20W)	2.95 (5)		O(5W) ···O(18W)		2.85(5)
O(5G4)···O(20W)	2.98 (4)		O(8W) ···O(14W)		2.64(5)
O(64A)···O(16W)	3.00 (4)		O(9W) ···O(12W)		2.84(3)
O(64B)···O(16W)	2.60 (4)		O(10W)···O(17W)		2.50(5)
O(5G5)···O(12W)	2.98 (3)		O(12W)···O(15W)		2.86(6)
O(6G5)···O(9W)	2.77 (2)		O(12W)···O(18W)		2.78(6)
O(6G7)···O(3W)	2.88 (1)		O(16W)···O(20W)		2.62(6)
O(1W) ···O(6G6) (h)	2.725(9)		O(10W)···O(11W)	(k)	2.80(4)
O(1W) ···O(3W) (h)	2.88 (1)		O(11W)···O(17W)	(l)	2.60(5)
O(2W) ···O(8W) (h)	2.80 (2)		O(12W)···O(13W)	(l)	2.78(4)
O(3W) ···O(7W) (i)	2.86 (2)		O(13W)···O(15W)	(l)	2.88(6)
O(6W) ···O(2G3) (a)	2.84 (1)		O(13W)···O(18W)	(l)	2.79(6)
O(7W) ···O(3G3) (j)	2.80 (2)		O(14W)···O(18W)	(f)	2.84(7)
O(7W) ···O(9W) (g)	2.88 (2)		O(15W)···O(17W)	(l)	2.68(6)
O(7W) ···O(14W)(b)	2.60 (5)		O(15W)···O(20W)	(l)	2.80(6)
O(9W) ···O(17W)(k)	2.48 (5)				

Equivalent positions

(a)	-x,	y+1/2,	-z+1/2
(b)	x-1,	y,	z
(c)	-x,	y-1/2,	-z+1/2
(d)	-x+1/2,	-y,	z-1/2
(e)	x+1,	y,	z
(f)	-x+1,	y-1/2,	-z+1/2
(g)	-x+1/2,	-y,	z+1/2
(h)	x-1/2,	-y+1/2,	-z+1
(i)	x+1/2,	-y+1/2,	-z+1
(j)	-x-1/2,	-y,	z+1/2
(k)	x+1/2,	-y+1/2,	-z
(l)	x-1/2,	-y+1/2,	-z

In contrast to DICLOFB, host molecules related by the twofold screw axis parallel to the *b*-axis and which passes through the cyclodextrin cavity do not shield the guest from the intermolecular space completely since the axis of the host makes an angle of 9.4° with the *b*-axis, leaving the guest exposed on one side (Figure 10). Successive guest molecules in this direction also do not show the same weakly attractive C-H•••π interaction as in DICLOFB, but nevertheless there is a close contact between a hydrogen atom of the phenylcarboxylate group and the methyl group of the dichloromethylphenyl moiety (Figure 11). This close contact is indicated in Table 4.

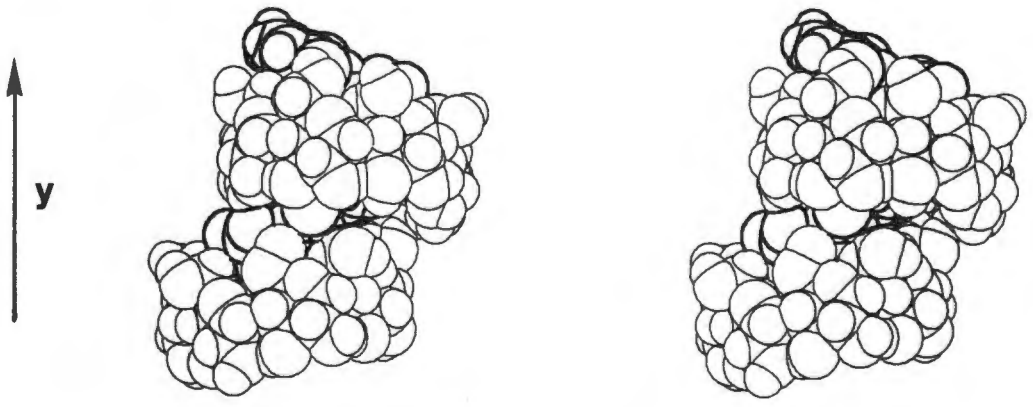

Figure 10 Two complex units related by the twofold screw axis parallel to the *b*-axis.

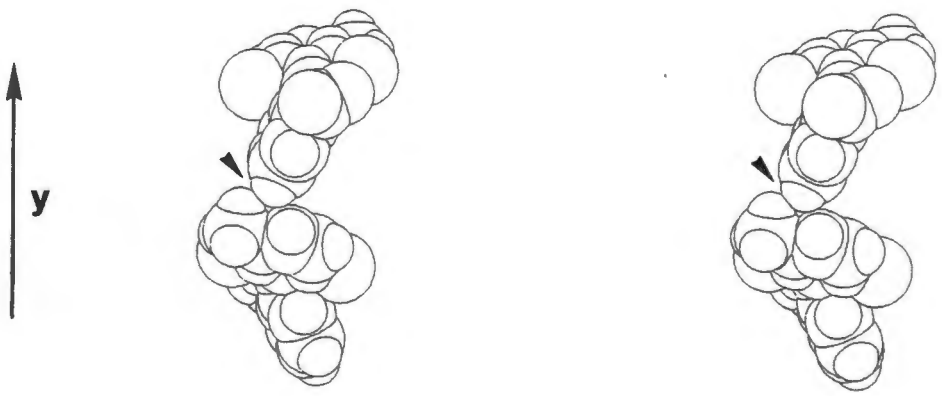

Figure 11 Two guest molecules related by the twofold screw axis parallel to the *b*-axis.

Monomeric β-cyclodextrin complexes usually pack in a herring-bone arrangement[8], but two which pack in molecular layers roughly perpendicular to the axes of the host

molecules have been reported, those of the pyridine-[9] and 1,4-diazabicyclo[2.2.2]octane-β-CD[10] complexes. SULFB (Chapter 3), which is isomorphous with the latter, and DICLOFB are also examples of monomeric β-CD complexes with layered structures. Although the MECLOFB complex is monomeric and columns of complex units stack head-to-tail in screw channel fashion along the *b*-axis as in the 1,4-diazabicyclo[2.2.2]octane-β-CD complex, SULFB and DICLOFB (*c*-axis in this case), the crystal packing arrangement does not form molecular layers. The two additional twofold screw axes parallel to the *a*- and *c*-axes, result in adjacent columns along the *c*-axis being antiparallel and shifted by approximately half a complex unit along *b* (Figure 12).

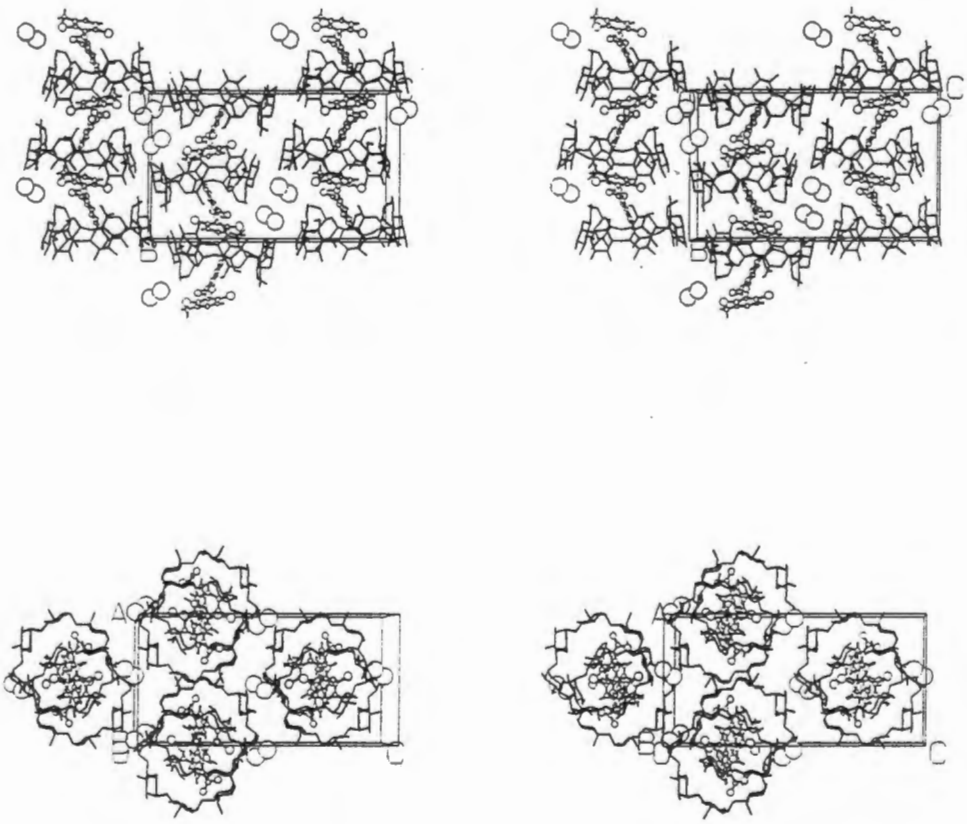

Figure 12 Stereo packing diagrams of MECLOFB viewed: above - down the *a*-axis, below - down the *b*-axis (the disordered Na^+ ion is represented by two large open circles, water molecules omitted).

This packing arrangement, although unique for a complex of unsubstituted β-cyclodextrin is not unlike the arrangement seen in complexes of heptakis(2,3,6-tri-O-methyl)-β-cyclodextrin (TRIMEB), which also crystallise in the space group $P2_12_12_1$[11,12,13,14]. The cell parameters for the *p*-iodophenol-TRIMEB complex[11] (PIPTMB) and those of the present complex are compared below. The *b*-axis in PIPTMB is longer by approximately 3.5 Å because of the additional methyl groups which increase the height of the host. The *c*-axis is shorter by approximately 1.5 Å despite the fact that the much larger tilt angles in TRIMEB, together with the presence of the methyl groups, are expected to increase the diameter of the host, at least at the O(2),O(3) side of the molecule. On closer inspection, however, the reason for the apparent anomaly becomes clearer. Adjacent columns along the *c*-axis are not as closely packed in MECLOFB because the Na^+ ions are accommodated between them (Figure 12). MECLOFB also contains in its crystal structure many more water molecules than PIPTMB (sixteen as opposed to four) which fill the intermolecular spaces.

	a (Å)	b (Å)	c (Å)
MECLOFB	15.087	17.967	29.634
PIPTMB	14.997	21.368	28.205

There are two direct hydrogen bonds between the primary hydroxyl face of one host and the secondary hydroxyl face of the screw-related cyclodextrin molecule along the *b*-axis i.e between hosts of adjacent complex units within a column. Apart from these there is also a hydrogen bond between a carboxylate oxygen atom, O(19), and a secondary hydroxyl group of the screw-related cyclodextrin molecule (Table 4). The only direct hydrogen bonding between adjacent columns is along the *a*-axis. One is between two host molecules and the other is between host and guest. In the former case, since as in DICLOFB each complex unit is equivalent, any given host acts as both donor and acceptor of the same hydrogen bond and therefore a particular host molecule is hydrogen bonded to the host molecule on either side in this direction. In the latter case, there is a hydrogen bond between O(18) of the guest and a secondary hydroxyl oxygen atom of a host molecule in an adjacent column (Table 4). The direct hydrogen bonds between host molecules are indicated in the hydrogen bonding table (Table 6).

XRD

Figure 13 shows the calculated and experimental XRD patterns for MECLOFB. The very close match in peak positions (2θ values) confirms the high purity of the sample as shown by the elemental analysis results. Differences in relative intensities are due to preferred orientation of the crystallites.

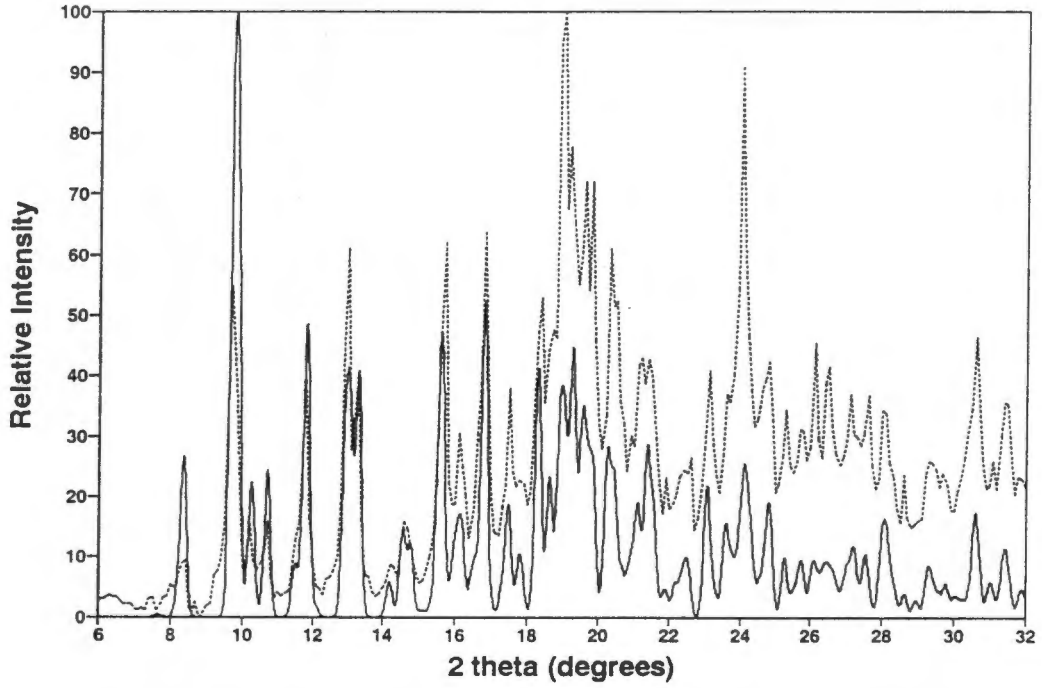

Figure 13 Calculated (——) and experimental (· · · · ·) XRD patterns for MECLOFB.

References

1. *The Merck Index*, 11th edition, edited by S. Budavari, M. J. O'Neil, A. Smith and P.E. Heckelman, Merck and Co., Inc., New Jersey, U.S.A., 1989.
2. K. Ikeda, K. Uekama, M. Otagiri and M. Hatano, *J. Pharm. Sci.*, 1974, **63**, 1168.
3. K. Ikeda, K. Uekama and M. Otagiri, *Chem. Pharm. Bull.*, 1975, **23**, 201.
4. M. Otagiri, J. H. Perrin, K. Uekama, K. Ikeda and K. Takeo, *Pharm. Acta Helv.*, 1976, **51**, 343.
5. *Cambridge Structural Database and Cambridge Structural Database System*, October 1995, Version 2.3.7, Cambridge Crystallographic Data Centre, University Chemical Laboratory, Cambridge, England.
6. V. Dhanaraj and M. Vijayan, *Biochim. Biophys. Acta*, 1987, **924**, 135.
7. W. Saenger, *Inclusion Compounds*, edited by J. L. Atwood, J. E. D. Davies and D. D. MacNicol, Academic Press, London, Volume 2, Chapter 8, 1984.
8. D. Mentzafos, I. M. Mavridis, G. Le Bas, and G. Tsoucaris, *Acta Crystallog.*, 1991, B**47**, 746.
9. C. de Rango, P. Charpin, J. Navaza, N. Keller, I. Nicolis, F. Villain and A. W. Coleman, *J. Am. Chem. Soc.*, 1992, **114**, 5475.
10. K. Harata, *Bull. Chem. Soc. Jpn.*, 1982, **55**, 2315.
11. K. Harata, K. Uekama, M. Otagiri and F. Hirayama, *Bull. Chem. Soc. Jpn.*, 1983, **56**, 1732.
12. K. Harata, K. Uekama, T. Imai, F. Hirayama and M. Otagiri, *J. Incl. Phenom.*, 1988, **6**, 443.
13. K. Harata, F. Hirayama, H. Arima, K. Uekama and T. Miyaji, *J. Chem. Soc., Perkin Trans. 2*, 1992, 1159.
14. D. Mentzafos, I. M. Mavridis and H. Schenk, *Carb. Res.*, 1994, **253**, 39.

Chapter 6 Heptakis(2,3,6-tri-O-methyl)-β-cyclodextrin

Introduction

Heptakis(2,3,6-tri-O-methyl)-β-cyclodextrin (TRIMEB) as a pharmaceutical carrier molecule offers various advantages over its unmethylated counterpart, amongst which are higher aqueous solubility and greater protection of the encapsulated drug from hydrolysis both in solution and in the solid state[1]. This chapter is devoted to the characterisation of a monohydrate of TRIMEB. Although the crystal structures of a number of complexes with this important host have been reported[2,3,4,5], that of the host alone has hitherto remained undetermined[6]. Since the structures of two complexes with TRIMEB are included in this thesis, namely those with (*S*)-naproxen (Chapter 7) and (*L*)-menthol (Chapter 8), the structure of TRIMEB monohydrate has also been solved for comparison of the conformation of uncomplexed TRIMEB with the complexed host in the solid state.

Preparation of TRIMEB monohydrate

Crystals of TRIMEB monohydrate were grown at approximately 50°C by slow evaporation of a dilute solution of TRIMEB in distilled water prepared at room temperature. The monohydrate crystallises as colourless needles shown in Figure 1. The density of the crystals was not measured because of the high solubility of the host in both aqueous solution and organic solvents.

Figure 1 TRIMEB monohydrate (32 X)

Thermal Analysis

TG and DSC traces for TRIMEB monohydrate are given in Figure 2. The TG trace

shows a gradual weight loss of 1.2% between 30 and 147°C. This corresponds to 1.0 water molecules per TRIMEB molecule. The DSC trace shows a very diffuse endotherm (A) in the temperature range of the water loss, followed by fusion of the dehydrated host (B) at 157°C (onset melting temperature).

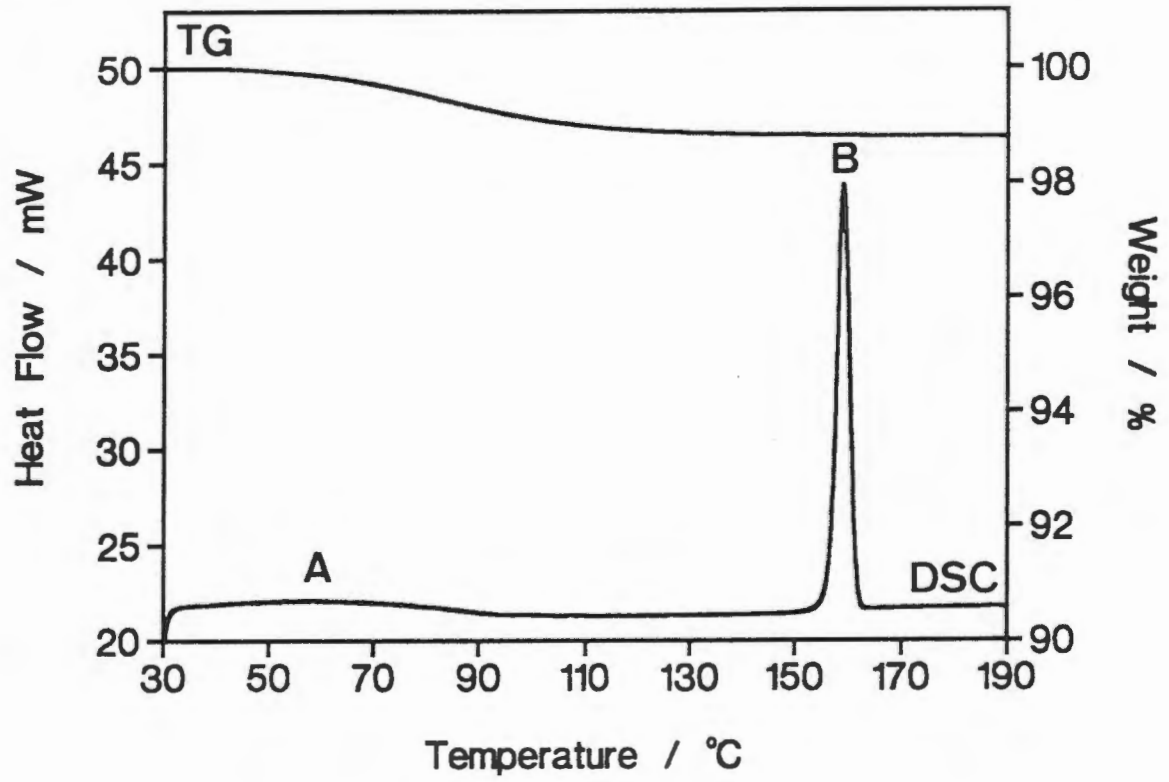

Figure 2 TG and DSC traces for TRIMEB monohydrate

Microanalysis

The water content is based on the result of thermogravimetric analysis. The molecular formula is as follows: $C_{63}H_{112}O_{35}.H_2O$

The results of the elemental analysis are reported as the average of duplicate determinations.

	Calculated (%)	Experimental (%)
Carbon	52.27	52.53
Hydrogen	7.94	7.90

Crystal structure solution

The structure of TRIMEB monohydrate proved difficult to solve. SHELX86 and PATSEE were both employed in trying to solve the structure. For PATSEE the skeleton atoms of a TRIMEB molecule in one of its complexes was used as the known fragment as it was assumed that the conformation of the cyclodextrin molecule would be similar in the monohydrate. After many unsuccessful attempts the structure was finally solved by direct methods (SHELX86). The co-ordinates of almost all of the non-hydrogen atoms were obtained from the direct methods solution (SHELX86 with parameters: TREF 5000 400 -20, SUBS 4) and the model was refined isotropically by full-matrix least-squares methods (SHELX76). The remaining non-hydrogen atoms and the water molecule were then located. Further refinement was carried out by the block-diagonal least-squares methods and anisotropic temperature factors were assigned to all non-hydrogen atoms except the disordered atoms and the water molecule. All hydrogen atoms of the host were fixed at idealised positions (C-H = 1.00 Å) in a riding-model. The methine and methylene hydrogen atoms of each methylglucose residue were assigned common variable isotropic temperature factors and all the methyl hydrogen atoms of the TRIMEB molecule were assigned a common variable isotropic temperature factor. The hydrogen atoms of the water molecule were not located.

Crystal structure

Crystal data, experimental and refinement parameters for TRIMEB monohydrate are listed in Table 1.

Table 1 Crystal data, experimental and refinement parameters (structure refined on F using SHELX76)

Molecular formula	$C_{63}H_{112}O_{35}.H_2O$
M_r ($g.mol^{-1}$)	1447.57
Crystal system	Orthorhombic
Space group	$P2_12_12_1$
Z	4

cont'd

Table 1 cont'd

a (Å)	14.818(4)
b (Å)	19.362(9)
c (Å)	26.51(2)
V ($Å^3$)	7606(6)
D_c ($g.cm^{-3}$)	1.264
μ (Mo Kα) (cm^{-1})	0.97
F(000)	3120
Crystal dimensions (mm)	0.43 x 0.50 x 0.50
Temperature of data collection	294K
Range scanned θ (°)	$1 \leq \theta \leq 25$
Scan type	ω-2θ
Index range	h 0,17: k 0,23: l 0,31
Scan width (°)	0.8 + 0.35 tanθ
Aperture width (mm)	1.12 + 1.05 tanθ
Std reflections monitored for decay	4,8,12 5,9,15 6,13,3
Decay (%)	3.3
No. of reflections collected	7366
No. of unique reflections	6366
R_{int}	0.00
No. of reflections with I > 2σ(I)	4286
No. of L.S. parameters	771
R	0.063
wR	0.067
w	$[\sigma^2(F_o) + 1.882 \times 10^{-3} F_o^2]^{-1}$
S	1.57
Shift/e.s.d. max, average	1.836, 0.010
$\Delta\rho_{max}$ final ($e.Å^{-3}$)	0.31
$\Delta\rho_{min}$ final ($e.Å^{-3}$)	-0.25

Figure 3 is a stereodiagram of TRIMEB monohydrate showing the numbering scheme (which is the same as that used for the host in the *p*-iodophenol-TRIMEB complex[7]) used in the crystal structure. The same numbering scheme will be used for this host in the (*S*)-naproxen and (*L*)-menthol complexes. All methylglucose

residues are in the $^4C_1$ chair conformation, except that of G2, which adopts the $^1C_4$ conformation. This is a most unusual finding as the inverted chair conformation is less stable (all except one of the substituents of the glucopyranose ring are in the axial position) and has not been previously observed in the cyclodextrins or their complexes in the solid state. The O(6) and C(9) atoms of residue G2 are disordered over two sites each, with occupancies of 0.63 and 0.37. The C(6) and O(6) atoms of G3 are similarly disordered with occupancies of 0.67 and 0.33. However, C(9G3) is not disordered.

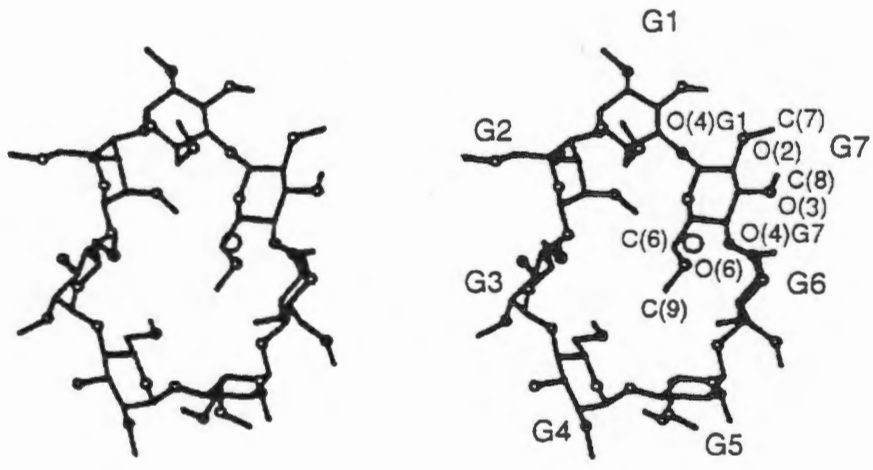

Figure 3 Stereodiagram of TRIMEB monohydrate viewed perpendicular to the least-squares plane through the seven O(4) atoms (the water molecule is represented by the single open circle).

The O(2)-C(7) bonds are directed away from the cavity and the O(3)-C(8) bonds are directed towards the cavity as observed in TRIMEB complexes[2,3,4,5], except in G2, where the inverted chair conformation causes O(2) and O(3) to be axial (torsion angle O(2G2)-C(2G2)-C(3G2)-O(3G2) 162.6°) instead of equatorial. This, together with a rather large negative tilt angle of 24.5° for G2, results in the C(7) methyl group pointing into the cavity and the C(8) methyl group pointing outwards. The C(6)-O(6) bonds of G1, G5, G6 and G7 are directed away from the cavity and are in the (-)-*gauche* conformation[8], while those of G3 and G4 are directed towards the cavity in the (+)-*gauche* conformation. The C(6)-O(6) group of G2 is also in the (+)-*gauche* conformation, but is directed away from the cavity on account of the inverted chair conformation and negative tilt angle of G2. The O(6)-C(9) bonds are *trans* to the C(5)-C(6) bonds, except those of G1 and G5, where the relationship is *gauche*.

Table 2 lists values for the tilt angles, O(4)···O(4')···O(4") angles of the O(4) heptagon, radii of the O(4) heptagon, O(4)···O(4') distances and deviations of the O(4) atoms from the least-squares plane through the O(4) atoms. The largest positive and negative tilt angles reported in inclusion complexes of TRIMEB are 51.7° and -16.3°, respectively[2,3,4,5]. O(4)···O(4')···O(4") angles in TRIMEB monohydrate range from 91.9° to 161.6°. These extreme values are approximately 22° lower and 10° higher respectively than the lowest and highest values found in TRIMEB complexes. The average, 124.5°, is slightly less than the averages for TRIMEB complexes which span a narrow range from 126.9° to 127.1°, close to the ideal value of 128.6° for a regular heptagon. The largest deviation from the least-squares plane of the seven O(4) atoms is 1.09 Å, compared with a maximum of only 0.66 Å in TRIMEB complexes. The radii of the O(4) heptagon range from 3.41 Å to 5.94 Å with an average of 4.82 Å. The *m*-iodophenol TRIMEB complex[4] (MIPTMB) has a minimum radius of 4.16 Å and a maximum radius of 5.47 Å with an average of 5.00 Å. The averages for the other TRIMEB complexes range from 4.98 Å to 5.01 Å. From these data it is evident that the conformation of the uncomplexed TRIMEB molecule is distorted to a remarkable extent, even when compared with the rather distorted conformations observed in its complexes.

Table 2 Geometrical data for TRIMEB in TRIMEB monohydrate.

i. Glycosidic oxygen angle(°) and radius (Å) of the O(4) heptagon (measured from the centre of gravity of seven O(4) atoms to each O(4) atom).

O(4G7)···O(4G1)···O(4G2)	119.1	G1	5.10
O(4G1)···O(4G2)···O(4G3)	91.8	G2	5.94
O(4G2)···O(4G3)···O(4G4)	161.6	G3	3.41
O(4G3)···O(4G4)···O(4G5)	118.1	G4	4.78
O(4G4)···O(4G5)···O(4G6)	116.0	G5	5.55
O(4G5)···O(4G6)···O(4G7)	120.3	G6	5.04
O(4G6)···O(4G7)···O(4G1)	144.4	G7	3.94
Average	124.5	Average	4.82

cont'd

Table 2 cont'd

ii. O(4)···O(4') distance (Å) and tilt angle (°)

O(4G1)···O(4G2)	4.09	G1	57.3
O(4G2)···O(4G3)	4.68	G2	24.5
O(4G3)···O(4G4)	4.28	G3	-24.7
O(4G4)···O(4G5)	4.24	G4	38.0
O(4G5)···O(4G6)	4.28	G5	21.0
O(4G6)···O(4G7)	4.46	G6	-4.6
O(4G7)···O(4G1)	4.61	G7	72.9
Average	4.38	Average	26.4

iii. Deviation of each O(4) atom (Å) from the least-squares plane through the seven O(4) atoms.

O(4G1)	O(4G2)	O(4G3)	O(4G4)	O(4G5)	O(4G6)	O(4G7)
1.09(2)	0.48(2)	0.62(2)	0.46(2)	0.38(2)	0.55(2)	0.28(2)

The O(6)-C(9) group of G7, which has the largest positive tilt angle, acts as a "lid", closing off the O(6) side of the TRIMEB molecule and making it cup-shaped (Figures 4 and 5). The water molecule occupies a site at the periphery of the O(2), O(3) side and is almost included by the host molecule. It forms a hydrogen bond with O(2G6) (O···O 2.80(2) Å) and is situated at 3.03(2) Å from $O(3G3)^{I}$ (I = 1/2+x, 1/2-y, 1-z). Due to the high thermal motion of the water molecule (U_{iso} = 0.269(6) $Å^2$), its hydrogen atoms could not be located, but the interaction $O(1W)\cdots O(3G3)^{I}$ probably represents a hydrogen bond as the $O(2G6)\cdots O(1W)\cdots O(3G3)^{I}$ angle of 98.5° is geometrically favourable. It occupies only one site and the formulation of the title compound as a monohydrate is based on thermogravimetric analysis.

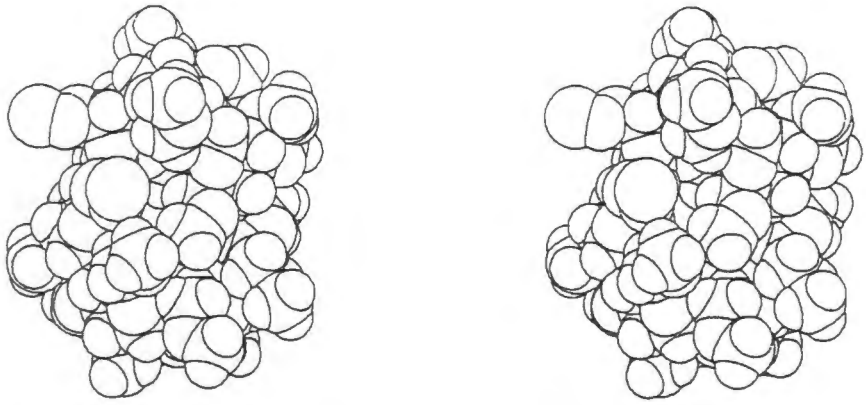

Figure 4 Space-filling diagram of TRIMEB monohydrate viewed from the O(6) side.

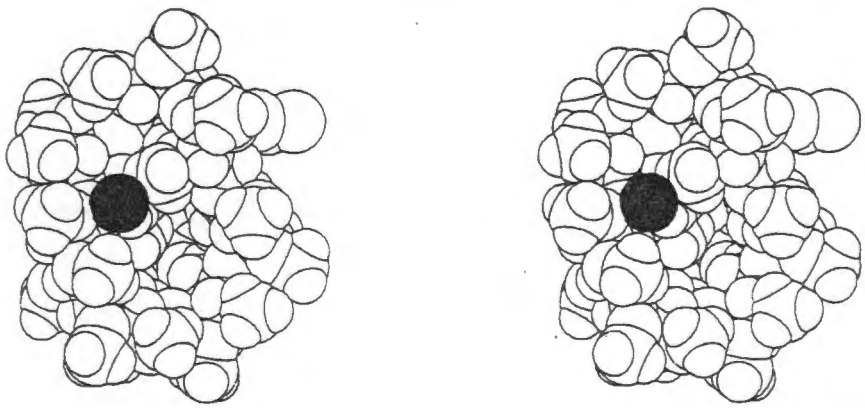

Figure 5 Space-filling diagram of TRIMEB monohydrate viewed from the O(2),O(3) side (the water molecule is represented by the shaded circle).

The conformation of the TRIMEB molecule is stabilised by a number of intramolecular C-H···O hydrogen bonds (Table 3), a common interaction found in carbohydrate crystal structures[9]. A significant interaction which appears to stabilise the $^{1}C_{4}$ conformation of G2 is C(5G2)-H···O(5G1). The orientation of residue G7, with the largest tilt angle, is partly maintained by the interaction C(1G6)-H···O(3G7). In addition, there are four C($6G_n$)-H···O($5G_{n-1}$) hydrogen bonds which are listed in Table 3. In the known crystal structures of TRIMEB complexes[2,3,4,5], five of the relevant C(6)···O(5) distances are in the range 3.0 - 3.4 Å; the two remaining (> 3.4 Å) involve O(5) atoms of those glucose residues with negative tilt angles. Therefore it is possible that these interactions are partly

responsible for the larger tilt angles observed both here and in complexes of TRIMEB, as compared with those found in complexes of unsubstituted cyclodextrins. Thus far, only steric repulsions and the absence of O(2)···O(3') hydrogen bonds have been invoked to explain unusually large tilt angles[3,10,11]. The somewhat collapsed structure of the uncomplexed TRIMEB molecule is due to numerous factors amongst which is an attempt to minimise the hydrophobic cavity in the absence of a hydrophobic guest, thereby facilitating more efficient packing whilst avoiding accommodation of water molecules in a relatively hydrophobic environment.

Table 3 Intramolecular C-H···O hydrogen bonds in TRIMEB monohydrate*.

			Distance (Å)			Angle (°)
C	H	O	C-H	H···O	C···O	C-H···O
C(6G1)-H(611)		O(5G7)	1.00	2.35	3.12 (1)	133
C(6G4)-H(642)		O(5G3)	1.00	2.48	3.37 (1)	148
C(6G5)-H(651)		O(5G4)	1.00	2.42	3.178(9)	133
C(6G6)-H(661)		O(5G5)	1.00	2.40	3.117(9)	128
C(5G2)-H(5G2)		O(5G1)	1.00	2.53	3.182(9)	123
C(1G6)-H(1G6)		O(3G7)	1.00	2.28	3.023(8)	130

* Parameters quoted are based on idealised hydrogen atoms.

The C(6)-O(6)-C(9) group of G2 is inserted in the cavity of a screw-related cyclodextrin molecule (Figure 6). This type of self-inclusion has also been observed in some complexes of DIMEB[12,13] and in γ-cyclodextrin hydrate[14]. TRIMEB molecules related by twofold screw axes pack in a herring-bone arrangement resulting in columns parallel to the *a*-axis. However, adjacent columns of TRIMEB molecules along the directions of the (0 1 1) and (0 1 -1) planes are not only antiparallel, but rotated by approximately 72° with respect to one another. This is illustrated more clearly in the stereo packing diagrams in Figures 7 and 8.

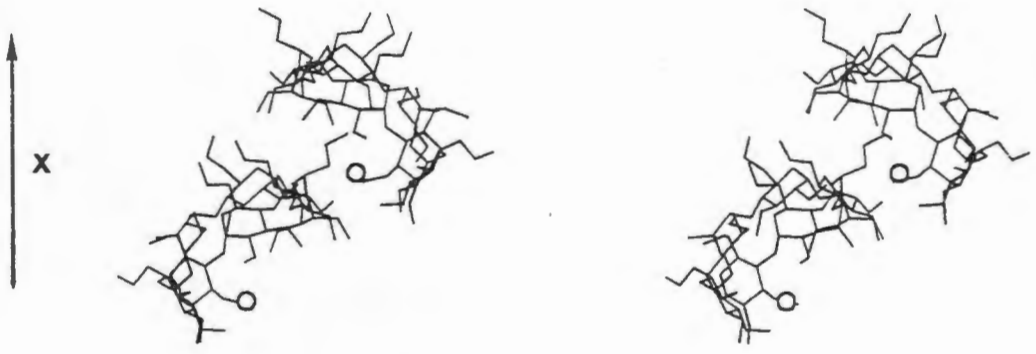

Figure 6 Two TRIMEB molecules related by the twofold screw axis parallel to the *a*-axis.

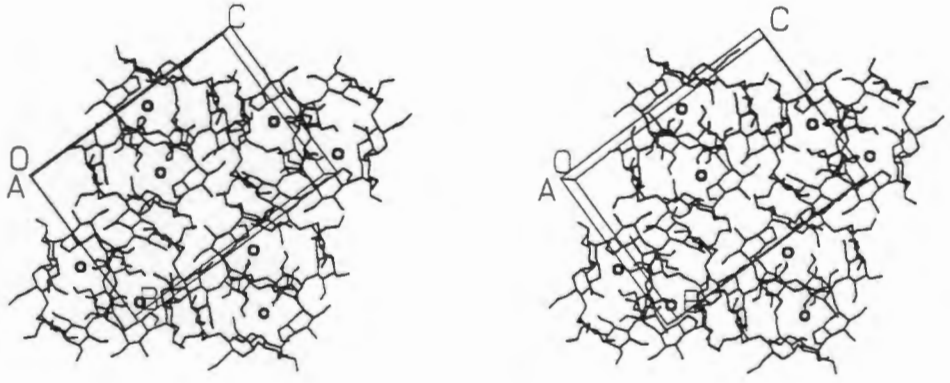

Figure 7 Packing diagram of TRIMEB monohydrate viewed down the *a*-axis.

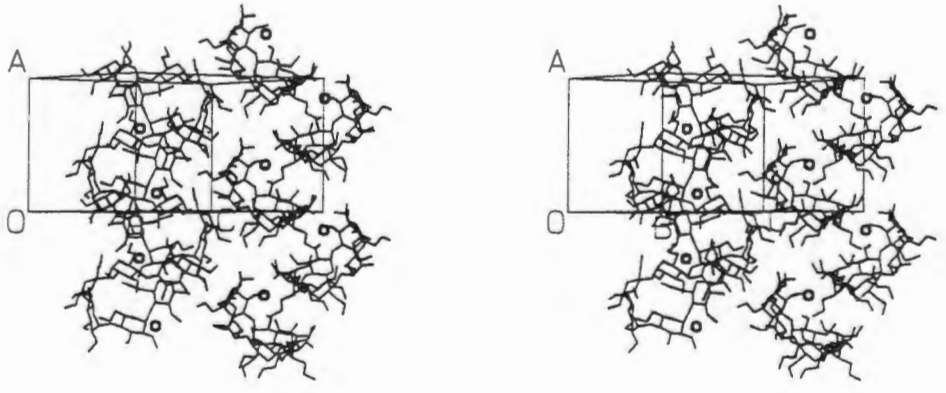

Figure 8 Packing diagram of TRIMEB monohydrate viewed perpendicular to the (0 1 -1) planes.

XRD

Experimental and calculated X-ray powder diffraction patterns are given in Figure 9. The very close match in peak positions (2θ values) means that the sample giving rise to the experimental pattern is an homogeneous preparation of TRIMEB monohydrate. The calculated pattern can be used as a fingerprint to differentiate between TRIMEB monohydrate and an inclusion complex of TRIMEB when the preparation of a TRIMEB complex is attempted, since the XRD pattern of a complex will be completely different (Chapters 7 and 8). The differences in relative intensities between calculated and experimental patterns are due to preferred orientation of the crystallites.

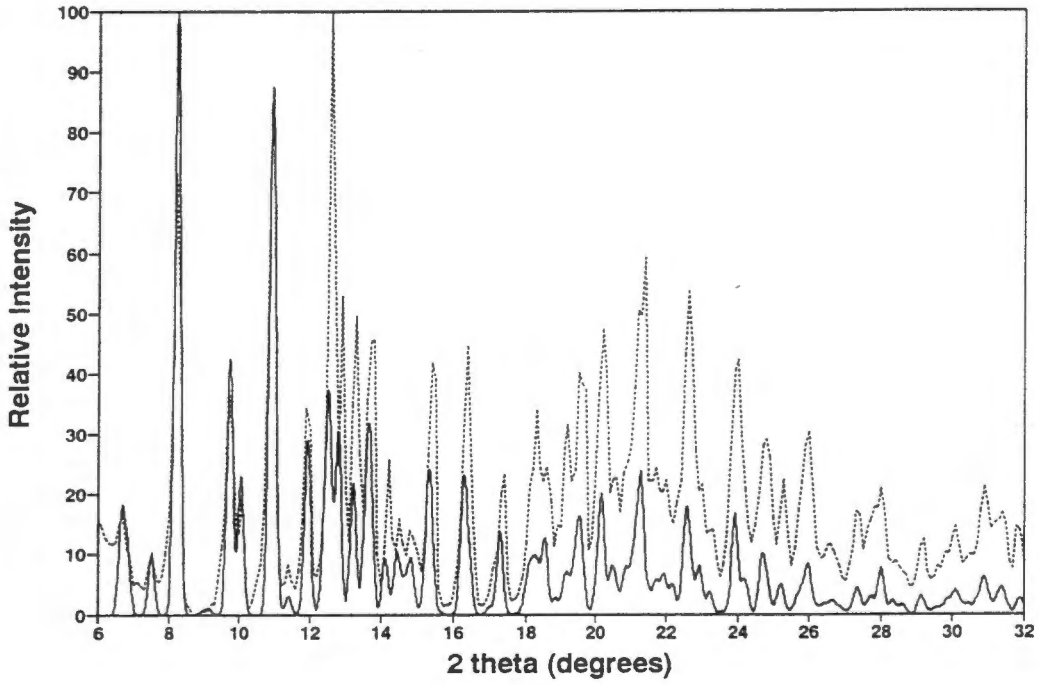

Figure 9 Calculated (——) and experimental (· · · · ·) XRD patterns for TRIMEB monohydrate.

References

1. J. Szejtli, *J. Incl. Phenom.*, 1992, **14**, 25.
2. K. Harata, K. Uekama, M. Otagiri and F. Hirayama, *Bull. Chem. Soc. Jpn.*, 1983, **56**, 1732.
3. K. Harata, K. Uekama, M. Otagiriand F. Hirayama, *J. Incl. Phenom.*, 1984, **1**, 279.
4. K. Harata, *J. Chem. Soc., Perkin Trans. 2*, 1992, 1159.
5. D. Mentzafos, I. M. Mavridis and H. Schenk, *Carb. Res.*, 1994, **253**, 39.
6. *Cambridge Structural Database and Cambridge Structural Database System*, October 1995, Version 2.3.7, Cambridge Crystallographic Data Centre, University Chemical Laboratory, Cambridge, England.
7. K. Harata, K. Uekama, M. Otagiri and F. Hirayama, *Bull. Chem. Soc. Jpn.*, 1983, **56**, 1732.
8. W. Saenger, *Inclusion Compounds*, ed. J. L. Atwood, J. E. D. Davies and D. D. MacNicol, 1984 Volume 2, 231.
9. T. Steiner and W. Saenger, *J. Am. Chem. Soc.*, 1992, **114**, 10146.
10. K. Harata, K. Uekama, M. Otagiri and F. Hirayama, *Bull. Chem. Soc. Jpn.*, 1983, **65**, 1732.
11. K. Harata, K. Uekama, T. Imai, F. Hirayama and M. Otagiri, *J. Incl. Phenom.*, 1988, **6**, 443.
12. K. Harata, *Bull. Chem. Soc. Jpn.*, 1988, **61**, 1939.
13. K. Harata, *J. Chem. Soc., Chem. Commun.*, 1993, 546.
14. K. Harata, *Bull. Chem. Soc. Jpn.*, 1987, **60**, 2763.

Chapter 7 Naproxen

Introduction

(*S*)-naproxen belongs to the arylpropionic acid derivative class of NSAIDs. The structure of naproxen, together with the numbering scheme used in the crystal structure analysis is shown in Figure 1. The interaction between naproxen and β-cyclodextrin has been investigated in solution and in the solid state[1,2,3,4,5,6,7,8]. Molecular modelling and NMR studies have generated proposals on the mode of inclusion of the drug by β-CD[1,4,5,6] and stability constants for the complex have been estimated by phase solubility, NMR, fluorescence, circular dichroism and UV techniques[1,4,5,6,7]. The ^{13}C-NMR study by Bettinetti *et al.*[1] also includes the calculation of stability constants in solution of naproxen complexes with some β-CD derivatives, amongst which is a partially methylated β-CD. The association constant for the complex of naproxen with this derivative was found to be higher than those for other derivatives and much higher than that of the parent cyclodextrin (1702 M^{-1} for β-CD and 6892 M^{-1} for the partially methylated derivative at pH 5).

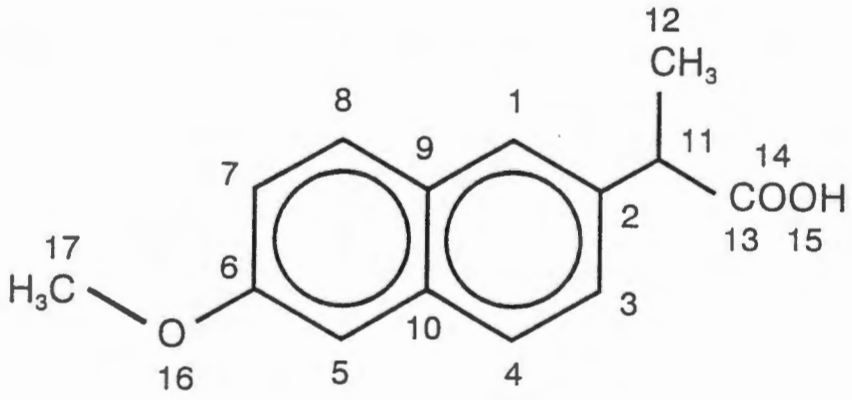

Figure 1 Naproxen

Preparation of the CD Complexes

Naproxen-β-cyclodextrin complex (NAPBmono)

0.30 mmol of naproxen and 0.30 mmol of β-cyclodextrin were dissolved in 2 ml distilled water at approximately 70°C. The pH was adjusted with a few drops of 0.1 M NaOH until almost all the naproxen had dissolved. The solution was then

filtered, diluted approximately 1 in 1.5 and cooled slowly to room temperature over three to four days in a thermos flask. A photograph of the NAPBmono complex is shown in Figure 2. Preparations of these crystals could not be kept in mother liquor for more than a few weeks as the crystals (monoclinic) would convert to the more stable NAPBorth complex (orthorhombic).

Naproxen-β-cyclodextrin complex (NAPBorth)

0.15 mmol of naproxen and 0.15 mmol of β-cyclodextrin were dissolved in 2 ml of distilled water at approximately 50°C. The pH was adjusted with 0.1 M NaOH until the naproxen had just dissolved. The solution was then left at room temperature to evaporate extremely slowly. The NAPBorth complex crystallised after about 1 year (Figure 2).

Naproxen-γ-cyclodextrin complex (NAPG)

0.01 mmol of naproxen and 0.15 mmol of γ-cyclodextrin were dissolved in 2 ml of distilled water at 70°C. The solution was filtered and cooled slowly to room temperature over three to four days in a thermos flask (Figure 2).

Naproxen-TRIMEB complex (NAPTMB)

0.04 mmol of naproxen and 0.04 mmol of TRIMEB were stirred at room temperature in 0.5 ml of distilled water until all the TRIMEB had dissolved. The temperature was raised to about 60°C and lowered again on ice several times. The solution was then kept on ice for about two hours. At this point almost all the naproxen had dissolved. The undissolved naproxen was filtered off and the solution was left at approximately 50°C for 2 hours. The crystals are colourless and prismatic (Figure 2). It was not possible to measure the density of the complex because of the high solubility of the host in both aqueous solution and organic solvents.

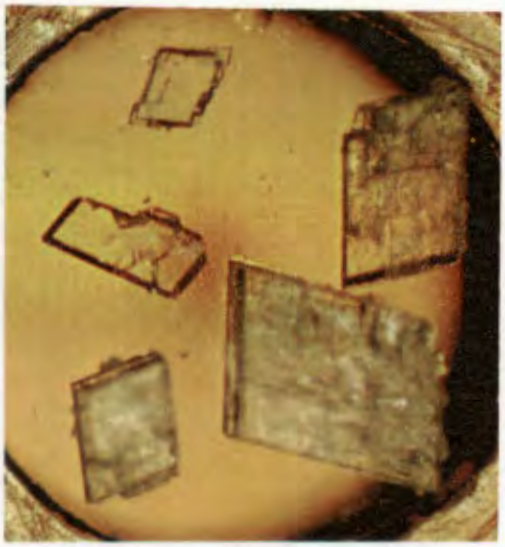

NAPBmono, 32 X

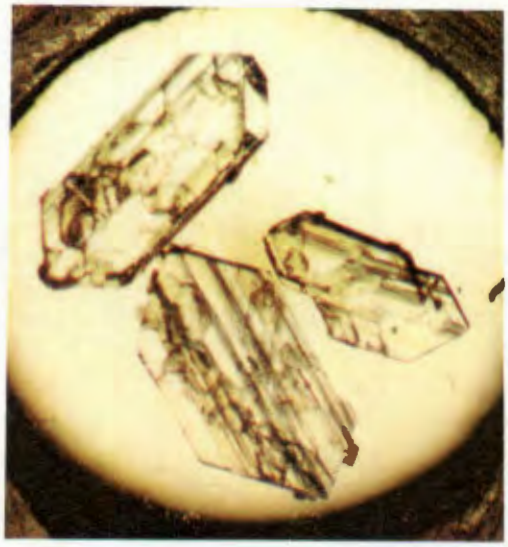

NAPBorth, 32 X

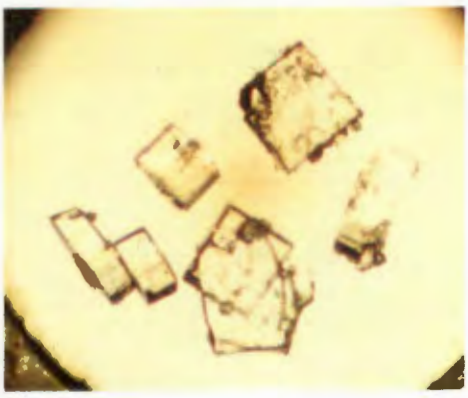

NAPG, 32 X

NAPTMB, 40 X

Figure 2 Photographs of the NAPBmono, NAPBorth, NAPG and NAPTMB complexes.

Thermal Analysis

The TG and DSC traces for the four naproxen complexes are given in Figure 3. TG data are summarised in Table 1.

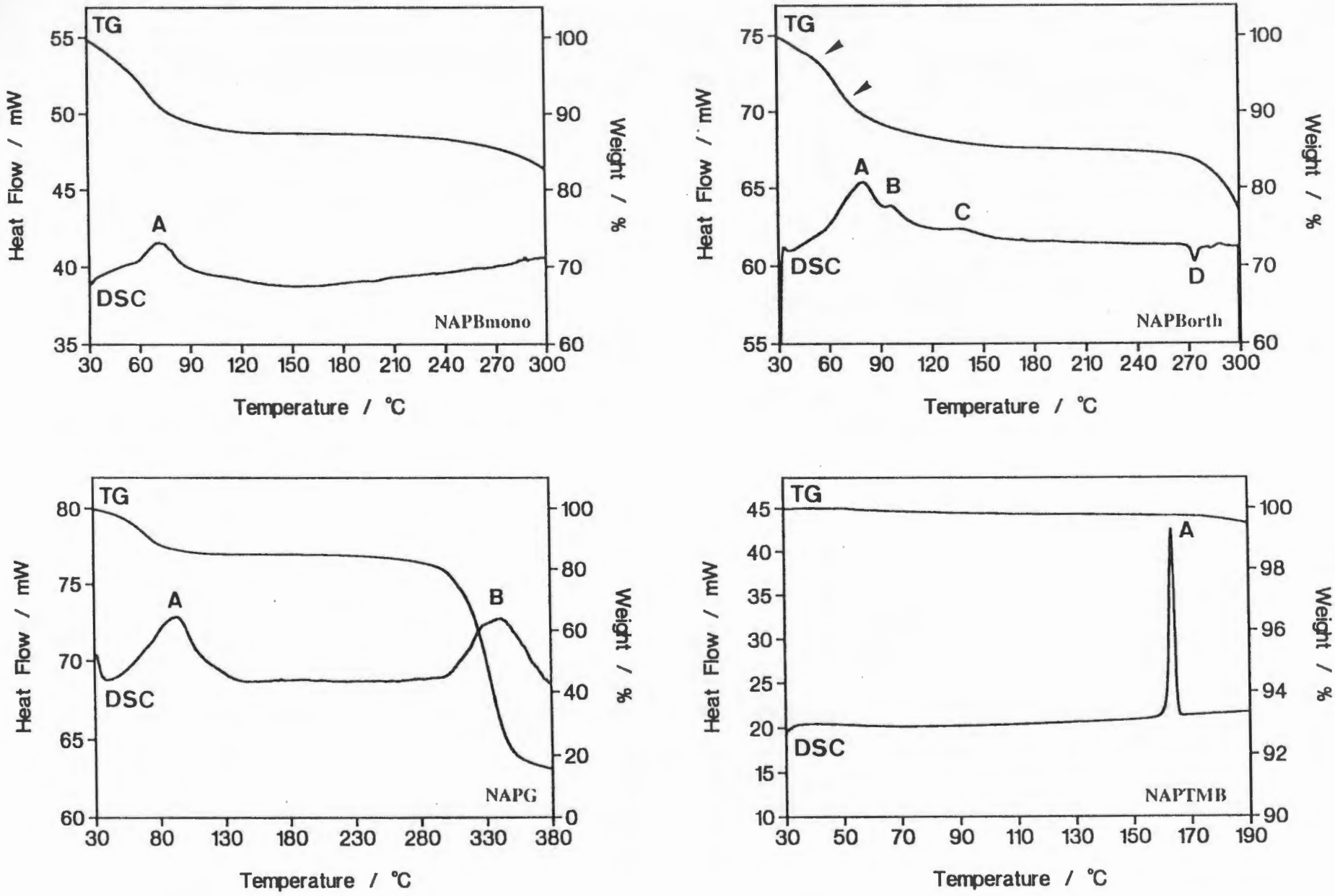

Figure 3 TG and DSC traces for NAPBmono, NAPBorth, NAPG and NAPTMB.

Table 1 TG data for the naproxen-CD complexes.

Complex	Weight loss	Temperature range	No. of water molecules
NAPBmono	12.6%	30 - 150°C	10.9
NAPBorth	14.8%	30 - 175°C	13.3
NAPG	15.1%	30 - 140°C	15.1
NAPTMB	0.2%	30 - 120°C	0.2

The DSC results for the four complexes are summarised in Table 2.

Table 2 DSC data for the naproxen-CD complexes.

Complex	Event	Temperature range (°C)	Onset (°C)	Peak (°C)
NAPBmono	Endotherm A	30 - 147	32	72
NAPBorth	Endotherm A	30 - 90	59	76
	Endotherm B	90 - 116	90	94
	Endotherm C	115 - 159	124	133
	Exotherm D	261 - 273	263	266
NAPG	Endotherm A	40 - 148	58	94
	Endotherm B	297 - 381	311	342
NAPTMB	Endotherm A	155 - 168	162	164

The endotherms (A in each case) representing water loss in the NAPBmono and NAPG complexes have similar profiles. Each has shoulders which suggest multi-step water loss, but since the separate peaks are not well-defined and the derivative of the TG trace did not show obvious points of inflection, no estimation of the number of water molecules in the separate steps was made.

In the case of NAPBorth, the DSC trace shows three endotherms for water loss (A, B and C) where the separate steps of water loss are much better resolved than in the previous two complexes. This appears to fit in with the trend which emerged in the thermal analysis of the β-CD complexes with the diclofenac and meclofenamic acid sodium salts (Chapters 4 and 5), where the endotherms for water loss in the DSC traces are much more well defined in their separation and the derivatives of the TG traces show that there are obvious points of inflection. In addition, the last water molecules lost are only relinquished some 20 to 30°C later on average than those from other complexes presented in this thesis which do not contain cations,

although this is also dependent on other factors as well, like crystal packing arrangement (although the scanning rate for the DSC trace given for NAPBorth is $20°.min^{-1}$, the scanning rate for the TG trace is the same as those for the TG traces of the other naproxen complexes i.e. $10°.min^{-1}$). The approximate number of water molecules involved in the three steps is 4, 4 and 5 respectively. Crystal structure solution of this complex is needed, which would, if there were found to be 5 water molecules coordinated to the Na^+ ion, provide more evidence in favour of this argument.

As is usually the case for cyclodextrin complexes where the host is unsubstituted, there are no well defined melting points. The NAPG complex shows a broad endotherm which occurs simultaneously with decomposition. However, the DSC trace of the NAPBorth complex does have a small exotherm (D) which seems to occur just prior to decomposition. This behaviour is similar to what was observed for the diclofenac complexes (Chapter 4). The NAPTMB complex, on the other hand, shows only a sharp endotherm (A) representing fusion of the complex. Since there are no water molecules present (the weight loss seen in TGA has been ascribed to surface water), the crystallinity of the sample is well retained until melting, hence the sharp melting point. The much lower melting point in comparison with the "melting points" of complexes of unsubstituted cyclodextrins is indicative of the weaker intermolecular interactions and is expected since methylation of all the hydroxyl groups precludes host-host intermolecular hydrogen bonding.

UV Spectrophotometry

Host:guest ratios determined by UV spectroscopy are as follows. The NAPTMB complex, whose crystal structure had been solved in this study (host:guest ratio of 1:1), was used as a reference compound to verify the reliability of the method. The wavelength used for naproxen was 230 nm and the correlation coefficient for the standard curve was 0.999.

Complex	Host:guest ratio
NAPBmono	1.00 : 0.90
NAPBorth	1.00 : 1.19
NAPG	1.00 : 1.03
NAPTMB	1.00 : 0.95

Microanalysis

The ratios in parentheses represent the host:guest:H_2O stoichiometry. The water content is based on the results of thermogravimetric analysis. Molecular formulae are as follows:

NAPBmono (1:1:10.9)	$C_{42}H_{70}O_{35}.C_{14}H_{14}O_3.10.9H_2O$
NAPBorth (1:1:13.4)	$C_{42}H_{70}O_{35}.C_{14}H_{13}O_3^-Na^+.13.4H_2O$
NAPG (1:1:15.1)	$C_{48}H_{80}O_{40}.C_{14}H_{14}O_3.15.1H_2O$
NAPTMB (1:1:0)	$C_{63}H_{112}O_{35}.C_{14}H_{14}O_3$

The results of the microanalyses are reported as the average of duplicate determinations.

	Calculated (%)		Experimental (%)	
	C	H	C	H
NAPBmono	43.07	6.83	43.10	6.62
NAPBorth	41.30	6.80	41.53	6.57
NAPG	41.38	6.96	41.68	6.79
NAPTMB	55.72	7.65	55.59	7.68

The calculated percentage carbon in NAPBmono if sodium were present would be 42.43% which is significantly different from what is observed. However, the calculated percentage carbon in NAPBorth if sodium were **not** present would be 42.03% which differs by 0.5% from the experimental value. Consequently, it could not be decided conclusively from the microanalysis results whether or not there was sodium present in NAPBorth and therefore the sample was analysed for sodium by atomic absorption. The result of the sodium analysis indicated the presence of sodium, but only approximately half the expected amount. Since the sodium concentration in the solution (1.1 ppm) was approaching the limit of detection due to insufficient material, it was decided to quote a molecular formula with one sodium ion per 1:1 host:guest. The microanalysis results and the measured density of the complex (given later with crystal data in Table 3) are consistent with the molecular formula given.

Crystal data for NAPBmono, NAPBorth and NAPG

Table 3 lists crystal data for NAPBmono, NAPBorth and NAPG (intensity data were not collected for these species).

Table 3 Crystal data for NAPBmono, NAPBorth and NAPG.

	NAPBmono	NAPBorth	NAPG
Mol. formula	$C_{42}H_{70}O_{35}.C_{14}H_{14}O_3.10.9H_2O$	$C_{42}H_{70}O_{35}.C_{14}H_{13}O_3^-Na^+.13.4H_2O$	$C_{48}H_{80}O_{40}.C_{14}H_{14}O_3.15.1H_2O$
M_r (g.mol^{-1})	1561.61	1628.63	1799.42
Crystal system	Monoclinic	Orthorhombic	Tetragonal
Space group	C2	$P2_12_12$	$P42_12$
Z	4	8	6
a (Å)	15.7(1)	30.2 (1)	23.8(1)
b (Å)	24.5(1)	32.0 (1)	
c (Å)	19.5(1)	15.47(5)	23.3(1)
β (°)	110.0(3)		
V (Å^3)	7048(66)	14950(83)	13198(97)
D_m (g.cm^{-3})	1.44(1)	1.44(1)	1.36(1)
D_c (g.cm^{-3})	1.47	1.45	1.36

The packing arrangement in the NAPBmono complex probably resembles that of other β-CD complexes which crystallise in the space group C2 with similar unit cell parameters[9,10,11]. This packing arrangement falls into the channel class of dimeric β-CD complex packing arrangements[12]. No complex of the unsubstituted β-CD has yet been reported in the space group $P2_12_12$ and therefore only crystal structure solution will reveal the nature of the packing arrangement and the host-guest interactions of the NAPBorth complex. In the case of the NAPG complex, the packing arrangement must resemble that found in the majority of γ-CD complexes which have been reported to date[13,14,15,16]. The naproxen molecule is probably fourfold disordered as the axis of the host molecule in this packing arrangement coincides with a crystallographic fourfold axis.

Crystal structure solution (NAPTMB)

To ensure accurate measurement of weak reflections, a pre-scan acceptance parameter of zero was chosen to force their final intensity scans up to a maximum time of 100 s per reflection. The structure was solved using published co-ordinates for the non-hydrogen cyclodextrin atoms (excluding the O(6), C(7), C(8) and C(9) atoms of each methylglucose residue) of the isomorphous *p*-iodophenol-TRIMEB tetrahydrate complex[17]. A difference Fourier synthesis after refinement by full-matrix least-squares techniques (SHELX93) revealed all the non-hydrogen atoms of the guest and many of the remaining non-hydrogen atoms of the host. Once all non-hydrogen atoms had been located from subsequent difference Fourier syntheses, all the cyclodextrin hydrogen atoms linked to carbon atoms were inserted at idealised positions with C-H = 1.00 Å. All the methyl hydrogen atoms were assigned a common variable isotropic temperature factor and the remaining hydrogen atoms of each methylglucose moiety were assigned common variable isotropic temperature factors. All non-hydrogen atoms were assigned anisotropic temperature factors, except for C(7G3), which was disordered, and C(1), C(5), C(9) and C(10) of the naproxen molecule, which, in addition, were refined subject to the following distance constraints, on account of abnormally long bond distances for C(1)-C(9) and C(5)-C(10): C(1)-C(2), C(1)-C(9), C(5)-C(6) and C(5)-C(10) with C-C = 1.42 Å, σ = 0.005 Å. The hydrogen atoms attached to the carbon atoms of the guest were also inserted at idealised positions with C-H = 1.00 Å and assigned a common isotropic temperature factor. The carboxyl hydrogen atom of the guest was located in a difference Fourier synthesis and allowed to refine subject to a distance constraint (O-H = 1.00 Å, σ = 0.05 Å).

Crystal structure (NAPTMB)

Table 4 lists crystal data, experimental and refinement parameters for NAPTMB (structure refined on F^2 using SHELX93).

Table 4 Crystal data, experimental and refinement parameters for NAPTMB (structure refined on F^2 using SHELX93)

Molecular formula	$C_{63}H_{112}O_{35}.C_{14}H_{14}O_3$
M_r (g.mol^{-1})	1659.82
Crystal system	Orthorhombic
Space group	$P2_12_12_1$
Z	4
a (Å)	15.179(4)
b (Å)	21.407(5)
c (Å)	27.67(1)
V (Å^3)	8991(5)
D_c (g.cm^{-3})	1.226
μ (Mo Kα) (cm^{-1})	0.92
F(000)	3568
Crystal dimensions (mm)	0.5 x 0.5 x 0.5
Temperature of dat coll.	258K
Range scanned θ (°)	$1 \leq \theta \leq 25$
Scan type	ω
Index range	h 0,18: k 0,25: l 0,32
Scan width (°)	0.8 + 0.35 tanθ
Aperture width (mm)	1.12 + 1.05 tanθ
Std reflections monitored for decay	2,3,15 2,16,8 10,3,13
Decay (%)	4%
No. of reflections collected	8655
No. of unique reflections	8613
R_{int}	0.1472
No. of reflections with I > 2σ(I)	6573
No. of L.S. parameters	1050
R1 (I > 2σ(I))	0.0571
wR2 (F^2)	0.1456
w	$[\sigma^2(F_o)^2 + (0.0859 \times P)^2 + (1.79 \times P)]^{-1}$ $P = (\max(F_o^2,0 + F_c^2)/3)$
Goof	1.120

cont'd

Table 4 cont'd

Shift/e.s.d. max, average	0.362, 0.006
$\Delta\rho_{max}$ final (e.Å^{-3})	0.56
$\Delta\rho_{min}$ final (e.Å^{-3})	-0.27

Figure 4 shows a diagram of the (*S*)-naproxen-TRIMEB complex illustrating the conformation of the host in which the methylglucose residues have been numbered. All seven methylglucose moieties of the TRIMEB molecule are in the $^4C_1$ chair conformation. Atom C(7G3) is disordered over three sites with site occupancies of 0.56, 0.22 and 0.22 (only the major site has been retained in the Figures). As is normally the case for TRIMEB, the O(2)-C(7) bonds are directed away from the cavity and the O(3)-C(8) bonds are directed towards the cavity[17,18,19,20,21]. The C(6)-O(6) bonds of residues G1, G3, G5, and G6 are directed away from the cavity in the *(-)-gauche* conformation[22], while those of G2, G4 and G7 point towards the cavity in the *(+)-gauche* conformation. The O(6)-C(9) bonds of all glucose residues are *trans* to the corresponding C(5)-C(6) bonds except in G6, where the relationship is *gauche*. Table 5 lists values for the O(4)···O(4')···O(4") angles of the O(4) heptagon, radii of the O(4) heptagon, O(4)···O(4') distances, tilt angles and deviations of the O(4) atoms from their least-squares plane. The values calculated for these parameters are comparable with those found for other TRIMEB complexes[17,18,19,20,21] and, as usual, two glucose moieties have negative tilt angles (in this case G3 and G6), while all the others have positive tilt angles[17]. The TRIMEB molecule is cup-shaped with the C(6)-O(6)-C(9) groups of G1, G2, G4, G5 and G7 almost closing off the O(6) side of the TRIMEB cavity.

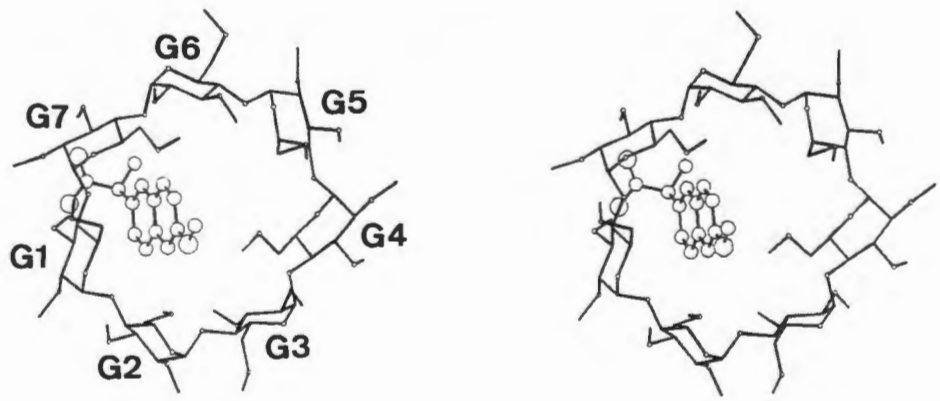

Figure 4 Stereodiagram of NAPTMB.

Table 5 Geometrical data for the TRIMEB molecule.

i. Glycosidic oxygen angle(°) and radius (Å) of the O(4) heptagon (measured from the centre of gravity of seven O(4) atoms to each O(4) atom).

O(4G7)···O(4G1)···O(4G2)	130.4	G1	4.86
O(4G1)···O(4G2)···O(4G3)	124.2	G2	5.21
O(4G2)···O(4G3)···O(4G4)	122.3	G3	5.14
O(4G3)···O(4G4)···O(4G5)	138.9	G4	4.64
O(4G4)···O(4G5)···O(4G6)	120.2	G5	5.17
O(4G5)···O(4G6)···O(4G7)	125.5	G6	5.12
O(4G6)···O(4G7)···O(4G1)	130.3	G7	4.86
Average	127.4	Average	5.00

ii. O(4)···O(4') distance (Å) and tilt angle (°)

O(4G1)···O(4G2)	4.51	G1	27.0
O(4G2)···O(4G3)	4.26	G2	20.7
O(4G3)···O(4G4)	4.55	G3	-9.4
O(4G4)···O(4G5)	4.25	G4	44.3
O(4G5)···O(4G6)	4.43	G5	34.5
O(4G6)···O(4G7)	4.38	G6	-14.4
O(4G7)···O(4G1)	4.27	G7	34.4
Average	4.38	Average	19.6

iii. Deviation of each O(4) atom (Å) from the least-squares plane through the seven O(4) atoms.

O(4G1)	O(4G2)	O(4G3)	O(4G4)	O(4G5)	O(4G6)	O(4G7)
0.429(3)	0.226(2)	0.505(3)	0.036(3)	0.581(3)	0.318(3)	0.376(3)

The distorted conformation of the TRIMEB molecule relative to the conformation observed for the parent β-cyclodextrin molecule is stabilised by numerous intramolecular C-H···O hydrogen bonds, a common interaction found in carbohydrate crystal structures[23]. In the crystal structure of TRIMEB monohydrate

(Chapter 6) the conformation of TRIMEB is stabilised by four intramolecular $C(6G_n)$-H···$O(5G_{n-1})$ hydrogen bonds. Furthermore, in the known crystal structures of TRIMEB complexes, five of the relevant C(6)···O(5) distances are in the range 3.0 - 3.4 Å. These hydrogen bonds are also present in the naproxen-TRIMEB crystal structure. In addition, there are two C-H···O hydrogen bonds stabilising the negative tilt angles of G3 and G6, namely C(1G3)-H···O(3G4) and C(1G5)-H···O(6G6). Table 6 lists C-H···O hydrogen bonding parameters.

Table 6 Intramolecular C-H···O hydrogen bonds in the naproxen-TRIMEB complex*.

			Distance (Å)			Angle (°)
C	H	O	C-H	H···O	C···O	C-H···O
C(6G1)-H(261)		O(5G7)	0.97	2.54	3.201(7)	125.5
C(6G2)-H(162)		O(5G1)	0.97	2.44	3.341(7)	155.1
C(6G3)-H(263)		O(5G2)	0.97	2.35	3.114(6)	134.9
C(6G5)-H(265)		O(5G4)	0.97	2.42	3.112(6)	128.5
C(6G6)-H(266)		O(5G5)	0.97	2.45	3.216(6)	136.2
C(1G3)-H(1G3)		O(3G4)	0.98	2.44	3.090(6)	123.5
C(1G5)-H(1G5)		O(6G6)	0.98	2.45	3.247(6)	138.1

* Hydrogen bonding parameters quoted based on idealised hydrogen atom positions.

Figure 5 is a stereoview of the NAPTMB complex viewed perpendicular to the axis of the host molecule. The naproxen molecule is inserted from the O(2),O(3) side of the TRIMEB molecule with the methoxy group buried in the cavity near the O(6) side and the propionic acid group protruding from the O(2),O(3) side. The guest is included at an angle of 23.3° relative to the least-squares plane through the seven O(4) atoms and the C(17) methyl group of the guest is in close contact with the "roof" of the cavity. Stereo space-filling diagrams in Figure 6 show how the naproxen molecule is shifted away from the host centre so that the methoxy group is situated in the deepest part of the cavity. Other close contacts between host and guest are listed in Table 7.

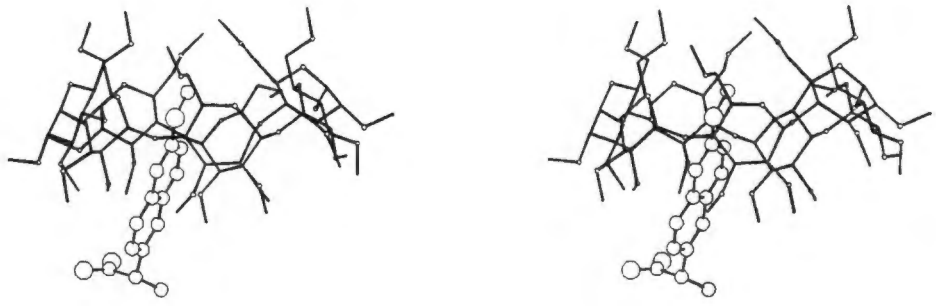

Figure 5 Stereodiagram of NAPTMB viewed perpendicular to the host axis.

Table 7 Close contacts between host and guest.

H(5) ···H(3G2)		2.358(9)
H(8) ···O(4G7)		2.76 (1)
H(17A)···C(9G4)		2.68 (8)
H(17A)···H(394)		2.27 (9)
H(17A)···O(6G4)		2.59 (8)
H(12C)···H(166)	(a)	2.46 (9)
H(12A)···O(5G3)	(b)	2.74 (8)
H(12A)···H(163)	(b)	2.33 (9)
O(15) ···H(2G2)	(c)	2.567(7)
H(15) ···C(2G2)	(c)	2.92 (7)
H(15) ···H(2G2)	(c)	2.41 (8)
H(15) ···C(3G2)	(c)	2.65 (6)
H(15) ···C(8G2)	(c)	2.8 (1)

Equivalent positions

(a)	-x+1,	y-1/2,	-z+1/2
(b)	-x+2,	y-1/2,	-z+1/2
(c)	x-1/2,	-y+1/2,	-z+1

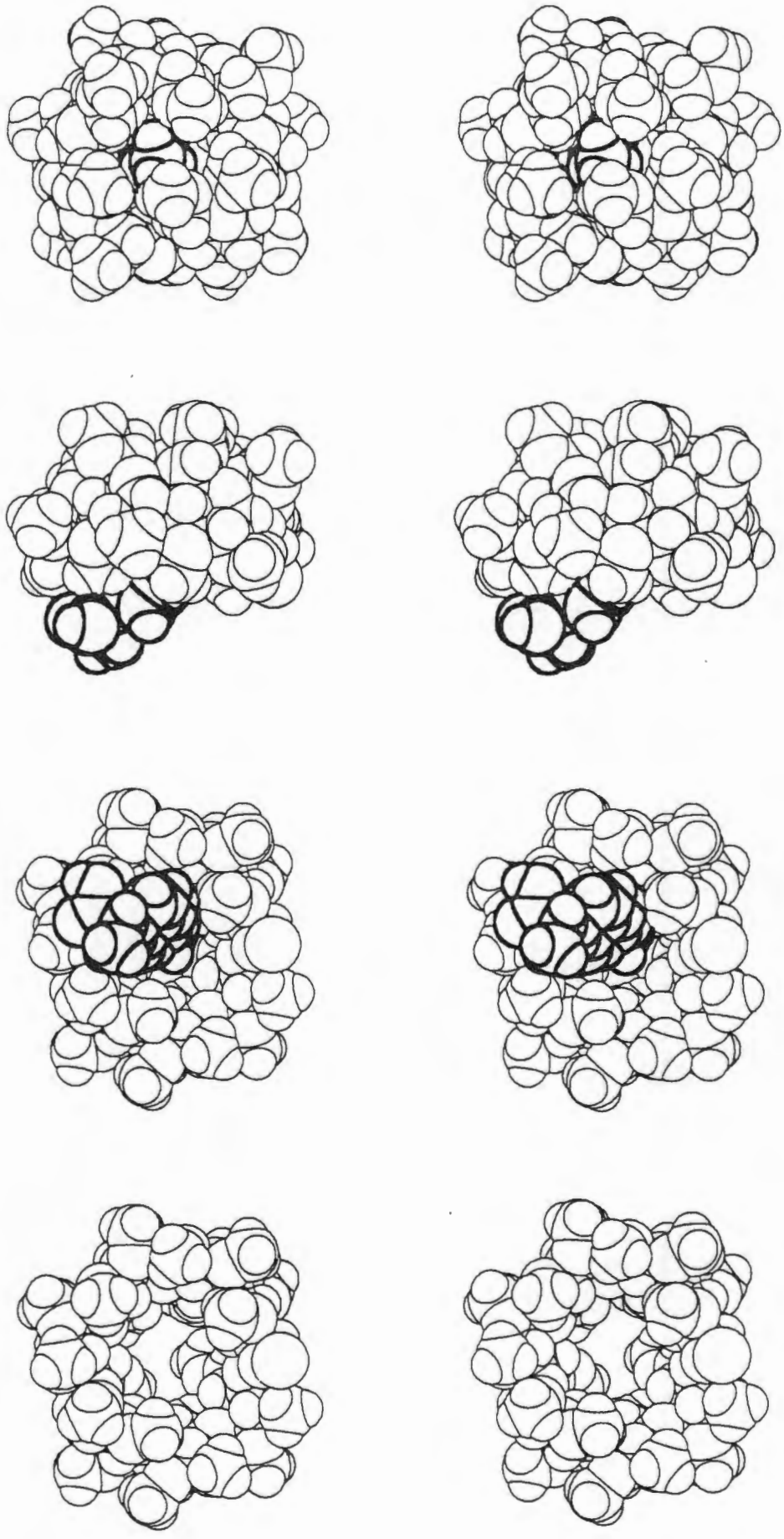

Figure 6 Stereo space-filling diagrams of NAPTMB viewed: top - from the O(6) side of the host, second - perpendicular to the host axis, third - from the O(2),O(3) side of the host, bottom - the same view as the diagram immediately above, but with the guest removed.

The way in which the naproxen molecule is included by TRIMEB in the solid state is similar to the modes of inclusion of naproxen by β-cyclodextrin proposed by Bettinetti et al.[1], Otero-Espinar et al.[4] and Ganza-Gonzalez et al.[6] on the basis of their NMR and/or molecular modelling studies. The guest is not as fully included in the TRIMEB molecule on account of the host's cup-like shape as opposed to the toroidal shape of β-cyclodextrin. However, the mode of inclusion proposed by Wang and Warner[5] in solution for naproxen and β-cyclodextrin, where the methoxy group is near the secondary hydroxyl side and the carboxyl group near the primary hydroxyl side, cannot be ruled out by the results of the present study as it has been noted by Harata that for some guests an "upside-down relationship is found between cyclodextrin complexes and methyl-cyclodextrin complexes"[18].

The uncomplexed TRIMEB molecule (Chapter 6) has a somewhat collapsed structure, partially attributed to its attempt to minimise the hydrophobic cavity size in the absence of a hydrophobic guest, thereby facilitating more efficient packing and simultaneously avoiding accommodation of water molecules in a relatively hydrophobic environment. On complexation with the (*S*)-naproxen molecule, the ellipticity of the TRIMEB molecule is significantly reduced. One of the seven methylglucose residues in uncomplexed TRIMEB adopts the unusual $^{1}C_{4}$ conformation in the crystal while the NAPTMB complex and other TRIMEB complexes contain only residues of the $^{4}C_{1}$ conformation. Since the most stable conformation of uncomplexed TRIMEB in solution may not coincide with that observed in the crystal, inclusion of guests by TRIMEB is not necessarily accompanied by the $^{1}C_{4}$ to $^{4}C_{1}$ conformational change.

The conformation of the methoxy group in naproxen with respect to the naphthalene ring is defined by the torsion angle $\tau 1$ C(5)-C(6)-O(16)-C(17) and that of the propionic acid substituent by $\tau 2$ C(1)-C(2)-C(11)-C(12), $\tau 3$ C(1)-C(2)-C(11)-C(13) and $\tau 4$ C(2)-C(11)-C(13)-O(15). The values for these torsion angles are -173.9(9), 48.1(8), -77.9(7) and -78.4(7)° respectively. The values for the corresponding torsion angles in the crystal structure of naproxen have been calculated for the (*S*)-isomer using the published co-ordinates[24] and are -2, -129, 112 and -90° (e.s.d.s ≤ 1°) respectively. The methoxy group, while still coplanar with the naphthalene ring has C(17) anti-periplanar to C(5) (as in Figure 1) as opposed to a syn-periplanar relationship in the naproxen crystal structure. The former conformation is favoured for inclusion as it reduces the width of the naproxen

molecule so that it can penetrate the deepest part of the cavity. The propionic acid substituent itself is in much the same conformation as that in the naproxen crystal structure, but, like the methoxy group, is rotated by approximately 180° with respect to the naphthalene ring (i.e. around C(2)-C(11)). The dihedral angle between the least-squares planes of the two rings of the naphthalene moiety is only 1.4(5)° compared with a value of 5.2(2)° in the naproxen crystal structure [18]. Calculation of the propionic acid group torsion angles in (*S*)-flurbiprofen using published co-ordinates for the crystal structures of flurbiprofen[25] and the (*S*)-flurbiprofen-TRIMEB complex[19] reveal similar conformations for the propionic acid substituent as in the (*S*)-naproxen-TRIMEB complex. The values for the torsion angles corresponding to $\tau 2$, $\tau 3$ and $\tau 4$ are 52, -70 and -102° respectively (e.s.d.s ≤ 1°) in uncomplexed (*S*)-flurbiprofen and 39, -87 and -88° respectively (e.s.d.s ≤ 1.6°) in the (*S*)-flurbiprofen-TRIMEB complex which implies that this residue of the (*S*)-flurbiprofen molecule undergoes little change in conformation on complexation with TRIMEB, in contrast to what is reported here for the complexation of naproxen by TRIMEB.

An intermolecular hydrogen bond between the carboxyl group of naproxen and a methoxy oxygen atom of a symmetry-related TRIMEB molecule, namely O(15)-H···O(3G2)^{I} (I = x - 1/2, -y + 1/2, -z + 1 with O···O 2.661(6), H···O 1.80(8) Å and O-H···O 141(12)°), stabilises the packing arrangement of the complex and could be the reason for the approximately 180° rotation of the propionic acid group relative to its orientation in the naproxen crystal structure. This hydrogen bond is also present in the (*S*)-flurbiprofen-TRIMEB crystal structure[19] as may have been expected, given the similar way in which this guest molecule interacts with the host compound. Figure 7 shows stereo packing diagrams for NAPTMB. Complex units pack in screw channel mode in a head-to-tail fashion with their axes almost parallel to the *b*-axis (3.5°). The similarity of the packing arrangement observed in MECLOFB with those of TRIMEB complexes has already been discussed (Chapter 5) and comparison of the packing diagrams of MECLOFB and NAPTMB illustrates this clearly. To date there is only one exception in packing arrangement amongst the known crystal structures of TRIMEB complexes, that of the *m*-iodophenol-TRIMEB complex[20] (MIPTMB), where the axis of the host molecule makes an angle of 26.2°C with the *b*-axis resulting in more of a cage-type packing arrangement. Figure 8 is a stereo space-filling diagram of two complex units related by the 2_1-axis parallel to the *b*-axis. The two host molecules are in

close contact on the one side and the portion of the guest molecule which protrudes from the O(2),O(3) side of the host fits in neatly next to the screw-related host, which is shifted slightly in the *ac*-plane relative to the host above.

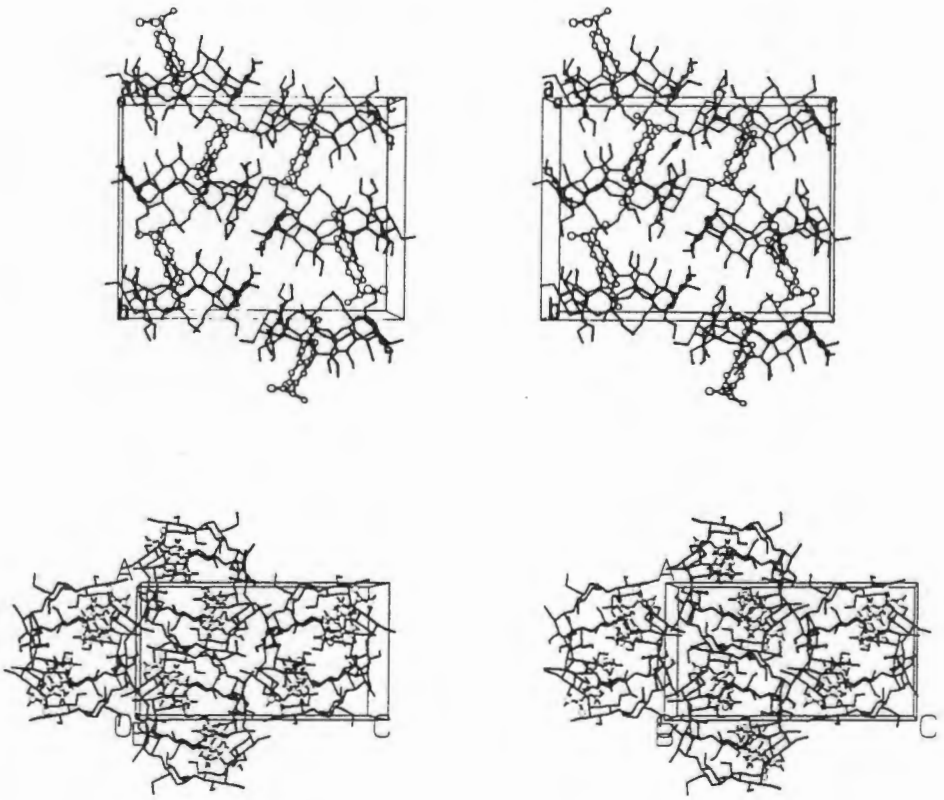

Figure 7 Stereo packing diagrams of NAPTMB viewed: above - down the *a*-axis, the O-H···O hydrogen bond is indicated by the dashed line, below - down the *b*-axis.

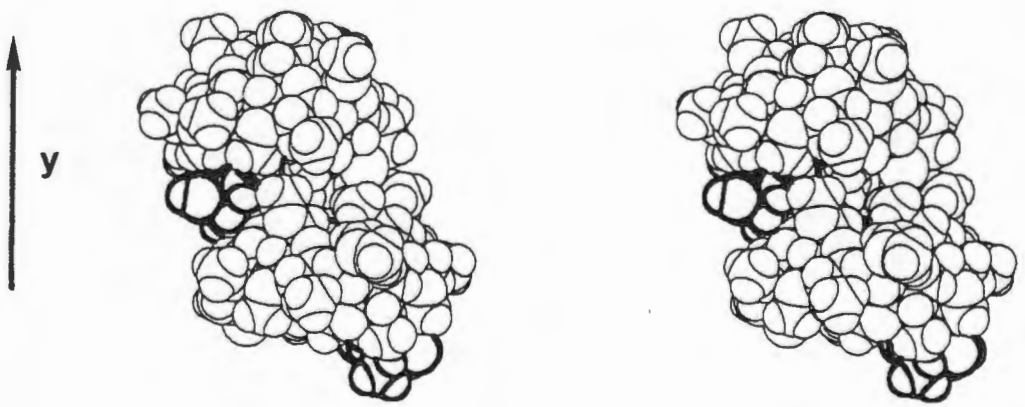

Figure 8 Two complex units related by the twofold screw axis parallel to the *b*-axis.

XRD

Calculated and experimental XRD patterns for NAPTMB are shown in Figure 9. The very close match between the calculated and experimental patterns shows the high purity of the sample.

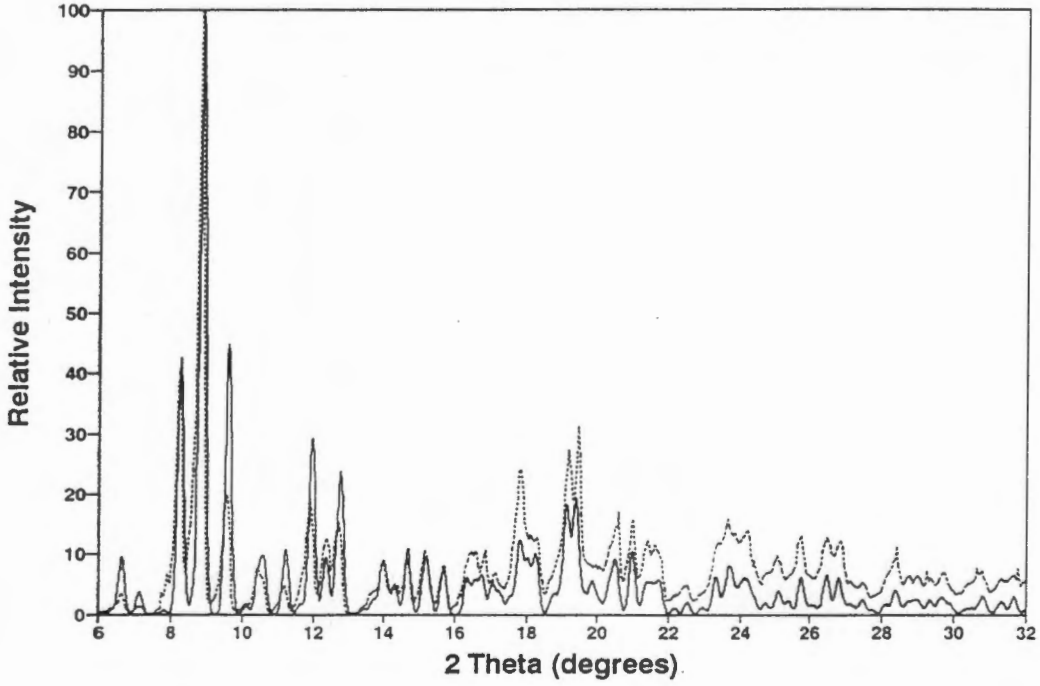

Figure 9 Calculated (——) and experimental (· · · · ·) XRD patterns for NAPTMB.

References.

1. G. Bettinetti, F. Melani, P. Mura, R. Monnanni and F. Giordano, *J. Pharm. Sci.*, 1991, **80**, 1162.
2. G. Bettinetti, A. Gazzaniga, P. Mura, F. Giordano and M. Setti, *Drug Dev. Ind. Pharm.*, 1992, **18**, 39.
3. N. Celebi and N. Erden, *Int. J. Pharm.*, 1992, **78**, 183.
4. F. J. Otero-Espinar, S. Anguiano-Igea, N. Garcia-Gonzalez, J. L. Vila-Jato and J. Blanco-Mendez, *Int. J. Pharm.*, 1992, **79**, 149.
5. J. Wang and I. M. Warner, *Microchemical J.*, 1993, **48**, 229.
6. A. Ganza-Gonzalez, J. L. Vila-Jato, S. Anguiano-Igea, F. J. Otero-Espinar and J. Blanco-Mendez, *Int. J. Pharm.*, 1994, **106**, 179.
7. T. Loftsson, B. J. Olafsdottir, H. Frioriksdottir and S. Jonsdottir, *Eur. J. Pharm. Sci.*, 1993, **1**, 95.
8. F. Melani, G. P. Bettinetti, P. Mura and A. Manderioli, *J. Incl. Phenom.*, 1995, 22, 131.
9. G. Le Bas, C. de Rango, N. Rysanek and G. Tsoucaris, *J. Incl. Phenom.*, 1984, **2**, 861.
10. I. M. Mavridis, E. Hadjoudis and G. Tsoucaris, *Carb. Res.*, 1991, **220**, 11.
11. J. A. Hamilton and M. N. Sabesan, *Carb. Res.*, 1982, **102**, 31.
12. D. Mentzafos, I. M. Mavridis, G. Le Bas and G. Tsoucaris, *Acta Crystallog.*, 1991, B**47**, 746.
13. S. Kamitori, K. Hirotsu and T. Higuchi, *J. Chem. Soc., Chem. Commun.*, 1986, 690.
14. S. Kamitori, K. Hirotsu and T. Higuchi, *J. Am. Chem. Soc.*, 1987, **109**, 2409.
15. S. Kamitori, K. Hirotsu and T. Higuchi, *Bull. Chem. Soc. Jpn.*, 1988, **61**, 3825.
16. J. Ding, T. Steiner and W. Saenger, *Acta Crystallog.*, 1991, B**47**, 731.
17. K. Harata, K. Uekama, M. Otagiri and F. Hirayama, *Bull. Chem. Soc. Jpn.*, 1983, **56**, 1732.
18. K. Harata, K. Uekama, M. Otagiri and F. Hirayama, *J. Incl. Phenom.*, 1984, **1**, 279.
19. K. Harata, K. Uekama, T. Imai, F. Hirayama and M. Otagiri, *J. Incl. Phenom.*, 1988, **6**, 443.
20. K. Harata, F. Hirayama, H. Arima, K. Uekama and T. Miyaji, *J. Chem. Soc. Perkin Trans. 2*, 1992, 1159.
21. D. Mentzafos, I. Mavridis and H. Schenk, *Carb. Res.*, 1994, **253**, 39.

22. W. Saenger, *Inclusion Compounds*, Volume 2, Chapter 8, London, Academic Press, edited by J. L. Atwood, J. E. D. Davies and D. D. MacNicol, 1984.
23. T. Steiner and W. Saenger, *J. Am. Chem. Soc.*, 1992, **114**, 10146.
24. K. Ravikumar, S. S. Rajan, V. Pattabhi and E. J. Gabe, *Acta Crystallog.*, 1985, C**41**, 280.
25. J. L. Flippen and R.D. Gilardi, *Acta Crystallog.*, 1975, B**31**, 926.

Chapter 8 Menthol

Introduction

The structure of (*L*)-menthol together with the numbering scheme used in the crystal structure analysis is shown in Figure 1. Menthol is used in a wide variety of skin emollients and protectants as it is mildly antipruritic and also in inhalants for symptomatic relief from nasal congestion[1]. In addition it has been shown to have antibacterial properties[2]. Stabilisation of volatile compounds like menthol can be achieved by complexation with the cyclodextrins[3,4] and cyclodextrin complexes with menthol have been exploited for this purpose in the tobacco industry[5] since it was found that the menthol flavour was only released when the tobacco product was smoked. A recent patent[6] describes the preparation of a menthol-β-CD complex for use as an inhalant in the treatment of respiratory ailments. Evolved gas analysis of the solid menthol-β-CD complex shows that menthol is only released from the complex at about 300°C[3,4,7]. However, on contact with hot water, an immediate and sustained release of the volatile component was found[7].

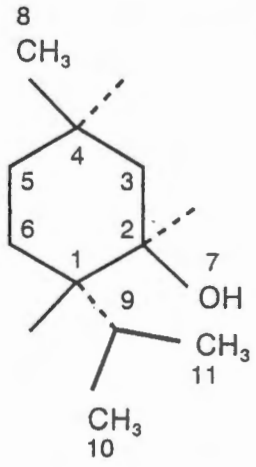

Figure 1 (*L*)-menthol

Preparation of the CD Complexes

(*L*)-menthol-β-cyclodextrin complex (MENTHB)

0.28 mmol of (*L*)-menthol and 0.16 mmol β-cyclodextrin were dissolved in approximately 18 ml of distilled water at 60°C. The solution was filtered and left at room temperature. Crystals of the MENTHB complex (Figure 2) crystallised in 7 to 14 days.

(*L*)-menthol-TRIMEB complex (MENTMB)

0.06 mmol of (*L*)-menthol and 0.12 mmol of TRIMEB were stirred at room temperature in 0.5 ml of distilled water until the TRIMEB had dissolved. The same procedure as for MENDMB was followed, except that the filtered solution was diluted approximately 1 in 2 with distilled water and left to crystallise at about 40°C. The complex crystallised as colourless needles (Figure 2) after 10 weeks of slow evaporation. In order to prepare the complex in sufficient quantities for XRD, the method of preparation was altered by using a 1:1 host:guest ratio and crystallising at a slightly higher temperature (about 50°C).

(*L*)-menthol-DIMEB complex (MENDMB)

The (*L*)-menthol-DIMEB complex was prepared by stirring 0.13 mmol of (*L*)-menthol and 0.26 mmol of DIMEB in 1 ml of distilled water at room temperature until all the DIMEB had dissolved. The temperature was increased to approximately 45° C (just high enough for the menthol to melt) and stirred until the sudden precipitation of the complex. The solution was then cooled in an ice bath to redissolve the complex, filtered and left at room temperature to evaporate very slowly. The complex crystallised as colourless plate-shaped crystals (Figure 2) after about 2 to 3 months. In order to prepare the complex in sufficient quantities for XRD, the method of preparation was altered by using a 1:1 host:guest ratio and making the solution more concentrated.

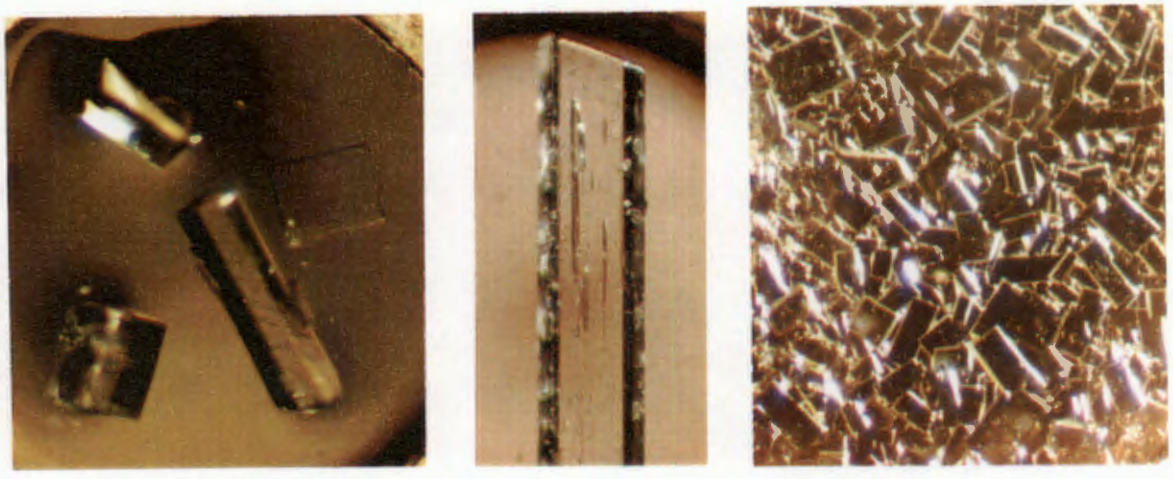

MENTHB, 30 X **MENTMB**, 30 X **MENDMB**, 48 X

Figure 2 Photographs of the MENTHB, MENTMB and MENDMB complexes.

Thermal Analysis

TG and DSC traces are shown in Figure 3.

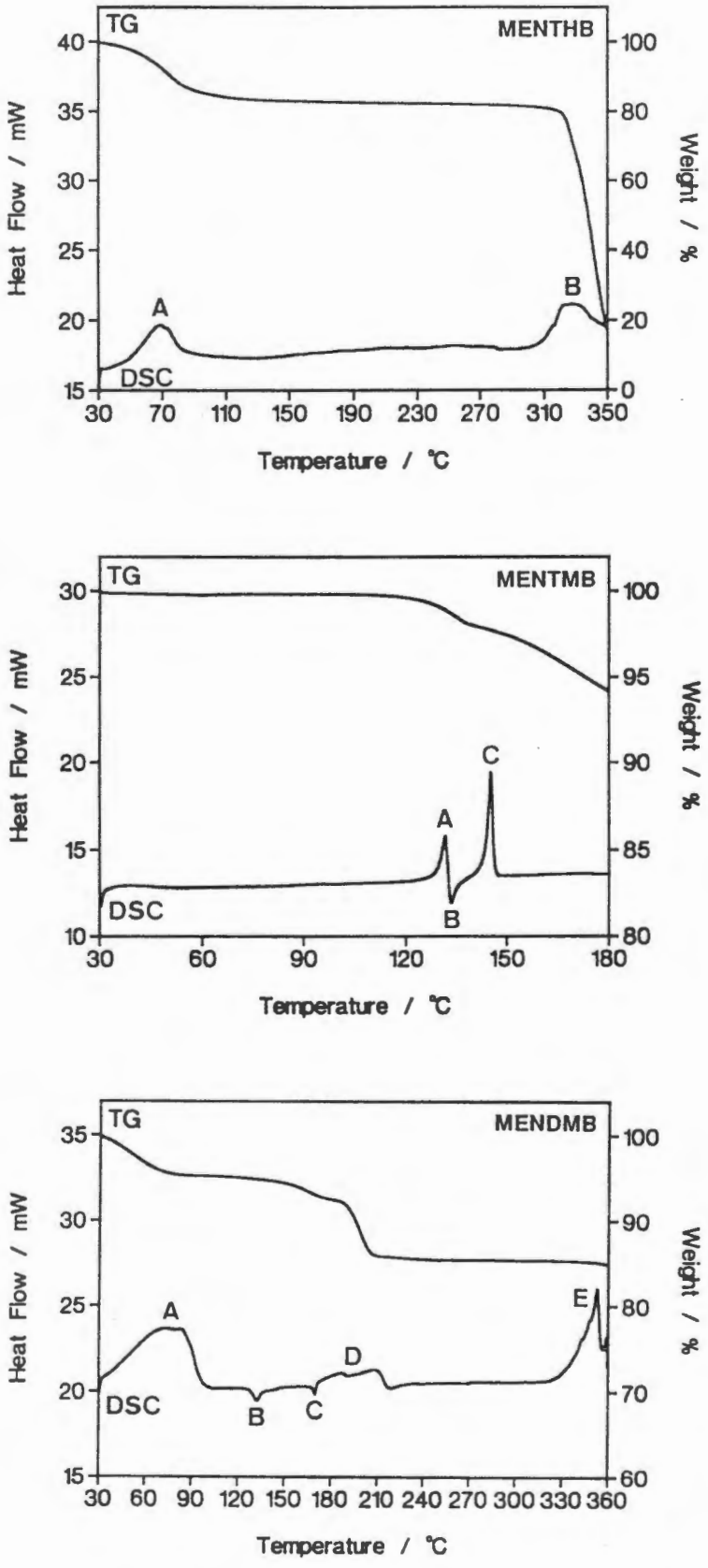

Figure 3 TG and DSC traces for MENTHB (top), MENTMB (middle) and MENDMB (bottom).

TG data are listed in Table 1.

Table 1 TG data for the menthol-CD complexes.

Complex	% weight loss	Temperature range (°C)	No. of molecules
MENTHB	16.8	30 - 135	14.5 (H_2O)
MENTMB	2.1	30 - 142	1.9 (H_2O)
MENDMB	4.7	30 - 93	4.1 (H_2O)
	9.9	93 - 280	1.0 (menthol)

DSC data are listed in Table 2.

Table 2 DSC data for the menthol-CD complexes.

Complex	Event	Temperature range (°C)	Onset (°C)	Peak(°C)
MENTHB	Endotherm A	30 - 130	47	68
	Endotherm B	300 - 350	314	323
MENTMB	Endotherm A	124 - 133	129	132
	Endotherm B	133 - 140	133	134
	Endotherm C	140 - 149	144	145
MENDMB	Endotherm A	30 - 105	30	74
	Exotherm B	125 - 155	128	132
	Exotherm C	166 - 173	168	170
	Endotherm D	173 - 220	180	177, 208
	Endotherm E	322 - 358	(348)	(353)

The DSC trace of the MENTHB complex shows two broad endotherms. The first (A) is associated with water loss and the second (B) with simultaneous melting and decomposition. It is the only β-CD complex presented in this thesis for which a melt of the dehydrated complex can be observed on the hot stage. The melt is different from that of β-CD alone in that there is vigorous foaming (Figure 4) while β-CD alone bubbles gently. It is probable that the guest is volatilised at this point as the characteristic smell of menthol can be detected together with the burnt sugar smell of the decomposing host. DSC of MENTMB shows an endotherm for water loss (A) and an exotherm interpreted as a phase change of the dehydrated complex (B) followed by a sharp endotherm due to fusion of the dehydrated complex (C). The

thermal analysis of these complexes will be discussed further in the crystal structure analyses.

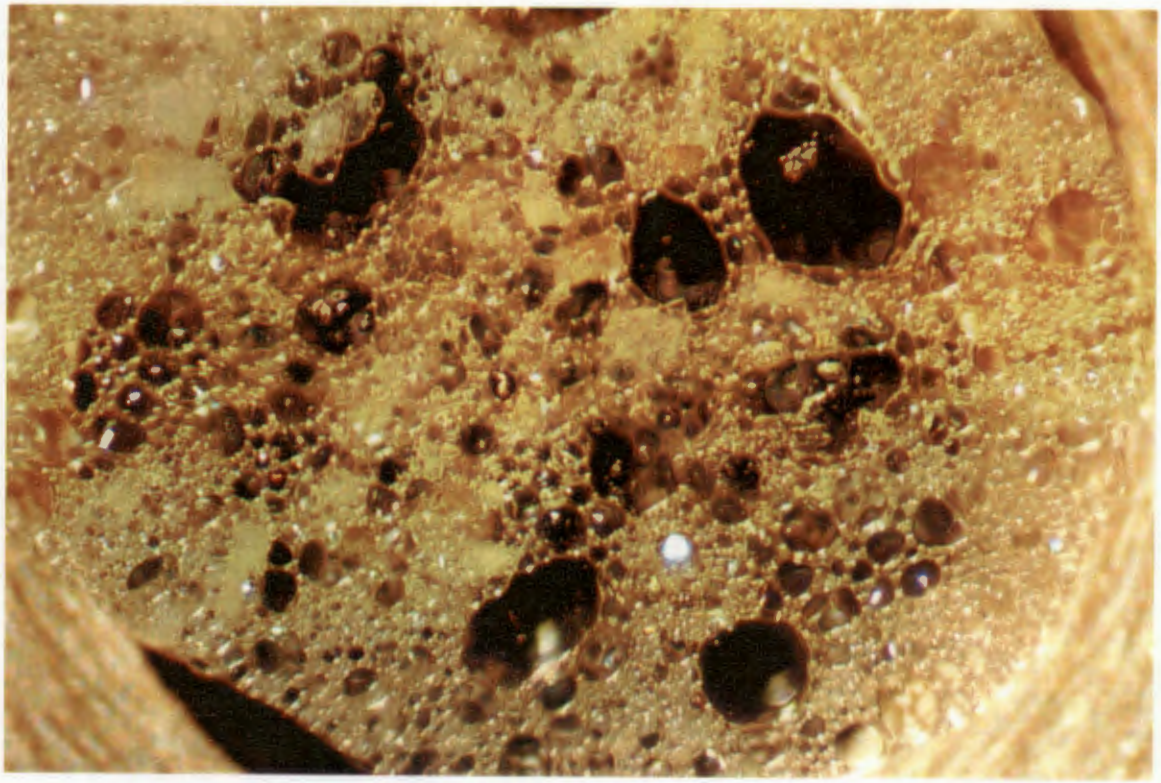

The melt of **MENTHB** (47 X)

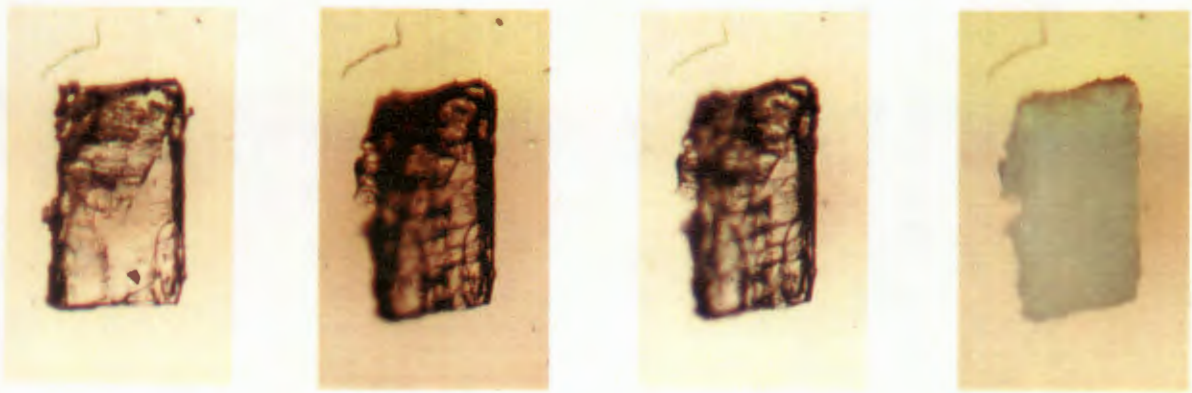

28°C, 47 X 100°C, 47 X 160°C, 47 X 200°C, 47 X

Figure 4 The melt of MENTHB (above) and MENDMB at various temperatures (below).

In contrast to the TG traces of the above two complexes, TG of MENDMB shows two weight losses. The first is associated with dehydration of the complex and the second corresponds to the loss of the menthol molecule. This weight loss is highly reproducible, giving 0.990(8) menthol molecules, n = 6 (assuming that the material remaining after this weight loss is the host alone). The assignment of a 1:1:4.1 DIMEB:menthol:H_2O complex is based on elemental analysis (given below) and the fact that an NMR spectrum of the material after the second weight loss shows no trace of the guest, but only signals for the host protons. In addition, a Debye-Scherrer photograph of this material (i.e. after the second weight loss) matches that of the host alone. The loss of the menthol molecule appears to be a two-step weight loss, but attempts to resolve the two steps at lower scanning rates were unsuccessful. The DSC trace of the MENDMB complex is complicated but reproducible. Endotherm A is unambiguously associated with water loss. Exotherm B is not associated with a weight loss and therefore must represent a phase change of the dehydrated complex. Exotherm C occurs from 166 - 173°C and since there is a lag of approximately 10°C in the DSC trace in relation to the TG trace, it is unlikely that this event is associated with a weight loss, but may be a further phase change which initiates the loss of the guest. Endotherm D corresponds to the loss of the menthol molecule and, as in the TG trace, indicates a two-step process. This may reflect more than one environment for the guest in the dehydrated complex which is not unlikely since the volume of the unit cell (unit cell data given later) for the hydrated complex indicates that there are two crystallographically independent complex units. The final event, Endotherm E, represents fusion of the host. Accurate onset and peak temperatures could not be obtained as the melt of the host involves bubbling with spillage onto the furnace. The separate losses of water and menthol can also be observed on the hot stage. Figure 4 shows how a crystal of the MENDMB complex cracks as it loses water and then becomes completely opaque over the narrow temperature range of 195 - 200°C as it loses the menthol molecule.

Microanalysis

The results of the microanalyses are given as the average of duplicate determinations. The ratio given in parentheses is the host:guest:H_2O stoichiometry. The water content is based on the results of thermogravimetric analysis. Molecular formulae are as follows:

MENTHB (1:1:14.5)	$C_{42}H_{70}O_{35}.C_{10}H_{20}O.14.5H_2O$
MENTMB (1:1:2)	$C_{63}H_{112}O_{35}.C_{10}H_{20}O.2H_2O$
MENDMB (1:1:4.1)	$C_{56}H_{98}O_{35}.C_{10}H_{20}O.4.1H_2O$

	Calculated (%)		Experimental (%)	
	C	H	C	H
MENTHB	40.23	7.73	40.49	7.50
MENTMB	54.06	8.45	54.32	8.41
MENDMB	50.77	8.15	50.81	8.08

Crystal data for MENDMB

Table 3 shows the crystal data for MENDMB.

Table 3 Crystal data for MENDMB

Molecular formula	$C_{56}H_{98}O_{35}.C_{10}H_{20}O.4.1H_2O$
M_r ($g.mol^{-1}$)	1561.50
Crystal system	Orthorhombic
Space group	$P2_12_12_1$
Z	8
a (Å)	15.52(5)
b (Å)	19.37(5)
c (Å)	60.9 (3)
V ($Å^3$)	18308(118)
D_c ($g.cm^{-3}$)	1.13

The unit cell parameters for MENDMB are similar to those for DIMEB complexes with *p*-iodophenol and *p*-nitrophenol[8], except that the unit cell length *c* is approximately doubled here. The guest molecules in the latter two complexes are not actually included in the host cavity, but are found in the intermolecular space, while the cyclodextrin cavity is occupied by water molecules. The similarity in unit

cell parameters (apart from the doubling in *c*) and the loss of the menthol molecule in the TG and DSC traces before the melting point may indicate that the guest is also located outside the cavity of the host in the MENDMB complex.

Crystal structure solutions.

Menthol-β-cyclodextrin complex.

Table 4 shows crystal data, experimental and refinement parameters for MENTHB. The numbering scheme for the β-cyclodextrin dimer in MENTHB differs slightly from that used thus far for this host because the asymmetric unit contains two independent host molecules and therefore the numbering scheme must distinguish between them. It is the same as that used in the (R)-fenoprofen-β-CD complex[9], where, for example, C(246) would be carbon atom number 6 of glucose residue number 4 in host molecule number 2 in the asymmetric unit. Similarly, there are two independent menthol molecules and therefore the non-hydrogen atoms of the guest included in host molecule number 2 are numbered from 21 to 31, instead of 1 to 11. Crystals of this species were very unstable, developing cracks immediately on removal from mother liquor. A single crystal was mounted in a Lindemann capillary which had been filled with quick-setting cyanoacrylate glue. The structure was solved using published co-ordinates for the non-hydrogen cyclodextrin atoms (excluding the primary hydroxyl oxygen atoms) of the isomorphous (R)-fenoprofen-β-cyclodextrin complex[9]. The y-coordinate of atom C(111) was fixed (space group $P2_1$) and a difference Fourier synthesis after refinement by full-matrix least-squares techniques revealed the remaining non-hydrogen atoms of the host molecules. All the non-hydrogen atoms of the two guest molecules were located in subsequent difference Fourier maps during refinement by the block-diagonal least-squares method. Subsequent refinement yielded abnormal bond lengths and angles for the guest molecules and therefore the two menthol molecules were refined as rigid bodies with C-C = 1.54, C-O = 1.44, C···C = 2.52 and C···O = 2.43 Å (σ = 0.01 Å). At this stage, the temperature factors of the guest atoms which had previously been refined were fixed, with those higher than 0.20 $Å^2$ being fixed at 0.20 $Å^2$. Water molecules were then located and the site occupancies of those with either abnormally high temperature factors or closer than 2.6 Å from other water molecules were refined. In order to refine the site occupancy factors of the disordered water molecules, their temperature factors were fixed at the average of the ordered water molecules (O(1W) to O(16W)). After refinement in this way, the

site occupancy factors of O(17W) to O(20W), which were close to 0.75, were fixed at 0.75 and their isotropic temperature factors were then refined. Similarly, the site occupancy factors of O(21W) to O(27W), which were close to 0.5, were fixed at 0.5 and their isotropic temperature factors were then refined. All hydrogen atoms attached to carbon atoms of both host molecules were inserted at idealised positions with C-H = 1.00 Å. The hydrogen atoms of each independent host molecule were assigned different common fixed isotropic temperature factors.

Menthol-TRIMEB complex

Table 5 shows crystal data, experimental and refinement parameters for MENTMB. The numbering scheme of the host is the same as that used in the NAPTMB complex (Chapter 7). Data were collected from a crystal mounted without mother liquor in a Lindemann capillary. To ensure accurate measurement of weak reflections, a pre-scan acceptance parameter of zero was chosen to force their final intensity scans up to a maximum time of 100s per reflection. Many direct methods runs (SHELX86) were unsuccessful, but the structure was finally solved using the following parameters: ESEL 1.6, TREF 10000 500 -20, SUBS 6. Most of the non-hydrogen atoms of the host and all of the non-hydrogen atoms of the guest were located in the resultant E-map. After refinement by full-matrix least-squares techniques, a difference Fourier map revealed the remaining non-hydrogen atoms of the host. Two water molecules were located in subsequent difference Fourier maps. Hydrogen atoms linked to carbons of both host and guest were inserted at idealised positions with C-H = 1.00 Å, provided that the relevant carbon atom was not disordered. Abnormally high temperature factors for several of the O(6)-C(9) groups of the host indicated disorder. However, attempts at modelling disorder for these groups did not result in any significant improvement and therefore only one position with full site occupancy for each of these atoms was retained. Anisotropic temperature factors were then assigned to all the non-hydrogen atoms, excluding those which were disordered and those for which anisotropic refinement resulted in unsatisfactory thermal parameters. The hydrogen atoms of each methylglucose residue and those of the guest molecule were assigned common variable isotropic temperature factors. The hydrogen atoms of the water molecules and of the hydroxyl group of the menthol molecule were not located.

Table 4 Crystal data, experimental and refinement parameters for MENTHB (structure refined on F using SHELX76)

Molecular formula	$C_{42}H_{70}O_{35}.C_{10}H_{20}O.14.5H_2O$
M_r (g.mol^{-1})	1552.47
Crystal system	Monoclinic
Space group	$P2_1$
Z	4
a (Å)	15.342(3)
b (Å)	32.54(2)
c (Å)	15.324(3)
β (°)	102.44(2)
V (Å^3)	7471(5)
D_m (g.cm^{-3})	1.37(1)
D_c (g.cm^{-3})	1.380
μ (Mo Kα) (cm^{-1})	1.15
F(000)	3340
Crystal dimensions (mm)	0.35 x 0.45 x 0.55
Temperature of data collection	294K
Range scanned θ (°)	$1 \leq \theta \leq 25$
Scan type	ω-2θ
Index range	h -18,18: k 0,38: l 0,18
Scan width (°)	0.75 + 0.35 tanθ
Aperture width (mm)	1.12 + 0.5 tanθ
Std reflections monitored for decay	6,-15,6 -2,-15,10 -1,-26,-1
Decay (%)	8
No. of reflections collected	13907
No. of unique reflections	9886
R_{int}	0.0254
No. of reflections with I > 2σ(I)	5469
No. of L.S. parameters	781
R	0.108
wR	0.113
w	$[\sigma^2(F_o) + 5 \times 10^{-3} F_o^2]^{-1}$
S	1.23

cont'd

Table 4 cont'd

Shift/e.s.d. max, average	0.525,0.011
$\Delta\rho_{max}$ final (e.Å^{-3})	0.74
$\Delta\rho_{min}$ final (e.Å^{-3})	-0.49

Table 5 Crystal data, experimental and refinement parameters for MENTMB (structure refined on F^2 using SHELX93).

Molecular formula	$C_{63}H_{112}O_{35}.C_{10}H_{20}O.2H_2O$
M_r (g.mol^{-1})	1621.85
Crystal system	Orthorhombic
Space group	$P2_12_12_1$
Z	4
a (Å)	11.060(3)
b (Å)	26.138(6)
c (Å)	29.669(6)
V (Å^3)	8576(2)
D_c (g.cm^{-3})	1.256
μ (Mo Kα) (cm^{-1})	0.94
F(000)	3512
Crystal dimensions (mm)	0.5 x 0.5 x 0.5
Temperature of dat coll.	248K
Range scanned θ (°)	$1 \leq \theta \leq 25$
Scan type	ω
Index range	h 0,13: k 0,31: l 0,35
Scan width (°)	0.5 + 0.35 tanθ
Aperture width (mm)	1.12 + 1.05 tanθ
Std reflections monitored for decay	2,9,20 8,8,4 7,11,6
Decay (%)	1.6
No. of reflections collected	8324
No. of unique reflections	8285
R_{int}	0.00
No. of reflections with I > 2σ(I)	4387

cont'd

Table 5 cont'd

No. of L.S. parameters	882
R1 ($I > 2\sigma(I)$)	0.105
wR2 (F^2)	0.3663
w	$[\sigma^2(F_o)^2 + (0.2182 \times P)^2 + (6.25 \times P)]$
	$P = (\max(F_o^2,0) + 2 \times F_c^2)/3$
Goof	1.028
Shift/e.s.d. max, average	2.703,0.080
$\Delta\rho_{max}$ final ($e.Å^{-3}$)	0.66
$\Delta\rho_{min}$ final ($e.Å^{-3}$)	-0.35

Crystal structures (MENTHB and MENTMB)

MENTHB complex

Figure 5 is a stereodiagram of the (*L*)-menthol-*β*-cyclodextrin complex in which the glucose residues in the two independent host molecules have been labelled. All seven glucose residues of each cyclodextrin molecule are in the $^4C_1$ chair conformation. Atom O(246) is disordered over two sites with site occupancies of 0.6 and 0.4. The C(6)-O(6) bonds are all in the (-)-*gauche* conformation[10], except in G2 of cyclodextrin 1 and G4 in cyclodextrin 2, where they are in the (+)-*gauche* conformation. Table 6 lists values for the O(4)···O(4')···O(4") angles, radii of the O(4) heptagon, O(4)···O(4') distances, tilt angles and deviations of the O(4) atoms from their least-squares plane for the two independent host molecules. It is evident from these parameters that the macrocyclic conformation of host 2 is slightly more distorted than that of host 1.

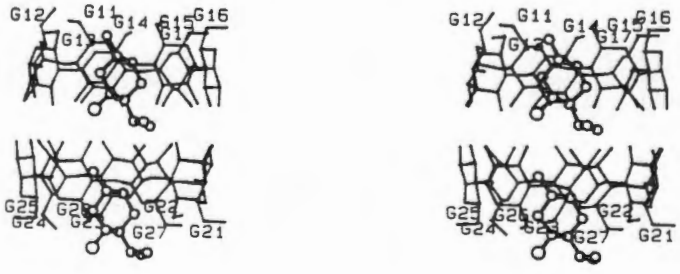

Figure 5 Stereodiagram of the (*L*)-menthol-*β*-CD complex.

Table 6 Geometrical data for the two independent β-CD molecules in MENTHB.

i. Glycosidic oxygen angle (°) and radius (Å) of the O(4) heptagon (measured from the centre of gravity of seven O(4) atoms to each O(4) atom).

	CD1	CD2		CD1	CD2
O(4G7)···O(4G1)···O(4G2)	128.2	124.0	G1	5.05	5.22
O(4G1)···O(4G2)···O(4G3)	125.7	130.1	G2	5.15	4.94
O(4G2)···O(4G3)···O(4G4)	130.5	132.4	G3	4.95	4.85
O(4G3)···O(4G4)···O(4G5)	130.3	124.9	G4	4.94	5.18
O(4G4)···O(4G5)···O(4G6)	126.1	127.2	G5	5.13	5.09
O(4G5)···O(4G6)···O(4G7)	128.7	131.9	G6	5.03	4.83
O(4G6)···O(4G7)···O(4G1)	130.6	129.5	G7	4.92	4.99
Average	128.6	128.6	Ave	5.02	5.01

ii. O(4)···O(4') distance (Å) and tilt angle (°)

	CD1	CD2		CD1	CD2
O(4G1)···O(4G2)	4.37	4.34	G1	4.2	5.0
O(4G2)···O(4G3)	4.32	4.44	G2	10.4	7.0
O(4G3)···O(4G4)	4.42	4.34	G3	7.7	12.0
O(4G4)···O(4G5)	4.33	4.28	G4	9.6	11.9
O(4G5)···O(4G6)	4.30	4.36	G5	8.7	10.2
O(4G6)···O(4G7)	4.38	4.45	G6	9.7	4.7
O(4G7)···O(4G1)	4.39	4.25	G7	5.6	5.0
Average	4.36	4.35	Average	6.6	8.0

iii. Deviations (Å) of O(4) atoms from the least-squares plane through the seven O(4) atoms (CD1 values above and CD2 values below).

O(4G1)	O(4G2)	O(4G3)	O(4G4)	O(4G5)	O(4G6)	O(4G7)
0.01(2)	0.01(2)	0.02(2)	0.02(2)	0.01(2)	0.00(2)	0.01(2)
0.03(2)	0.03(2)	0.01(2)	0.01(2)	0.02(2)	0.02(2)	0.00(2)

As is the case in the majority of β-cyclodextrin complexes, two host molecules form a head-to-head dimer stabilised by hydrogen bonding[11]. It has been suggested that the more fully included the guest in the host cavity, the less the distortion of the conformation of the host[11]. This is also the case in the MENTHB complex as the guest of CD1 is more fully included in its host cavity than the guest of CD2. The guest molecules are oriented differently in the cavities of the two crystallographically independent cyclodextrin molecules comprising the dimer (Figure 5). This type of head-to-tail orientation of guest molecules has also been observed in the racemic fenoprofen, phenobarbital and (*S*)-fenoprofen complexes with β-cyclodextrin[9,12,13]. Both menthol molecules have their hydroxyl and isopropyl substituents protruding from, and their methyl substituents buried in, the cavities of their respective host molecules. However, one protrudes from the primary hydroxyl side and the other from the secondary hydroxyl side of its host (Figure 5). This results in the unusual situation where the hydroxyl group of a guest molecule is found at the interface of the cyclodextrin dimer. Furthermore, this hydroxyl group is not within hydrogen bonding distance of the cyclodextrin secondary hydroxyl groups. The hydroxyl group of the other menthol molecule which protrudes from the dimer cavity is within hydrogen bonding distance of a water molecule. The guest molecules are therefore held in the cyclodextrin cavities only by hydrophobic forces.

Stereo space-filling diagrams of each independent host molecule with its guest (Figure 6) show that the menthol molecules are held relatively loosely in the dimer cavity. Although the guest hydrogen atoms were not placed in the crystal structure, they have been included at calculated positions in the space-filling diagrams. Table 7 lists the few close contacts between the hosts and guests of the dimer complex unit.

Table 7 Close contacts (Å) between hosts and guests of the dimer complex unit.

H(4) ···H(125)	2.40*
H(14)···H(223)	2.36
C(23)···H(255)	2.88(7)
H(23)···H(255)	2.35

* No e.s.d.s quoted for distances involving H atoms of the guests since they were not actually included in the crystal structure.

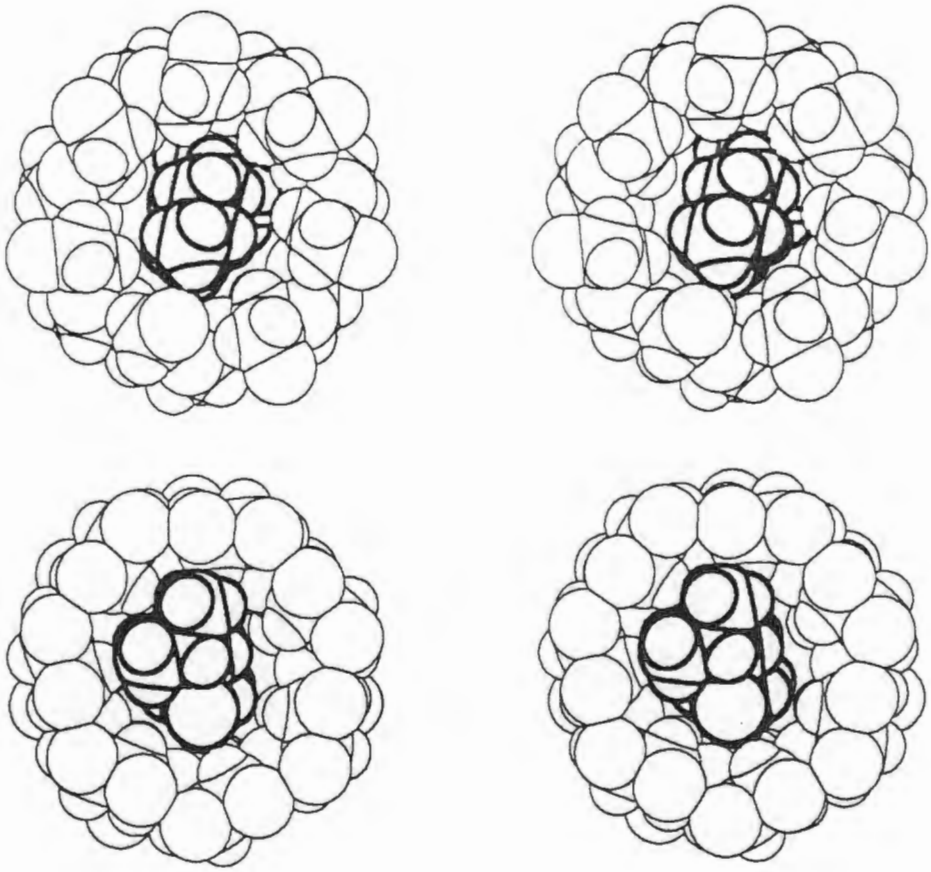

Figure 6A Space-filling diagrams of CD1 with its guest viewed: above - from the primary hydroxyl side, below - from the secondary hydroxyl side.

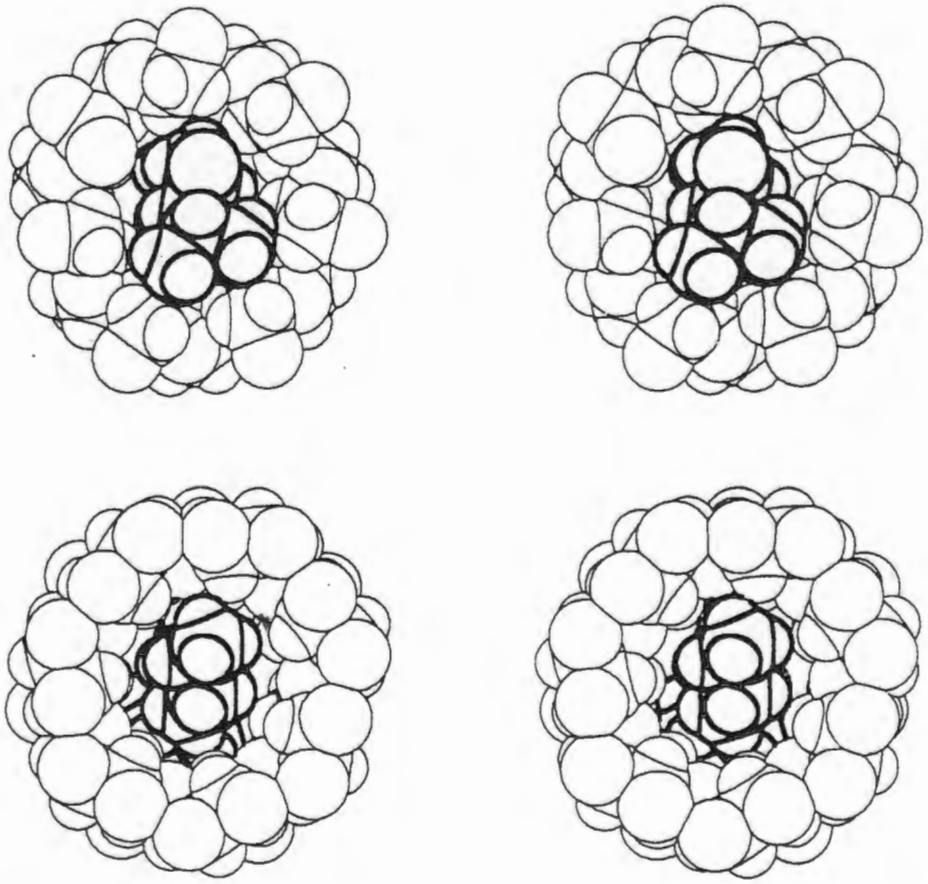

Figure 6B Space-filling diagrams of CD2 with its guest viewed: above - from the primary hydroxyl side, below - from the secondary hydroxyl side.

Figure 7 is a stereo space-filling diagram of the dimer complex showing how the two independent guest molecules are in close contact (H(13)···H(32) 2.32 Å, hydrogen atoms inserted at calculated positions for the two independent guests are numbered consecutively H(1) to H(19) and H(21) to H(39)) and fill the available space of the dimeric cavity at the dimer interface. Although other dimeric β-CD complexes occasionally have the polar groups of their guests at the dimeric interface[9,11,12,13], those which are not hydrogen bonded to a host secondary hydroxyl group are usually hydrogen bonded to a water molecule[14,15,16]. In this instance it is clear that there is no space in the dimeric cavity for a water molecule at the interface.

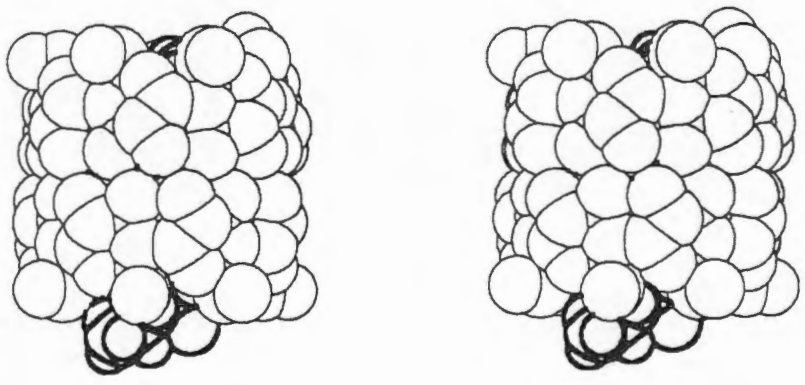

Figure 7 Space-filling diagram of the dimer complex unit in MENTHB.

Thermogravimetric analysis of the complex gave a weight loss which corresponds to 29 water molecules per dimer complex unit. In addition, the C, H microanalysis results are within 0.3% of the calculated values for a 2:2:29 menthol:β-cyclodextrin:water complex and the measured density of the complex, 1.37(1) $g.cm^{-3}$, gives 27.7 ± 1.3 water molecules per 2:2 menthol:β-cyclodextrin complex unit. Only 22.5 of the 29 water molecules were placed owing to extensive disorder which was complicated further by decay of the crystal during data collection. Sixteen of these were ordered and the remaining 6.5 water molecules located were disordered over 11 sites. Table 8 gives a list of all O···O contact distances of 3.0 Å and less.

Table 8 O···O contact distances less than 3.0 Å in the MENTHB complex.

O	O	Distance (Å)	O	O	Distance (Å)
O(113)	O(122)	2.83(2)	O(163)	O(22W)	2.92(4)
O(123)	O(132)	2.80(2)	O(216)	O(8W)	2.82(3)
O(133)	O(142)	2.88(2)	O(222)	O(14W)	2.76(4)
O(143)	O(152)	2.76(2)	O(212)	O(21W)	2.76(4)
O(153)	O(162)	2.79(2)	O(2W)	O(4W)	2.87(2)
O(163)	O(172)	2.72(2)	O(3W)	O(9W)	2.76(3)
O(173)	O(112)	2.74(2)	O(3W)	O(13W)	2.85(5)
O(213)	O(222)	2.75(2)	O(4W)	O(8W)	2.78(4)
O(223)	O(232)	2.79(2)	O(5W)	O(7W)	2.98(3)
O(233)	O(242)	2.83(2)	O(5W)	O(10W)	2.94(3)
O(243)	O(252)	2.82(2)	O(5W)	O(26W)	2.93(6)
O(253)	O(262)	2.76(2)	O(6W)	O(14W)	2.92(5)
O(263)	O(272)	2.71(2)	O(8W)	O(17W)	2.86(5)
O(273)	O(212)	2.81(2)	O(9W)	O(16W)	2.72(4)
O(113)	O(263)	2.83(2)	O(9W)	O(20W)	3.00(7)
O(123)	O(253)	2.87(2)	O(10W)	O(14W)	2.68(5)
O(133)	O(243)	2.76(2)	O(11W)	O(18W)	2.47(6)
O(143)	O(233)	2.85(2)	O(15W)	O(17W)	2.55(6)
O(153)	O(223)	2.75(2)	O(15W)	O(25W)	2.85(6)
O(163)	O(213)	2.86(2)	O(19W)	O(20W)	2.57(9)
O(173)	O(273)	2.81(2)	O(20W)	O(27W)	2.9 (1)
O(153)	O(6W)	2.84(2)	O(22W)	O(23W)	2.98(5)
O(163)	O(21W)	3.00(4)	O(26W)	O(27W)	2.5 (1)

O	O	Symmetry operation			Distance (Å)
O(116)	O(156)	x-1,	y,	z	2.86(2)
O(126)	O(216)	-x,	y+1/2,	-z	2.69(2)
O(136)	O(176)	x,	y,	z-1	2.93(2)
O(152)	O(262)	x+1,	y,	z	2.73(2)
O(172)	O(242)	x,	y,	z+1	2.70(2)

cont'd

Table 8 cont'd

O(226)···O(266)	x+1,	y,	z	2.77(2)
O(27) ···O(12W)	x-1,	y,	z-1	3.00(3)
O(1W) ···O(243)	x+1,	y,	z+1	2.82(2)
O(1W) ···O(272)	x+1,	y,	z	2.66(2)
O(1W) ···O(16W)	-x+1,	y+1/2,	-z+1	2.95(4)
O(2W) ···O(226)	x,	y,	z+1	2.77(2)
O(2W) ···O(256)	x+1,	y,	z+1	2.69(3)
O(3W) ···O(176)	-x,	y-1/2,	-z+1	2.75(3)
O(4W) ···O(136)	-x,	y-1/2,	-z	2.67(3)
O(4W) ···O(236)	x,	y,	z+1	2.72(3)
O(5W) ···O(126)	-x,	y-1/2,	-z	2.76(3)
O(5W) ···O(266)	x+1,	y,	z	2.66(2)
O(6W) ···O(112)	x+1,	y,	z	2.75(3)
O(7W) ···O(116)	-x,	y-1/2,	-z	2.72(2)
O(7W) ···O(146)	-x+1,	y-1/2,	-z	2.81(3)
O(9W) ···O(156)	-x+1,	y-1/2,	-z+1	2.79(3)
O(10W)···O(446)	x+1,	y,	z+1	2.80(4)
O(11W)···O(236)	x+1,	y,	z+1	2.63(4)
O(11W)···O(276)	x+1,	y,	z	2.52(4)
O(12W)···O(116)	-x,	y-1/2,	-z+1	2.84(3)
O(16W)···O(132)	-x,	y-1/2,	-z	2.67(4)
O(16W)···O(25W)	-x+1,	y-1/2,	-z+1	2.85(7)
O(17W)···O(256)	x+1,	y,	z+1	2.88(4)
O(18W)···O(136)	-x+1,	y-1/2,	-z	2.80(5)
O(18W)···O(166)	-x+1,	y-1/2,	-z+1	2.80(5)
O(19W)···O(123)	-x,	y-1/2,	-z	2.96(6)
O(19W)···O(24W)	-x+1,	y-1/2,	-z+1	2.75(9)
O(20W)···O(166)	-x+1,	y-1/2,	-z+1	2.89(6)
O(21W)···O(233)	x,	y,	z+1	2.79(5)
O(22W)···O(142)	x,	y,	z+1	2.69(4)
O(23W)···O(232)	x,	y,	z+1	2.68(4)
O(23W)···O(253)	x+1,	y,	z+1	2.89(4)

cont'd

Table 8 cont'd

O(24W)···O(122)	x+1,	y,	z+1	2.73(4)
O(24W)···O(143)	x,	y,	z+1	2.86(5)
O(24W)···O(253)	x+1,	y,	z+1	2.96(5)
O(25W)···O(252)	x+1,	y,	z+1	2.75(5)
O(26W)···O(446)	x+1,	y,	z+1	2.86(7)
O(26W)···O(276)	x+1,	y,	z	2.70(7)
O(27W)···O(146)	-x+1,	y-1/2,	-z	2.98(9)

The dimer axis is almost parallel to the crystal *b*-axis (interaxial angle approximately 8°) and successive cyclodextrin dimers in this direction are related by a two-fold screw axis creating an endless zigzag channel which is occupied by the guest molecules. Figure 8 is a stereo space-filling diagram of two dimer complex units related by the twofold screw axis parallel to the *b*-axis and shows how the guest hydroxyl group which protrudes from the dimer is situated so that it is accessible for hydrogen bonding to a water molecule. Figure 9 shows the close proximity of guest 1 to guest 2 of the screw-related dimer.

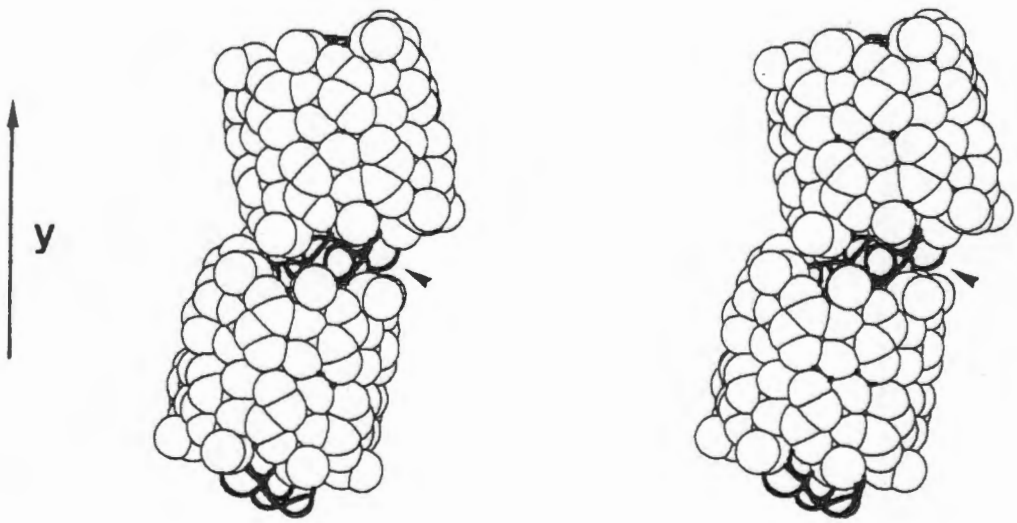

Figure 8 Space-filling diagram of two dimer complex units related by the twofold screw axis parallel to the *b*-axis.

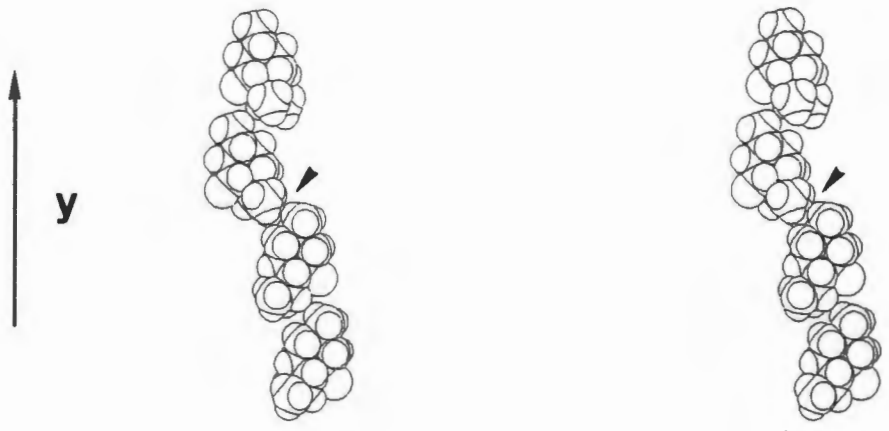

Figure 9 The four guest molecules which occupy two cyclodextrin dimers related by the twofold axis parallel to the *b*-axis.

The resulting layered structure is typical of the packing arrangement usually observed in dimeric β-CD complexes crystallising in $P2_1$ and classed as screw channel packing[11]. Figures 10 and 11 are stereo packing diagrams illustrating the layered and screw channel features of this packing arrangement. In this type of packing arrangement, there are usually quite a number of direct hydrogen bonds between adjacent dimers within a layer, but direct inter-layer hydrogen bonding has been found to be rare[11]. However, in this case there does appear to be a direct hydrogen bond between dimers in adjacent layers. Hydrogen bonding is inferred from a close contact between O(126) and $O(216)^{I}$ (I -x, y+1/2, -z 2.69(2) Å, C(126)-O(126)···$O(216)^{I}$ angle = 103° and $C(216)^{I}$-$O(216)^{I}$···O(126) angle = 123°).

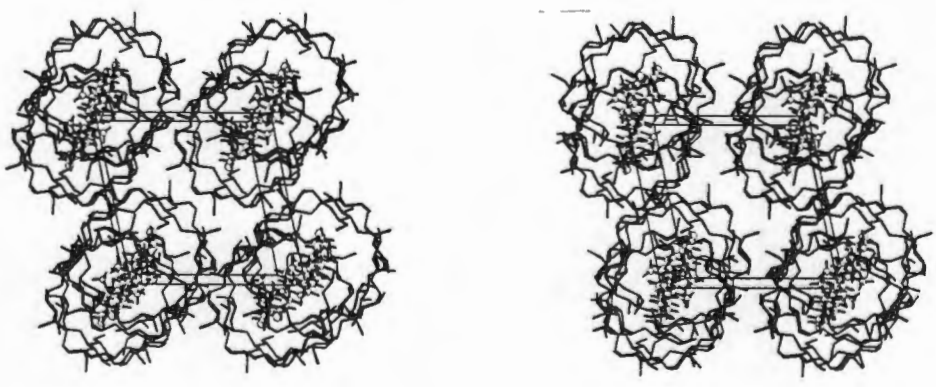

Figure 10 Packing diagram of the MENTHB complex viewed down the *b*-axis (water molecules have been omitted).

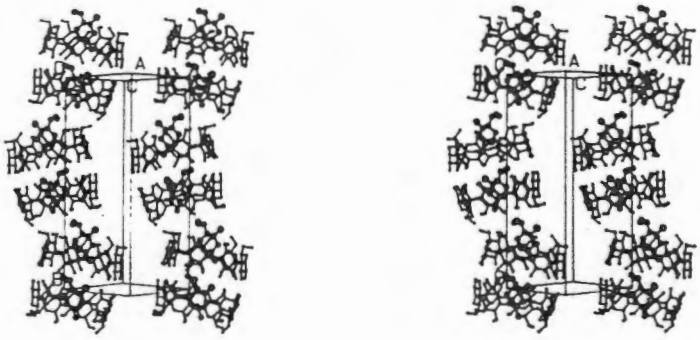

Figure 11 Packing diagram of the MENTHB complex viewed perpendicular to the *b*-axis (water molecules have been omitted).

MENTMB complex

Figure 12 shows a stereodiagram of the (*L*)-menthol-TRIMEB complex in which the glucose residues have been numbered. All seven methylglucose moieties of the TRIMEB molecule are in the $^4C_1$ chair conformation. Atom C(8G2) is disordered over two sites with site occupancies of 0.6 and 0.4. Bond lengths are within the e.s.d.s of those reported for other cyclodextrin complexes, except for O(2G1)-C(7G1) and C(5G4)-C(6G4) (1.31(1) and 1.68(2) Å, respectively). This is probably due to residual disorder which was not modelled. The C(6)-O(6) bonds are in the (-)-*gauche*[10] conformation, except in G4 and G5, where they have the (+)-*gauche* conformation. All O(6)-C(9) bonds are *trans* to the corresponding C(5)-C(6) bonds, except in G4 and G6, where the relationship is *gauche*. Table 9 lists O(4)···O(4')···O(4") angles, radii of the O(4) heptagon, O(4)···O(4') distances, tilt angles and deviations of the O(4) atoms from their least-squares plane. As observed in previous complexes, the TRIMEB molecule is cup-shaped with the O(6)-C(9) groups of G1, G2, G4, G5 and G7 almost completely closing off the O(6) side of the TRIMEB molecule (Figure 13).

Figure 12 A stereodiagram of the MENTMB complex viewed perpendicular to the host axis.

Table 9 Geometrical data for TRIMEB in the menthol-TRIMEB complex.

i. Glycosidic oxygen angle (°) and radius (Å) of the O(4) heptagon (measured from the centre of gravity of seven O(4) atoms to each O(4) atom.

O(4G7)···O(4G1)···O(4G2)	120.0	G1	5.25
O(4G1)···O(4G2)···O(4G3)	122.5	G2	5.39
O(4G2)···O(4G3)···O(4G4)	129.4	G3	4.83
O(4G3)···O(4G4)···O(4G5)	139.0	G4	4.65
O(4G4)···O(4G5)···O(4G6)	115.0	G5	5.53
O(4G5)···O(4G6)···O(4G7)	124.4	G6	5.14
O(4G6)···O(4G7)···O(4G1)	142.7	G7	4.40
Average	127.6	Average	5.03

ii. O(4)···O(4') distance (Å) and tilt angle (°)

O(4G1)···O(4G2)	4.26	G1	26.5
O(4G2)···O(4G3)	4.46	G2	-10.2
O(4G3)···O(4G4)	4.54	G3	7.4
O(4G4)···O(4G5)	4.37	G4	47.7
O(4G5)···O(4G6)	4.26	G5	25.1
O(4G6)···O(4G7)	4.55	G6	-9.3
O(4G7)···O(4G1)	4.40	G7	46.5
Average	4.41	Average	19.1

iii. Deviations (Å) of O(4) atoms from the least-squares plane through the seven O(4) atoms.

O(4G1)	O(4G2)	O(4G3)	O(4G4)	O(4G5)	O(4G6)	O(4G7)
0.514(8)	0.009(7)	0.418(6)	0.120(6)	0.466(6)	0.390(6)	0.283(8)

In contrast to the inclusion of menthol by β-cyclodextrin, the menthol molecule here has its hydroxyl and isopropyl substituents buried in the cup-shaped TRIMEB cavity and its methyl substituent protruding slightly from the O(2),O(3) face (Figure 12). The hydroxyl group is not within hydrogen bonding distance of any of the O(4)

atoms of the TRIMEB molecule and the fact that this group is found buried in the cavity, instead of protruding from the O(2),O(3) face of the host (where it could form a hydrogen bond with an O(2) or O(3) atom) is further evidence that the extent of hydrophobic host-guest interactions is sufficient for complex stabilisation with menthol as guest. There are only two close contacts between host and guest i.e. H(32)···H(86C) 2.36(2) Å and O(7)···H(5G5) 2.75(1) Å. Despite only two close contacts, stereo space-filling diagrams (Figure 13) show that the menthol molecule fits the cavity of the TRIMEB host better than the rounder, more symmetrical cavity of the parent cyclodextrin.

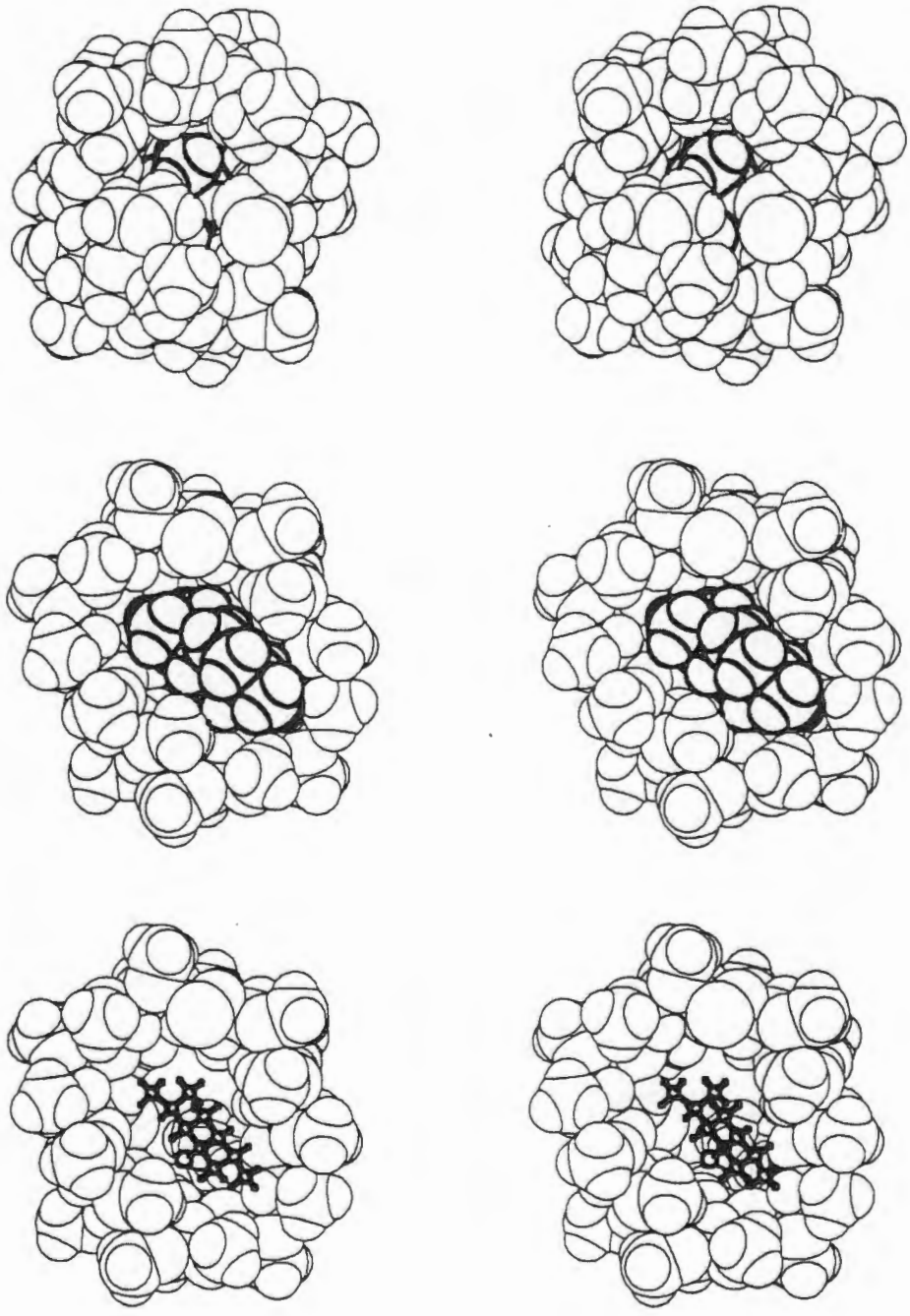

Figure 13 Space-filling diagrams of the MENTMB complex viewed: top - from the O(6) side of the host, middle and bottom - from the O(2),O(3) side of the host (stick representation of guest in the bottom diagram).

Thermogravimetric analysis gave a weight loss which corresponds to almost two water molecules per 1:1 complex unit. These water molecules were located in the X-ray analysis and although their temperature factors were rather high, were refined with full site occupancy as there were no indications for any alternative positions. The water molecules are situated at the periphery of the cyclodextrin molecule and fill a small intermolecular space between complex units. Close O···O contacts for these water molecules, indicative of hydrogen bonding, and parameters for a C-H···O(1W)[17] hydrogen bond are given in Table 10.

Table 10 O···O contacts less than 3.0 Å and C-H···O hydrogen bonds in the MENTMB complex.

O	O	Symmetry operation			Distance (Å)
O(1W)···O(3G5)		-x+1,	y+1/2,	-z+1/2	2.71(2)
O(1W)···O(2W)		x-1,	y,	z	2.93(3)
O(2W)···O(3G2)		x+1/2,	-y-1/2,	-z	2.62(2)
O(2W)···O(6G2)		x+1,	y+1,	z	2.87(2)

			Distance (Å)			Angle (°)
C	H	O	C···O	C-H	H···O	C-H···O
C(1G2)-H(1G2)		O(1W) (a)	3.18(3)	0.98	2.43	132.8
C(6G1)-H(612)		O(5G7)	3.17(2)	0.97	2.36	140.3
C(6G2)-H(622)		O(5G1)	3.17(2)	0.97	2.41	133.9
C(6G3)-H(632)		O(5G2)	3.22(1)	0.97	2.58	122.9
C(6G5)-H(651)		O(5G4)	3.16(1)	0.97	2.28	149.7
C(6G6)-H(662)		O(5G5)	3.12(1)	0.97	2.42	128.7
C(1G6)-H(1G6)		O(3G7)	3.06(2)	0.98	2.39	125.3

(a) x, y-1, z

The conformation of the TRIMEB molecule is stabilised by six intramolecular C-H···O hydrogen bonds, five of the type $C(6G_n)$-H···$O(5G_{n-1})$. These hydrogen bonds also exist in the (*S*)-naproxen-TRIMEB complex (Chapter 7) and in TRIMEB monohydrate (Chapter 6). Calculation of the $C(6G_n)$···$O(5G_{n-1})$ distances in other TRIMEB complexes shows that five of them in each case are less than 3.4 Å. Table 10 also lists these C-H···O hydrogen bonds. Figure 14 shows

stereo packing diagrams for the (*L*)-menthol-TRIMEB complex. Complex units stack in columns in head-to-tail mode, forming what appear to be continuous channels along the *a*-axis. However, a space-filling diagram of the host (Figure 13) shows that the O(6)-C(9) methoxy groups almost completely block off the O(6) side of the molecule and therefore the packing is more accurately described as cage-type packing.

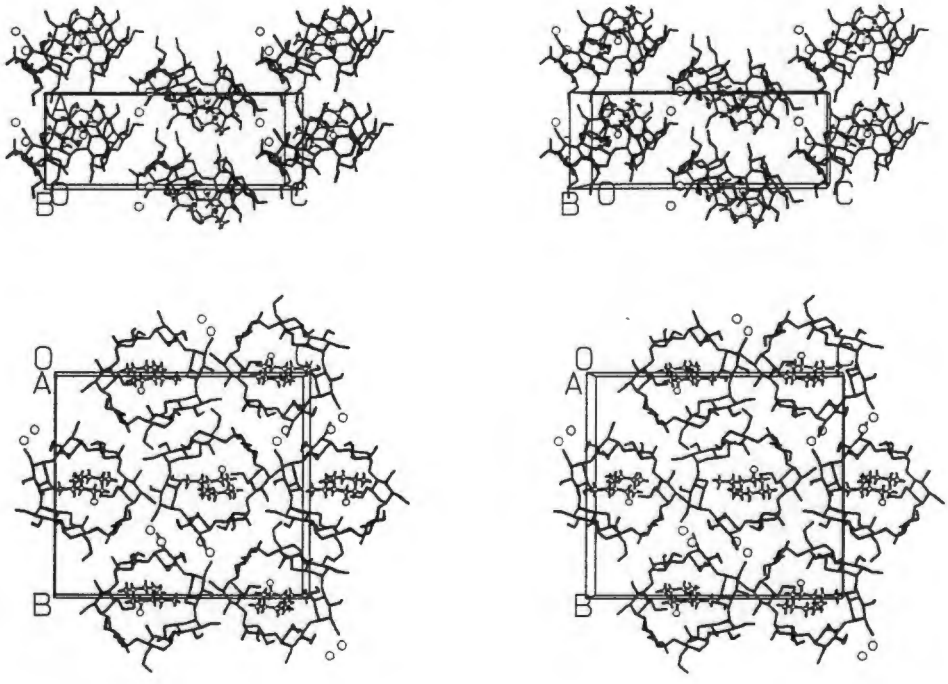

Figure 14 Packing diagrams for MENTMB viewed: above - down the *b*-axis, below - down the *a*-axis.

This packing arrangement is different from those observed thus far in TRIMEB complexes. All but one of the complexes published to date pack in "screw channel" mode along the *b*-axis[18,19,20,21]. The exception to these is the *m*-iodophenol complex[20] (MIPTMB), where the axis of the TRIMEB molecule makes an angle of 26.2° with the *b*-axis, resulting in a herring-bone packing arrangement. One of the methylglucose residues of the host in this complex is in the $^{O}S_{2}$ twist boat conformation, but apart from this, the authors found that the TRIMEB conformation was very similar to that in the 4-biphenylacetic acid complex[20]. In the present complex, the *a*-axis direction corresponds with the direction of the *b*-axes in all the other complexes. However, the twofold screw axis parallel to the *a*-axis does not pass through the host cavity, but to the side of the host and therefore complex units related by the 2_1-axis in this direction are members of adjacent columns. This

results in a much shorter cell length *a* than the cell lengths *b* in other complexes and therefore successive complex units within a column are related by a unit cell translation rather than by a twofold screw axis as in other complexes.

Despite the reported occurrence of three different packing arrangements and a range of very different guests, the TRIMEB molecule has a remarkably similar conformation in all of these complexes, the major differences lying in the different conformations of the O(6)-C(9) methoxy groups which determine the relative extent to which the O(6) side of the molecule is closed off. The comparison of the tilt-angles of the methylglucose residues in the three different packing arrangements shows the similarity in the conformations of the TRIMEB molecule (Table 11). The conformation of the TRIMEB molecule observed in its inclusion complexes thus appears to be a preferred one which is independent of guest or crystal packing, although the latter two factors could induce small local conformational differences. It therefore seems reasonable to conclude that the $C(6G_n)$-H···$O(5G_{n-1})$ hydrogen bonding, which invariably occurs in TRIMEB complexes, plays an important role in stabilising the conformation of this host molecule in the solid state, in much the same way as the O(2)···O(3') hydrogen bonding does in the parent cyclodextrin.

Table 11 Tilt angles (°) for the methylglucose residues in the three packing arrangements of TRIMEB complexes and in TRIMEB monohydrate.

	PIP[a]	MIP[b]	MENTMB	TRIMEB[c]
G1	28.6 ± 1.5	27.7	26.5	38.0
G2	17.3 ± 1.9	13.3	10.2	21.0
G3	-12.1 ± 1.1	-6.1	-7.4	-4.6
G4	43.6 ± 0.4	45.2	47.7	72.9
G5	35.3 ± 0.9	28.3	25.1	57.3
G6	-14.5 ± 0.7	-13.6	-9.3	-24.5
G7	39.4 ± 3.1	51.7	46.5	24.7

a *p*-iodophenol-TRIMEB complex[18]. The values quoted are the averages with mean deviations for this complex together with four isomorphous complexes[19,20] and Chapter 7 - NAPTMB.
b *m*-iodophenol-TRIMEB complex[20].
c TRIMEB monohydrate (Chapter 6).

The conformation of the TRIMEB molecule in TRIMEB monohydrate (Chapter 6) is much more distorted than in its complexes (one methylglucose residue adopting a $^1C_4$ conformation), yet the overall trend in the tilt angles is comparable with those in the complexes (Table 11). This distorted conformation, characterised by very large tilt angles, has been attributed to the reduction of the hydrophobic cavity size in the absence of a guest molecule so that more efficient packing is attained (Chapter 6). It is possible that an additional factor causing such large tilt angles is the maintenance of the $C(6G_n)$-H$\cdots$O$(5G_{n-1})$ hydrogen bonding.

Thermal analyses of the menthol-CD complexes in relation to their crystal structures

Knowledge of the detailed crystal structures of the MENTHB and MENTMB complexes facilitates the interpretation of the different thermal behaviour of these two complexes with respect to the loss of water of crystallisation. The loss of water molecules from β-CD hydrate and complexes of native β-CD is typically the first event on heating and usually occurs between 30 and 130°C[22,23,24,25,26]. The crystal structures always contain many water molecules which fill the intermolecular spaces. In contrast, DIMEB and TRIMEB complexes contain fewer or no water molecules[18,19,20,21], presumably because of their decreased hydrogen bonding capability and the presence of methyl groups with rotational freedom which help to maximise the efficiency of crystal packing. Although water loss occurs between 30 and 135°C in the MENTHB complex and between 30 and 90°C in the DIMEB complex, the onset of water loss from the MENTMB complex does not occur until shortly before the melt of the complex. This is probably because the water molecules are relatively tightly held in a small, closed intermolecular space in the crystal structure (Figure 15). While it is true that the water molecules in the MENTHB complex are also involved in extensive hydrogen bonding (indicated by many close O$\cdots$O contacts), it is possible that the sheer number of water molecules, coupled with the fact that they occupy "channels" inbetween columns of screw-related dimer complex units (Figure 16), facilitates disruption of the integrity of the crystal structure on heating with subsequent escape of water molecules. In the case of the DIMEB complex, if the water molecules are indeed situated in the cyclodextrin cavity (as suggested by the analogy with other DIMEB complexes), then they are likely to be disordered and therefore not particularly tightly bound. However, crystal structure solution would be necessary for the unambiguous

interpretation of the thermal behaviour.

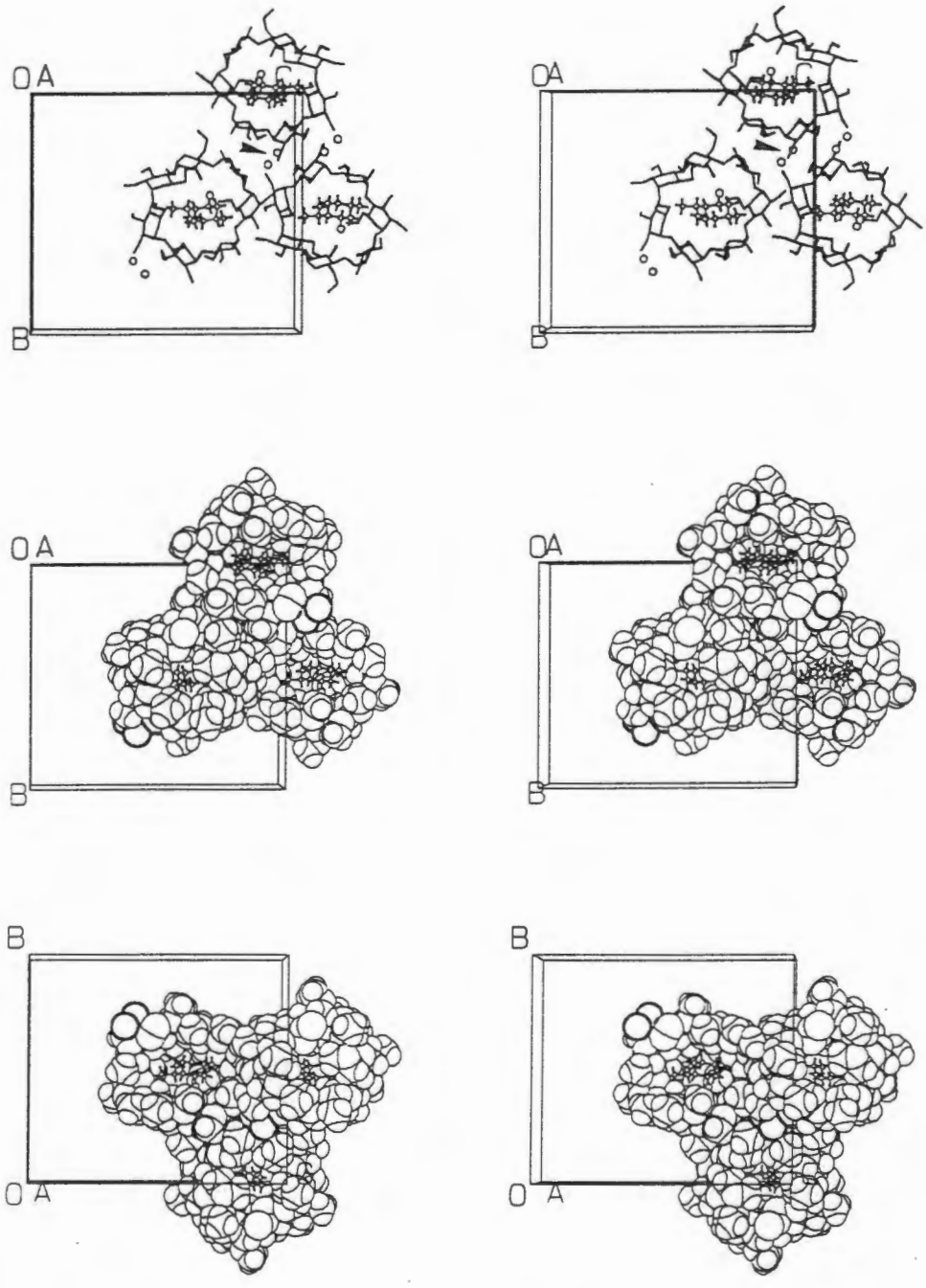

Figure 15 A partial packing diagram for MENTMB, showing how the water molecules are situated in a closed intermolecular space. The middle diagram is the same as the top diagram, except that van der Waals radii have been used for the host and the water molecules. In the bottom diagram the same three complex units are viewed from the other side i.e. the diagram has been rotated through 180° top to bottom.

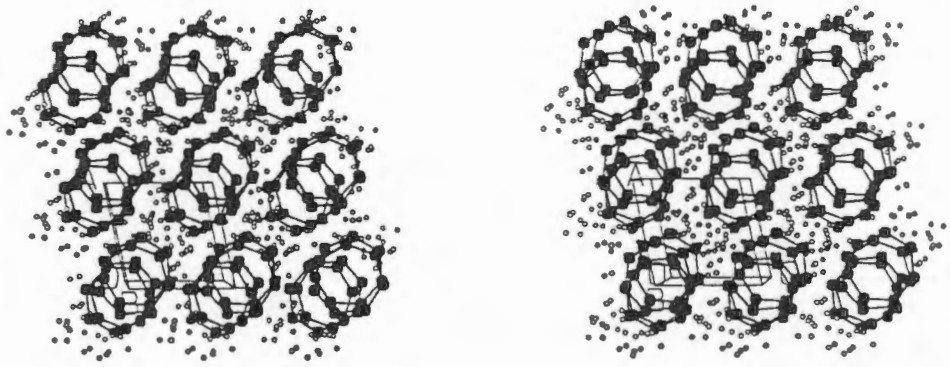

Figure 16 Simplified packing diagram for MENTHB showing how the water molecules occupy large regions of intermolecular space. Each cyclodextrin molecule is represented by its O(4) heptagon (shaded atoms) and the menthol molecules have been omitted.

XRD

Figures 17 and 18 show the calculated and experimental XRD patterns for MENTHB and MENTMB, respectively. Differences in intensities between calculated and experimental patterns are due to preferred orientation of the crystallites and, in the case of MENTHB, an incomplete theoretical model which does not include contributions from the hydrogen atoms of the guest or water molecules and the hydroxyl groups of the host. The very close match in the peak positions shows the high purity of the samples. Figure 19 shows the XRD patterns for the DIMEB complex and for a 1:1 physical mixture of (*L*)-menthol and DIMEB. The appearance of new peaks with different 2θ values and the disappearance of others in the pattern of the complex relative to the pattern of the physical mixture demonstrate the existence of a different phase.

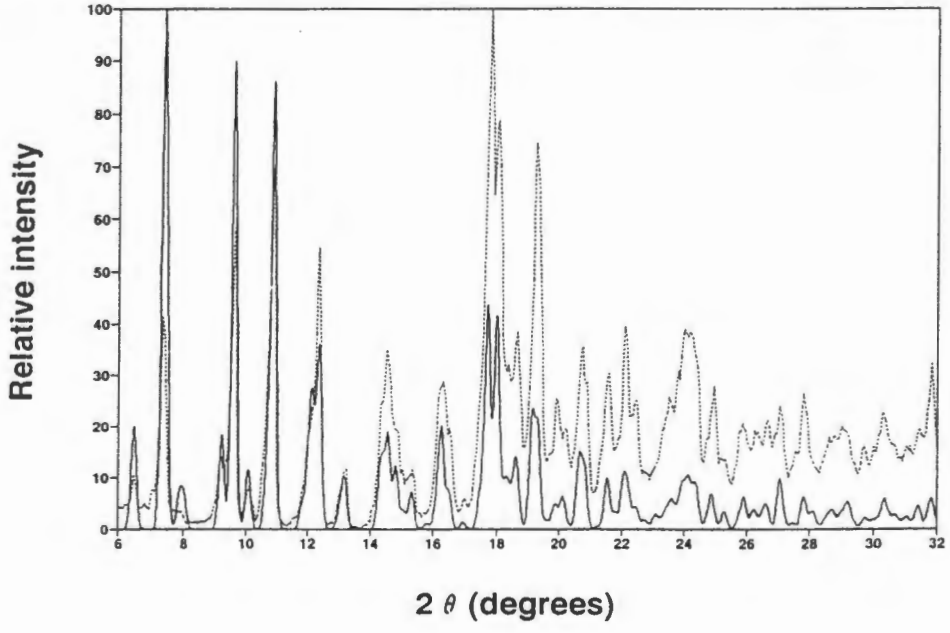

Figure 17 Calculated (——) and experimental (· · · · ·) XRD patterns for MENTHB.

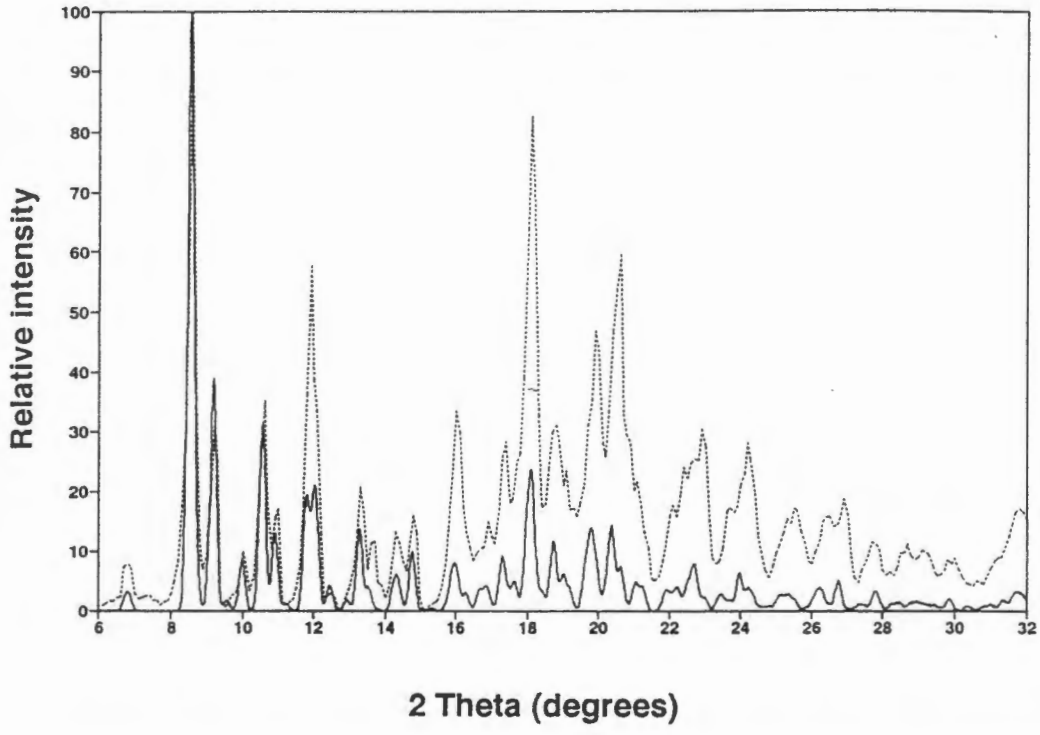

Figure 18 Calculated (——) and experimental (· · · · ·) XRD patterns for MENTMB.

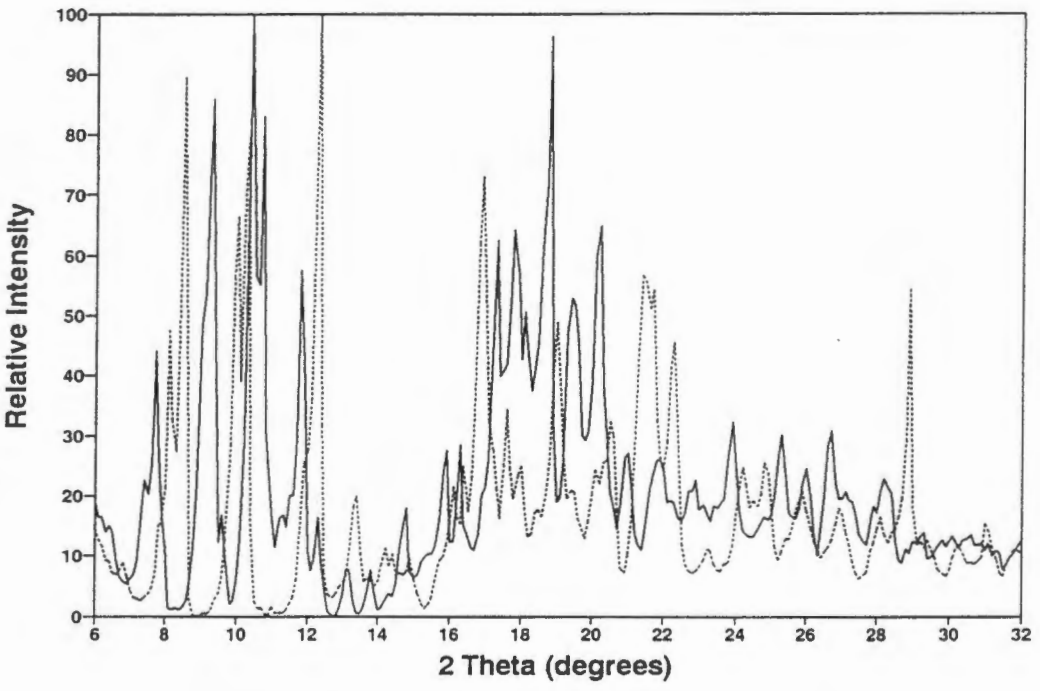

Figure 19 XRD patterns for MENDMB (——) and a 1:1 physical mixture of (*L*)-menthol and DIMEB (· · · · ·).

References

1. *South African Medicines Formulary*, edited by C. J. Gibson and C. R. Swanepoel, CTP Book Printers, Western Cape, South Africa, 1995.
2. O. P. Shukla, *Proc. 11th Int. Congr. Essent. Oils, Fragrances Flavours*, 1989, 137.
3. J. Szejtli, *Topics in Inclusion Science - Cyclodextrin Technology*, Dordrecht, The Netherlands, Kluwer Academic Publishers, 1988.
4. K-H Frömming and J. Szejtli, *Topics in Inclusion Science - Cyclodextrins in Pharmacy*, Volume 5, Dordrecht, The Netherlands, Kluwer Academic Publishers, 1994.
5. A. Bavley and E. W. Robb, *Chem. Abs.*, 1962, **57**, 17091.
6. G. Koczka and A. Hung, *Chem. Abs.*, 1992, **117**, 448.
7. L. Szente, J. Szejtli and M. Gal-Füzy, *J. Incl. Phenom.*, 1984, **2**, 631.
8. K. Harata, *Bull. Chem. Soc. Jpn.*, 1988, **61**, 1939.
9. J. A. Hamilton and L. Chen, *J. Am. Chem. Soc.*, 1988, **110**, 4379.
10. W. Saenger, *Inclusion Compounds*, Volume 2, Chapter 8, London, Academic Press, edited by J. L. Atwood, J. E. D. Davies and D. D. MacNicol, 1984.
11. D. Mentzafos, I. M. Mavridis, G. Le Bas and G. Tsoucaris, *Acta Crystallog.*, 1991, B**47**, 746.
12. I. Nakanishi, T. Fujiwara and K. Tomita, *Acta Crystallog.*, 1984, **A**, C78.
13. J. A. Hamilton and L. Chen, *J. Am. Chem. Soc.*, 1988, **110**, 5833.
14. T. Tokuoka, T. Fujiwara and K. Tomita, *Acta. Crystallog.*, 1981, B**37**, 1158.
15. J. A. Hamilton and M. N. Sabesan, *Carb. Res.*, 1982, **102**, 31.
16. I. M. Mavridis, E. Hadjoudis and G. Tsoucaris, *Carb. Res.*, 1991, **220**, 11.
17. T. Steiner and W. Saenger, *J. Am. Chem. Soc.*, 1993, **115**, 4540.
18. K. Harata, K. Uekama, M. Otagiri and F. Hirayama, *Bull. Chem. Soc. Jpn.*, 1983, **56**, 1732.
19. K. Harata, K. Uekama, T. Imai, F. Hirayama and M. Otagiri, *J. Incl. Phenom.*, 1988, **6**, 443.
20. K. Harata, F. Hirayama, H. Arima, K. Uekama and T. Miyaji, *J. Chem. Soc. Perkin Trans. 2*, 1992, 1159.
21. D. Mentzafos, I. M. Mavridis and H. Schenk, *Carb. Res.*, 1994, **253**, 39.
22. S. Senel, O. Cakoglu, M. Sumnu, D. Duchene and A. A. Hincal, *J. Incl. Phenom.*, 1992, **14**, 171.
23. E. Redenti, M. Passini, P. Ventura, A. Spisni, M. Vikmon and J. Szejtli, *J. Incl. Phenom.*, 1993, **15**, 281.

24. S. Kohata, K. Jyodoi and A. Ohyoshi, *Thermochimica Acta*, 1993, **217**, 187.
25. S. Szafranek and J. Szafranek, *J. Incl. Phenom.*, 1993, **15**, 351.
26. M. Bilal, C. de Brauer, P. Claudy, P. Germain and J.M. Létoffé, *Thermochimica Acta*, 1995, **249**, 63.

Chapter 9 Conclusion

Crystal structure solution of cyclodextrin-drug complexes provides unequivocal confirmation of complex formation and detailed information regarding the stoichiometry, mode of inclusion and host-guest interactions. This information is useful in the pharmaceutical industry, where strict characterisation is important for patenting and registration. Once a crystal structure is available, a calculated XRD pattern can be used as a standard when bulk preparation of the complex is desired. Relatively few of the reported structures of cyclodextrin complexes have drug molecules as guests. In this study thirteen different cyclodextrin-drug complexes have been characterised and the crystal structures of six of these have been solved. In addition, the crystal structure of a monohydrate of TRIMEB has been determined.

Hot stage microscopy - a useful tool

Simple observation of thermal events on a hot stage microscope proved to be one of the most reliable methods of testing putative inclusion complexes of the native cyclodextrins. The hot stage behaviour of most of the complexes with β-CD and γ-CD presented in this study was remarkably similar and differed from that of the relevant host alone. Crystals of complexes retained their shape but became opaque as water of crystallisation was lost and then turned black, decomposing with no clear melting point. Crystals of the pure cyclodextrins, on the other hand, tended to break up on heating with concomitant water loss, followed by melting with gentle bubbling. The one exception to this was the (*L*)-menthol-β-CD complex which melted with rather vigorous frothing. The TRIMEB complexes were more problematic because the behaviour of the complexes was not markedly different from that of TRIMEB monohydrate. The (*L*)-menthol-DIMEB complex was interesting in that the guest was also lost from the complex in addition to water and these separate losses could clearly be seen on the hot stage microscope. This behaviour and the similarity in unit cell parameters (except for an approximate doubling in c) with reported DIMEB complexes led to the proposal that the guest is located outside the host cavity as in the published structures.

Thermal analysis

The observations made by hot stage microscopy could be correlated with the thermal analysis, where weight losses and endotherms associated with the loss of water were seen in the TG and DSC traces, respectively. Exotherms or endotherms related to decomposition could also be identified. Weight losses obtained for water loss were generally very reproducible, emphasising the reliability of thermogravimetric analysis in estimating the water content of cyclodextrin complexes as opposed to crystal structure solution, where high thermal motion and disorder often cause uncertainty in the placing of water molecules. Both TG and DSC indicated that water losses from complexes of native cyclodextrins are multi-step processes, a finding observed previously, pointing to different populations of water molecules. This can be rationalised with the crystal structures, where some water molecules are involved in a complex network of hydrogen bonds. A related trend which emerged, was the tendency for complexes of the unsubstituted cyclodextrins which contained cations to retain water molecules to higher temperatures than other complexes. This explanation appears to be supported by the crystal structures of the β-CD complexes with diclofenac sodium and meclofenamate sodium, where the number of water molecules coordinated to the Na^+ ions is in agreement with the estimation of the number of water molecules lost in the later weight losses seen in the TG traces.

Crystal structure

Very few crystal structures of cyclodextrins complexed with large anionic guests have been reported. Although many solution studies have shown that the association constant for a given guest decreases dramatically (at least for β-CD) with increasing ionisation, the results of this study, where a number of β-CD complexes and a γ-CD complex with ionised guests have been presented, show that solid inclusion complexes with relatively large anionic guests can be isolated. This may also be the reason why these complexes have packing arrangements (DICLOFB - $P6_1$, MECLOFB - $P2_12_12_1$) and crystallise in space groups that have not been encountered previously in complexes with native β-CD and γ-CD (FENACBK and FENACBCs - $P2_12_12_1$, DICLOFG - $P2_1$, NAPBorth - $P2_12_12$). Furthermore, the DICLOFB complex not only has a unique packing arrangement, but is also the first example of a β-CD complex crystallising in the hexagonal crystal system.

Interactions between host and guest in the various complexes for which crystal structures were solved range from the relatively snug fit of the diclofenac anion to the loose fit of (*L*)-menthol in the cavity of β-cyclodextrin. It has been suggested that the solvation of a guest molecule's polar group/s is an important factor in determining the orientation of inclusion[1]. Therefore the situation in the menthol complexes, where the hydroxyl group plays a rather passive role, is unexpected. However, it is interesting to note that the two independent guest molecules in the menthol-β-CD complex have very similar orientations in the dimeric cavity. Perhaps the dipole moments of the guest molecules are oriented such that they oppose the resultant dipole moment of the cyclodextrin dimer (assuming this is not close to zero) and that greater complex stabilisation is achieved in this way than by host-guest hydrogen bonding.

The inclusion of the structural isomers, diclofenac sodium and meclofenamate sodium, by β-CD is similar. Examples are seen in these two complexes of the host's ability to discriminate between mirror image conformers of guest molecules[2]. Both conformers of these guest molecules are present in crystal structures containing the diclofenac and meclofenamate anions, but only the one is selected in the crystal structures of their β-CD complexes. The packing arrangements of these two complexes, on the other hand, are somewhat different. Apart from the fact that complex units stacking head-to-tail are related by sixfold and twofold screw axes in the former and latter complexes respectively, one of the most obvious differences is that in the diclofenac sodium complex these columns are unidirectional while in the meclofenamate sodium complex adjacent columns are antiparallel.

In the SULFB complex, the guest is also found in what appears to be a preferred conformation (by comparison with the conformations adopted in other crystal structures in which sulfathiazole is present). The low energy conformations preferred by the guests in the solid state therefore seem to be maintained, if possible, upon complexation with a cyclodextrin host. This particular complex was exceptionally stable in comparison with other β-CD complexes. This is probably due to the number of hydrogen bonds in which the guest molecule is involved which serve as anchorage. As the first reported crystal structure of a sulfonamide-β-CD complex, SULFB can serve as a reference structure for modelling sulfonamide-β-CD interactions.

The crystal structures of several TRIMEB complexes have already been reported, revealing the rather distorted conformation of this host in comparison with the parent cyclodextrin. In this study the crystal structure of a monohydrate of TRIMEB was solved. Not only is the conformation of the uncomplexed host distorted to a remarkable extent even compared with the conformations observed in its complexes, but one of the methylglucose residues adopts the unusual $^{1}C_{4}$ inverted chair conformation. The latter has not been found previously in the cyclodextrins or their complexes in the solid state. It was also noted in this study that the TRIMEB molecule takes on a similar conformation in all of its complexes reported to date despite a range of guests and three different packing arrangements. This is attributed to the C(6G_n)-H···O(5G_{n-1}) intramolecular hydrogen bonds which may play a significant role in the stabilisation of the conformation of TRIMEB in the solid state in much the same way as the O(2)···O(3') hydrogen bonds do in the parent cyclodextrin. Although attention has already been focussed on C-H···O hydrogen bonding in carbohydrate and cyclodextrin crystal structures in particular, the systematic presence of the C(6G_n)-H···O(5G_{n-1}) intramolecular hydrogen bonds in TRIMEB crystal structures has not been noted previously.

XRD

XRD patterns calculated from the crystal structures solved in this study matched the experimental patterns of the prepared samples well, showing their high purity. Since hot stage microscopy is not as useful for detecting the formation of TRIMEB complexes as for those of native cyclodextrins, the calculated XRD pattern of TRIMEB monohydrate can be used as a fingerprint to differentiate between this phase and inclusion complexes of TRIMEB.

References

1. D. Mentzafos, I. M. Mavridis, G. Le Bas and G. Tsoucaris, *Acta Crystallog.*, 1991, B47, 746.
2. G. Tsoucaris, G. Le Bas, N. Rysanek and F. Villain, *J. Incl. Phenom.*, 1987, **5**, 77.